

University of Warwick institutional repository: <http://go.warwick.ac.uk/wrap>

A Thesis Submitted for the Degree of PhD at the University of Warwick

<http://go.warwick.ac.uk/wrap/3973>

This thesis is made available online and is protected by original copyright.

Please scroll down to view the document itself.

Please refer to the repository record for this item for information to help you to cite it. Our policy information is available from the repository home page.

**“Fundamental Studies and Instrumental Methodology
in the Mass Spectrometric Analysis of
Low-Mass Polymeric Systems”**

by

Mark Stanton Woodward

Submitted for the degree of Doctor of Philosophy in Chemistry

University of Warwick, Department of Chemistry

September 2001

**“Fundamental Studies and Instrumental Methodology
in the Mass Spectrometric Analysis of
Low-Mass Polymeric Systems”**

by

Mark Stanton Woodward

Submitted for the degree of Doctor of Philosophy in Chemistry

University of Warwick, Department of Chemistry

September 2001

Table of Contents

Chapter One – Introduction

i.	Overview of Mass Spectrometry	11
ii.	Historical Perspective	16
iii.	Ionisation Techniques	20
	a. Electrospray Ionisation	21
	b. Matrix-assisted Laser Desorption / Ionisation	27
iv.	Separation Techniques	37
	a. Time-of-Flight	37
	b. Fourier Transform Ion Cyclotron Resonance	42
v.	Polymer Science	51
vi.	Structural Analysis	57

Chapter Two - Experimental

i.	Commercial Laser Desorption Mass Spectrometers	61
ii.	Commercial Electrospray-based Mass Spectrometer	63
iii.	Research Mass Spectrometers	66
iv.	Chromatographic Systems	71
v.	Chemicals and Experimental Samples	72

Chapter Three – Matrix-assisted Laser Desorption / Ionisation

i.	Overview	77
ii.	Discussion of Sample Preparation Issues	78
iii.	Presentation of Sample Preparation Results	81
	a. Sample Application Techniques	81
	b. Low-mass Polymer Samples	91
iv.	Mass-bias Effects	94
	a. Effect of Instrumental Variables	96

b.	Effect of Attached Cations	100
c.	Rationalisation of Bias Effects	107
v.	Other Samples	127
vi.	Mass Reliability	132

Chapter Four – Electrospray Ionisation

i.	Overview	135
ii.	Conformational Studies	137
iii.	Mass and Charge Bias Experiments	145
a.	Capillary and Skimmer Effects	148
b.	Hexapole Effects	159

Chapter Five – Structural Analysis

i.	Overview	166
ii.	Discussion of MAG-TOF	172
iii.	Carbon-60 Results	174
iv.	Fragmentation of Oxygenate Polymers	182

Chapter Six – Conclusions	200
----------------------------------	------------

Table of Figures

Chapter One - Introduction

1a - Simplified schematic of a mass spectrometer	11
1b - Simplified diagram of a typical mass spectrum	14
1c – Simplified explanation of the cathode ray experiment	16
1d - Double focusing instrument design using Nier-Johnson geometry	17
1e - Formation of cations by electron impact ionisation	18
1f - Formation of cations by chemical ionisation using ammonia	18
1g - Simplified schematic of a generic electrospray source	22
1h - Showing the shrinking and fission process of ion formation	23
1i - Showing the basis for the acquired charge in the IEM theory	25
1j - Schematic of the basic process of ion formation by MALDI	29
1k - Schematic of the basic process of separation by linear tof	38
1l - Schematic of the basic process of separation by reflectron tof	39
1m – Two separate representations of cyclotron and magnetron motion	43
1n – Simplified diagram of the common design for FTICR cells	47
1o - Relation of resolving power to m/z for different magnet strengths	49
1p - Polymerisation by a free radical process	52
1q - Visual representation of the different classes of polymer tacticity	54
1r - Visual representation of the different classes of co-polymer system	54
1s - Pictorial description of the size exclusion principle	55
1t - Simplified model of the process of collision-induced dissociation	58

Chapter Two - Experimental

2a - Simplified layout of the Kompact IV MALDI mass spectrometer	61
2b - Schematic of the MALDI slide used by the Kompact instruments	63
2c - Schematic of the source region of the electrospray source	64
2d - Top-down schematic of the Mag-TOF instrument	67

2e - Diagram showing a simplified operation of the ion buncher	70
2f - Structure of PEG / PPG and their simple block co-polymer	72
2g - Chemical structure of Needol showing a C12 and C13 variation	73
2h - Structure of CoBF showing its binding to a growing polymer chain	74
2i - Catalytic chain transfer polymerisation mediated by cobalt	74
2j - Structure of methyl, benzyl and hydroxyethylmethacrylate polymers	75
2k - Common matrix systems used in this study	75

Chapter Three - Matrix-assisted Laser Desorption / Ionisation

3a - Schematic of the “blank” MALDI slide for the Kratos instrument	82
3b - Schematic of the “templated” slide showing location of the mask	83
3c - Ion intensity across the sample for a non-templated slide	84
3d - Ion intensity across the sample for a templated slide	84
3e - Structure of poly(glycerolmethacrylate)	85
3f – Schematic of the process in preparing a templated MALDI slide	87
3g – Graph of ion intensity loss for higher mass tail	88
3h – Graph of ion loss by mass of oligomer	89
3i – Mass accuracy shown as a function of oligomer mass	90
3j – Structure of parent alcohol of the C12 species	91
3k – Structure of methyl and benzyl polymer systems	93
3l - Comparison of MALDI and gel permeation results at low-mass	95
3m – Schematic of the instrument showing the variable settings	98
3n – Intensity and normalised bar charts of ion affinity	102
3o – Schematic showing coiled and linear salt attachment	106
3p – Model to explain the effect of chain length on salt attachment	106
3q – Intensity plots showing Gaussian and decremental patterns	107
3r – Overlaid spectra of a bimodal sample at various laser powers	108
3rr – Overlaid spectra of bimodal sample at two acceleration voltages	108b
3s – Graph of laser power effect on HEMA polymer system	110
3t – Graph of acceleration voltage effect on the HEMA polymer system	111

3u – Pictorial representation of the two dominant envelope shapes	112
3v – Bar graph showing overall trend for the aCCa matrix system	115
3w – Bar graph showing overall trend for the DHB matrix system	116
3x – Bar graph showing overall trend for the dithranol matrix system	117
3y – Bar graph showing overall trend for the super-DHB matrix system	118
3z – Enlargement of the high mass area of the spectra	120
3aa – Overall trend in Mn values for matrices and laser power	122
3ab – Overall trend in Mn values for matrices and laser power	123
3ac – Overall trends in polydispersity for matrices and laser power	125
3ad – Structure of poly(propylene)	128
3ae – Predicted structure of two of the organometallic additives	129
3af – Spectra of the molybdenum dithiocarbamate sample	131

Chapter Four – Electrospray Ionisation

4a – Electrospray spectra of BPTI under ‘harsh’ source conditions	139
4b - Electrospray spectra of BPTI under ‘mild’ source conditions	140
4c – Theoretical isotope distribution for BPTI	141
4d – Enlarged spectra showing the possible 16 mass loss	142
4e – Enlarged spectra showing the recurring three ion pattern	143
4f - Schematic of the ESI source showing the variable settings	147
4g – Ion intensity given as a function of different skimmer voltages	150
4h – Charge states by skimmer voltage of the 3k polymer	151
4i – Charge states by skimmer voltage of the 11k polymer	152
4j – Overlay of spectra showing the visible effect of skimmer voltage	154
4k - ESI spectra of 3k polymer at the base settings	155
4l – Close-up of 3k polymer showing the isotope pattern	156
4m – Representation of the focusing effect of the skimmer	157
4n – Comparison of the deconvoluted envelope patterns	158
4o – Mass averages shown as a function of the skimmer voltage	159
4p – Mass average and intensity as function of dwell time	161

4q – Mass average as a function of the offset voltage	163
4r – Mass average as a function of the extract voltage	163
4s – Mass average as function of both the extract and offset voltage	164

Chapter Five - Structural Analysis

Figure 5a – Ion gating to isolate a particular mass of ion	169
Figure 5b – MAG-TOF schematic	173
Figure 5c – Carbon-60 3-dimensional structure	175
Figure 5d – Tree diagram of initial loss of a 2-carbon unit	176
Figure 5e – Initial loss Venn diagram	177
Figure 5f – Second loss Venn diagram	178
Figure 5g – Tree diagrams of second loss of a 2-carbon unit	178
Figure 5h – Theoretical isotope distribution for the first two losses	180
Figure 5i – CID spectrum of carbon-60	181
Figure 5j – Needol structure	183
Figure 5k – Linear tof spectra of Needol sample	184
Figure 5l – Calculated masses of Needol combinations	185
Figure 5m – Radical mechanism for the formation of the C _n fragments	186
Figure 5n – CID spectra of the isolated C ₁₂ -EO ₅ species	187
Figure 5o – CID spectra of the isolated C ₁₃ -EO ₅ species	188
Figure 5p – Rearrangement leading to the formation of A fragments	189
Figure 5q – Rearrangement leading to the formation of B fragments	189
Figure 5r – Homolytic fission leading to the formation of the C fragments	190
Figure 5s – Masses of various EO / PO combinations	192
Figure 5u – Number-average mass values for a wider distribution sample	195
Figure 5v – Bar chart of the raw intensities of the fractions	196
Figure 5w – Bar chart of the normalised intensities of the fractions	196
Figure 5x– Composited intensities from the normalised data series	197
Figure 5y – Table showing masses and end-group confirmations	198

Acknowledgements

I would like to take the opportunity to acknowledge the support of my supervisor Professor Peter J Derrick and other members of the Institute of Mass Spectrometry.

I would further thank Malcolm Salisbury of Shell Global solutions as my industrial liaison and further Shell Research Ltd for their financial support of this project.

For the opportunity to study in Budapest I would thank the British Council and more importantly Professor Karoly Vekey and his group for their hospitality.

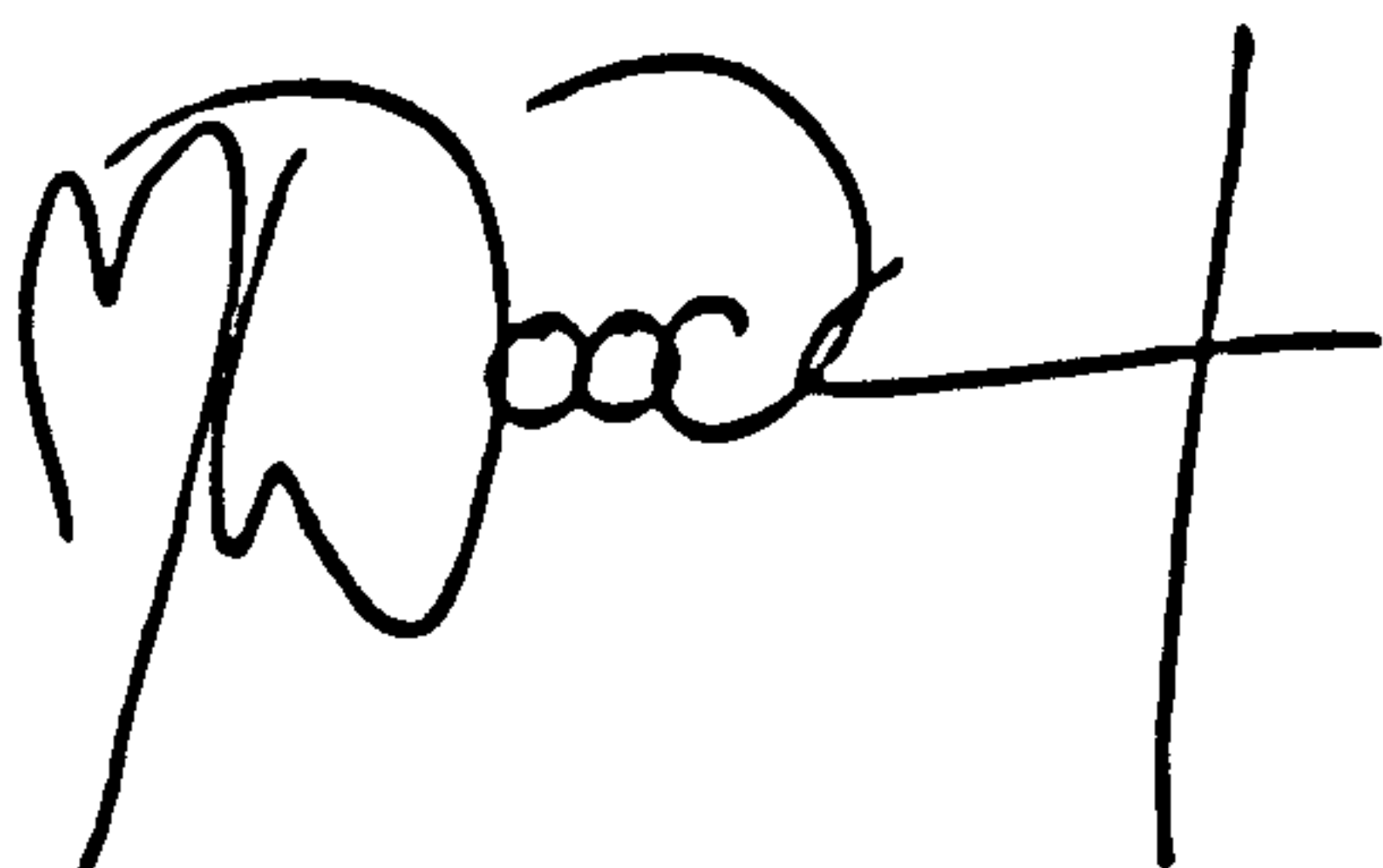
In appreciation of his friendship and as a co-conspirator on a number of studies I would show my appreciation for my colleague Sajid Bashir.

Finally for their enduring love and support I would be remiss not to thank my parents Brenda and Stanley Woodward.

Declaration

I declare that the material presented within has not been used in a prior examination and represents my own work conducted during the three year period of the degree unless as specified within the thesis. The material has further not been submitted in whole or part as qualification for a degree at any other university or college.

Signed :

A handwritten signature in black ink, consisting of a large, stylized 'W' followed by a horizontal line and a vertical line.

Summary of Thesis

The analysis of polymer systems is a crucial field in modern petrochemicals and also other sectors of the chemical industry. This analysis stretches from simple mass measurement, to sample identification and structural studies. Mass spectrometry is one of a number of analytical fields that are used to investigate such samples, but it has been shown to have certain limitations for the routine analysis of polymers.

Chapter one discusses the development of mass spectrometry and the progression that has led to the development of the methods of sample ionisation and separation that are most used today. It also discusses the field of polymer analysis and the other analytical techniques that are applied to such investigations in industry.

Chapter two details the instrumentation used in this study and also the nature of the main samples that were investigated.

Chapter three covers analysis by the technique of matrix-assisted laser desorption / ionisation which is the major mass spectrometric method currently for polymer analysis. Details of work investigating sample preparation are given leading into a larger discussion of the mass biases that arise in such polymer analysis and a rationalisation of their causes.

Chapter four details investigations of polymer analysis using an electrospray source on a Fourier-transform ion cyclotron resonance instrument. The added complexity of charge states is discussed leading to further study of the mass and charge variations given by instrumental conditions.

Chapter five presents a small body of work in the field of structural analysis by the technique of collision-induced dissociation. Work with buckminsterfullerene and a range of ethoxylate polymers is given to demonstrate the capabilities of such analysis.

Chapter six concludes the thesis with a discussion of the topics raised in the previous chapters and how they affect the use of mass spectrometry as a routine tool for the industrial analysis of polymeric systems.

CHAPTER ONE

Introduction

i. Overview of Mass Spectrometry

Mass spectrometry as an analytical technique is fundamentally based on the separation of molecules according to their masses¹. This approach differs from many chromatographic techniques that are based on affinity of some functional group to a stationary phase², and from other spectroscopic methods, such as infrared³ or nuclear magnetic resonance⁴, where the irradiation of a ground state molecule leads to a discernible change. This separation by mass takes place in the gas phase as a result of the behaviour of charged ions within magnetic and / or electric fields. Instrumentation for mass spectrometric analysis can effectively be visualised as being broken down into three parts: a source for the gas-phase ions, a mass separator and some form of detector. Many designs are available in each area and specific combinations are often used to facilitate particular capabilities⁵.

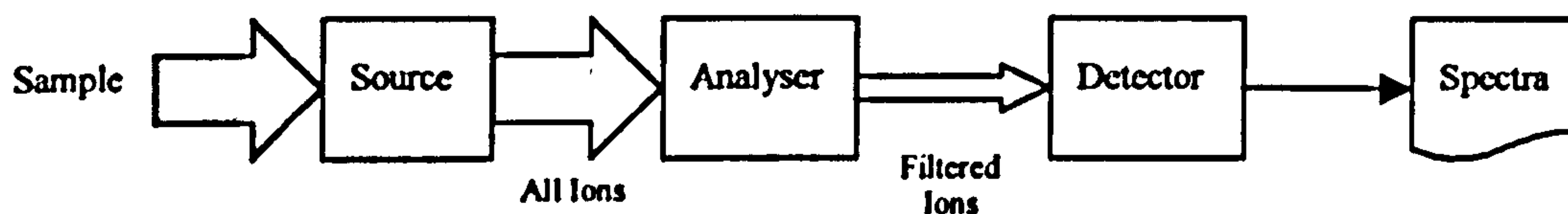


Figure 1a - Simplified schematic of a mass spectrometer

The source part of the instrumentation takes the presented analyte and, assuming it is not already gaseous, transfers it into the gas phase and ionises it to either a positive or negative ion. This process can be carried out as a continuous stream or in a pulsed mode and which one is used determines the specifics of the separation and detection. The ionisation is commonly designated as either “soft” or “hard”, as a rough guide to the energy involved in the process. So-called “hard” ionisation techniques, such as high-

¹ RAW Johnstone, ME Rose, *Mass Spectrometry for Chemists and Biochemists*, Cambridge University Press, (1996)

² K Vekey, *J Chrom A*, 921, 227, (2001)

³ M Coskun, Z Ilter, E Ozdemir, K Demirelli, M Ahmedzade, *Polym Degrad Stabil*, 58, 193, (1997)

⁴ IIN Cheng, TA Early, *Macromol Symp*, 86, 1, (1994)

⁵ RW Purves, L Li, *J Am Soc Mass Spectrom*, 8, 1085, (1997)

energy (70eV) electron impact⁶, have a higher probability of breaking up the analyte molecule into fragments, which is something that is not always wanted. “Soft” ionisation techniques, such as electrospray⁷ and matrix-assisted laser desorption / ionisation⁸ tend to lead to a reduced level fragmentation compared to the “hard” forms. Reduced fragmentation allows easier analysis of mixtures, where otherwise it would have been a challenging task to distinguish fragment ions from parent ions. Since virtually all stable molecules have an even-electron configuration, ionisation by removal of an electron by such means as electron impact, leads to the formation of a radical cation of the molecule which is termed a “molecular ion”. Fragmentation of the molecular ion can lead to charged and neutral daughter species, some of which can give key structural clues to the original molecule. This area of mass spectrometry is well documented, with mechanisms postulated for the fragmentation and rearrangements of most important chemical moieties⁹.



The mass separation is perhaps the most variable of the three stages in the experiment. Different systems give various performance characteristics, from the relatively straightforward time-of-flight¹⁰ to the high-resolution capabilities of ion cyclotron resonance^{11,12,13}. Until recently at least, if most people visualised a mass spectrometer, it would invariably be a sector separator¹⁴. In a sector mass spectrometer, a beam of analyte

⁶ W Bleakney, Phys Rev, 34, 157, (1929)

⁷ SJ Gaskell, J Mass Spectrom, 32, 677, (1997)

⁸ PA Limbach, Spectroscopy, 13, 16, (1998)

⁹ HIF Grutzmacher, Int J Mass Spectrom Ion Proc, 118, 825, (1992)

¹⁰ C Weickhardt, F Moritz, J Grotemeyer, Mass Spec Rev, 15, 139, (1996)

¹¹ A Marshall, Mass Spec Rev, 17, 1, (1998)

¹² PO Stancke, Spectroscopy, 13, 145, (1997)

¹³ JJ Amster, J Mass Spectrom, 31, 1325, (19)

¹⁴ PA Dagostino, JR Hancock, LR Provost, PD Semchuk, RS Hodges, Rapid Comm Mass Spectrom, 9, 597, (1995)

ions is directed into a curved path by magnetic and electrostatic fields applied perpendicular to the direction of motion. How much the various ions are deviated from their path is related to their mass and charge, so the fields can be altered so that a particular mass of ion is focused at a certain point in space. This is a form of mass filtration, since all other masses in the sample are lost to the experiment. Once the ions have been separated based on their masses, they need to be detected and a response can be recorded as a mass spectrum. This process of detection can either be destructive, such as impinging on a particle-sensitive plate, or non-destructive and in principle allowing for the analyte ions to be used in further experiments.

The results of the detection are typically displayed as intensities of ions against what is derived into the form of a scale of mass / charge. Some source techniques, such as matrix-assisted laser desorption / ionisation, which will be discussed later, tend to produce only singly charged ions and so the mass / charge scale is effectively the mass of the analyte plus any attached species. Other techniques produce multiple or higher charge states and special consideration must be given to the interpretation of results so as to ensure that the correct mass is identified. This concept of mass / charge, or m/z as it is usually abbreviated, is crucial to the discussion of mass spectrometry. Masses are quoted in Daltons (Da), the standard values identifiable from a periodic table of the elements where a single unit represents 1/12th of the mass of a carbon atom ($1.661 \times 10^{-27} \text{kg}$). The actual value of m/z is somewhat infrequently given in units known as Thomsons (Th), but are perhaps more strictly written as if dimensionless, as is the z value which represents a discrete multiple of the electron charge ($1.602 \times 10^{-19} \text{C}$). As most separations are mass and charge dependent, an ion with twice the mass as another but also twice the charge will have the same m/z ratio and hence will appear in the same place in the mass spectrum. Techniques such as ion cyclotron resonance use their high resolution to circumvent this problem in practice, as will be discussed later.

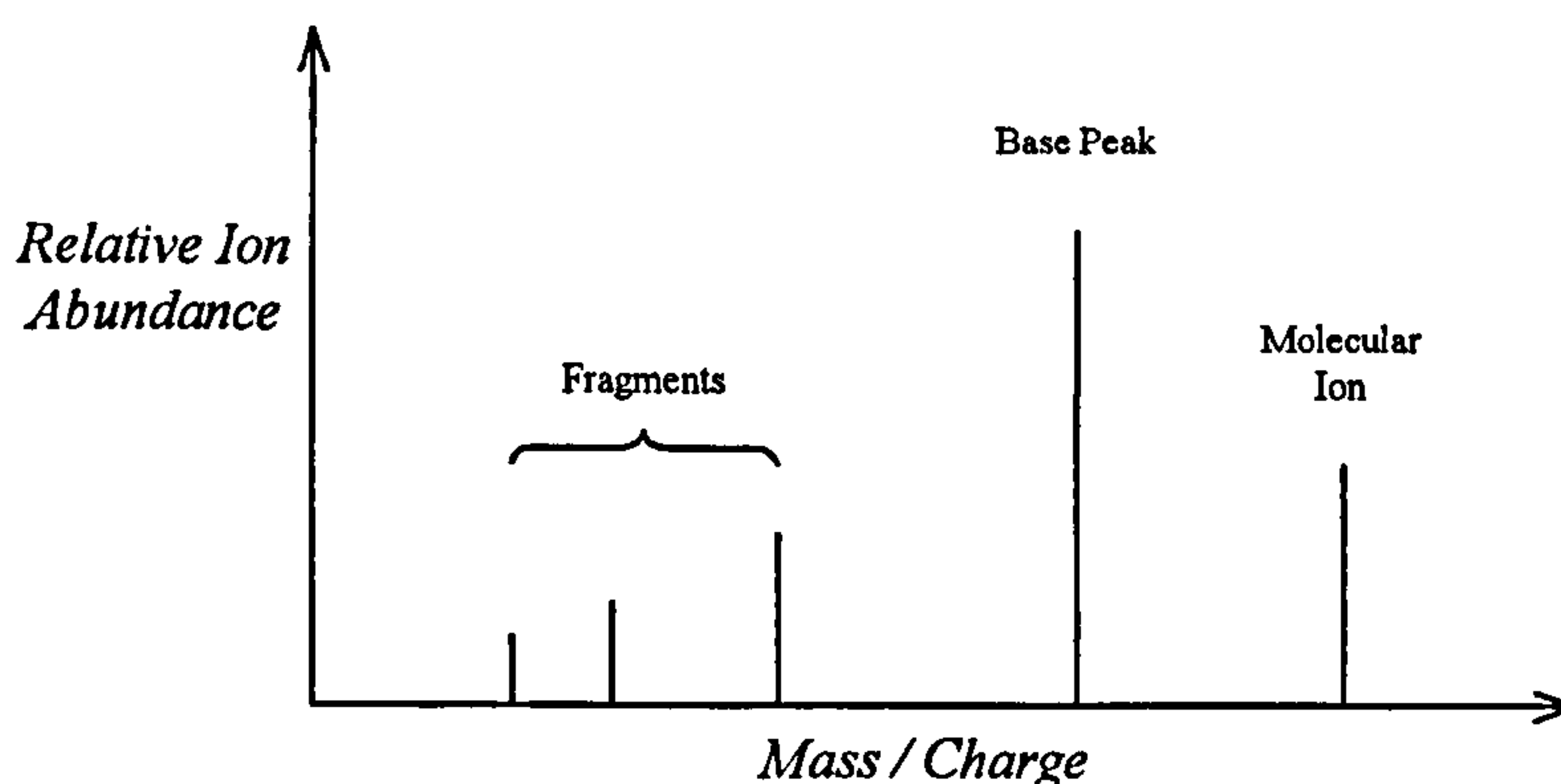


Figure 1b - Simplified diagram of a typical mass spectrum

The mass spectrometry experiment can also involve the deliberate breaking of covalent bonds within the target molecules. This fragmentation can be carried out by a number of routes, and as mentioned earlier some source techniques automatically tend to fragment the analyte in the course of their operation. Through the process of isolating an ion of a particular mass and then fragmenting it, information can be acquired on the structure of the molecule by identifying the fragments and working out how they were joined together¹⁵. For unknown species this process can be used for identification. With known systems, such as co-polymers and complexes, it can potentially be used to explore their macrostructures or architecture. This being how they are oriented in space, which is not often apparent even from their structural formula¹⁶.

So, from mass spectrometry it is possible to achieve molecular mass and structural information, depending on the specific technique used and the requirements of the analysis. For this reason, the technique has found use in a wide range of applications, either exclusively or in conjunction with other methodology^{17,18,19,20}. In the field of

¹⁵ RA Yost, DD Fetterolf, Mass Spec Rev, 2, 1, (1983)

¹⁶ S Koster, MC Duursma, JJ Boon, MWF Nielen, CG de Koster, RMA Heeren, J Mass Spectrom, 35, 739, (2000)

¹⁷ JF Banks, Electrophoresis, 18, 2255, (1997)

¹⁸ WMA Niessen, J Chrom A, 856, 179, (1999)

bioanalysis it has allowed sequencing of complex proteins and also investigation of non-covalent interactions^{21,22}, such as those of enzymes and substrates. Routine analysis of organic molecules has aided modern synthetic routes and product analysis. The high limits of detection can be exploited for trace analysis in complex commercial application, which is of course essential in areas such as the pharmaceutical market^{23,24}.

The field of proteomics²⁵ has seen a steady rise in the use of mass spectrometry in recent years, with automation of protein identification and sequencing²⁶. This has been made possible by advances in instrument design, which has in turn spurred on new developments itself in the application of the technique. Much of the recent development of methodology and the understanding of the underlying principles has been driven by industry. While experimental systems can be useful, it is not until they are sufficiently understood and controlled that they can gain use in the commercial sector.

In the important area of polymer analysis however, mass spectrometry has not made the inroads that would be expected. Routine analysis is still mainly carried out by chromatographic methods, with mass spectrometry used nearly exclusively for structural studies^{27,28,29}. While this area of analysis is an important one in the development of new synthetic materials and complex architectures, it is very notable that routine mass analysis is a far more common procedure. The reasons for this hesitancy are many and much of this is the focus of this work.

¹⁹ MS Montaudou, C Puglisi, F Samperi, G Montaudou, *Rapid Comm Mass Spectrom*, 12, 519, (1998)

²⁰ AL Gusev, *Fresenius J Anal Chem*, 366, 691, (2000)

²¹ MR Larson, P Roepstorff, *Fresenius J Anal Chem*, 366, 677, (2000)

²² DJ Harvey, *Mass Spec Rev*, 18, 349, (1999)

²³ RK Boyd, *Rapid Comm Mass Spectrom*, 7, 257, (1993)

²⁴ JB Landis, DS Aldrich, MA Smith, *Abstr Pap Am Chem Soc*, 209, 92, (1995)

²⁵ J Godovac-Zimmermann, LR Brown, *Mass Spectrom Rev*, 20, 1, (2001)

²⁶ R Aebersold, DR Goodlet, *Chem Rev*, 101, 269, (2001)

²⁷ R Lehrle, DS Sarsons, *Rapid Comm Mass Spectrom*, 9, 91, (1995)

²⁸ PM Lloyd, KG Suddaby, JE Varney, E Scrivener, PJ Derrick, DM Haddleton, *Eur Mass Spectrom*, 1, 293, (1995)

²⁹ HJ Rader, J Spickermann, M Kreyenschmidt, K Mullen, *Macromol Chem Phys*, 197, 3285, (1996)

ii. Historical Perspective

It is useful at this juncture to relate the evolution of mass spectrometry and the path that led to the techniques that are in use today. The modern form of mass spectrometry developed out of the cathode ray experiments of JJ Thomson that lead directly to his parabola mass spectrograph in 1912³⁰. Goldstein had earlier observed in 1886 that at low pressures a high potential applied between two electrodes gave rise to a current³¹. A stream of negatively charged particles was detected passing between the electrodes and were termed “cathode rays”. This experiment was developed further by perforating the cathode and showing that a stream of positive ions were produced in the opposite direction to the negative rays. This new “ion” beam, the name being derived from the Greek for ‘travellers’, could be deflected by both magnetic and electric fields³².

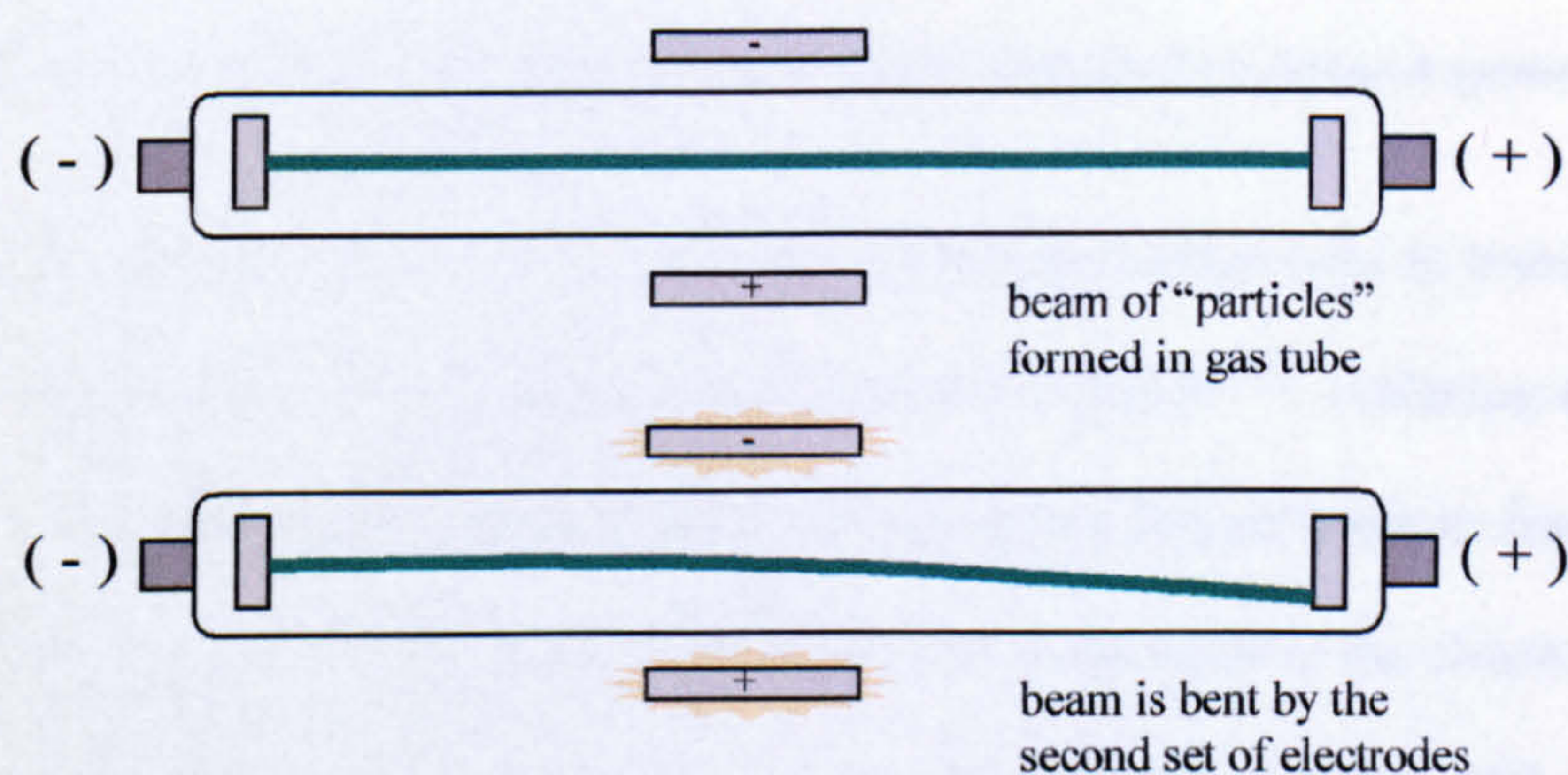


Figure 1c – Simplified explanation of the cathode ray experiment

Aston, following on from Thompson’s work, refined the approach by separating the functions of the magnetic and electric fields through moving the two sections apart in his

³⁰ JJ Thomson, *Rays of Positive Electricity and their Application to Chemical Analysis*, Longmans Green, London, (1913)

³¹ E Goldstein, *Berl Ber*, 39, 691, (1886)

³² W Wein, *Verhanal Phys Ges*, 17, (1898)

instrument design³³. The electric sector dispersed the collimated beam of ions according to their kinetic energy, so that a slit could be used to filter off a homogenous portion of the total population. This could then be passed through a magnetic sector and so dispersed according to their momentum. It is this principle that lead directly to the double-focusing system of Nier and Johnson, which is shown schematically below³⁴.

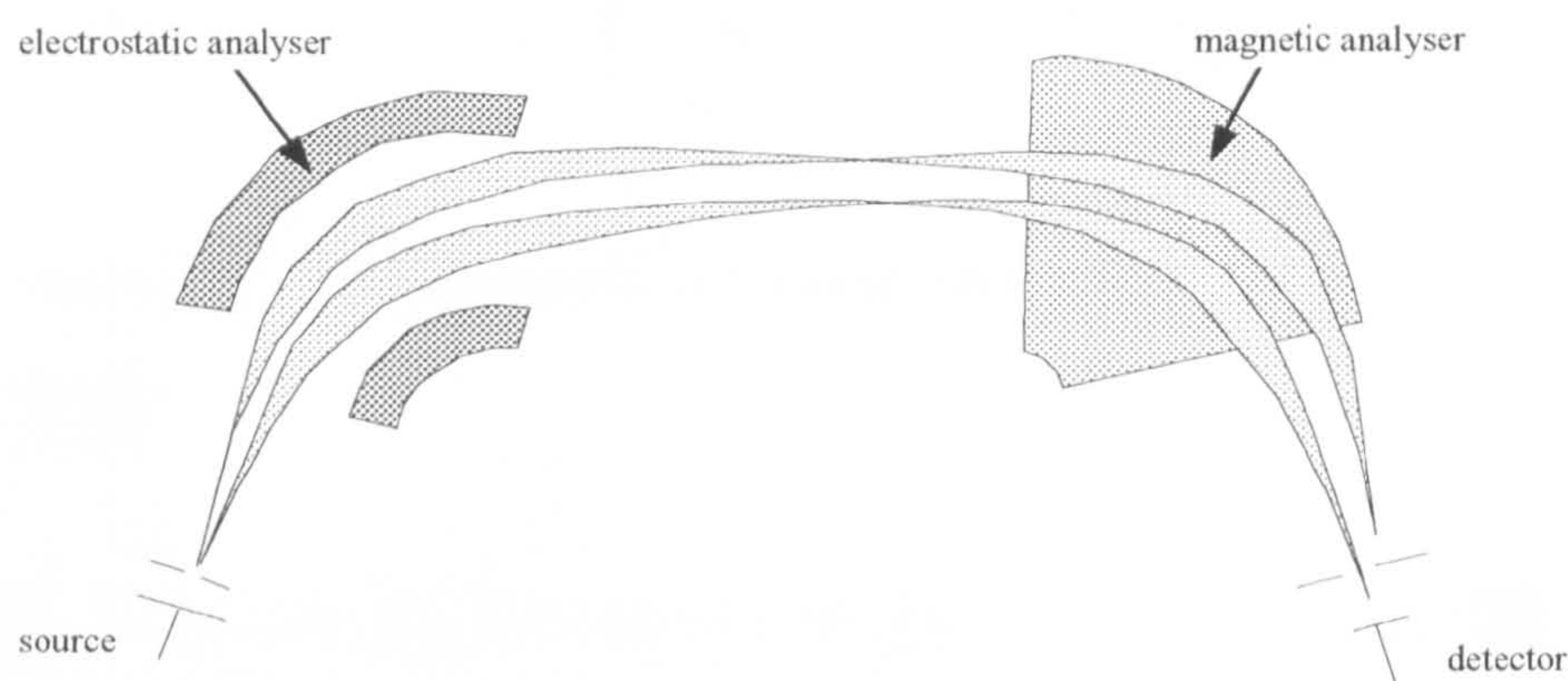


Figure 1d - Double focusing instrument design using the Nier-Johnson geometry

At the time of Nier and Johnson's work, the dominant method used to transport the sample into the state of a gas-phase ion was electron impact^{35,36}, replacing the discharge tubes of the earlier physics experiments. Using electron impact tends to fragment molecules easily due to the high energies involved, unless that is the electron acceleration voltage is kept just slight above the ionisation potential of the analyte. Other source techniques developed in tandem with improvements in the design of the spectrometer, such as chemical ionisation^{37,38,39} (CI) and field desorption^{40,41} (FD) in the latter half of

³³ FW Aston, Philos Mag, 38, 707, (1919)

³⁴ AO Nier, J Am Soc Mass Spectrom, 2, 447, (1991)

³⁵ W Bleakney, Phys Rev, 34, 157, (1929)

³⁶ AO Nier, Rev Sci Instrument, 18, 415, (1947)

³⁷ MSB Munson, FH Field, J Am Chem Soc, 88, 2681, (1966)

³⁸ AG Harrison, *Chemical Ionisation Mass Spectrometry*, CRC Press, Boca Raton, Florida, (1983)

³⁹ M Vincenti, E Pelizzetti, A Guarini, S Constanzi, Anal Chem, 64, 1879, (1993)

⁴⁰ HD Beckey, *Principles of Field Ionisation and Field Desorption in Mass Spectrometry*, Pergamon Press, Oxford, (1977)

⁴¹ H-R Shulten, RP Lattimer, Anal Chem, 61, 1201A, (1989)

instrument design³³. The electric sector dispersed the collimated beam of ions according to their kinetic energy, so that a slit could be used to filter off a homogenous portion of the total population. This could then be passed through a magnetic sector and so dispersed according to their momentum. It is this principle that lead directly to the double-focusing system of Nier and Johnson, which is shown schematically below³⁴.

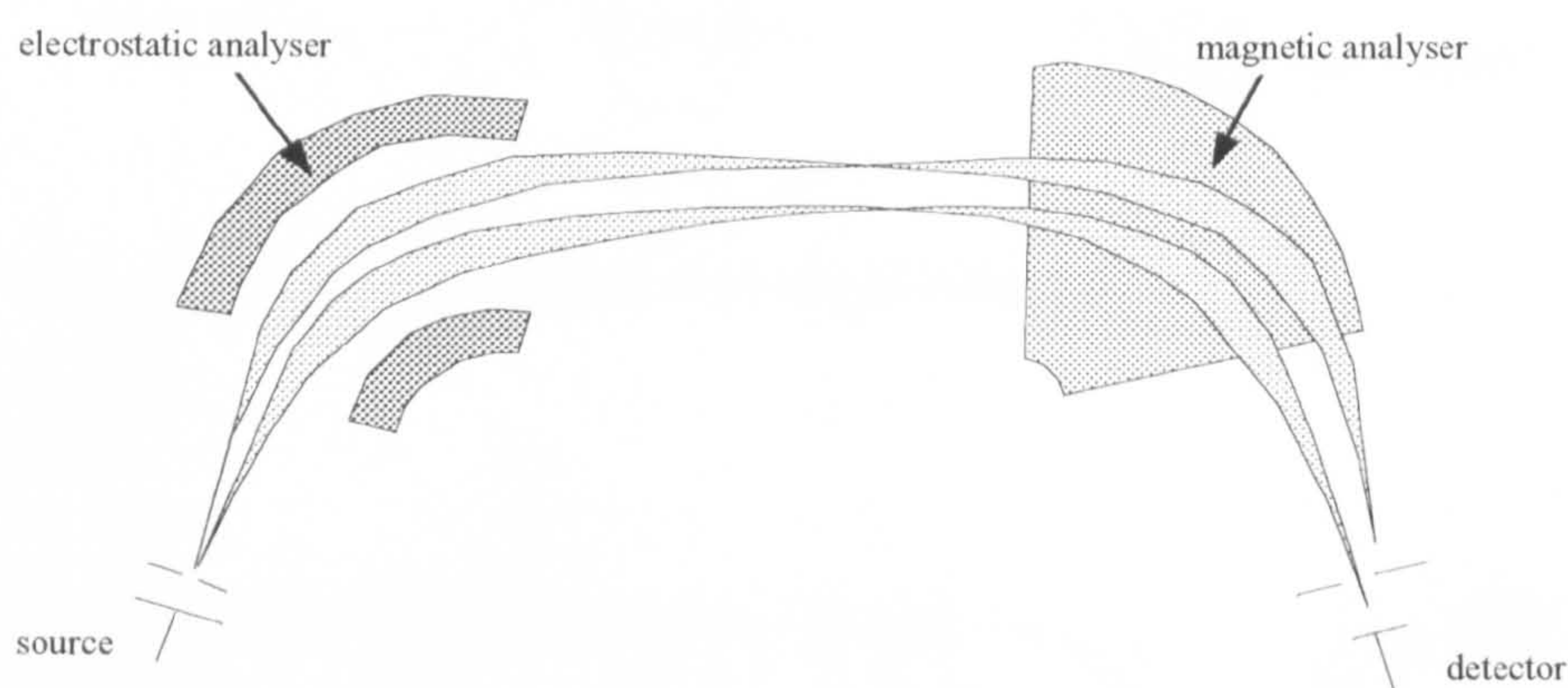


Figure 1d - Double focusing instrument design using the Nier-Johnson geometry

At the time of Nier and Johnson's work, the dominant method used to transport the sample into the state of a gas-phase ion was electron impact^{35,36}, replacing the discharge tubes of the earlier physics experiments. Using electron impact tends to fragment molecules easily due to the high energies involved, unless that is the electron acceleration voltage is kept just slight above the ionisation potential of the analyte. Other source techniques developed in tandem with improvements in the design of the spectrometer, such as chemical ionisation^{37,38,39} (CI) and field desorption^{40,41} (FD) in the latter half of

³³ FW Aston, Philos Mag, 38, 707, (1919)

³⁴ AO Nier, J Am Soc Mass Spectrom, 2, 447, (1991)

³⁵ W Bleakney, Phys Rev, 34, 157, (1929)

³⁶ AO Nier, Rev Sci Instrument, 18, 415, (1947)

³⁷ MSB Munson, FH Field, J Am Chem Soc, 88, 2681, (1966)

³⁸ AG Harrison, *Chemical Ionisation Mass Spectrometry*, CRC Press, Boca Raton, Florida, (1983)

³⁹ M Vincenti, E Pelizzetti, A Guarini, S Constanzi, Anal Chem, 64, 1879, (1993)

⁴⁰ HD Beckey, *Principles of Field Ionisation and Field Desorption in Mass Spectrometry*, Pergamon Press, Oxford, (1977)

⁴¹ H-R Shulten, RP Lattimer, Anal Chem, 61, 1201A, (1989)

the 1960's. However, most of these have lessened considerably in use over time in favour of the most recent developments of “soft” ionisation.

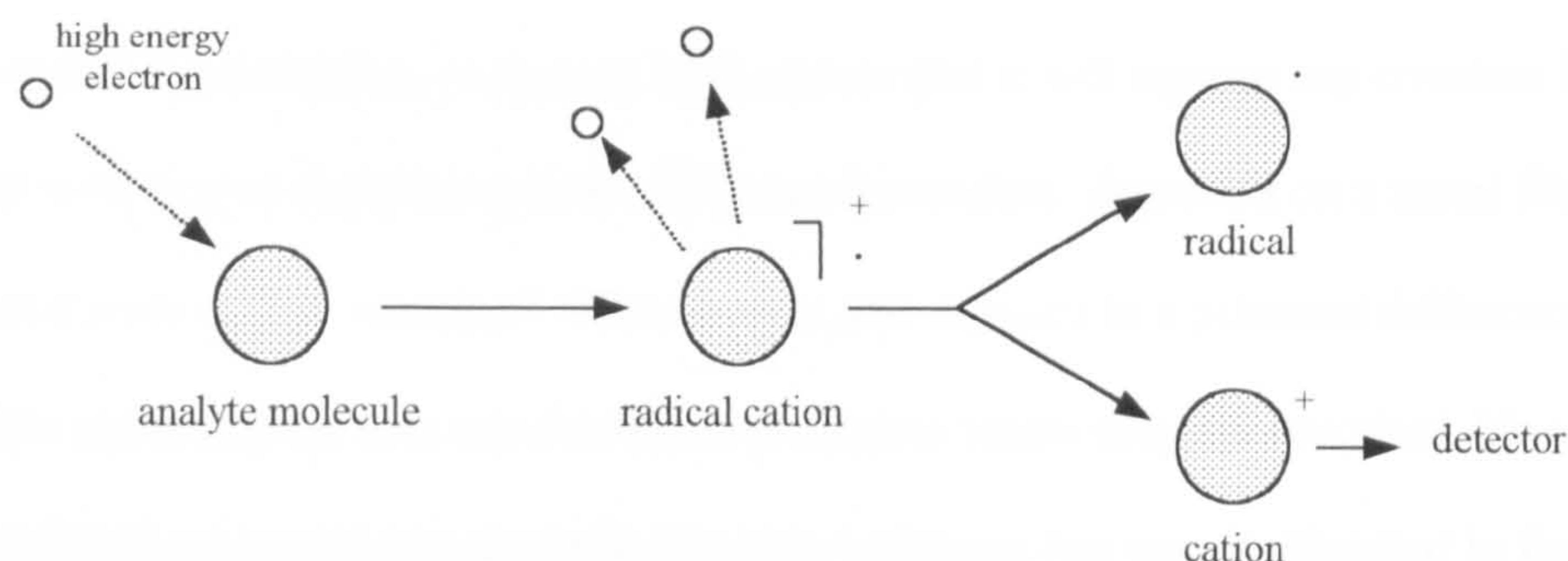


Figure 1e - Formation of cations by electron impact ionisation

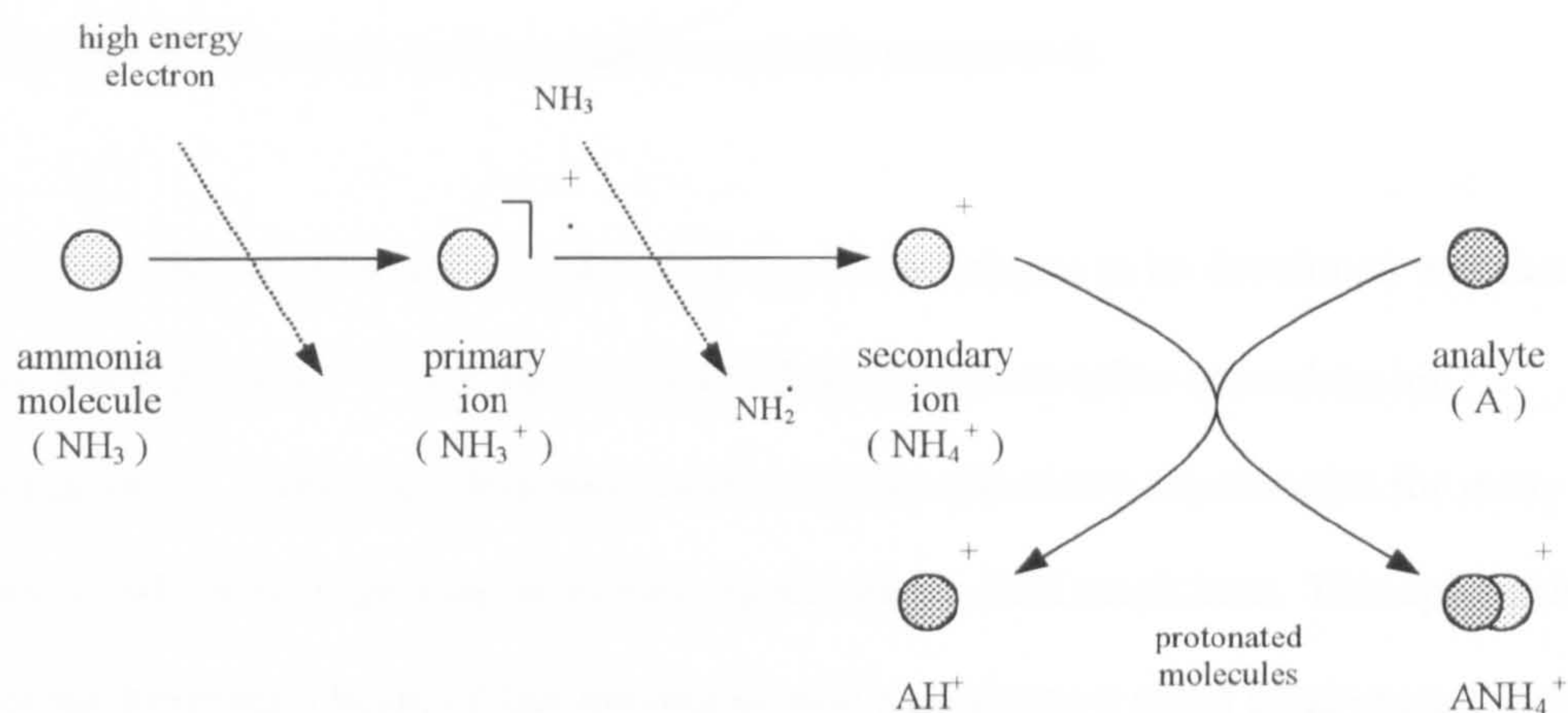


Figure 1f - Formation of cations by chemical ionisation using ammonia

Chemical ionisation works by the collision of the neutral analyte molecule with another ion formed from a reagent gas, such as methane or ammonia. As the reagent gas is dominant in pressure over the analyte, an electron entering the source will preferentially ionise it over the analyte. The reagent ion then collides with other molecules forming an ionised plasma by a series of ion-molecular reactions. Further reactions can lead to proton transfer to the analyte, hydride abstractions or even electron capture of slower thermal electrons. This leads to the formation of positive and negative analyte ions in the source region that can be analysed by the instrument. In comparison, field ionisation works by holding a sharp point or edge at a high potential. An atom nearing this edge experiences a

strong potential gradient and can lose its outermost electron to form a positive ion, but since the edge is also positively charged the newly formed ion is repelled into the analyser region. The advantage of this technique is that the ion gains little excess energy above that for ionisation, so there is little chance that it will rupture any covalent bonds. What is termed as field desorption (FD) has the analyte deposited on a metal filament covered with carbon “needles”. When heated and exposed to a potential difference, the sample melts and the ions move towards the points where they are desorbed. However, the difficulty in producing electrodes for this technique has seen it relegated in face of other potentially easier “soft” ionisation techniques but it remains a useful method for the ionisation of high-mass and especially non-polar compounds.

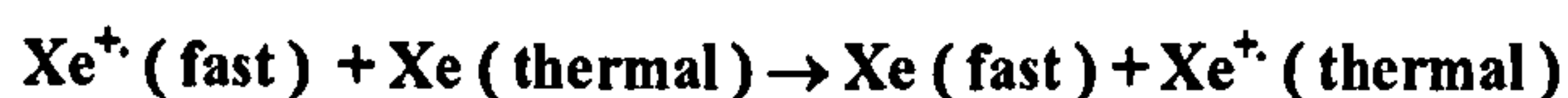
One of the first of what are considered the “soft” techniques to be developed was fast atom bombardment^{42,43,44} (FAB), which followed on from other secondary ion techniques^{45,46}. Although it had been used in surface chemistry experiments for many years, it did not find application in mass spectrometry until much later. This approach involves directing a beam of fast moving neutral atoms onto a metal plate coated with the sample. It is found that much of the kinetic energy of the beam is transferred into the analyte on impact. This energy can dissipate in a number of ways, some of which lead to the ionisation of the molecule and so production of a population of analyte ions for analysis. The beam of neutrals is usually an inert gas such as xenon or argon, produced by colliding a fast moving stream of accelerated ions of the gas into a chamber containing more gas in the ground state. Collisions here lead to charge exchange and the formation of fast moving neutrals that can be separated from the now thermal ions by means of a deflection plate.

⁴² M Barber, RS Bardoli, RD Sedgewick, AH Tyler, J Chem Soc Chem Commun, 325, (1981)

⁴³ M Barber, RS Bardoli, DV Garner, DB Gordon, RD Sedgewick, LW Tetler, AN Tyler, Biochem J, 197, 401, (1981)

⁴⁴ G Montaudo, E Scamporrino, D Vitalini, Macromolecules, 24, 376, (1991)

⁴⁵ IV Bletsos, DM Hercules, JH Magil, D van Leyen, E Niehuis, A Benninghoven, Anal Chem, 60, 938, (1988)



These neutrals then impact on the sample, which is usually dissolved in a relatively involatile matrix substance such as glycerol. Since both positive and negative ions will be produced by this process, holding the metal probe at a potential leads to only one type of ion being repelled and so directed into the analyser region of the instrument. Although structural fragments result from this process, FAB does not usually produce the molecular ion⁴⁷. One advantage over techniques such as FD is that the ion stream lasts for a reasonable length of time, allowing good signal collection or facilitating so-called MS / MS experiments⁴⁸. That is when a particular m/z is isolated, fragmented and then analysed again so as to give structural information on that single species or parent fragment. As this name suggests, this is the equivalent of performing mass spectrometry on the sample multiple times in series.

iii. Ionisation Techniques

As mentioned in the introduction, the source is responsible for transferring the sample, be it a solid or liquid, into the gas-phase ion. The ionisation part of this can be accomplished by electron capture / loss, proton attachment / detachment or the attachment of a metal cation. In the case of the two sources used in most modern mass spectrometry systems for life science and polymers, and those under study in this work, it is the latter two routes that are significant. These techniques are electrospray ionisation^{49,50,51,52} (ESI) and

⁴⁶ YL Kim, DM Hercules, *Macromolecules*, 27, 7855, (1994)

⁴⁷ MW Senko, SC Bue, FW McLafferty, *J Am Soc Mass Spectrom*, 6, 229, (1995)

⁴⁸ FW McLafferty, IJ Amster, MA Baldwin, MP Barbalas, MT Cheng, SL Cohen, PO Danis, GH Kruppa, CJ Proctor, F Turecek, *Int J Mass Spectrom Ion Proc*, 45, 323, (1982)

⁴⁹ M Yamashita, JB Fenn, *J Chem Phys*, 80, 4451, (1984)

⁵⁰ MG Ikononou, AT Blades, P Kebarle, *Anal Chem*, 62, 957, (1990)

matrix-assisted laser desorption / ionisation^{53,54,55} (MALDI). These approaches differ greatly, the first being a continuous technique that produces a stream of ions from an analyte solution, while the second gives a pulse of ions from a laser shot onto a solid sample. This diversity in sample type and the nature of the ions produced allow these two techniques alone to cover most of the range of applications for commercial analysis.

a. Electrospray Ionisation

Fenn and co-workers are credited with first developing electrospray ionisation⁵⁶, although Dole had recognised the potential earlier when he was working with ion-drift spectrometers⁵⁷. In essence, an analyte solution is passed through a capillary held at a high potential. The electric field has the effect of turning the emerging liquid into a fine spray of charged droplets^{58,59}. A nebulising gas is sometimes used down the outside of the capillary to assist the droplet formation⁶⁰. A counter-directional flow of heated gas can also be used to facilitate solvent evaporation or the spray can equally be directed into a second capillary heated by an electric coil. The exact mechanism of transfer of the analyte droplets to gas-phase ions is the subject of much debate. There are two basic theories that differ only in their last stages, however both of these models suppose that the analyte picks up charge from the droplet while a small body of other work suggests a role for ions pre-formed in the solution phase^{61,62}. The two theories of ion formation are the charge

⁵¹ RD Smith, JA Loo, CG Edmons, CJ Barinaga, HR Udseth, Anal Chem, 62, 882, (1990)

⁵² M Mann, Ord Mass Spectrom, 25, 575, (1990)

⁵³ J Gross, Trends in Anal Chem, 17, 470, (1998)

⁵⁴ KJ Wu, RW Odom, Anal Chem, 70, 465A, (1998)

⁵⁵ DJ Harvey, Mass Spec Rev, 18, 349, (1999)

⁵⁶ M Yamashita, JB Fenn, J Chem Phys, 80, 4451, (1984)

⁵⁷ J Gieniec, LL Mack, K Nakamae, C Gupta, V Kumar, M Dole, Biomed Mass Spectrom, 11, 259, (1984)

⁵⁸ P Kobarle, L Tang, Anal Chem, 65, 972A, (1993)

⁵⁹ A Gomez, K Tang, Phys Fluids, 6, 404, (1994)

⁶⁰ AP Bruins, TR Covey, JD Henion, Anal Chem, 59, 2642, (1987)

⁶¹ H Ehring, C Costa, PA Demirev, BUR Sundqvist, Rapid Comm Mass Spectrom, 10, 821, (1996)

⁶² YF Zhu, KL Lee, K Tang, SL Allman, NI Taranencko, CH Chen, Rapid Comm Mass Spectrom, 9, 1315, (1995)

residue model (CRM) proposed by Dole⁶³ and extended by Röhlgen^{64,65}, and the ion evaporation model (IEM) of Iribarne and Thomson^{66,67}.

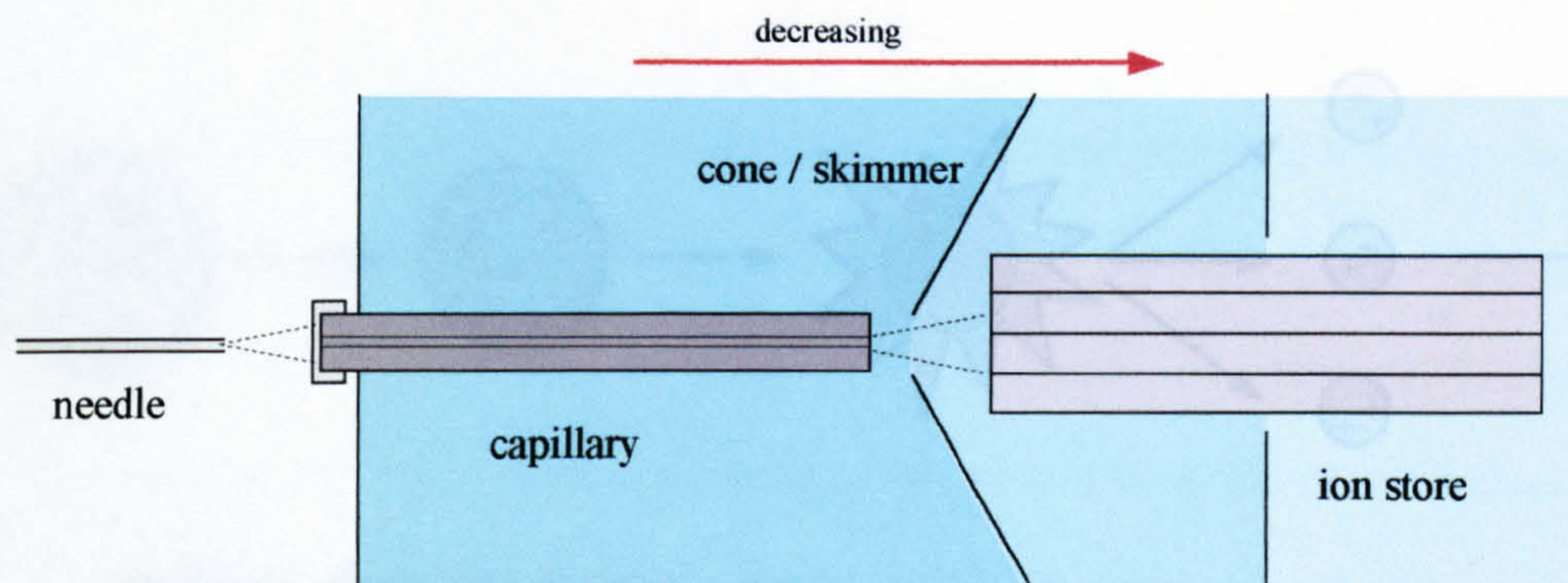


Figure 1g - Simplified schematic of a generic electrospray source

At the end of the spraying capillary, assuming a positive potential, the positive ions in solution accumulate at the surface which is so drawn out in the direction of the field as to form a 'Taylor cone'^{68,69}. With the high field imposed, the tip is pulled finer and finer so that droplets are formed where the electrostatic forces are able to overcome the surface tension. This part of the process is most certain, with visual studies made of the Taylor cone formation under various conditions. Both of the desorption methods then proceed with the droplet gradually shrinking due to solvent evaporation as they move along the pressure gradient of the source area. This evaporation leads to a decrease in the diameter of the droplet and so an increase in charge density within. At below the point known as the 'Rayleigh limit'⁷⁰, the magnitude of the charge is sufficient to overcome the surface tension holding the droplet together, and so fission occurs leading to two or more smaller droplets. These so-called 'Coulomb explosions' together with gradual solvent evaporation

⁶³ M Dole, LL Mack, RL Hines, RC Mobley, LD Ferguson, MB Alice, J Chem Phys, 49, 2240, (1968)

⁶⁴ FW Röhlgen, E Bramer-Weger, Lbütfering, J Phys, 48, C6253, (1987)

⁶⁵ G Schmelzensen-Redeker, L Bütfering, FW Röhlgen, Int J Mass Spectrom Ion Proc, 128, 123, (1993)

⁶⁶ JV Iribarne, BA Thomson, J Chem Phys, 64, 2287, (1976)

⁶⁷ JV Iribarne, BA Thomson, J Chem Phys, 71, 4451, (1979)

⁶⁸ MS Wilm, M Mann, Int J Mass Spectrom Ion Proc, 136, 167, (1994)

⁶⁹ T Dulcks, R Juraschek, J Aerosol Sci, 30, 927, (1999)

⁷⁰ Lord Rayleigh, Philos Mag, 14, 184, (1882)

lead to increasingly smaller and smaller droplets^{71,72}. It is at this point that the two models diverge.

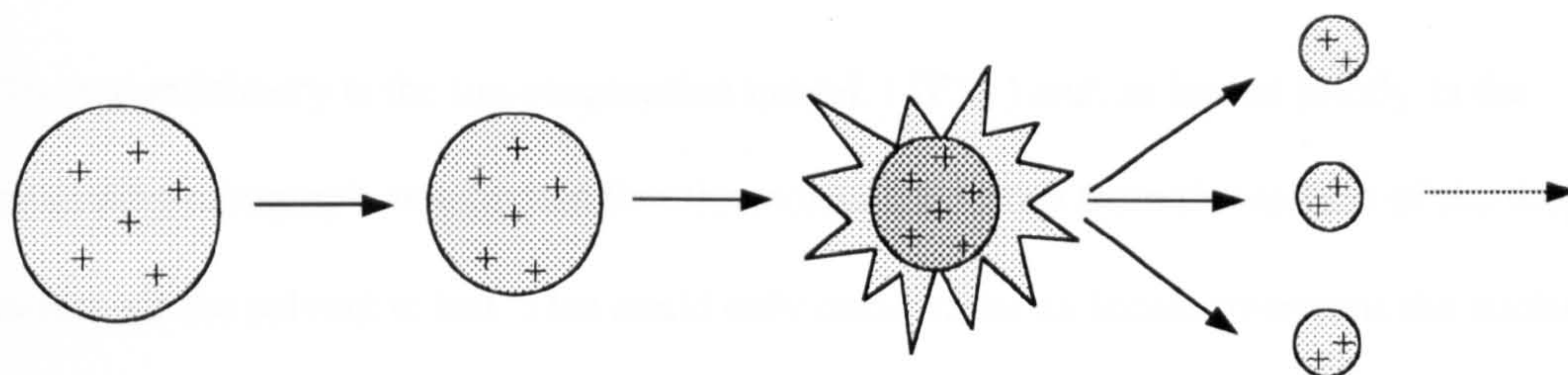


Figure 1h - Showing the shrinking and fission process of ion formation

The charge residue model (CRM) theory suggests that the shrinking process continues until each droplet only contains one analyte molecule. The charge that molecule takes into the gas phase is then the residual charge left in the droplet at the stage when all the solvent has been removed. This model has its strengths for large analyte molecules where the field desorption of the IEM model discussed next is most uncertain. In the case of large proteins which can form a spherical shape⁷³, field desorption from a droplet is perhaps less likely than charge residue, which Fernandez de la Mora et al have also suggested goes more towards explaining the observed range of charge states for these species^{74,75}. However, for polymers which are generally considered to be extended rod arrangements, then both models seem to have shortcomings. The surface charge would appear by Fenn's experiments to be too low to allow field desorption⁷⁶, but for charge residue the droplet must be considered to deform along the axis of the molecule. If this is not accounted for then the charge that would result from a spherical droplet with a

⁷¹ J Fernandez de la Mora, IG Loscertales, J Fluid Mech, 243, 561, (1994)

⁷² A Gomez, K Tang, Phys Fluids, 6, 404, (1994)

⁷³ M Gamero-Castãno, Thesis, Yale University, (1999)

⁷⁴ IG Loscertales, J Fernandez de la Mora, J Chem Phys, 103, 5041, (1995)

⁷⁵ P Kebarle, Y Ho, *Electrospray Ionisation Mass Spectrometry*, Wiley, New York, (1997)

⁷⁶ JB Fenn, J Rose, CK Meng, J Am Soc Mass Spectrom, 8, 1147, (1997)

diameter equivalent to the length of the polymer chain, would it has been argued give a much higher value than that observed in practice⁷⁷.

The second theory is the ion evaporation model (IEM) and, as hinted briefly in the preceding paragraph, it supposes that the molecules desorb from the surface of the droplet before all the solvent is lost. This could only occur if the molecule overcame the surface tension and also any hydrogen bonding or other interactions with the solvent molecules. This is now generally thought to be the predominant mode of operation for lower-mass species, which can be visualised as existing on the surface of the droplet. Since, by an extension of Coloumb's law, it would be suggested that the charges in the droplet move to be equidistant over the surface of the sphere, the charge density is very important. The analyte molecule will be in proximity to a number of charged sites dependent on their density and the hydrodynamic volume of the molecule. It is these charges that it is said to carry into the gas phase on field desorption. Experimental work has used this assumption to try and gain a measure of the surface charge density by observing charge numbers for various analyte molecules. Using a series of simple, and more importantly generally linear, poly(ethyleneglycol) molecules, Fenn and co-workers found the smallest mer unit for each charge state and so arrived at an estimate of charge density on the surface of the droplet in the region of 1.46 to 2.66 V/nm depending on the solvent used⁷⁸. These figures vary slightly from those of Fernandez de la Mora et al⁷⁹, who had derived values of 1.00 to 1.76 V/nm by looking at fully evaporated 'droplets' and arguing that once the ion desorption process starts the field on the droplet is maintained at a constant value.

⁷⁷ T Nohmi, JB Fenn, J Am Chem Soc, 114, 3241, (1992)

⁷⁸ JB Fenn, J Rose, CK Meng, J Am Soc Mass Spectrom, 8, 1147, (1997)

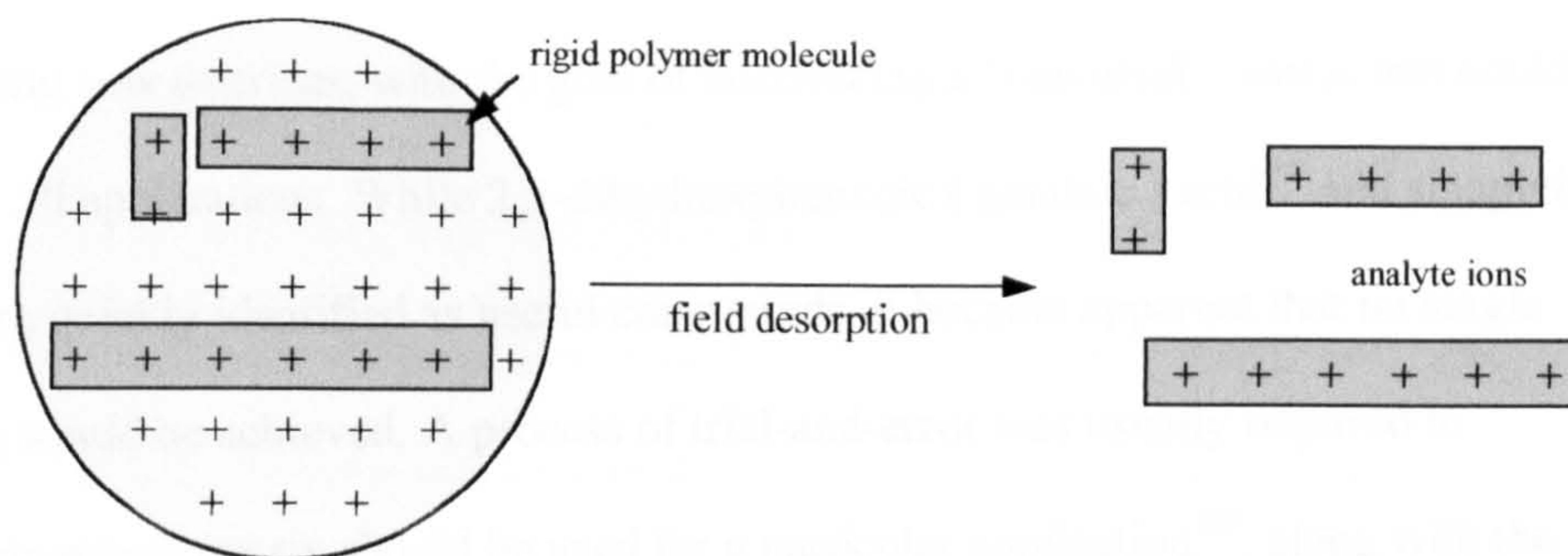


Figure 1i - Showing the basis for the acquired charge in the IEM theory

Experiments used to probe both of these routes have usually taken assumptions based on the two theories and so have led to conflicting arguments in some cases⁸⁰. It is generally accepted now however that IEM is the most probable mechanism for small molecules and linear polymeric systems, the CRM route tending to be preferred in particular for globular proteins and very large analyte molecules. That said, there is also a small body of work suggesting the influence of pre-formed ion on the process^{81,82}. That is, analyte molecules becoming associated with a charged species while in the condensed phase⁸³. In most cases, however, the gas-phase system bears only a token resemblance to the condensed. For instance, protonated proteins have been observed from strongly basic systems where no protonated species would be normally found⁸⁴. The only associations that have been consistently observed to be carried through to the gas phase are those such as the non-covalent bonding of small peptides to receptor proteins that would be very unlikely to arise from gas-phase processes. Pre-formed ions are also even more unlikely for polymeric systems, which do not on the whole tend to have obvious centres for ion attachment in the solution phase.

⁷⁹ J Fernandez de la Mora, IG Locertales, J Fluid Mech, 243, 561, (1994)

⁸⁰ V Katta, AL Rockwood, ML Vestal, Int J Mass Spectrom Ion Proc, 103, 129, (1991)

⁸¹ T Blades, P Jayaweera, MG Ikononou, P Kebarle, J Chem Phys, 92, 5900, (1990)

⁸² M Pechke, AT Blades, P Kebarle, Int J Mass Spectrom, 185 / 186 / 187, 685, (1999)

⁸³ P Kebarle, L Tang, Anal Chem, 65, 972, (1993)

⁸⁴ MA Kelly, MM Vesting, CC Fenselau, PB Smith, Org Mass Spectrom, 27, 1143, (1992)

The early experiments in MALDI were mainly concerned with discovering and developing new matrices, with the goal of uncovering a “universal” matrix that could be used for all applications. While 2,5-dihydroxybenzoic (gentisic) acid¹⁰⁵ and sinapinic acid were quickly identified as useful compounds, it became apparent that no single solution would be achieved. A process of trial-and-error was usually required to determine which matrix should be used for a particular application¹⁰⁶, along with the solvent system and the ratio of matrix to analyte, which can vary from 100:1 up to as much as 50,000:1. These ratios show that the vast bulk of the crystal structure will be composed of matrix compound. The fact that the matrix ion signal is not such an order of magnitude higher than most analytes is an effect known as ‘matrix suppression’ and is invaluable to the success of the technique¹⁰⁷.

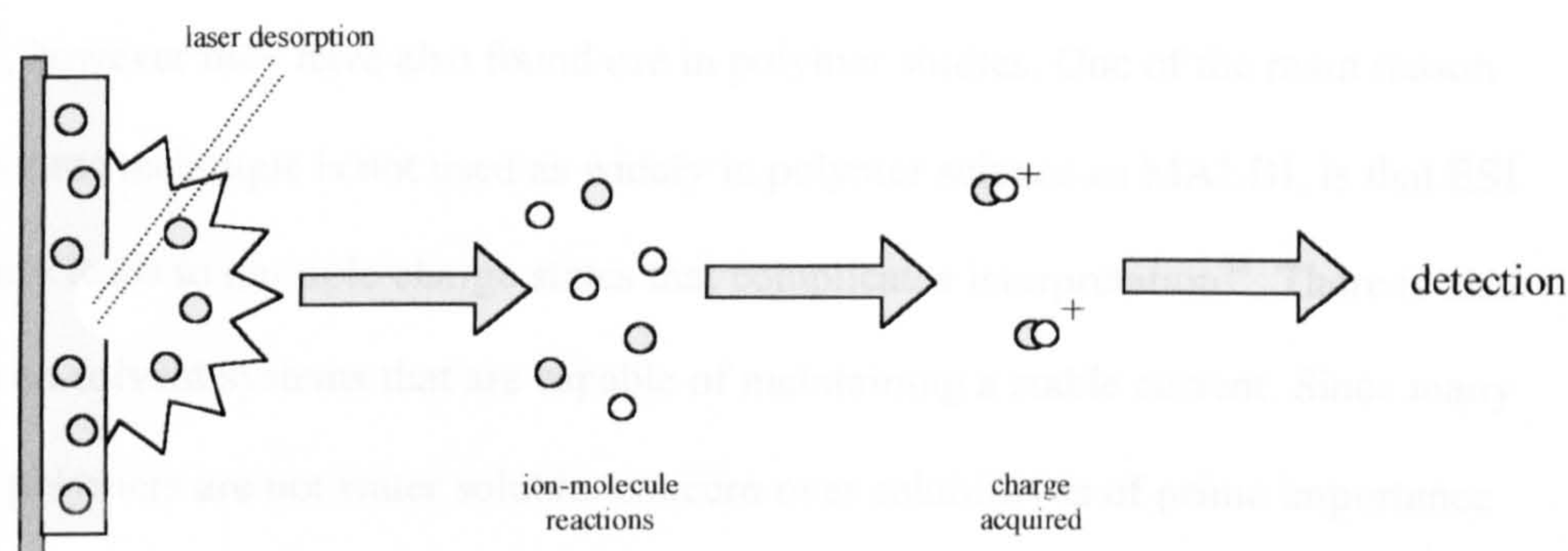


Figure 1j - Schematic of the basic process of ion formation by MALDI

An exact mechanism of the MALDI process is still not agreed^{108,109}. A large number of experiments having been performed in attempts to understand the process^{110,111,112}, for instance by separating the desorption and ionisation steps through having the co-

¹⁰⁴ PO Danis, DE Karr, YS Xiong, KG Owens, Rapid Comm Mass Spectrom, 10, 862, (1996)

¹⁰⁵ RC Beavis, BT Chait, Rapid Comm Mass Spectrom, 3, 233, (1989)

¹⁰⁶ MC Fitzgerald, GR Parr, LM Smith, Anal Chem, 65, 3204, (1993)

¹⁰⁷ R Knochenmuss, F Dubois, MJ Dale, R Zenobi, Rapid Comm Mass Spectrom, 10, 871, (1996)

¹⁰⁸ R Zenobi, R Knochenmuss, Mass Spec Reviews, 17, 337, (1998)

¹⁰⁹ P-C Liao, J Allison, J Mass Spectrom, 30, 408, (1995)

¹¹⁰ M Karas, D Bachmann, F Hillenkamp, Anal Chem, 57, 2935, (1985)

¹¹¹ H Ehring, M Karas, F Hillenkamp, Org Mass Spectrom, 27, 427, (1992)

¹¹² PC Liao, J Allison, J Mass Spectrom, 30, 408, (1995)

A variation on the theme of electrospray was developed by Wilm and Mann⁸⁵, and is now referred to as ‘nanospray’⁸⁶. This operates at low nl min^{-1} flow rates leading to droplets with diameters in the nanometer range instead of the μm of standard electrospray. In place of a pumped source, this approach uses a metal-plated glass needle that acts as its own reservoir with the spraying process itself providing the impetus for the flow. The efficiency of the system in the production of ion signal has been shown to be approximately two orders of magnitude greater and the production of clusters is lessened. For this reason, nanospray is more tolerant of systems containing salts, such as buffer systems, and has found use in the characterisation of proteins at the sub-picomole level.

Both electrospray and nanospray are used extensively in the analysis of biological samples⁸⁷, however they have also found use in polymer studies. One of the main reason that this source technique is not used as widely in polymer science as MALDI, is that ESI by its nature leads to multiple charge states that complicates interpretation⁸⁸. There is also a reliance on solvent systems that are capable of maintaining a stable current. Since many industrial polymers are not water soluble, concern over solubility is of prime importance and has ruled out or made very difficult the analysis of certain polymer types. The multiple charging of polymers is an interesting phenomenon in its own right which has undergone much study over recent years. The number of charges a polymer molecule acquires is based on its length, longer polymers have higher charge states so bringing all results down into a lower and similar mass / charge range. The fact that all polymer systems are “reduced” down to this relatively low range of m / z values is of great advantage. It allows analysis of very large polymers that would be impossible or poorly resolved, depending on the separation and detection techniques, if they had been only

⁸⁵ MS Wilm, M Mann, *Int J Mass Spectrom Ion Proc*, 136, 167, (1994)

⁸⁶ M Karas, U Bahr, T Dulcks, *Fresenius J Anal Chem*, 336, 669, (2000)

⁸⁷ M Mann, MS Wilm, *Trends in Biochemical Sciences*, 20, 219, (1995)

⁸⁸ CN McEwan, WJ Simonsick, BS Larsen, K Ute, K Hatada, *J Am Soc Mass Spectrom*, 6, 906, (1995)

singly charged. Unlike proteins, the charges in polymeric systems are more directly linked to size and do not appear to be related as strongly to specific and identifiable charge sites. Work looking at the conformation of poly(ethyleneglycol) molecules using mass spectrometry combined with an ion chromatographic technique, suggested that the polymer chains wrap around the relatively large sodium ions in a roughly spiral arrangement so that the charges interact with the electron-rich oxygen centres⁸⁹. Also, in difference to biological systems, polymers do not in general gain charge by protonation but rather by the attachment of small metal cations. The most ubiquitous cation is sodium, which is present in nearly all solutions and samples. However, the systems can be doped with other salts to promote attachment. There is interest in looking at the result of the favouring of different salts and their effect on the resultant mass spectrum as with other parts of the sample preparation.

b. Matrix-assisted Laser Desorption / Ionisation

Matrix-assisted laser desorption / ionisation (MALDI) can be considered as a progression from direct laser desorption^{90,91}. It was first described by Tanaka et al in 1988⁹², who had observed that the addition of an absorbing species, known as the matrix, made possible the acquisition of spectra from high mass molecules. In their experiment, the analyte was mixed with finely divided cobalt and suspended in glycerol. In this case, an N₂ laser was used to give a beam within the maximum absorbance region of the cobalt. This preparation was used to measure glycol-based polymers with masses in the order of 25-100 kDa, without significant fragmentation but unfortunately with considerable broadening of the peak widths. It was soon found that small aromatic molecules could

⁸⁹ J Gidden, T Wittenbach, AT Jackson, JH Scrivens, MT Bowers, J Am Chem Soc, 122, 4692, (2000)

⁹⁰ LM Nuwaysir, CL Wilkins, WJ Simonsick Jnr, J Am Soc Mass Spectrom, 1, 66, (1996)

⁹¹ CW Ross, WJ Simonsick Jnr, Int J Mass Spectrom Ion Proc, 157, 379, (1996)

⁹² K Tanaka, W Hiroaki, Y Ido, S Akita, Y Yoshida, T Yoshida, Rapid Comm Mass Spectrom, 2, 151, (1988)

perform a similar function to the cobalt, leading to the development of a series of matrix systems^{93,94}. By 1992, the use of sinapinic acid as a matrix had been established as a common method for the analysis of biomolecules^{95,96,97}. Danis et al applied this procedure with success to a number of water-soluble synthetic polymers, such as poly(acrylic acid)⁹⁸.

Karas and Hillenkamp carried out the first systematic study of synthetic polymers by the MALDI technique⁹⁹. These experiments compared the responses of poly(methylmethacrylate), poly(ethyleneglycol) and poly(propyleneglycol) over different mass ranges using 2,5-dihydroxybenzoic acid as the matrix. Polymers up to 40 kDa were successfully analysed, although often requiring the addition of alkali salts to aid cationisation. Unlike the poly(acrylic acid), these polymers are not particularly water-soluble and so raise complications in sample preparation. Danis proposed indoleacrylic acid as a matrix for polymer systems that require organic solvents to avoid precipitation¹⁰⁰. The next major step in the analysis of polymers, was the successful detection of a non-polar system. Polystyrene was the first such polymer analysed, in the initial experiment using a liquid 2-nitrophenyl octyl ether matrix and silver trifluoroacetate as a source of cations¹⁰¹. While the matrix requirements would later be simplified, silver has remained as a key feature of the analysis of such polymer systems^{102,103,104}.

⁹³ M Karas, D Bachmann, U Bahr, F Hillenkamp, *Int J Mass Spectrom Ion Proc*, 78, 53, (1987)

⁹⁴ F Hillenkamp, M Karas, RC Beavis, BT Chait, *Anal Chem*, 63, 1193, (1991)

⁹⁵ F Hillenkamp, M Karas, A Ingeldoh, B Stahl, *Biological Mass Spectrometry*, Elsevier, Amsterdam, 49, (1990)

⁹⁶ M Karas, F Hillenkamp, *Anal Chem*, 60, 2229, (1988)

⁹⁷ RC Beavis, BT Chait, *Rapid Comm Mass Spectrom*, 3, 233, (1989)

⁹⁸ PO Danis, DE Karr, F Mayer, A Holle, CH Watson, *Org Mass Spectrom*, 27, 843, (1992)

⁹⁹ U Bahr, A Deppe, M Karas, F Hillenkamp, *Anal Chem*, 64, 2866, (1992)

¹⁰⁰ PO Danis, DE Karr, *Org Mass Spectrom*, 28, 923, (1993)

¹⁰¹ JW Leon, MJ Frechet, *Polymer Bulletin*, 35, 449, (1995)

¹⁰² H Rashidzadeh, BC Guo, *J Am Soc Mass Spectrom*, 9, 724, (1998)

¹⁰³ AM Belu, JM DeSimone, RW Linton, GW Lange, RM Friedman, *J Am Soc Mass Spectrom*, 7, 11, (1996)

The early experiments in MALDI were mainly concerned with discovering and developing new matrices, with the goal of uncovering a “universal” matrix that could be used for all applications. While 2,5-dihydroxybenzoic (gentisic) acid¹⁰⁵ and sinapinic acid were quickly identified as useful compounds, it became apparent that no single solution would be achieved. A process of trial-and-error was usually required to determine which matrix should be used for a particular application¹⁰⁶, along with the solvent system and the ratio of matrix to analyte, which can vary from 100:1 up to as much as 50,000:1. These ratios show that the vast bulk of the crystal structure will be composed of matrix compound. The fact that the matrix ion signal is not such an order of magnitude higher than most analytes is an effect known as ‘matrix suppression’ and is invaluable to the success of the technique¹⁰⁷.

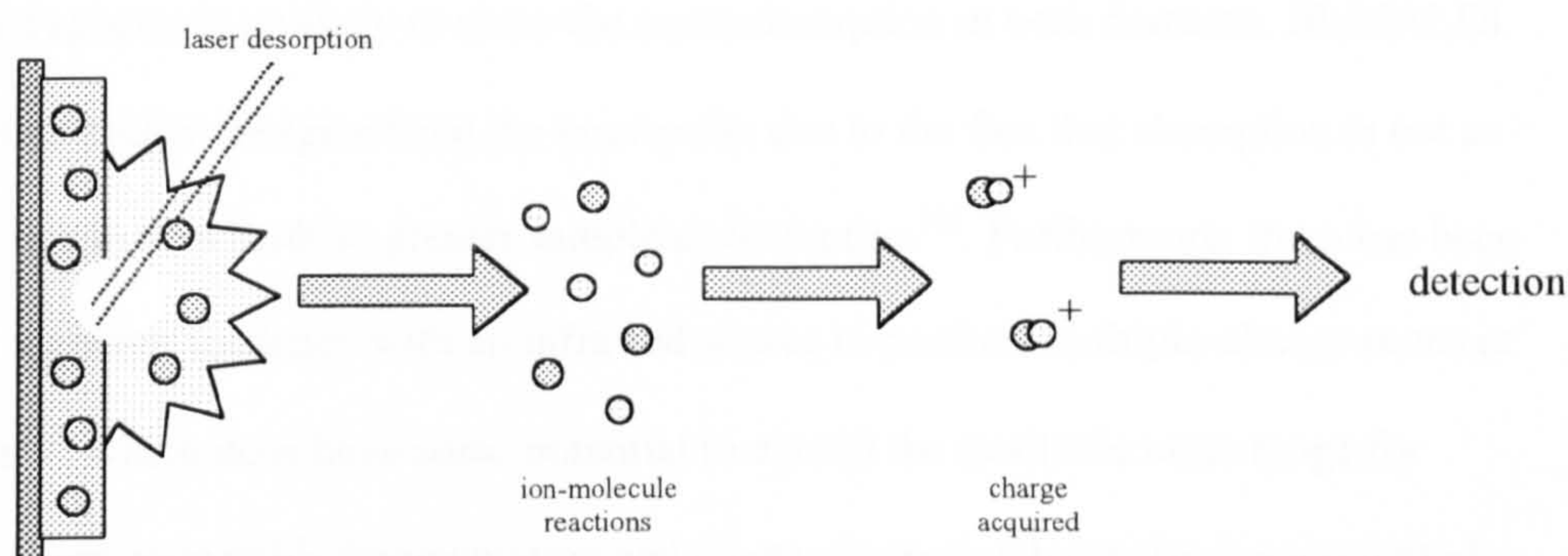


Figure 1j - Schematic of the basic process of ion formation by MALDI

An exact mechanism of the MALDI process is still not agreed^{108,109}. A large number of experiments having been performed in attempts to understand the process^{110,111,112}, for instance by separating the desorption and ionisation steps through having the co-

¹⁰⁴ PO Danis, DE Karr, YS Xiong, KG Owens, Rapid Comm Mass Spectrom, 10, 862, (1996)

¹⁰⁵ RC Beavis, BT Chait, Rapid Comm Mass Spectrom, 3, 233, (1989)

¹⁰⁶ MC Fitzgerald, GR Parr, LM Smith, Anal Chem, 65, 3204, (1993)

¹⁰⁷ R Knochenmuss, F Dubois, MJ Dale, R Zenobi, Rapid Comm Mass Spectrom, 10, 871, (1996)

¹⁰⁸ R Zenobi, R Knochenmuss, Mass Spec Reviews, 17, 337, (1998)

¹⁰⁹ P-C Liao, J Allison, J Mass Spectrom, 30, 408, (1995)

¹¹⁰ M Karas, D Bachmann, F Hillenkamp, Anal Chem, 57, 2935, (1985)

¹¹¹ H Ehring, M Karas, F Hillenkamp, Org Mass Spectrom, 27, 427, (1992)

¹¹² PC Liao, J Allison, J Mass Spectrom, 30, 408, (1995)

ordinating salt physically removed from the analyte source area¹¹³. One of the main problems is that the variations in the experimental setup, from the sample preparation through to the choice of matrix, have a fundamental effect on the ion formation process. It has also been shown by Puretzky and Geohegan that the conversion of ions is not that highly favoured¹¹⁴, with an neutral to ion ratio in the order of 10^4 . This means that the ion formation process leads to a minority species, with a number of different potential routes possible opens up this difficulty in describing and understanding the process¹¹⁵.

The form of MALDI generally carried out is using a laser that produces light in the ultra-violet (UV) region, however the technique also works with IR lasers. There are a number of experimental differences between the two methods, notably the choice of matrix as a species is unlikely to show the same absorption in both domains. IR-MALDI also requires higher energies from the laser pulse due to the fact that absorption is not as efficient, this in turn leads to greater sample consumption¹¹⁶. Furthermore, there has been observed a greater tendency with an infra-red source to produce multiple-charge states at high mass¹¹⁷, which does have some potential to extend the available mass range for detection. Less metastable fragmentation and cluster formation have also been reported with IR-MALDI¹¹⁸.

The MALDI process is usually considered in two parts, the desorption of the matrix¹¹⁹ and the ionisation of the analyte. The analyte is taken into the gas phase by the momentum of the bulk matrix which acquires the energy from the laser pulse. Models describing the nature of this desorption process are varied but generally fall into

¹¹³ ME Belov, CP Myatt, PJ Derrick, Chem Phys Lett, 284, 412, (1998)

¹¹⁴ AA Puretzky, DB Geohegan, Chem Phys Lett, 286, 425, (1997)

¹¹⁵ CD Mowry, MV Johnston, J Phys Chem, 98, 1904, (1994)

¹¹⁶ S Niu, W Zhang, BT Chait, J Am Soc Mass Spectrom, 9, 1, (1998)

¹¹⁷ A Overberg, M Karas, U Bahr, R Kaufmann, F Hillenkamp, Rapid Comm Mass Spectrom, 4, 293, (1990)

¹¹⁸ S Berkenkamp, F Kirpekar, F Hillenkamp, Science, 281, 260, (1998)

¹¹⁹ A Vertes, G Irinyi, R Gijbels, Anal Chem, 65, 2389, (1993)

thermal¹²⁰ or jet expansion systems^{121,122}. Thermal models assume that the energy from the laser pulse is distributed to a certain depth, giving the lattice enough energy to evaporate effectively into a given volume of gas-phase molecules. The exact proportion of energy taken in by the matrix depends on its absorption profile and the depth of solid material. Some models suggest a portion, if not a majority, of the energy passes straight through to the metal substrate and so leads to a thermal spike beneath the matrix layer causing the lattice to break into a jet expansion outwards¹²³. Experiments, showing that a salt placed under the matrix and analyte is incorporated into gas-phase ions, can be thought of as potentially supporting this idea¹²⁴. For a more gentle thermal evaporation, the flux of the material ejected is dependent on the surface ‘temperature’ and since most matrices are reasonably volatile such enhanced sublimation models are attractive¹²⁵. The yield of ions has been shown to rise steeply with fluence, differing from other models where a linear trend is observed¹²⁶.

Expansion models basically divide into either a progressive, or layered, approach or the jet expansion of a much larger volume of matrix¹²⁷. The progressive system gives desorption in relation to locally deposited energy that is assumed not to be distributed widely through the bulk solid. At higher fluences the volume affected will increase and more distribution would be supposed, leading to a move towards the thermal evaporation models. This layered desorption has been shown by Johnson to be dependent on the incident angle of the laser¹²⁸, and so in turn the laser spot size and penetration depth. In contrast, volume ejection or pressure-pulse is the rapid and impulsive expansion of a

¹²⁰ Dreisewerd, *Int J Mass Spectrom Ion Proc*, 141, 127, (1995)

¹²¹ RE Johnson, BUR Sundqvist, *Rapid Comm Mass Spectrom*, 5, 574, (1991)

¹²² RE Johnson, *Int J Mass Spectrom Ion Proc*, 139, 25, (1994)

¹²³ DA Allwood, PE Dyer, RW Dreyfuss, *Rapid Comm Mass Spectrom*, 11, 499, (1997)

¹²⁴ AM Hoberg, DM Haddleton, PJ Derrick, J Scrivens, *Eur Mass Spectrom*, 3, 471, (1996)

¹²⁵ CD Mowry, MV Johnston, *J Phys Chem*, 98, 1904, (1994)

¹²⁶ Z Szilágyi, JE Varney, PJ Derrick, K Vékey, *Rapid Comm Mass Spectrom*, 12, 489, (1998)

¹²⁷ LV Zhigitei, BJ Garrison, *Rapid Comm Mass Spectrom*, 12, 1273, (1998)

¹²⁸ RE Johnson, Y LeBeyec, *Int J Mass Spectrom*, 177, 111, (1998)

larger volume of sample in response to the net momentum imparted on the lattice by the deposited energy. This does not depend on the angle of the incoming light and is thought to show a linear trend with laser fluence¹²⁹.

As suggested with the layer effect, the model that most accurately applies to the mechanics can change with fluence and also as the whole process advances. Matrices can be more prone to a particular route, depending on their solid-state characteristics such as sublimation enthalpy and absorption efficiency at the wavelength of the laser. Both Ens¹³⁰ and Beavis¹³¹ have reported results in which ion yields were near linear just above threshold, before changing their relationship and later becoming linear with a shallower gradient at higher laser fluence. The assignment of thresholds is potentially complicated, with detector efficiency affected by both mass and also laser fluence. With a particularly volatile matrix, there is a good probability that the matrix and analyte thresholds will differ, meaning that the laser fluence must be higher to obtain an analyte signal than it would be for solely the matrix.

Ionisation can take place in the solid phase, just after desorption or in the gas-phase plume by the addition of additional photons. Where in the overall process ionisation occurs will determine, in part, the energy necessary to form ions. The simplest model for the process is single molecule multiphoton ionisation of the matrix so as to give a radical cation. Ehring, Karas and Hillenkamp consider this a primary route to all observed MALDI ions¹³², with the wavelength dependence of the technique indicating the reliance on excited matrix molecules^{133,134}.

¹²⁹ R Knochenmuss, F Dubois, MJ Dale, R Zenobi, *Rapid Comm Mass Spectrom*, 10, 871, (1996)

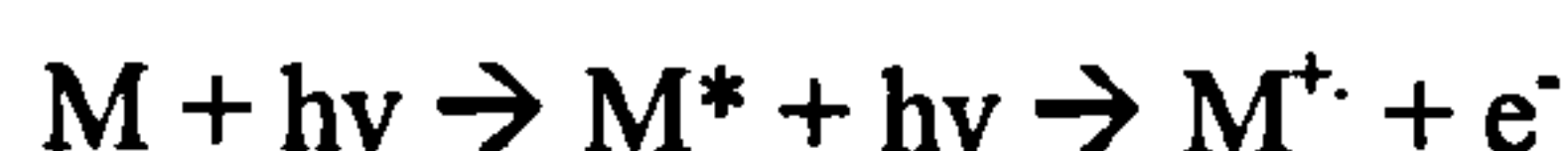
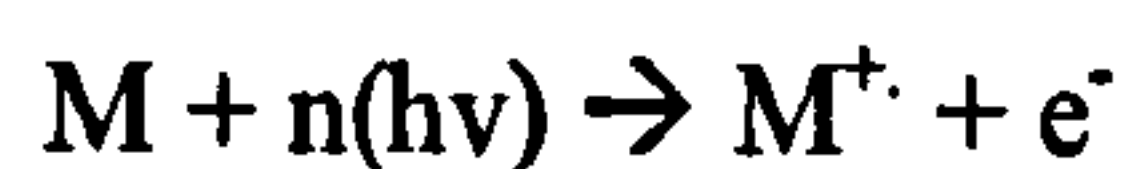
¹³⁰ W Ens, Y Mao, F Mayer, KG Standing, *Rapid Comm Mass Spectrom*, 5, 117, (1991)

¹³¹ RC Beavis, *Org Mass Spectrom*, 27, 864, (1998)

¹³² H Ehring, M Karas, F Hillenkamp, *Org Mass Spectrom*, 27, 472, (1992)

¹³³ LM Preston-Schaffter, GR Kinsel, DH Russell, *J Am Soc Mass Spectrom*, 5, 800, (1994)

¹³⁴ H Ehring, BUR Sundqvist, *Appl Surf Sci*, 96, 577, (1996)



It is unlikely that the second step shown here would be a multiphoton process since calculations have shown that the fluences in the typical experiment are too low for such an occurrence. Whether two photons alone is sufficient to achieve ionisation is unclear¹³⁵, with ionisation potentials for large aggregate systems still generally unknown although they would be theorised as being lower than the corresponding individual species¹³⁶. However, values from isolated matrix molecules tend to be in the region of 8-10eV and as such can be considered to be too high given the 7.36eV (707 kJ/mol or 169 kcal/mol) imparted by two nitrogen laser photons¹³⁷. This shortfall in acquired energy could be accounted for by a contribution from thermal ionisation routes. Such effects can result from the pooling of energy between a number of excited matrix molecules, resulting in the production of a single radical species. Strong interactions between chromophores such as this are known and given the conditions in the gas plume such a process is certainly feasible¹³⁸.



As shown above, the route can also lead directly to analyte ions. This direct ionisation route does give a clue to the matrix suppression effect, which with higher concentrations

¹³⁵ DA Allwood, PE Dyer, PW Dreyfus, Rapid Comm Mass Spectrom, 11, 499, (1997)

¹³⁶ R Cramer, RF Haglund, F Hillenkamp, Int J Mass Spectrom Ion Proc, 169/170, 51, (1997)

¹³⁷ V Karbach, R Knochenmuss, Rapid Comm Mass Spectrom, 12, 968, (1998)

¹³⁸ M Handschuh, S Nettesheim, R Zenobi, Applied Surf Sci, 137, 125, (1999)

of analyte can lead to a total loss of matrix ion signal in the eventual spectra¹³⁹. Most calculations for nearest-neighbour energy pooling, such as those by Knochenmuss et al., have given reasonable expected ion yields. But since the effect of clusters has not been modelled in these calculations, the ionisation potentials could be even more favourable¹⁴⁰.

The second most supported mechanism is proton transfer from an excited matrix molecule, which is assumed to be more acidic than in its ground state¹⁴¹. It is certainly known that excitation of aromatic hydroxyls in solution show enhancements in pK values¹⁴². Experiments with derived systems to remove these free hydroxyls have met with mixed results, some showing a lowering of MALDI efficiency and others little change. It is still generally thought though, that the carboxylic group of a number of matrix systems is less likely to be involved in the transfer process and esters have been shown to be valid matrices in certain applications¹⁴³. Work looking at the structural isomers of dihydroxybenzoic acid (DHB) shows that only the 2,5 form is particularly useful¹⁴⁴, suggesting the importance of the hydroxyls and their specific local environment.



A significant doubt in the importance of excited-state proton transfer (ESPT) is that compounds known to exhibit such a characteristic in the solution phase have tended not to show good MALDI performance¹⁴⁵. Some matrices, such as salicylic acid, do

¹³⁹ R Knochenmuss, V Karbach, U Wiesli, K Breuker, R Zenobi, *Rapid Comm Mass Spectrom*, 12, 529, (1998)

¹⁴⁰ R Knochenmuss, F Dubois, MJ Dale, R Zenobi, *Rapid Comm Mass Spectrom*, 10, 871, (1996)

¹⁴¹ RW Taft, RD Topson, *Prog Phys Org Chem*, 16, 1, (1987)

¹⁴² JF Ireland, PA Wyatt, *Adv Phys Org Chem*, 12, 131, (1976)

¹⁴³ J Krause, M Stoeckli, UP Schlunegger, *Rapid Comm Mass Spectrom*, 10, 1927, (1996)

¹⁴⁴ S Bashir, M Mormann, PJ Derrick, D Kuck, *J Am Soc Mass Spectrom*, 11, 544, (2000)

¹⁴⁵ V Karbach, R Knochenmuss, *Rapid Comm Mass Spectrom*, 12, 968, (1998)

however bear a structural similarity to known ESPT-active species. The fact that some matrices will give signal in negative mode suggests that a disproportionation route is also feasible. A possible mechanism for such a process would be by multi-centre ionisation, leading to an excited-state proton transfer¹⁴⁶. A direct proton ejection from a single matrix molecule is rather unfeasible, with the energy needed by DHB for example being in the order of 14eV¹⁴⁷.



Most of the reactions so far discussed concern the matrix molecule. Either the analyte must undergo a similar set of reactions or the charge is transferred from another species. For the latter to occur there must be sites within the analyte that are amenable to charge attachment, either in the form of a proton or the addition of a small cation. In proteins the obvious positions are nitrogen centres, which are well documented with localised charge in the solution and solid phases. In comparison, polymers tend not to protonate or appear as a pure analyte ion. Rather, nearly all systems pick up charge by attachment of metal cations, most usually sodium or potassium which are both present at sufficient levels in most commercial compounds¹⁴⁸. It can be speculated that the salt ions will be liberated in the plume formed by the laser impact and be allowed to attach to the more electron-rich areas of the polymer. Although most do not demonstrate specific binding sites, systems such as polyglycols have nucleophilic oxygen groups that are the most obvious point of contact for the charged species. The chain can be visualised to be wrapped around the cation, however unlike in electrospray ionisation here there is only a single charge and ipso facto charge is not dependent on the length of the oligomer. In fact, where there are cations with a natural charge of more than one unit, it has been observed that charge is

¹⁴⁶ ME Gimón, LM Preston, T Solouki, MA White, DH Russell, *Org Mass Spectrom*, 27, 827, (1992)

¹⁴⁷ K Breuker, R Knochenmuss, R Zenobi, *Int J Mass Spectrom*, 184, 25, (1999)

lost from the resultant analyte ion in the form of protons so as to reduce the overall charge species down to a unit charge. This is not a major consideration given that the most common cations used are the singly-charged alkali metals¹⁴⁹. However, more complex systems containing transition metals are sometimes used in order to ionise certain polymer systems. These polymers tend to be those, such as polystyrene, with less obvious binding units where the cation must presumably interact with the electron density of an aromatic system in some form of Π -stacking arrangement^{150,151}. Completely non-polar systems such as polyethylene have so far resisted all attempts to achieve reliable MALDI results.

The attachment process can be studied using the process of delayed extraction, that is by allowing the natural expansion of the plume before applying the extraction potential. This prolongs the time spent by the ions and other species in the higher density region of the source. The enhancement of sodiated peaks observed by Wang¹⁵² shows that a significant part of the ion attachment takes place in this gas plume a period after desorption.

Measurements suggest that without this delay, ions are generated with velocities out of the plume in the region of 1000 m/s, the exact value depending on the matrix system employed¹⁵³. Further evidence can be gleaned using polymer systems that do not attach common cations such as sodium. This means that the source from which the sample gains counter-ions can be better controlled. If a chosen salt is placed in a layer above the analyte, then the most likely time for attachment would be following successful desorption. The cation affinities of small molecules can be measured by spectroscopic

¹⁴⁸ D Dogruel, RW Nelson, P Williams, *Rapid Comm Mass Spectrom*, 10, 801, (1996)

¹⁴⁹ JS Klassen, SG Anderson, AT Blades, P Kebarle, *Phys Chem*, 100, 1421, (1996)

¹⁵⁰ CF Llenes, RM O'Malley, *Rapid Comm Mass Spectrom*, 6, 564, (1992)

¹⁵¹ AM Belu, JM DeSimone, RW Linton, GW Lange, RM Friedman, *J Am Soc Mass Spectrom*, 7, 11, (1996)

¹⁵² J Wang, P Sporns, *J Agr Food Chem*, 48, 5887, (2000)

¹⁵³ RC Beavis, BT Chait, *Chem Phys Lett*, 181, 479, (1991)

means and are shown to be in the order of 25-50 kcal/mol for singly charged species, which is considerably lower than equivalent values determined for protons¹⁵⁴.

iv. Analysers

What is often considered erroneously as the detection of the ions, is in fact a mass separation or filter and can be better considered as an “analyser”. The physics behind the various types of analyser are often very different, giving a range of degrees of performance and abilities. Some are better suited to certain types of source, while others form the core of an instrument on which a number of different sources can be used.

a. Time-of-Flight

Perhaps the simplest analyser is based on the principle of time-of-flight (TOF), a theory that dates back to at least the end of the nineteenth century¹⁵⁵. In fact, Werehart used the basis of the technique to measure the m / q value of the ‘rays’ produced by Thompson’s cathode experiments¹⁵⁶. Today the technique is almost synonymous with the source technique of MALDI and the discussion will be focused on this application in particular, although a number of recent ESI-TOF systems have demonstrated good resolution and performance¹⁵⁷. The technique relies on the fact that if a potential of V_x is applied to an ion of mass m and charge q , then it acquires a constant energy qV_x . The time it takes this ion to traverse a field-free region of distance L can be then be described by the following equation.

¹⁵⁴ RD Burton, CH Watson, JR Eyler, GL Lang, DH Powell, MY Avery, Rapid Comm Mass Spec, 11, 443, (1997)

¹⁵⁵ C Weickhardt, Mass Spec Rev, 15, 139, (1996)

¹⁵⁶ J Mattingly, Stud Hist Phil Modern Phys, 32B, 53, (2001)

¹⁵⁷ JG Boyle, CM Whitehouse, Anal Chem, 64, 2084, (1992)

$$t = L (m / 2qV_x)^{1/2}$$

Using such a pulsed source, the time required for an ion to move to a detector is related to a mass/charge value. With the different oligomer masses of typical polymers the time interval between the arrival of subsequent ions will be very small. Utilisation of this principle for a mass analyser has therefore been predicated by the development of high-speed processing of ion signals^{158,159}. The resolution of the system is still not as high as other techniques and tends to decrease as the mass of the ion is increased, as the longer flight time of a larger ion leads to a broadening of the peak. This resolution is limited mainly by the fact that the ions start in a small but finite volume and have an initial amount of kinetic energy. As ions must be produced in a small time period, in the order of 0.1 μ s in the case of MALDI, each pulse contains very few of them and so a mass spectrum must be formed by summing a number of ion creation and detection events.

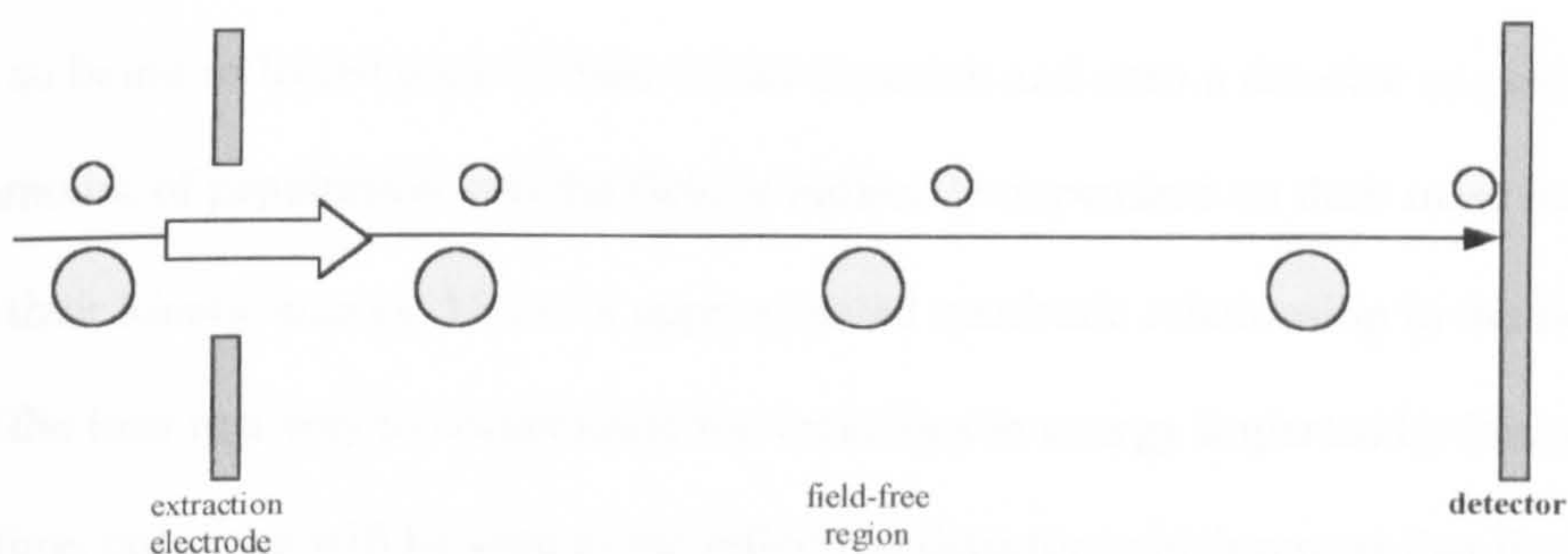


Figure 1k - Schematic of the basic process of separation by linear time-of-flight

¹⁵⁸ WC Wiley, JB McLaren, Rev Sci Instruments, 26, 1150, (1955)

¹⁵⁹ H Wollnik, Mass Spectrom Rev, 12, 89, (1993)

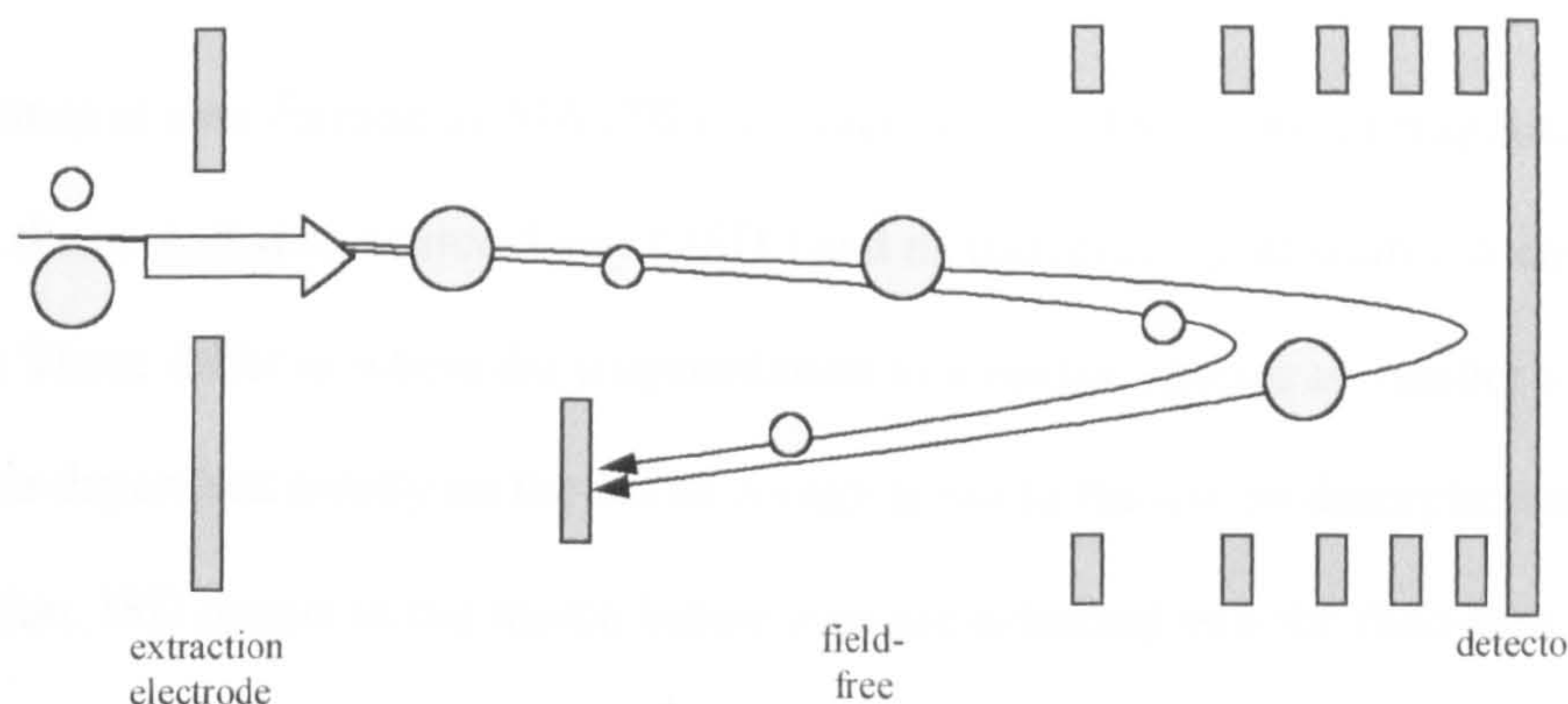


Figure 11 - Schematic of the basic process of separation by reflectron time-of-flight

Detection of ions at the end of the flight path can be carried out in either linear or reflectron modes. Linear systems are those where the particle detector is simply placed at the end and collects all species that reach that point. Both ions and also any neutrals formed indirectly by the ionisation process are detected. Using a reflectron improves the performance of the system over that achieved with linear systems¹⁶⁰. The ion mirror of this approach reverses the motion of the ions as they move into a progressive electrostatic field, so being reflected back in their initial direction and onto a detector so positioned. The amount of penetration into the field is indirectly dependent on their mass but directly so on their kinetic energy. Use of a approximated quadratic relationship in the field can focus the ions in a way to compensate for variations in energy imparted by ionisation. By its nature, only ions will be seen at the reflectron detector, which means that the spectra will be much cleaner, in addition to the improvements in peak width and shape. Ion population after the reflectron will tend to be lower than with linear detection, meaning that the technique requires a high initial ion yield else low intensity species may be lost to the background.

¹⁶⁰ TJ Cornish, RJ Cotter, Rapid Comm Mass Spectrom, 7, 1037, (1993)

The nature of ions formed by MALDI is characterised by two forms of fragmentation or decay, the so-called in-source decay (ISD) and metastable or post-source decay¹⁶¹ (PSD). These differ in where the fragmentation to a neutral species or smaller ion occurs, which is dependent mostly on the initial energy given to the ion on desorption and ionisation. ISD occurs in the source before ions are extracted into the field-free region, which would be expected if molecules acquire far too much energy during the ionisation process. Obviously anything that prolongs their time in the source, such as delayed extraction, will also lead to more of this fragmentation taking place. Since the ions can lose their charge before extraction, the movement of the resultant neutrals will be random and so very few will move in the direction of the detector and be successfully counted. Fragments in the source can also acquire charge from the morass of cations still remaining in the plume, these species will be extracted and move down the drift path in true relation to their eventual mass. These fragment ions will therefore be detected and appear in the mass spectrum. If these can be identified and also related to a particular parent ion, then they can give valuable structural information.

In comparison, species that fragment in the field-free region will give neutrals and smaller ions that have a momentum related to their initial parent mass exposed to the accelerating potential. This metastable decay occurs in molecules than have less energy than those that fragment in the source, but still have too much to remain as a stable ion species while traversing the drift tube. Neutrals formed by this process represent the majority of neutrals seen at the linear detector¹⁶², since they have been extracted and directed towards the detector while still carrying a charge. The pathways leading to the in-source and post-source decay products are reliant on the energy taken in by the analyte molecules, either from the laser pulse or through collisions with matrix molecules in the

¹⁶¹ B Spengler, D Kirsch, R Kaufmann, J Phys Chem, 96, 9678, (1992)

¹⁶² KG Standing, *The Analysis of Peptides and Proteins by Mass Spectrometry*, Wiley, New York, (1998)

source region. Both of these processes can therefore lead to structural fragments so long as they can be successfully detected and also identified. One method of clarifying this process is to use an ion gate, that is a deflection plate positioned just after the extraction potential. This can be used to eject all but the parent ion of interest from the system, so that only the single species fragments and it can be certain that all observed fragments result from that species. Using a reflectron also means that neutral fragments are not observed, so the signals that result are genuine ions appearing at the correct value for their mass.

The two main variables open to time-of-flight analysis are the extraction potential and the length of the flight path. Most instruments are anything up to one metre, which gives a reliable performance with a good range of masses. Increasing the length does increase the separation of masses and so would give better resolution if the frequency of the detection remained constant. However, the increased distance also amplifies any slight variations of velocity in the time-of-flight of molecules with the same mass, which leads to a decrease in effective resolution. The extraction or acceleration potential is usually kept stationary on most instruments, this is for the purpose of calibration as the relation of the time measured to mass will be dependent on this setting. Commercial instruments tend not to give ability to alter the value freely, but rather limit to a small number of settings that are suited to different mass ranges. This means that any one setting does not give good performance across a very wide mass range, which is especially true with MALDI-TOF which does not work well at all with polymers exhibiting a high degree of polydispersity, usually considered as being anything over a PDI value of 1.4^{163,164}.

¹⁶³ G Montaudo, E Scamporrino, D Vitalini, P Mineo, *Rapid Comm Mass Spectrom*, 10, 1551, (1996)

¹⁶⁴ K Martin, J Spickermann, HJ Rader, K Mullen, *Rapid Comm Mass Spectrom*, 10, 1471, (1996)

b. Fourier-Transform Ion Cyclotron Resonance

The separation technique of Fourier-transform ion cyclotron resonance (FTICR) is a relatively new addition to the battery of mass spectrometric capabilities^{165,166}. It offers a previously almost unprecedented degree of resolution and mass accuracy, so opening up new experimental possibilities¹⁶⁷. The phenomenon of ion cyclotron motion has been known for a long period, but in itself has no analytical use until its inception as a high-resolution mass spectrometer^{168,169}. The effect occurs when an ion moving within a uniform magnetic field has a force applied to it as described by the following well-known equation.

$$\text{Force} = \text{Mass} \times \text{Acceleration} = m \times (dv / dt) = qv \times B_0$$

Where

B_0 - magnetic field

m - ionic mass

q - charge of ion

v - velocity of ion

If the ion is assumed in the ideal case to maintain a constant speed with no collisions, then the magnetic field will bend its path into a true circle. Positive and negative ions are of course bent in opposite directions by this process¹⁷⁰.

¹⁶⁵ A Marshall, Mass Spec Rev, 17, 1, (1998)

¹⁶⁶ IJ Amster, J Mass Spectrom, 31, 1325, (1996)

¹⁶⁷ JE Bruce, X Cheng, R Bakhtiar, Q Wu, SA Hofstadler, GA Anderson, RD Smith, J Am Chem Soc, 116, 7839, (1994)

¹⁶⁸ ML Gross, DL Rempel, Science, 226, 261, (1984)

¹⁶⁹ AG Marshall, Actual Chimique, 1, 18, (2001)

¹⁷⁰ L Schweikhard, AG Marshall, J Am Soc Mass Spectrom, 4, 433, (1993)

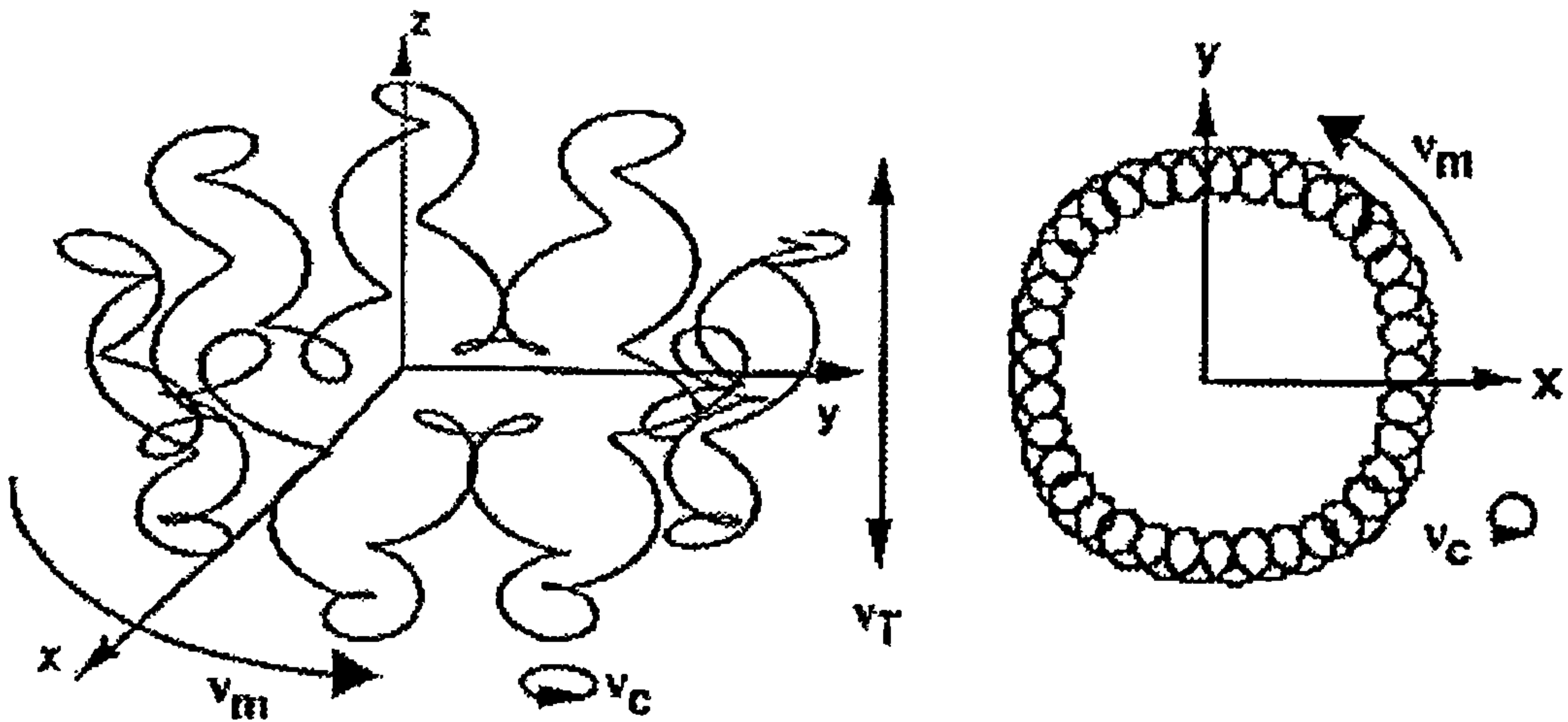


Figure 1m – Two separate representations of the cyclotron and magnetron motions of an ion

Denoting the ion velocity in the xy plane as $v_{xy} = \sqrt{(v_x^2 + v_y^2)}$ and with the angular acceleration also given by $|dv/dt| = v_{xy}^2/r$, the initial simple equation above can be changed to give a more complex one.

$$\frac{m v_{xy}^2}{r} = q V_{xy} B_0$$

Since angular velocity around the z -axis can be defined as $\omega = v_{xy}/r$ (in radians/sec), this can however also be incorporated into the equation to give the so-called “cyclotron” equation. Here, the velocity is given in terms of Hertz, the magnetic field in Tesla and charges as multiples of the elementary charge.

$$m \omega^2 r = q B_0 \omega r \quad \text{or} \quad \omega_c = q B_0 / m$$

The ω_c term in this equation is the cyclotron frequency of the “unperturbed” ion. An interesting development of this derivation is that all ions of a given m/z value will have the same cyclotron frequency, independent of their initial velocity. This feature is useful

for mass spectrometry, as it means that extensive focusing of the translational energies of the source ions is not required for the precise determination of m/z . More derivations can also lead to a relation between the ion cyclotron radius and temperature.

$$r = \frac{1.33651 \times 10^{-6}}{z B_0} \sqrt{mT}$$

From this equation it can be seen that the movement of the ions over a wide range of masses still have a radii of under a centimetre. So ions of thermal energy up to a very high mass limit can be confined to an orbit conveniently small for excitation and detection. Of course, increasing the magnetic field strength decreases the ion radius and so in itself extends the mass range. Since the radius is m/z dependent and not simply mass, it also means that ionisation techniques that lead to multiple charge states reduce the ionic radius and extend the effective mass range.

The majority of FTICR systems use an external ion source^{171,172}, especially for ionisation at high or even atmospheric pressures. This requires that the analyte ions be conveyed through ion optics into the cell^{173,174}. One such source that is now very common in FTICR systems is electrospray¹⁷⁵, this being the technique used in the majority of the work documented here. MALDI is interesting as a source^{176,177}, being either external to the magnet or carried out within the high-vacuum region at the centre of the instrument. The ions are contained in this cell by trapping voltages applied to two or more of the

¹⁷¹ IJ Amster, JA Loo, JJP Furlong, FW McLafferty, *Anal Chem*, 59, 313, (1987)

¹⁷² SA Hofstadler, DA Laude, *J Am Soc Mass Spectrom*, 3, 615, (1992)

¹⁷³ P Kofel, M Allemann, H Kellerhals, K-P Wanczek, *Int J Mass Spectrom Ion Proc*, 72, 53, (1986)

¹⁷⁴ RT McIver, RL Hunter, WD Borvers, *Int J Mass Spectrom Ion Proc*, 64, 67, (1985)

¹⁷⁵ KD Henry, FW McLafferty, *Org Mass Spectrom*, 25, 490, (1990)

¹⁷⁶ JA Castoro, C Köster, C Wilkins, *Rapid Comm Mass Spectrom*, 6, 239, (1992)

¹⁷⁷ RL Hettich, MV Buchanan, *Int J Mass Spectrom Ion Proc*, 111, 365, (1995)

component plates¹⁷⁸. When the ions enter the cell, the phases of their orbits are randomly distributed. In order for detection to be performed they must be brought into spatial coherence, else the ions at opposite extremes of the orbit will in effect balance each other and so give a net charge of zero on the detection plates. This detection is carried out by exciting the ion packets into a larger orbit using a uniform electric field that is oscillating near the cyclotron range for the particular m/z under study. Calculations on the excitation of ions within the cell show that the post-excitation radius is independent of the m/z value. This obviously means that all ions will be excited to the same orbital radius, dependent only on the fields involved in the process. The ion image of the moving ions will then be induced on detection plates and so converted to a mass spectrum¹⁷⁹. The excitation stage can also be used to push the ion energies over the threshold for collisional dissociation or eject them entirely from the cell. The former practice gives another experimental capability that incorporates techniques such as sustained off-resonance irradiation¹⁸⁰ (SORI) and will be discussed in more detail later in this work.

The development that made all of this potential into a viable analytical technique was the application of Fourier transformation (FT) mathematics to the detection. This means that all the ions of differing m/z values are detected simultaneously, with the ion currents formed being measured as a function of time. This gives vast improvements over having to scan each channel separately¹⁸¹ and also has advantages over other applications of FT, such as nuclear magnetic resonance (NMR) spectroscopy¹⁸², in that the values can be measured to a very high degree of accuracy. This technique of Fourier transform ion cyclotron resonance, also sometimes known more generally as Fourier-transform mass

¹⁷⁸ RT McIver, Rev Sci Instruments, 41, 555, (1970)

¹⁷⁹ MB Comisarow, J Chem Phys, 69, 4097, (1978)

¹⁸⁰ JW Gauthier, TR Trautman, DB Jacobson, Anal Chem Acta, 246, 211, (1991)

¹⁸¹ AG Marshall, FR Verdun, *Fourier Transforms in NMR, Optical and Mass Spectrometry*, Elsevier, Amsterdam, (1990)

¹⁸² AG Marshall, Acc Chem Res, 9, 307, (1996)

spectrometry (FTMS), has grown rapidly since its inception in 1974 by Marshall and Comisarow^{183,184}. There are now reported to be over 300 installations world-wide, ranging from high-field research instruments to those used in industry for more routine sample analysis¹⁸⁵. The high-resolution capability extends to being able to identify the carbon-13 isotope distribution in large organic molecules. This combined with a high degree of mass accuracy, allows a good deal of certainty in the identification of molecules, either singularly or in complex mixtures. The isotopic resolution is also used to determine charge state of any given ion signal, by comparing the separation of the isotope peaks to that of the single atomic mass unit that it would be if the charge was singular. Using this process to find the charge state means that the exact mass may be calculated from the m/z value. From the very high degree of accuracy in this mass for the analyte, it is possible to identify analytes based on elemental composition with a high level of certainty. If a particular species is suspected or known, the theoretical mass can be compared to a level of confidence of two or more decimal places, dependent on the mass of the subject. For unknown molecules this is slightly more complex, with spectral libraries used to suggest analytes based on their mass that can be confirmed by other techniques or even by observing other mass peaks or fragment species.

When combined with ionisation methods such as electrospray ionisation, the result tends to be multiply-charged analyte ions. FTICR is usually capable of resolving even the complex spectra produced by these multiple series, so leading to what Fenn et al termed a “revolution” in the detection of high-mass species¹⁸⁶. Proteins with masses in excess of 100kDa have been detected^{187,188}, since the multiple charge state brings the m/z value

¹⁸³ MB Comisarow, AG Marshall, Chem Phys Lett, 25, 282, (1974)

¹⁸⁴ MB Comisarow, AG Marshall, Chem Phys Lett, 26, 489, (1974)

¹⁸⁵ B Asamoto, Spectroscopy, 3, 38, (1988)

¹⁸⁶ JB Fenn, M Mann, CK Meng, SF Wong, CM Whitehouse, Science, 246, 64, (1989)

¹⁸⁷ NL Kelleher, MW Senko, MM Siegel, FW McLafferty, J Am Soc Mass Spectrom, 8, 380, (1997)

¹⁸⁸ MV Buchanan, RL Hettich, Anal Chem, 65, 245, (1995)

into a region capable of being contained and detected. Sensitivity can also be pushed so that samples in the sub-attomole range have been successfully detected using the technique¹⁸⁹.

Developments in the instrumental side for FTMS have mainly concentrated on cell design and that of the process of moving the ions into the cell from the ion source¹⁹⁰. Since all of the plates that generate the excitation and trapping potentials are finite, the electric field produced is non-linear and less than that which would result from the theoretical situation of two infinitely-extended parallel plates. Cells have been developed from the simple cubic design used by Comisarow et al, in order to try and make excitation as linear as possible and also reduce any ion loss ('ejection') along the z-axis¹⁹¹.

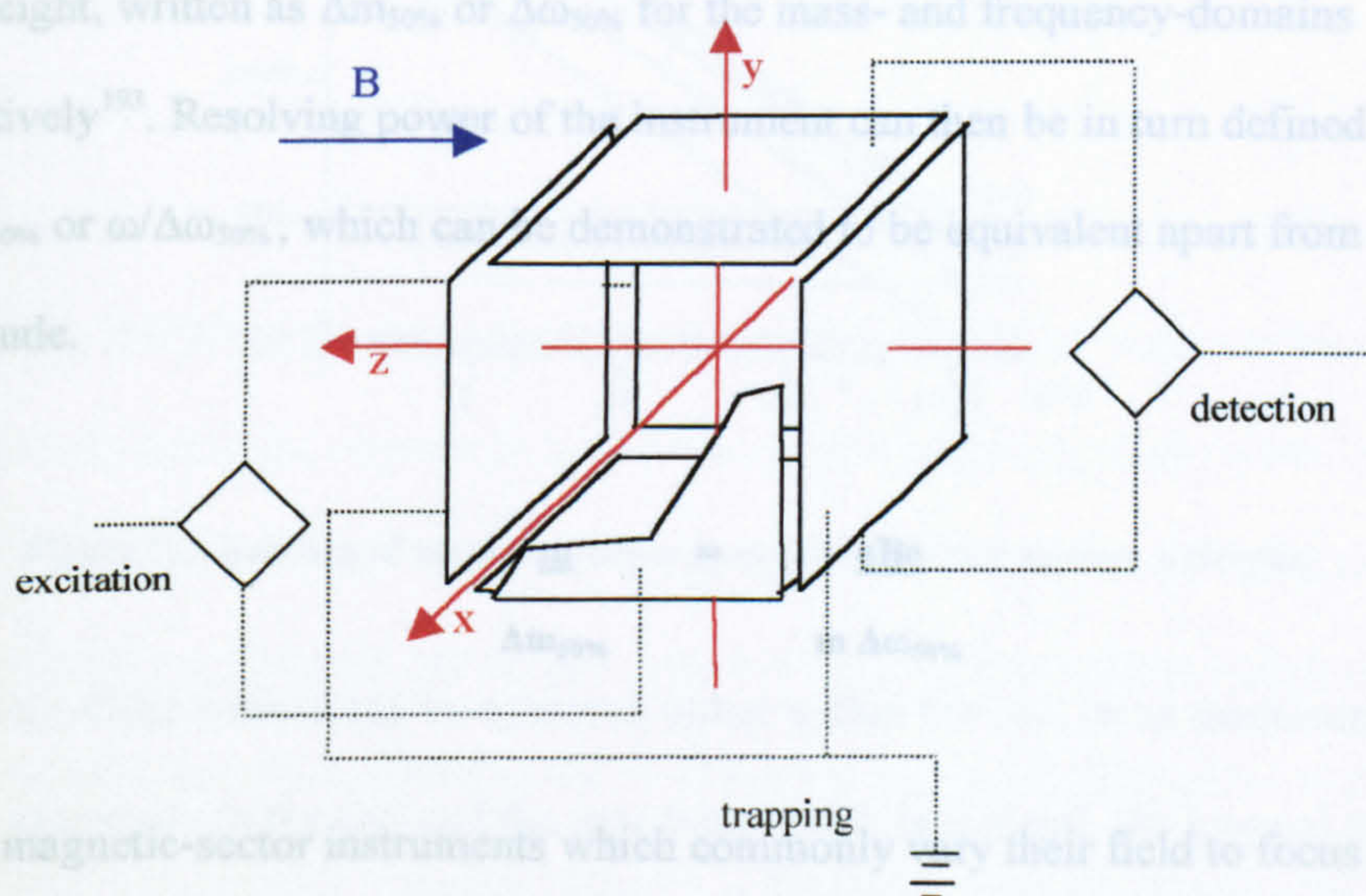


Figure 1n – Simplified diagram of the common design for FTICR cells

The radial electric field imposed on the ion in the cell produces its own force, opposing the Lorentz force from the magnetic field. The implication of this is that along with the

¹⁸⁹ GA Valaskovic, NK Kelleher, FW McLafferty, Science, 273, 1199, (1996)

¹⁹⁰ DA Laude, Mass Spec Rev, 14, 1, (1995)

¹⁹¹ SH Guan, AG Marshall, Int J Mass Spectrom Ion Proc, 146, 261, (1995)

effect of the trapping potential, the observed ion cyclotron frequency is reduced. Without this deficiency, the mass scale could be calibrated from a single ion of known composition, but in practice a number of species near or across the mass range under study must be used. The highest degree of accuracy is achieved by internal calibration, that is having the calibrant materials with the sample. This works only so long as the ion density in the cell remains sufficiently low that space-charge perturbation is not significant¹⁹². External calibration with a mixture designed for the role can be easier, especially if the samples under study are themselves complex mixtures of different masses.

Resolution in FTMS is usually defined as the full peak-width at half of the maximum peak height, written as $\Delta m_{50\%}$ or $\Delta \omega_{50\%}$ for the mass- and frequency-domains respectively¹⁹³. Resolving power of the instrument can then be in turn defined as $m/\Delta m_{50\%}$ or $\omega/\Delta \omega_{50\%}$, which can be demonstrated to be equivalent apart from the sign of magnitude.

$$\frac{m}{\Delta m_{50\%}} = \frac{qB_0}{m \Delta \omega_{50\%}}$$

Unlike magnetic-sector instruments which commonly vary their field to focus on certain masses, FTICR systems operate with a fixed magnetic field. This both allows higher magnetic strengths to be employed and also results in a much better homogeneity, so resulting in an improved mass resolving power. It is important to note that the resolution does vary in an inversely proportional relationship with m/z . Some instruments use a

¹⁹² JB Jeffries, SE Barlow, GH Dunn, Int J Mass Spectrom Ion Proc, 54, 169, (1983)

¹⁹³ AG Marshall, MB Comisarow, G Parisod, J Chem Phys, 71, 4434, (1979)

permanent magnet to generate the field¹⁹⁴, however these only give low fields strengths and so super-conducting systems are more often used.

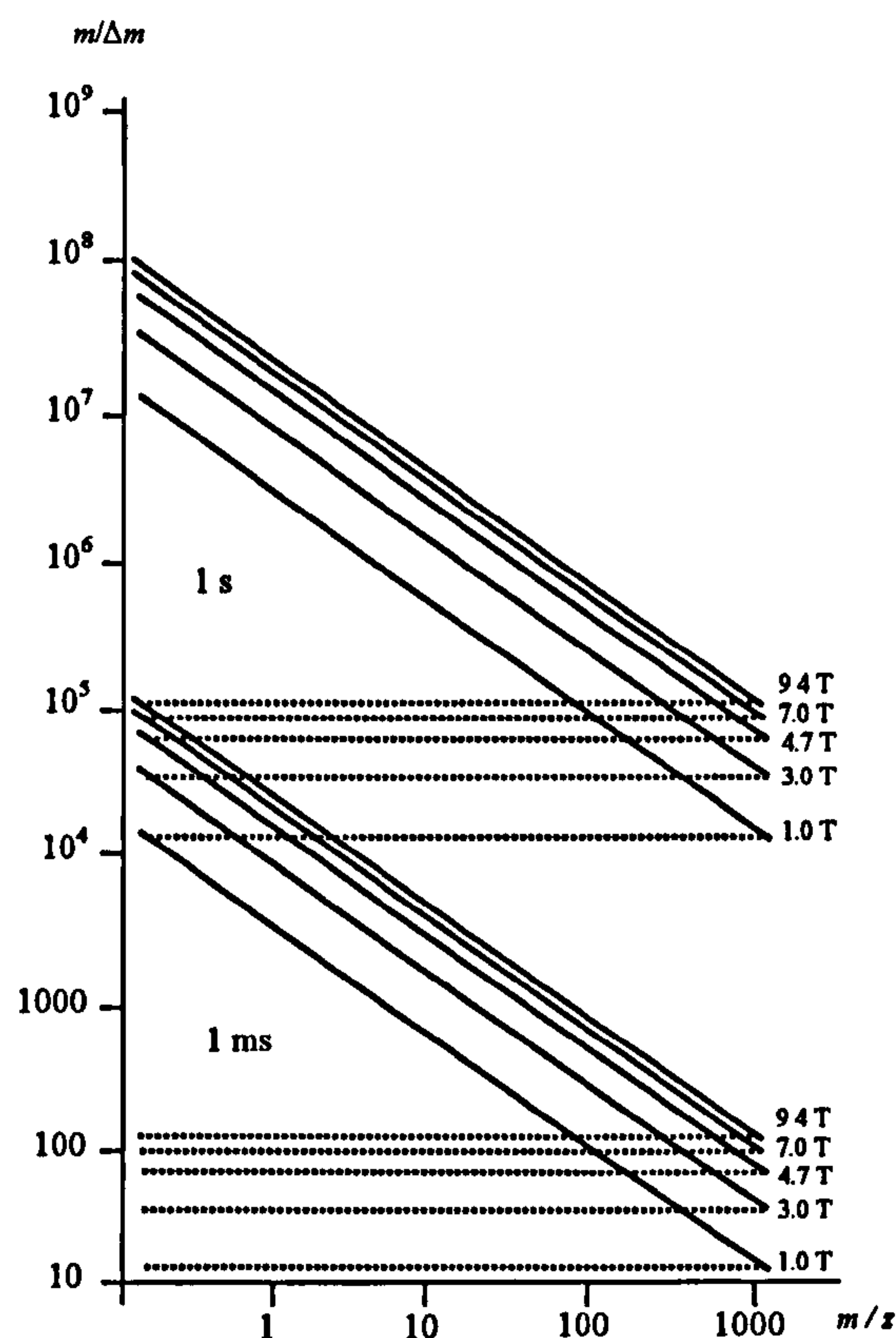


Figure 10 - Relation of resolving power to m/z for different magnet strengths

Ionisation of the analyte can be achieved either within the cell, or as mentioned briefly earlier, externally to the cell and the ions transferred. In general, the internal techniques have been replaced in routine operation by the external coupling of modern ion sources. Internal ionisation requires the analyte to be present in the cell in a gaseous form, which usually necessitates it being sufficiently volatile. The material can then be ionised by techniques such as passing an electron beam through the cell or perhaps by a photochemical process stimulated by a laser shot. Any ions so produced are then hopefully trapped in the cell while the other species are pumped away. In direct

¹⁹⁴ LC Zeller, JM Kennedy, H Kenttamaa, JE Campana, Anal Chem, 65, 2116, (1993)

comparison, external sources can be used with a wider range of samples using various methods of desorption or volatilisation and subsequent ionisation¹⁹⁵. The transfer process then also means that only ions are directed into the cell, reducing the amount of extraneous material that could affect the integrity of the high vacuum within the cell region. With an external source, the low pressure in the cell is maintained by using a progressive series of pumped regions. Some external techniques, such as electrospray for instance, start at atmospheric pressure and operate at relatively high values (approx. 1 torr) compared to that needed in the cell for resolution (approx. 1×10^{-10} torr). The nature of this pumping arrangement is that ions will be generated a distance outside the magnetic field of the instrument and so will require to be guided through the fringe field of the magnet into the cell. External sources also allow the coupling of chromatographic systems, which can be used to separate and in essence purify and concentrate the sample. This is important to many industrial applications where the high-mass accuracy can be used to rapidly identify components in a complex mixture¹⁹⁶. The other feature in FTICR that is very useful in this role is the ease in carrying out tandem mass spectrometry experiments, that is the sequential fragmentation and detection of an isolated mass species¹⁹⁷. The trapping and excitation potentials of the cell can be so manipulated that these forms of experiments can be carried out on a relatively small population of generated ions. It is the application of an additional time-dependent electric field that causes the fragmentation in this instance, a technique that will be discussed in more detail later.

¹⁹⁵ KD Henry, FW McLafferty, *Org Mass Spectrom*, 25, 490, (1990)

¹⁹⁶ MW Senko, CL Hendrickson, MR Emmett, SD-H Shi, AG Marshall, *J Am Soc Mass Spectrom*, 8, 970, (1997)

v. Polymer Science

Polymers, or plastics as they are often referred to by the general populace, are a major class of modern synthetic chemicals¹⁹⁸. They find use in countless applications depending on their varied properties, both chemical and mechanical. The whole range of masses are also represented, from high-weight systems used for structural applications through the mid-range malleable plastics and gels to low-mass liquids used as lubricants, detergents and other additives. Formed in most part by intermediates from the petrochemical industry, common polymers are produced in vast quantities.

Regardless of the large-scale production method, polymers are formed by fundamentally one of two processes - addition or condensation. While the end result is the linking of a defined repeat unit into an extended chain, these two routes affect the conditions used and are dictated in part by the structure of the monomer. A classic example of a condensation polymer is nylon, where an amine and carboxylic acid combine and in doing so release the water molecule that gives the synthesis its name¹⁹⁹. In comparison, addition polymers are mostly formed by a radical process and are usually evident by a carbon-carbon double bond in the monomer, such as that with the acrylate or styrene systems. The radical process is broken down into three stages - initiation, propagation and termination²⁰⁰. The relative rates of these three processes determine the length of chains produced and can be controlled in a number of ways, such as the amount of radical initiator or the temperature used for the synthesis²⁰¹. Greater control can be achieved using a moderated synthesis

¹⁹⁷ S Koster, MC Duursma, JJ Boon, MWF Nielen, CG de Koster, RMA Heeren, *J Mass Spectrom*, 35, 739, (2000)

¹⁹⁸ G Challa, *Polymer Chemistry*, Ellis Harwood, London, (1993)

¹⁹⁹ S Nakata, J Brisson, *J Polym Sci A*, 35, 2379, (1997)

²⁰⁰ D Kukulj, TP Davis, *Macromol Chem Physic*, 199, 1679, (1998)

²⁰¹ C Barner-Kowollik, TP Davis, *Macromol Theor Simul*, 10, 255, (2001)

such as the atom-transfer characterised by the use of the TEMPO intermediate²⁰² or the cobalt-based macrocycles²⁰³.

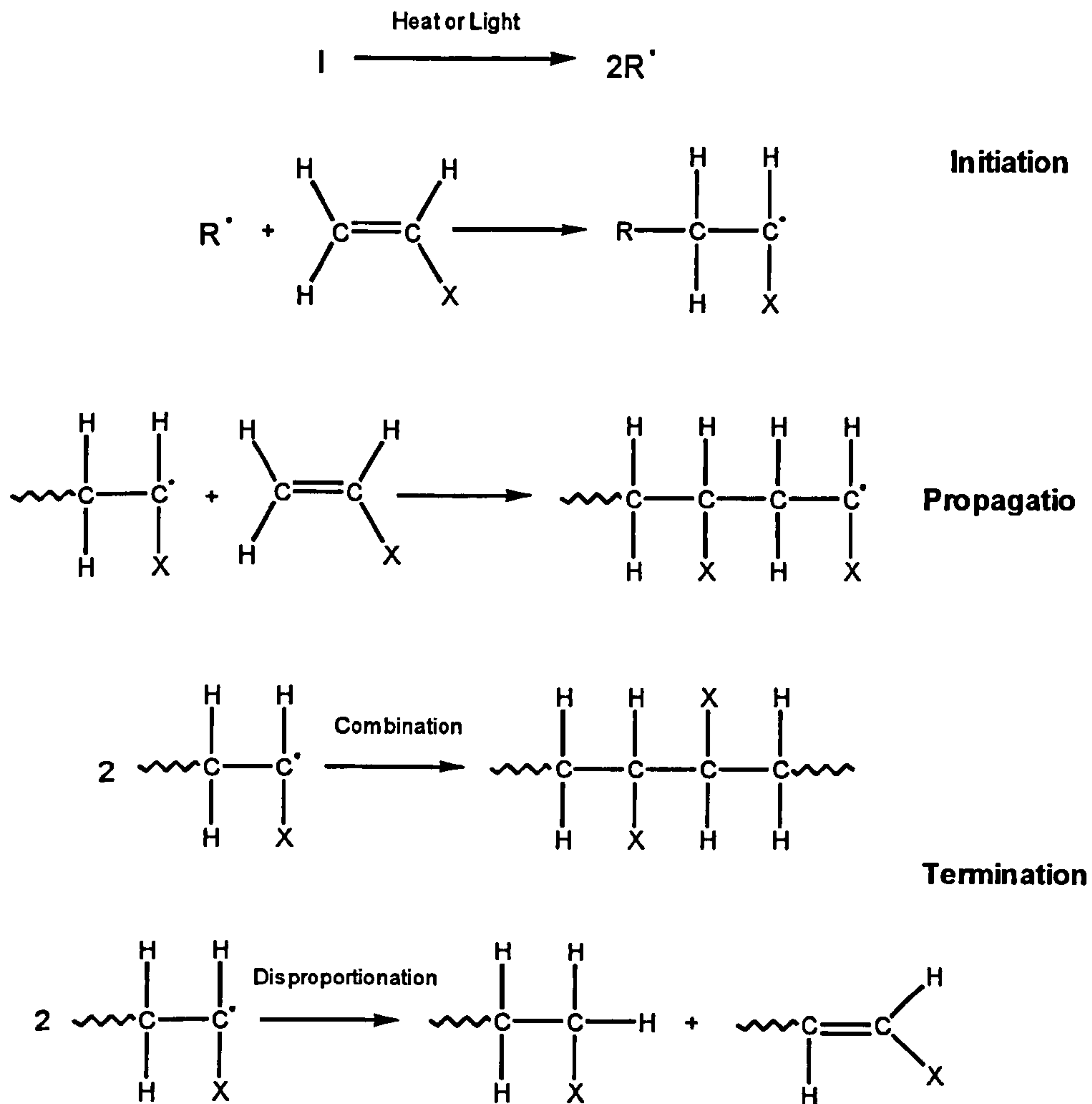


Figure 1p - Polymerisation by a free radical process

On the industrial scale, both processes are used with close control of conditions to give a very defined product with the necessary properties. Since production facilities are designed for particular systems, it is rare that new monomer systems would be introduced and so, apart from a few specialised applications, research concentrates more on the process specifics and architecture of the polymer. Polymer architecture goes beyond simple chain length to explore the effect of macrostructure on the behaviour, such as that

²⁰² D Greszta, K Matyjaszewski, *Macromol*, 329, 7661, (1996)

given by cross-linking, co-polymerisation and tacticity²⁰⁴. The property known as tacticity describes the geometry of functional groups in relation to the carbon chain in much the same way as the phenomenon of chirality in complex organic molecules. This is most important for addition polymers, where the side chain of a simple carbon backbone gives the characteristics of that particular polymer. Systems can have all of the groups to one side of the backbone (isotactic), alternating sides (syndiotactic) or completely random (atactic) which is, perhaps surprisingly, rare in synthetic polymers. This arrangement affects the macrostructure of the polymer, in particular the way in which the chains can fit together and so strongly influence physical properties such as thermal characteristics and transparency. Cross-linking is a stronger model of how chains relate to each other, often drastically increasing the effective mass of the polymer macromolecule. Such structures do make mass analysis more difficult, with fragmentation more complex and spectroscopic techniques mainly concerned with the backbone structure²⁰⁵. In comparison, co-polymers are an interesting area to study in this regard, either by detailed fragmentation or other methods. The most straightforward form of co-polymer is where two different polymers are effectively joined together at the ends to form a “co-block” structure. This type of arrangement is relatively simple to synthesis, however with more careful control other possibilities can be achieved including gradient, alternating, graft and totally random (terpolymer) co-polymer systems. Each of these requires careful choice of monomer and conditions, resulting in products with varying physical properties often different from those of the parent homopolymers²⁰⁶.

²⁰³ TP Davis, D Kukulj, DM Haddleton, Trends Polym Sci, 3, 365, (1995)

²⁰⁴ G Challa, *Polymer Chemistry*, Ellis Horwood, London, (1993)

²⁰⁵ SY Chang, NS Wang, ACS Sym Series, 147, (1995)

²⁰⁶ AK Kashyap, V Kalpagam, J Sci Ind Res, 40, 113, (1981)

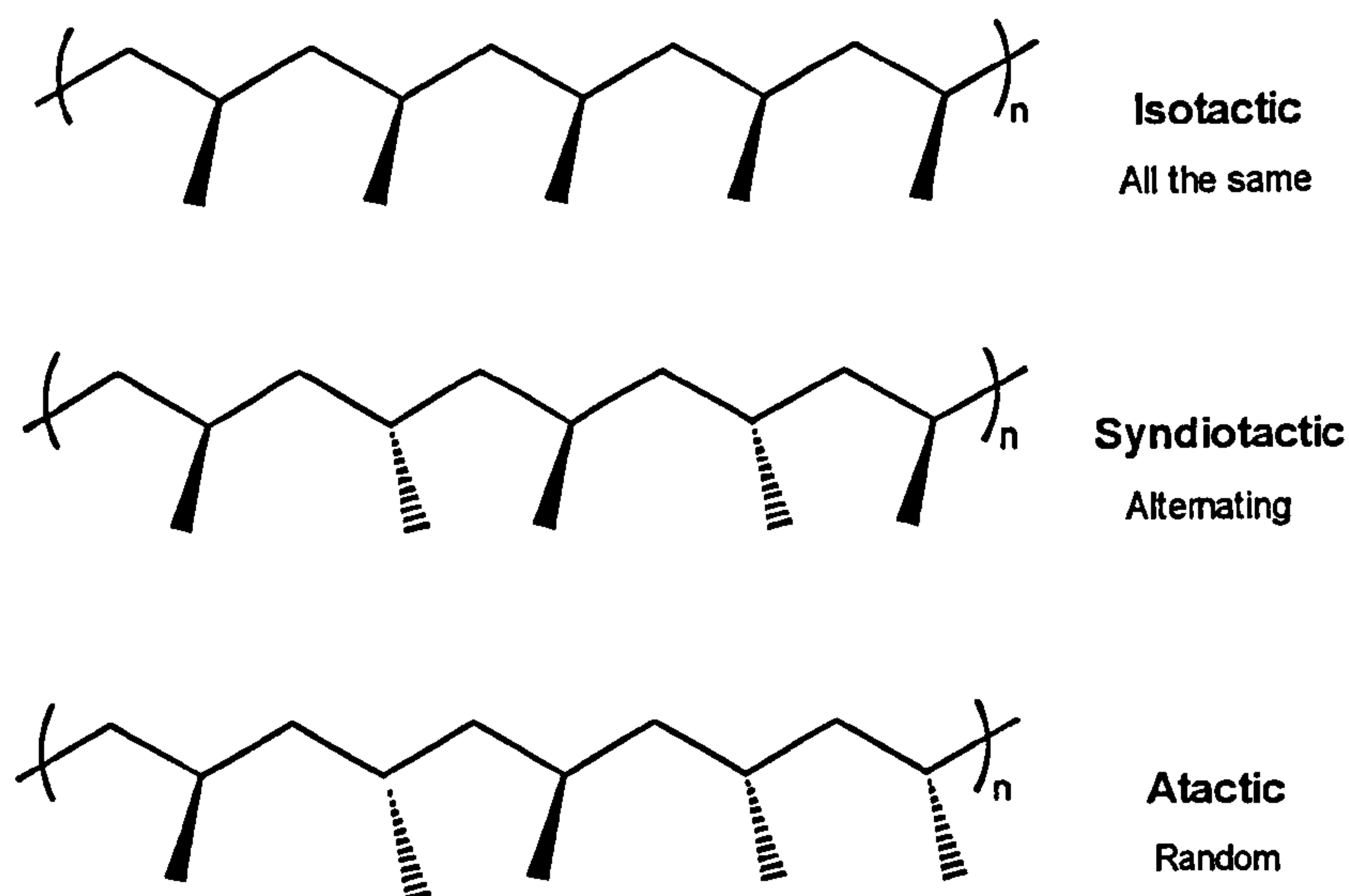


Figure 1q - Visual representation of the different classes of polymer tacticity

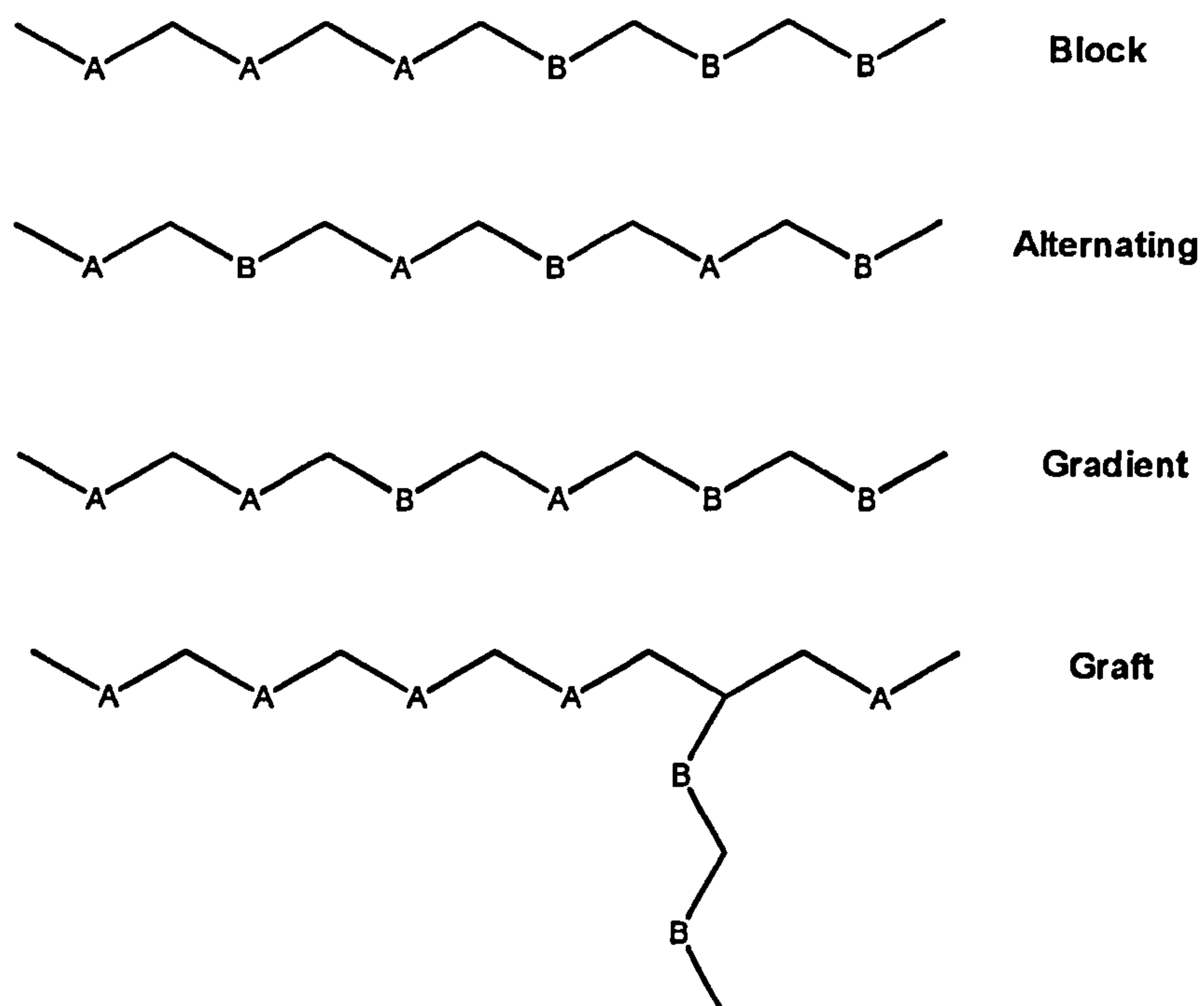


Figure 1r - Visual representation of the different classes of co-polymer system

Analysis of mass values for polymers is traditionally carried out by chromatography, most notably size exclusion chromatography (SEC) or as it is also known gel permeation

chromatography (GPC)²⁰⁷. This technique separates the sample by its hydrodynamic volume, that is the amount of space it occupies when dissolved in a specified solvent. The recognition of size is achieved using a porous material in the chromatographic column, with cavities usually of the order of 3-5 μm in diameter. Basically, as the sample passes through the column, the molecules permeate the cavities in the material and the amount of this penetration depends on their own size. Logically, sample molecules that interact in this way will take longer to pass through and be eluted from the column. In a similar way to liquid chromatography, the distribution of molecules is graduated over a period of time. However unlike with traditional liquid chromatography, the separation is not based on affinity of groups but the physical size of the molecule, which for a homologous series is of course related to its mass. In fact, SEC results in a separation of the quick-eluting high masses decreasing over time, or more precisely elution volume.

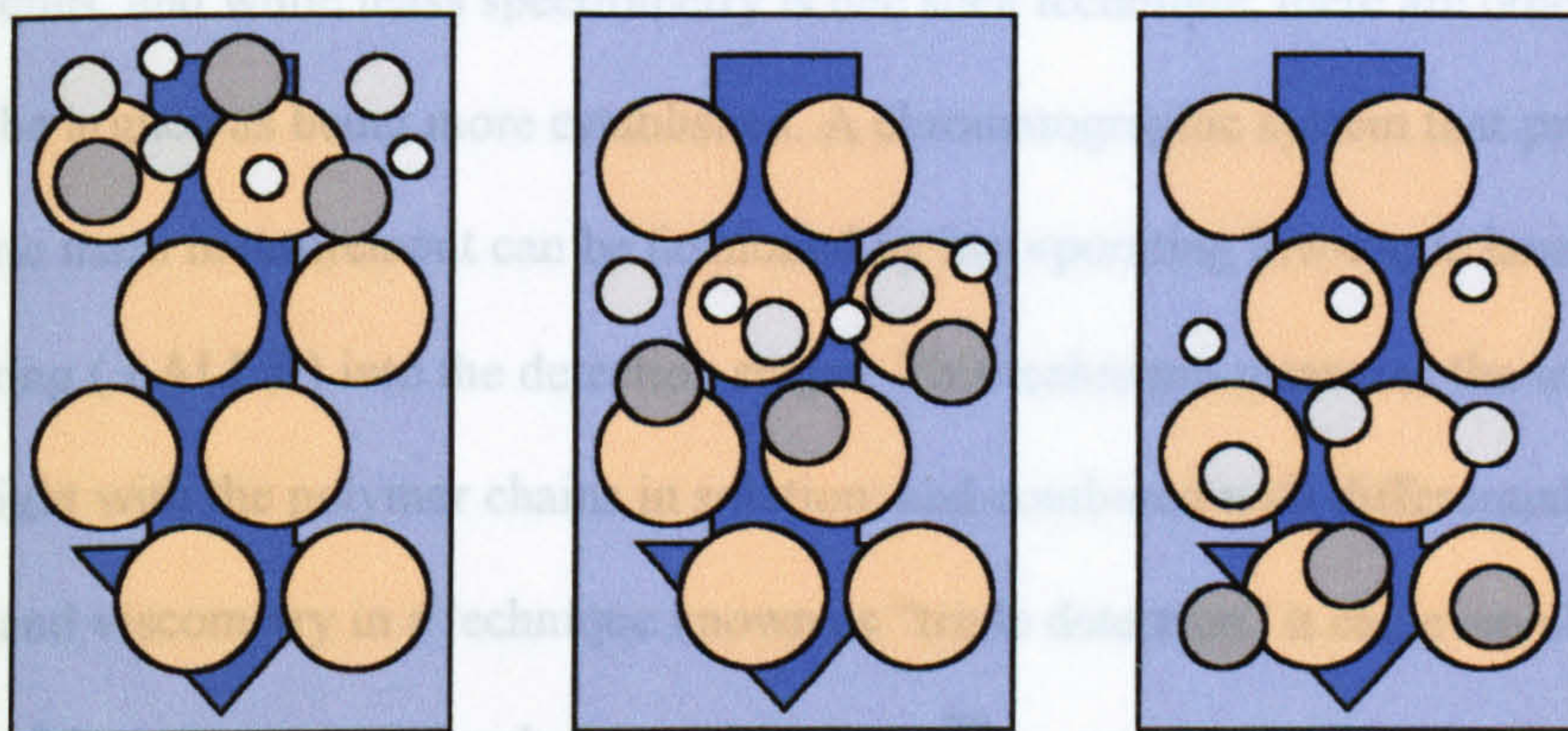


Figure 1s - Pictorial description of the size exclusion principle of mass separation

The main issue with SEC is that it is a relative technique. The time of elution is proportional to mass but must be calibrated against a known and also narrow mass standard. Since different polymers will give slightly different geometries in solution and have different atoms in their functional groups, the calibration must be performed using

²⁰⁷ ST Balke, TH Mourey, TC Schunk, Polym React Eng, 7, 429, (1999)

the actual polymer for the correct degree of accuracy^{208,209}. For the important polymers these standards do exist over a useful mass range, having been prepared from synthetic systems by preparative-scale liquid chromatographic techniques. However, even with the most common systems, the presence of any cross-linking, additional side-chains or other structural feature can change the shape of the polymer in solution and so its interaction in the SEC column. The result of this is the calibration of the system with a straight-chain standard will over-estimate the mass of the mass of the analyte. Co-polymers are also a major problem as their behaviour is obviously different from the homopolymer, so a good calibration would only be achieved using standards that are known to closely match the analyte in structure which is very often not possible. All of these concerns mean that SEC alone, while being an excellent tool for routine analysis, becomes less favourable when used as a method for novel synthesis and research in polymer systems. Here other techniques, and while mass spectrometry is one such technique, there are others that could be argued as being more established. A chromatographic system that provides absolute mass measurement can be fashioned by incorporating low-angle laser light scattering (LALLS) into the detection stages. This technique measures the interaction of laser light with the polymer chains in solution, and combined with differential refractive index and viscometry in a technique known as “triple detection” it can even allow limited study of the more complex polymer architectures²¹⁰.

Vapour-point osmometry was once a fairly well-used technique for mass determination, since the thermal properties of polymers will vary with the mass average and also distribution²¹¹. Nuclear magnetic resonance (NMR) can also be used to give fairly

²⁰⁸ S Mori, Anal Chem, 53, 1813, (1981)

²⁰⁹ M Kubin, J Liq Chem, 7, 41, (1984)

²¹⁰ MD Zammit, TP Davis, Polymer, 38, 4455, (1997)

²¹¹ A Eliassi, H Modarress, Eur Polym J, 37, 1487, (2001)

reliable results for homopolymers using a method known as “end-group analysis”²¹². This process compares the integrated intensity of the endgroup carbons with those of one of the CH₂ groups in the backbone. The ratio of these two signals gives a measurement of the chain length, and since the backbone intensity is the sum total of all chains this results in the number-average molecular weight. Again this method has problems with certain architectures, ignoring cross linking completely since it does not change the ratio of end-groups to mer units to any great extent. The ability to identify the two important signals is of paramount importance, so weak end-groups or complex pendant systems can hamper the system. Mass spectrometry would seem to be the ideal alternative, since it works on absolute mass values and is not affected by chemical concerns in the way of some other techniques. However, as this work will show there are significant problems with its use for routine analysis that go towards explaining why chromatography is still dominant.

As a polydisperse system, it is of limited value to quote fixed mass values for samples. Polymer analysis nearly always leads to three specific statistical values, those being number-average molecular weight (M_n), weight-average molecular weight (M_w) and polydispersity. These values are mathematically derived from the abundance of the various oligomeric species and together describe the distribution of masses within a system. The exact calculation for these values is somewhat dependent on the analysis technique, but the standard forms are given here. As can be seen, the weight-average biases for high masses with its square term. This means that weight-average molecular weight will always be higher than number-average, and from this polydispersity will have a value greater than one where one itself is a monodisperse system.

$$M_n = \frac{\sum \text{mass} \times \text{abundance}}{\sum \text{abundance}}$$

$$M_w = \frac{\sum \text{mass}^2 \times \text{abundance}}{\sum \text{mass} \times \text{abundance}}$$

²¹² K Hatada, T Kitayama, K Ute, Y Terawaki, T Yanagida, *Macromol*, 30, 6754, (1997)

vi. Structural Analysis

While there are well established techniques for mass measurement and certain architectures as described above, mass spectrometry may be suited to the study of polymer structure where other methods are incapable or have other problems. The analysis is usually carried out in mass spectrometry by breaking up the molecule and detecting the fragments produced²¹³. Fragmentation often occurs in the formation of ions, especially with the ‘hard’ ionisation techniques, but this is usually an unwanted side-effect and lacks the control needed for a careful analysis. Certain re-arrangement and fragmentation pathways are however well documented for organic molecules in this way, such as the McLafferty mechanism for the re-arrangement of carbonyl groups²¹⁴. For polymers, the most commonly observed result of fragmentation is in effect a reverse of the polymerisation, as the chains “unzip” back to the monomer and smaller oligomer lengths²¹⁵. More controlled fragmentation can be achieved by collision-induced dissociation (CID). This method uses a non-reactive gas placed in the path of the ion beam, causing the analyte ions to collide at high energy and so break into smaller ‘daughter’ species²¹⁶. The gases used must of course be non-reactive so as not to form chemical compounds with the analyte, for this reason nitrogen, helium and the other noble gases are commonly used. Since the technique entails releasing a gas into the vacuum system of the mass spectrometer, the operation is controlled to prevent contamination of the detection system usually in a small gas chamber with just enough of the collision gas to give the required fragmentation.

²¹³ AG Craig, H Bennich, PJ Derrick, *Austr J Chem*, 45, 403, (1992)

²¹⁴ FW McLafferty, *Interpretation of Mass Spectrometry*

²¹⁵ M Tsunekawa, S Nishio, H Sato, *J Appl Phys*, 76, 5598, (1994)

²¹⁶ AL Burlingame, DS Millington, DL Norwood, DH Russell, *Anal Chem*, 62, 268, (1990)

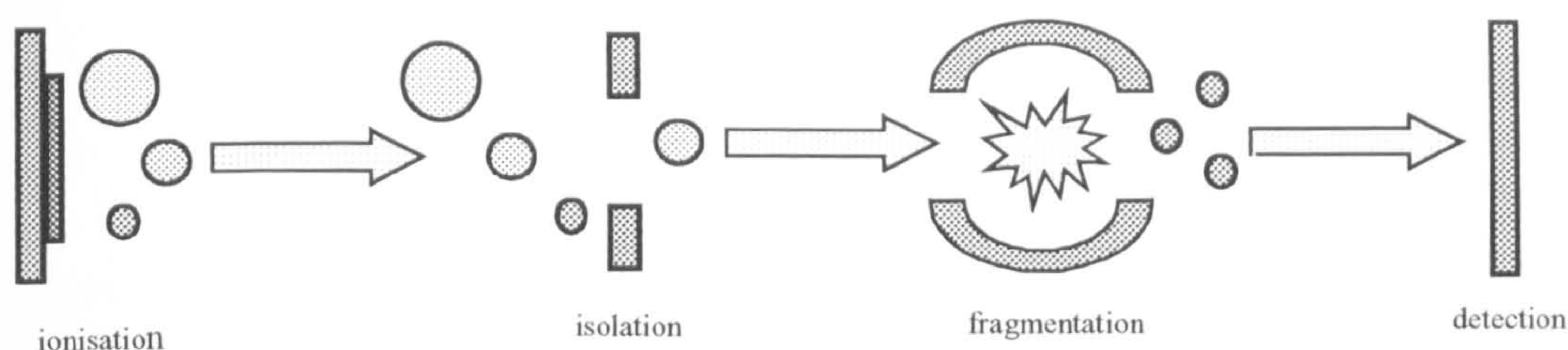


Figure 1t - Simplified model of the process involved in collision-induced dissociation

Of course, if too high a pressure of gas is used or the analyte molecules hit with too much energy, the result can be the production of exclusively small fragments that do not give structural information. For the assignment of a structure to a large molecule, an entire range of fragments is needed from the parent molecule down in a statistically-evident decreasing pattern. Such work also relies on isolating a single species to fragment, else it would be almost impossible to determine which fragment results from what parent species. This isolation can be carried out in a number of ways, the most obvious being by the action of a sector instrument. Usually the degree of isolation does not need to be too high for polymers since the separation between oligomers is typically over 20 mass units, while a window of a few mass units is typically achieved. The isolation would ideally be carried out on the most intense species possible, but to make the fragmentation easier to understand it is beneficial to use the monoisotopic signal, that is the species that is comprised of solely carbon-12 atoms. If the conditions for fragmentation are favourable, the spectra that result should allow at least major structural features to be identified. With polymers, the most obvious moieties are the repeat unit and any end-groups. Since polymers tend to fragment from the end of the chain, the detection and identification of these is one of the more facile experiments. One concern with this type of study of polymers is that the large number of species reduces the available intensity of the isolation ion. This can be overcome by various sample preparation steps including preparative-scale chromatography^{217,218}, as will be discussed in chapter five.

²¹⁷ MS Montaudou, C Puglisi, F Samperi, G Montaudou, *Rapid Comm Mass Spectrom*, 12, 519, (1998)

²¹⁸ XW Lou, JLJ van Dongen, EW Meijer, *J Chrom A*, 896, 19, (2000)

CHAPTER TWO

Experimental

i. Commercial Laser Desorption Mass Spectrometers

A number of different systems were used at various parts of this work, however they can basically be categorised in terms of the source that was interfaced to them for the experiments. The primary MALDI instruments were the Kratos Kompact MALDI IV at Warwick and the Bruker BioFlex III for the work carried out in Budapest¹. There were slight differences in the design of these two instruments, mainly in the method of loading the sample. The Bruker instrument was equipped with a reflectron detector which was used in the series of experiments carried out on it, while the majority of the work at Warwick involved linear detection for the increased signal response that provided. Equally both systems used the same type and make of laser for desorption and ionisation, although the scales for the power output differ making direct comparison impossible. However trends observed on the two systems were shown to hold to a pattern. Since the Kratos instrument was used for the larger amount of time, it will be described in more detail here.

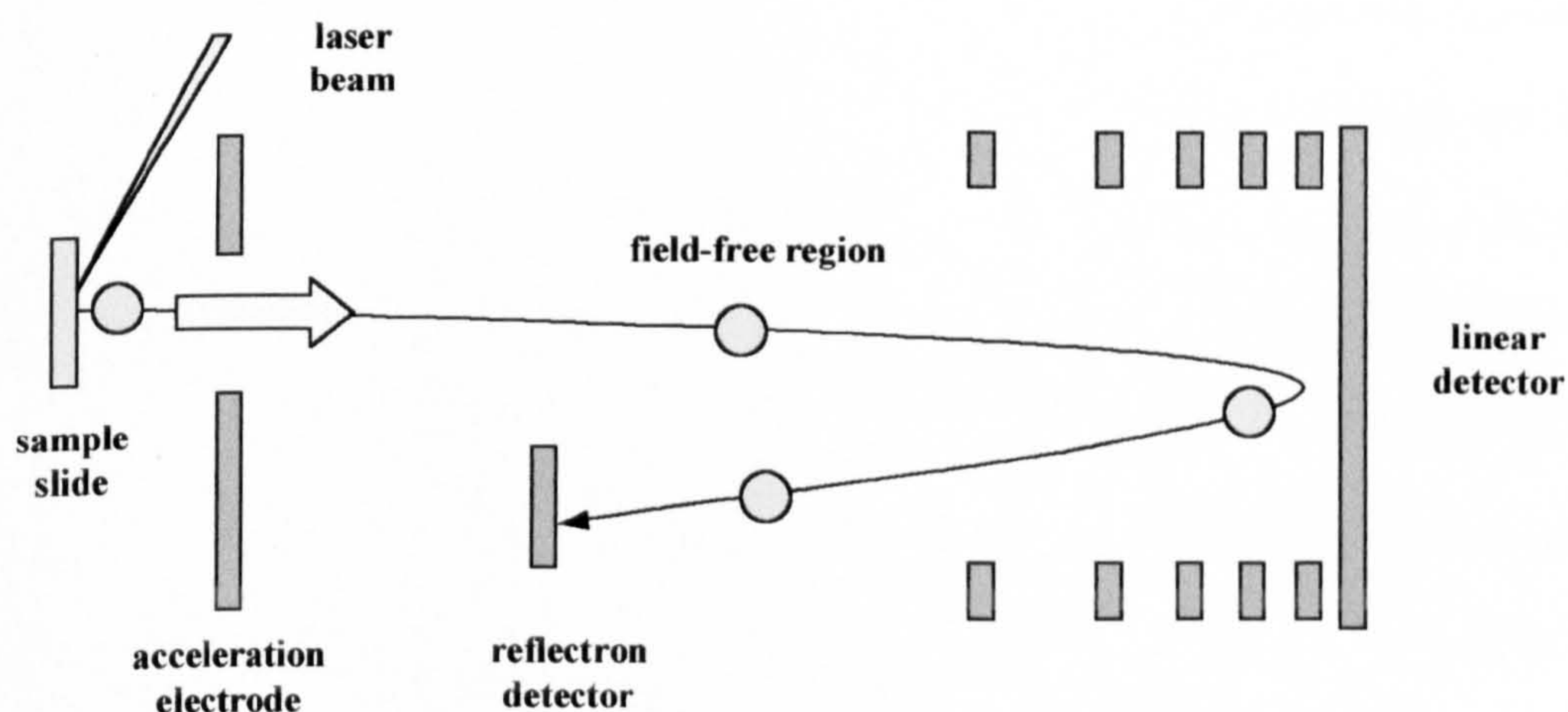


Figure 2a - Simplified layout of the Kompact IV MALDI mass spectrometer

¹ Z Szilagyi, JE Varney, PJ Derrick, K Vekey, Rapid Comm Mass Spectrom, 12, 489, (1998)

The Kompact instrument used the typical laser wavelength of 337 nanometres, provided by a nitrogen laser with a 3ns pulse width. The laser shot produced was attenuated by a neutral density filter, so giving a logarithmic scale that was fully controlled from within the computer software. An acceleration potential of +20kV was generally used to extract the ions into the flight region and towards the detector. This potential could be lowered by selecting a “low mass” mode for the instrument and could even be converted to guide negative ions, although this setting was limited in application and had not been shown to give directly comparable performance².

Although not used in the majority of the experiments, a “curved-field” reflectron is located at the end of the field-free region, which is essentially acting as a quadratic-effect electrostatic field³. This gave the instrument the capability of performing post-source decay experiments, as well as simply being used for higher mass-resolution and the filtering out of neutral species. The nature of the field in the ion mirror meant that the fragmentation experiments could be carried out without the need to step the potential. This differed in design from the detection system used in the Bruker instrument, which implemented a simpler two-stage reflectron using two variable potential gradients⁴. Here the voltages had to be more carefully selected to match the energy and mass of the ions, especially in post-source decay where the potentials were stepped through a defined sequence and the computer mathematically composited the various spectra into the final result. Apart from this distinction, the operation of the two instruments was very similar, with only the mechanism of presenting the slide being of obvious difference. In the Kompact, the rectangular slide attached to a protruding bar that was manoeuvred into the vacuum region by the machine. The Bruker had a slightly more manual approach, where the sample was put on a circular slide and attached to an externally mounted probe. After

² R Knochenmuss, V Karbach, U Wielsi, K Breuker, R Zenobi, *Rapid Comm Mass Spectrom*, 12, 529, (1988)

³ AW Colburn, AE Giannakopoulos, PJ Derrick, M von Raumer, *Eur J Mass Spectrom*, 6, 523, (2000)

being sealed, the probe was move forward into the instrument by the operator. The end result was the same however, in that the MALDI sample was positioned a set distance from the detector and oriented for the laser shots to hit the samples in turn.

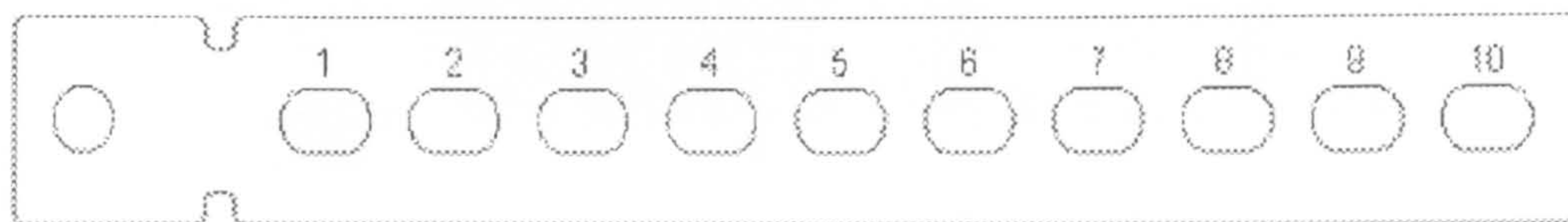


Figure 2b - Schematic of the MALDI slide used by the Kompact instruments

ii. Commercial Electrospray-based Mass Spectrometer

A single instrument was used for all of the electrospray results presented here. This was the BioAPEX-94e developed by Bruker Daltonics (Billerica, USA), a Fourier-transform ion cyclotron resonance system with 9.4 Tesla super-conducting magnet located at Warwick⁵. Although this system can also be equipped with an interim MALDI source, this was not used for any significant experiments due to issues at the time with the design of the source. The Bruker system used an Analytica electrospray source, incorporating a single hexapole in the transfer region⁶. The source could be presented with either a standard electrospray needle connected to a syringe on a stepper motor stage, or the newer nanospray needle design which formed its own reservoir system. The entire progression of the source area is shown below along with the various pumping stages that brought the system down to the high vacuum needed in the cell cavity.

⁴ WB Brinckerhoff, GG Manadagzo, RW McEntire, AF Cheng, WJ Green, Rev Sci Instrum, 71, 536, (2000)

⁵ M Palmblad, K Hakansson, P Hakansson, XD Feng, HJ Cooper, AE Giannakopoulos, PS Green, PJ Derrick, Eur J Mass Spectrom, 6, 267, (2000)

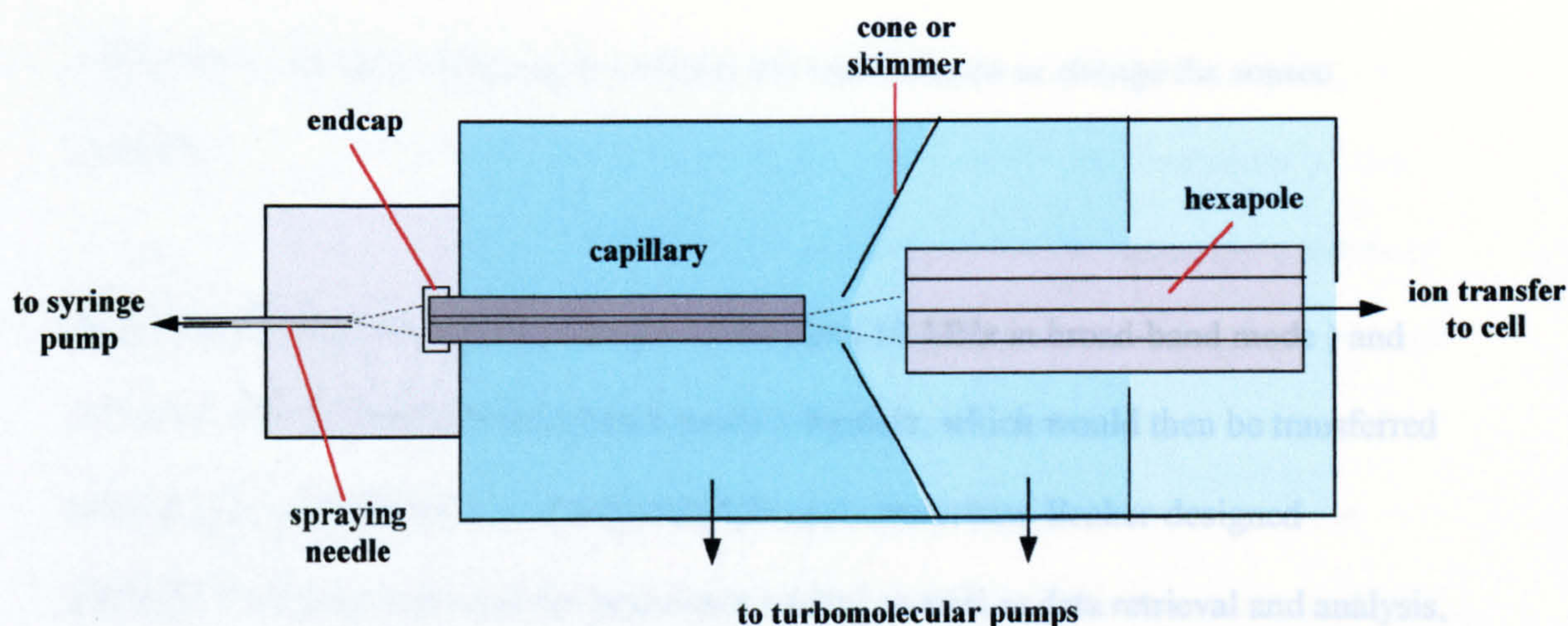


Figure 2c - Schematic of the source region showing the Analytica electrospray system

The horizontal bore magnet was housed in the large metal frame, which contained passive shielding to reduce the stray field. The magnet itself was a super-conducting niobium-tin (Nb_3Sn) system cooled by liquid helium and in turn by a greater volume of liquid nitrogen. At the centre of the magnetic field lay the InfinityTM cell, a cylindrical arrangement of a pair of detection plates with two offset excitation plates⁷. The cell was capped with a third set of plates, which provided an annular entrance to allow access of ions from the external source. A small potential was applied perpendicular to the motion of the ions as they entered the cell, referred to as SidekickTM, which decreased their forward motion and increased the chance of them being retained in the cell volume⁸. The entire area was held at a ultra-high vacuum using cryogenic pumps to sustain a base pressure below 5×10^{-9} mbar. Extra pumping was also required in the source region to cope with the ambient conditions present at the beginning of the process. The ESI source used a mechanical pump combined with a turbomolecular pump, which together allowed a wide range of reagent and buffer gases to be used. A gate valve isolated the cell

⁶ MV Gorshkov, L PasaTolic, JE Bruce, GA Anderson, RD Smith, Anal Chem, 69, 1307, (1997)

⁷ P Caravatti, M Allemann, Org Mass Spectrom, 26, 514, (1991)

⁸ SA Hofstadler, KA Sannos-Lowrey, RH Griffey, Rapid Comm Mass Spectrom, 15, 945, (2001)

completely in the case of having to perform any maintenance or change the source assembly.

Data from the cell was acquired using a 12-bit fast (10 MHz in broad-band mode) and 14/16-bit slow (400 kHz in heterodyne mode) digitiser, which would then be transferred onto an Indy workstation over a dedicated Ethernet connection. Bruker-designed XMASSTM software was used for instrument control as well as data retrieval and analysis, running under the IRIX operating system. Data storage could be made to magneto-optical disc, DAT tape or transfer by network FTP to other IBM-type computers within the group running a Microsoft Windows-compatible version of the XMASS system.

The ESI source (Analytica, Branford, CT, USA) centred around a glass capillary 15 centimetres in length and with an internal diameter of 0.5mm. The solvent was directed into the capillary from a stainless steel spraying needle with a 0.1mm internal diameter, with a stream of nitrogen acting as a nebulising gas to assist in the spraying process. A heated gas was also used in the counter-direction to speed the solvent evaporation. The needle tip could be accurately controlled in all three directions to aim the spray into the opening of the end cap of the capillary. Following exit from the capillary, a skimmer separated the expanding Taylor cone from another pumped region. The skimmer sampled from the ion population and introduced them into a computer-controlled hexapole ion trap. The ions were then accumulated in the trap for a certain dwell time before being pulsed into the spectrometer. The entire process was automated, the sample being continuously supplied from a syringe locked into a stepper-motor pump and connected to the spray needle by a short length of small bore tubing.

The resolving power of the instrument is defined by $m/\Delta m_{\text{fwhm}}$, the latter part being the width of the peak at half of the maximum intensity (“full width - half maximum”). This resolution is orders of magnitude higher than was necessary for the successful analysis of the polymer samples for this work. It is also observed that the increased magnetic strength reduced the likelihood of peak coalescence, which can reduce the ability to use the full resolving power of the instrument, and also prevent the observation of fine structure present in the spectra. The mass accuracy, that is the accuracy of the values obtained for the sample masses, was very high. Experiments carried out by the group at Warwick regularly gave accuracies in the order of a few ppm or better over a significant mass range. The calibration of the system was usually carried out using a commercial mixture of seven peptides (Calibrant G2421A, Hewlett Packard) which gives peaks in the m/z range of 118 to 2722. The XMASS software was then capable of performing a two or three point calibration with a linear regression or, for a greater degree of matching, a quadratic expression. This level of accuracy and the impressive dynamic range of the system were, as stated before, much higher than actually required for the polymer analysis undertaken. However, the capabilities were useful in the absolute identification of novel polymers and also fragments produced by SORI or other such techniques⁹.

iii. Research Mass Spectrometers

The final instrument used in a significant amount of work detailed here was a hybrid tandem mass spectrometer known as the Mag-TOF¹⁰. The majority of tandem systems employ scanning across a mass range for detection just as described for sector instruments. This means that a large percentage of the produced ions are in fact wasted. Sensitivity is a great concern, as a high signal must be produced to ensure adequate

⁹ SJ Pastor, CL Wilkins, Int J Mass Spectrom, 175, 81, (1998)

detection. The Mag-TOF system avoided this problem by employing a reflectron time-of-flight analyser which by its nature detected all produced ions simultaneously. This detector was referred to as MS-2, as it represents the second stage of the tandem system. The first stage (MS-1) located before the collision cell comprised a modified Kratos Concept H double-focusing magnetic sector instrument. This instrument used the Nier-Johnson geometry for the ion path as described in the introduction and is shown in schematic below.

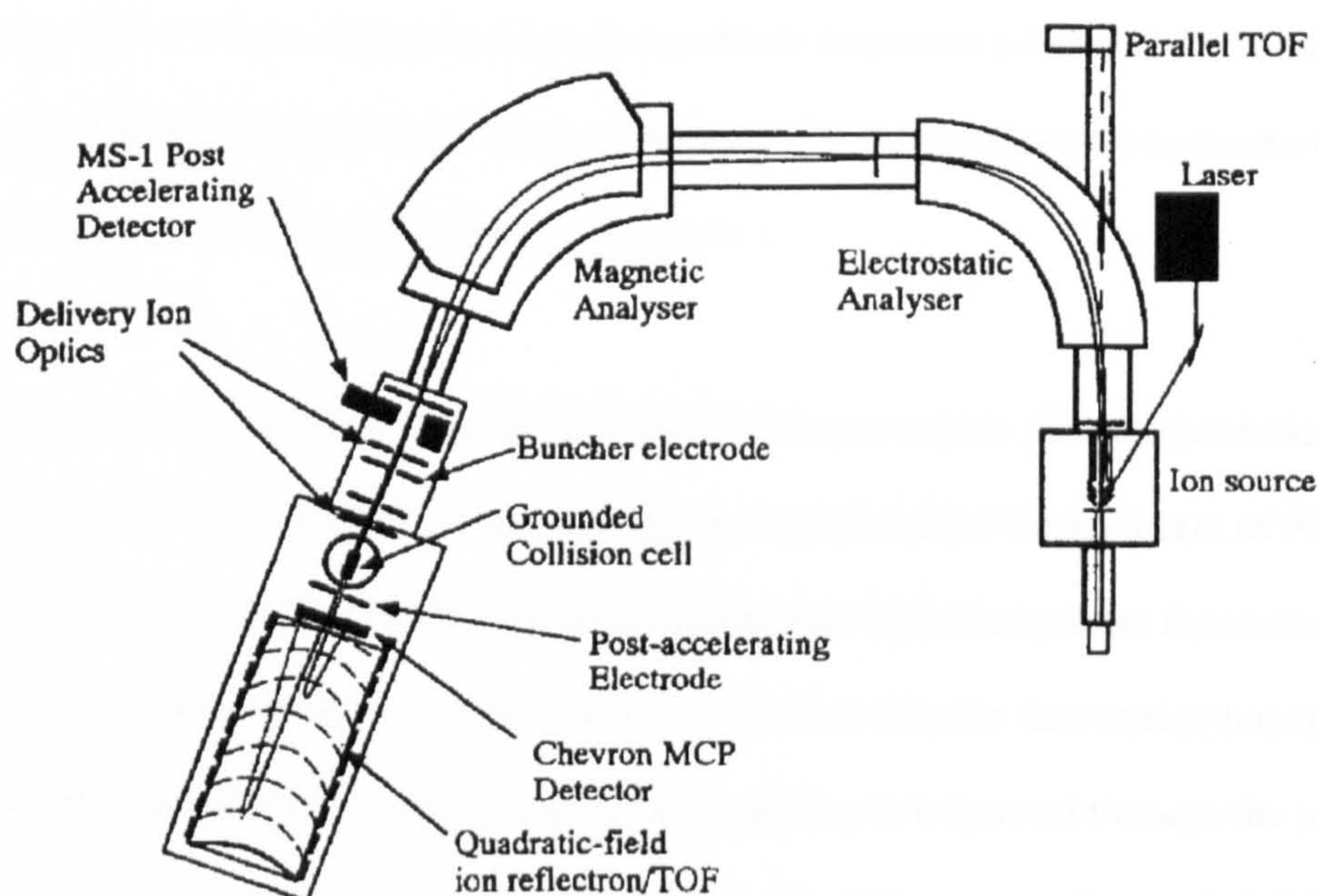


Figure 2d - Top-down schematic of the Mag-TOF instrument

The preferred source used in this system was MALDI, although the design was such that it is capable of using a range of other pulsed techniques. The sample was loaded onto a single sample spot located on the top of a probe which could be manipulated to move the tip in all three directions. The fact that it was a pulsed source improved acquisition of the

¹⁰ UN Anderson, AW Colburn, AA Makarov, EN Raptakis, DJ Reynolds, SC Davis, AD Hoffman, S Thomson, PJ Derrick, Rev Sci Instrum, 69, 1650, (1998)

CID spectra, but did bring with it its own complications such as the timing of the various operations and issues of calibration. The MALDI source centred around a 337 nanometre nitrogen laser (Laser Science Inc, Newton, USA) external to the source region which could produce up to 250 μ J per 3ns pulse. A variable density wheel positioned between the laser and entry into the machine allowed computer control of the laser power delivered to the sample. The laser impacted on the sample on its electrically isolated stage, with the important z-axis position controlled by a vernier screw to the side of the probe. This distance was set so the surface of the tip touched the source cradle and sits just behind a plate design to direct the ion beam formed in a forward direction. The accelerating electrode was held at a potential of 8kV, giving source ions entering the instrument a laboratory-frame energy of 8keV

The sector part of the instrument followed the source region. The electrostatic analyser being formed from two curved plates giving a deflection of the ion beam of 90 degrees, which also had a hole positioned on the initial axis of the beam from the source and leading to a linear time-of-flight detector. This first detector was used to tune the source parameters and ensured a high enough ion intensity to be passed through the rest of the instrument and in particular the collision cell. The hole was small enough however so that it did not have a detrimental effect on the field within the electrostatic sector during its operation. The subsequent magnetic sector bent the ion beam to a lower angle of 60 degrees, focusing the ions to a point just after the exit slit. In order to optimise the ion transmission through the mass analyser, a second detector was located at this point and monitored using an electronic oscilloscope. This allowed the double-focusing part of the instrument to be tuned for optimum performance and accurate selection of the mass peak to be isolated, which was the monoisotopic species in most cases.

As the ions move through an instrument, they lose spatial and temporal focus. The spatial component in this case was dealt with by the action of the two sectors, but ions of the same mass still became spread out over an increased time-of-flight. This had to be rectified before the ions entered the collision cell, else the times-of-flight of the fragments in the MS2 detector would not be accurate to their mass. The correction was carried out by insertion of an ion buncher at the egress of the magnetic sector and following the in-line detector. Consisting of two charged plates of 1mm stainless steel separated by a gap of 3cm, the buncher was large enough to completely contain an ion packet with a spread of up to 25eV. A high-voltage pulse was applied to the first electrode using a Behlke (Frankfurt, Germany) high-speed and high-voltage switch. This pulse was timed on a delay from the initial laser shot and controlled from the computer based on the entered mass of the isolated ion packet. Since the second electrode, the one nearest the MS2 detector, was grounded the pulse affected the ions in the buncher depending on their distance from the first plate¹¹. This imparted an amount of kinetic energy onto the ions that was proportional to their progress, so effectively giving the later ions a boost. The process had the effect of compressing the ion packet and focusing it at a point just inside the start of the reflectron time-of-flight detector. Although this corrected the temporal spread, it in doing so created a large energy spread that has no effect on the quadratic-field time-of-flight detection.

The collision cell that followed the buncher was a 10mm by 7mm cavity that allowed entry of a chosen gas by means of a small leak valve. The gases usually employed were helium and argon from dedicated cylinders within the laboratory and using an interchangeable regulator to control the pressure. This gave a gas pressure in the collision cell that was approximately an order of magnitude higher than for the rest of the

¹¹ AR Bottrill, AE Giannakopoulos, C Waterson, DM Haddleton, KS Lee, PJ Derrick, Anal Chem, 71, 3637, (1999)

spectrometer (around 10^{-4} torr), which resulted in a transmission of ions from the parent beam of about 60-70%. Ion optics following the cell consists of an extraction electrode held at -2150V and a z-deflector that imparted a slight upward vector to the beam. This redirection targeted the beam onto the microchannel plate detector after the reflection in the ion mirror.

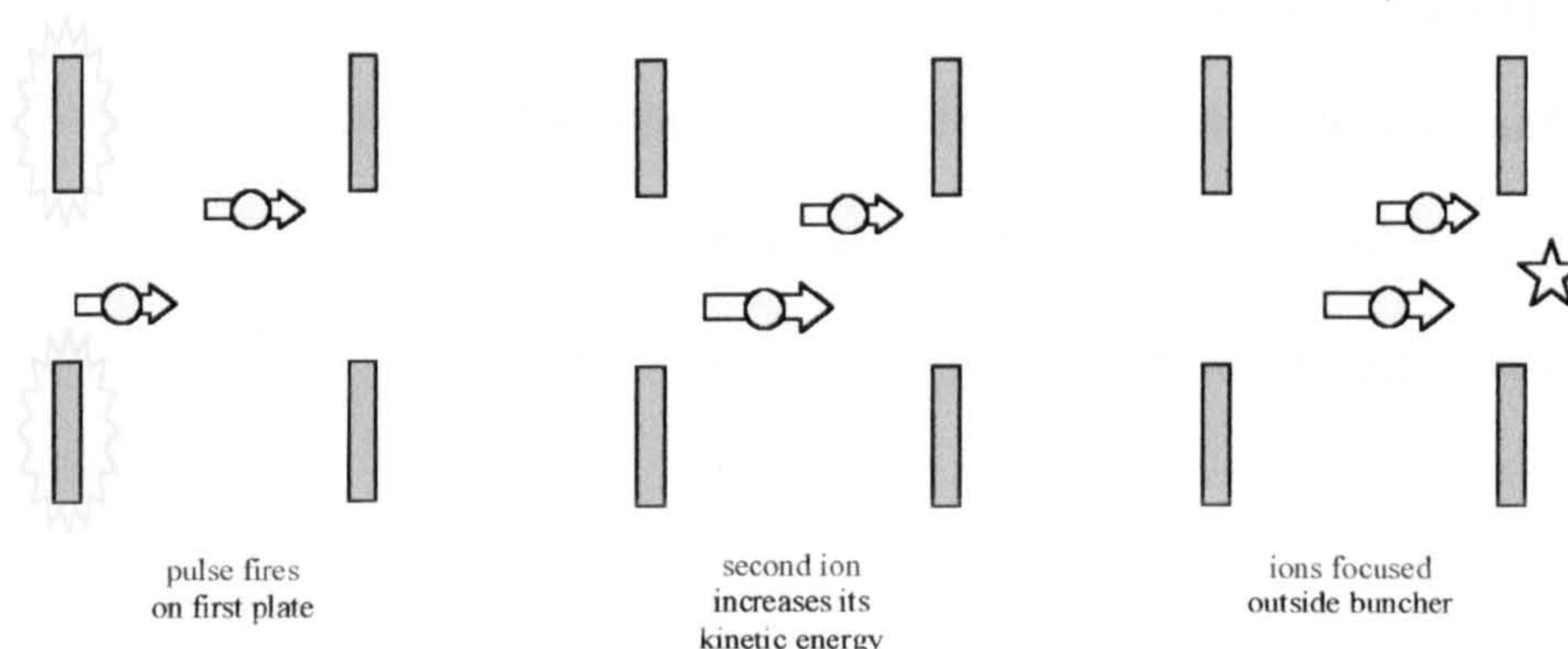


Figure 2e - Diagram showing a simplified representation of the operation of ion buncher

The ion mirror created a field shaped to fit a quadratic equation by means of 38 shaped copper electrodes with small insulating gaps between them. A resistor chain running along the mirror provided a controlled field that increases into the mirror, where the density of electrodes was greatest. The potential of the mirror therefore varied from -2.15kV at the front to +12kV at the extreme rear, supplied to the instrument by a purpose-built power source (HD Technologies, Manchester). The ion beam was directed by this arrangement with a high precision onto the detector, which was situated directly above the initial entry into the chamber. The 10×8cm microchannel plate detected all of the ions, the signal being passed to the computer where the masses were summated. With the low intensity of the signals, a large number of shots were required and acquisitions can often run to a number of hours for a high-quality CID spectrum.

iv. Chromatographic Systems

At various stages of the work, chromatography was used to gauge a benchmark value for samples or to verify the masses of unknown commercial analytes. The majority of the time this was carried out using gel permeation chromatography on one of the systems located in the Department of Chemistry within Professor Haddleton's research group. Results were also available from certain samples run on systems at Shell research. The Warwick systems were based on PL mixed bed columns and usually ran on tetrahydrofuran, although in later work an aqueous eluent system was also used for certain samples¹².

The SEC system comprised of a high-performance piston pump (ICI Instruments) with an injection valve and loop capable of holding 20 μ l of sample. The pump ran the solvent through the columns at 1ml min⁻¹, usually with tetrahydrofuran but an aqueous system also existed and was used for later work. This took the sample through the column set and to a refractive index detector, which worked by comparing the eluent against a base reference of pure solvent. Toluene (0.2% w/w) was used as an internal calibrant as it produced a sharp and high intensity peak at low mass. The columns were preceded by a 5 μ bead-size guard column to filter out an undissolved particulate matter that could block the main separating columns. Separation was then achieved by a 300x7.5mm Mixed-E column with a 3 μ m bead which gave a good dynamic range that was capable of being calibrated to a mass of over 10,000 units. The signal that this sent from the detector was passed by a data capture unit (DCU) to a PC using Polymer Laboratories Calibre™ software. Once the toluene peak was identified, the sample envelope and baseline could be manually set and so led to a calculation of the mass-average values.

v. Chemicals and Experimental Samples

Very few actual samples were used given the large volume of data acquired, this being in order to maximise the ability to cross-compare results and improve reliability of the information. The largest class used were polyglycols, a relatively simple oxygen-centred condensation polymer, which was commercially available with a range of different repeat units, co-polymer combinations and of course mass averages. The commercial samples tended to be formed from a liquid chromatographic fraction, which gives a fairly consistent mass distribution and also a narrower range than would have been the case even for a moderated synthesis. The smallest of the glycols used was poly(ethyleneglycol) which its mer unit mass of 44, compared to a repeat of every 58 units for its larger brother poly(propyleneglycol). Co-polymers of the two were also explored using dissociation experiments to try and observe the architecture of the polymer chain.

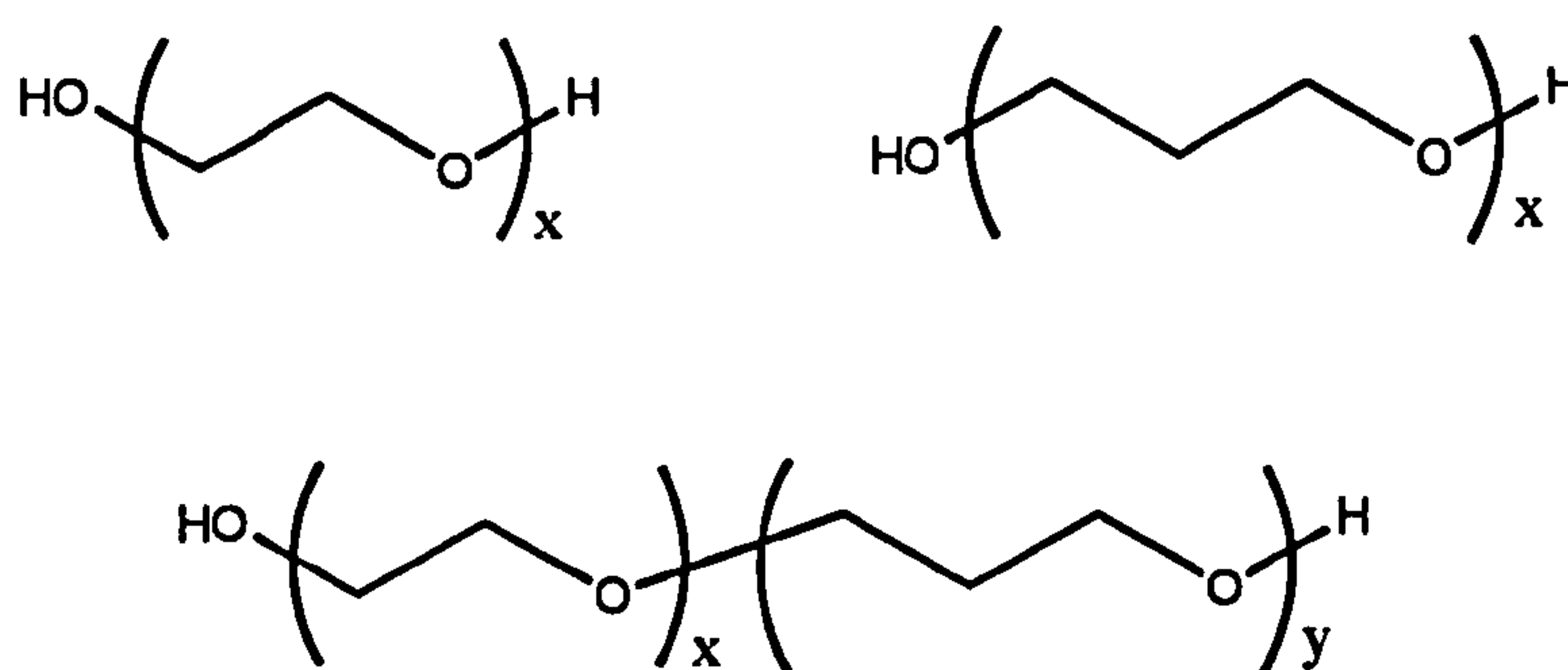


Figure 2f - Structure of PEG / PPG and their simple block co-polymer

A subtle variant on poly(ethyleneglycol), which tended to be terminated by a hydroxy group, were the range of α -ethoxylate detergents manufactured by Shell UK under the tradename Needol™. These combined the oxygenate polymer with a hydrocarbon tail

¹² JE Rollings, A Bose, JM Caruthers, GT Tsao, MR Okos, Adv Chem Series, 203, 345, (1983)

that led to their surfactant action¹³. Most of the commercial samples comprised a distribution of ethoxy group lengths and also a selection of different hydrocarbon moieties. This had the effect of presenting a homologous series of polymers, especially since the hydrocarbon is not synthesised to a statistical distribution but rather resulted from a petrochemical fraction. To simplify the situation for analysis, a series of product standards were acquired from Shell that had only on average two or three ethoxy groups, so giving a very narrow distribution. The more commercially-natured Needol23-6.5 however, presented a reasonable number of repeat units with its average at 6.5 but extending to over fifteen. The 23 component of the name indicated that there were twelve carbon and thirteen carbon long chains in the system. The distribution given from these systems was hence unlike the standard Gaussian form of higher mass polymers, in fact it more resembled an exponential decay after the peak maxima. To achieve this effect with pure glycols would have required extremely low mass that brought with it added handling complications. Whereas the long hydrocarbons of the Needols made them fairly viscous liquid and also more importantly not overly volatile.

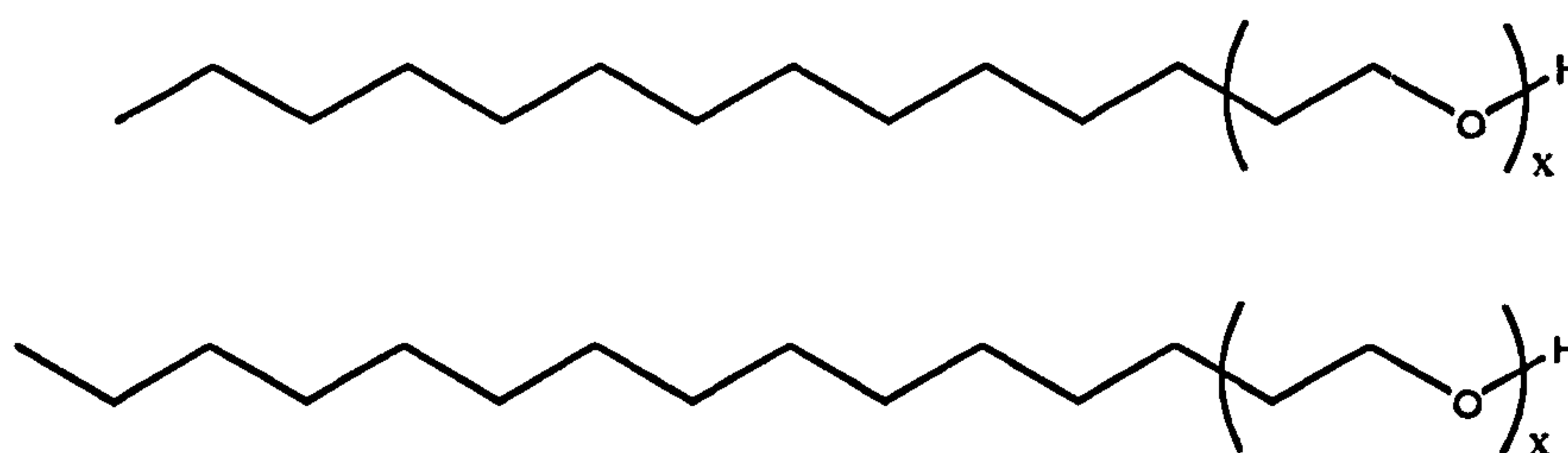


Figure 2g - Chemical structure of Needol showing a C12 and C13 variation

The acrylate polymers used in this study were all synthesised by Professor Haddleton's group. The process used a free-radical addition moderated by the presence of small amounts of cobaloxime boron trifluoride (CoBF). This cobalt-containing macrocycle was capable of intercepting the radical propagation as shown below¹⁴. By varying the

¹³ I Hama, M Sakaki, H Sasamoto, J Am Oil Chem Soc, 74, 823, (1997)

¹⁴ TP Davis, D Kulkulj, DM Haddleton, Trends Polym Sci, 3, 365, (1995)

amount of CoBF, although still at catalytic levels, it was therefore possible to control the length of the polymer chains and also affect the polydispersity of the resultant polymer. A wide range of substituted acrylates, as well as other monomeric systems, could be treated in this way such as the poly(hydroxyethylmethacrylate) used in the Budapest MALDI work documented herein.

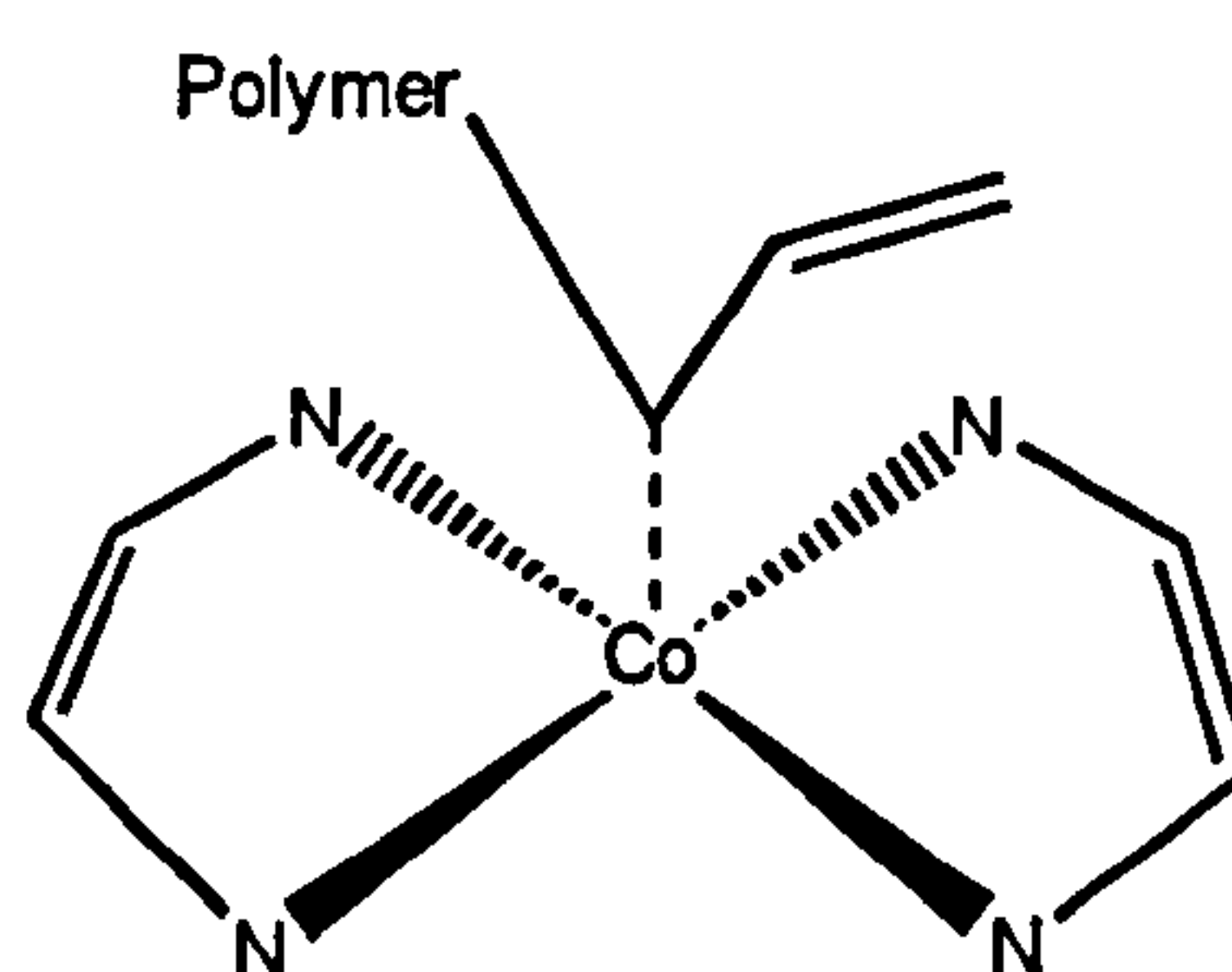


Figure 2h - Structure of CoBF showing its binding to a growing polymer chain

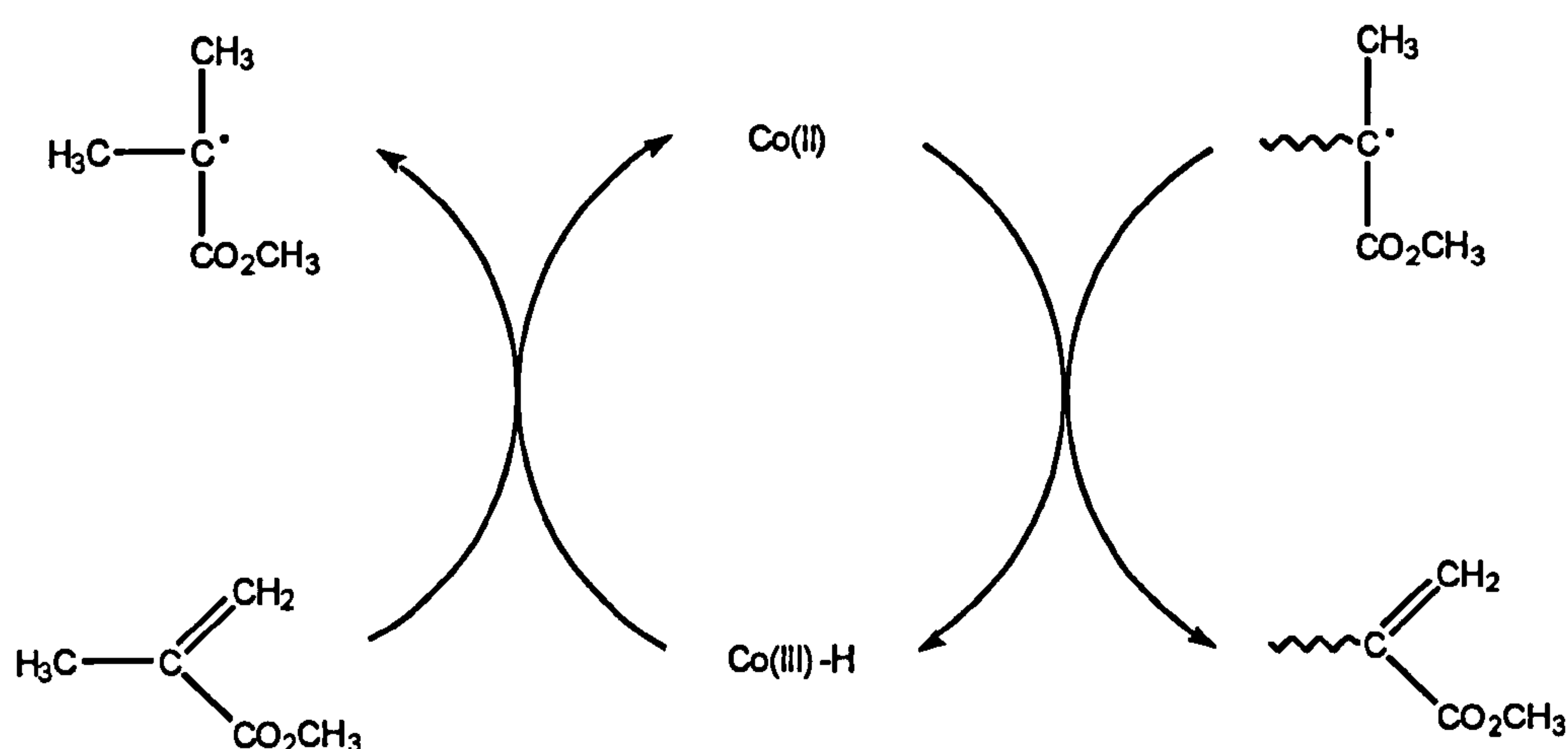


Figure 2i - Catalytic chain transfer polymerisation mediated by cobalt

A wide range of polymers can be produced by this method, including the series of acrylates studied in this work. As well as the more typical poly(methylmethacrylate) and poly(benzylmethacrylate), a sample of polymerised hydroxyethylmethacrylate (HEMA) was used which is better solvated in aqueous systems and also has a greater proportion of oxygen atoms in the chain.

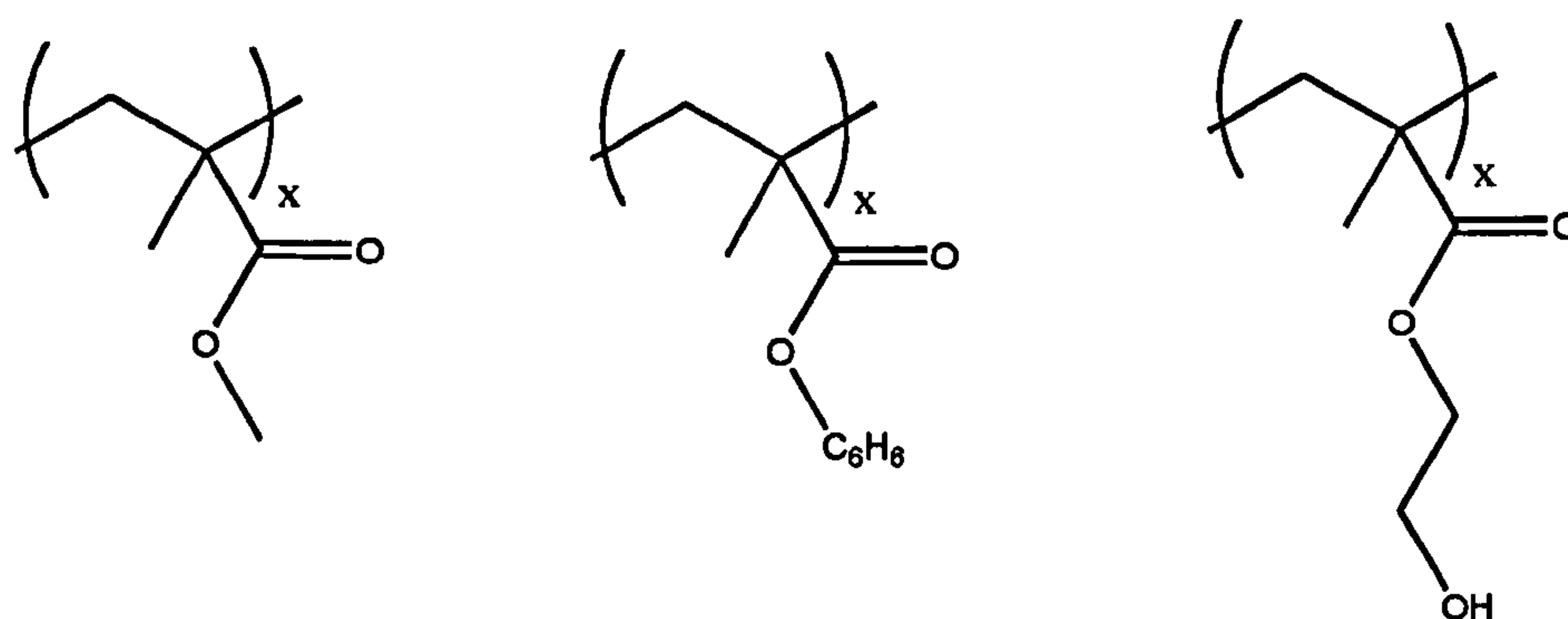


Figure 2j - Structure of methyl, benzyl and hydroxyethylmethacrylate polymers

All of the matrices used in the work were readily obtained from Sigma-Aldrich, the most prominent being 2,5-dihydroxybenzoic acid (DHB), sudan orange G (an azo dye), and dithranol. The structures of all the major matrices used are shown below, demonstrating the fact that most active matrix compounds are based around an aromatic core group. Nearly all of these matrices are soluble in aqueous systems, which commonly had fairly high percentages of organic solvent add to make it more amenable to any interaction with the polymer solutions. Standard grade solvents were used in all preparations, chromatographic purity not being required especially in the case of MALDI where the solvent is not thought to be present to any great extent in the final prepared sample.

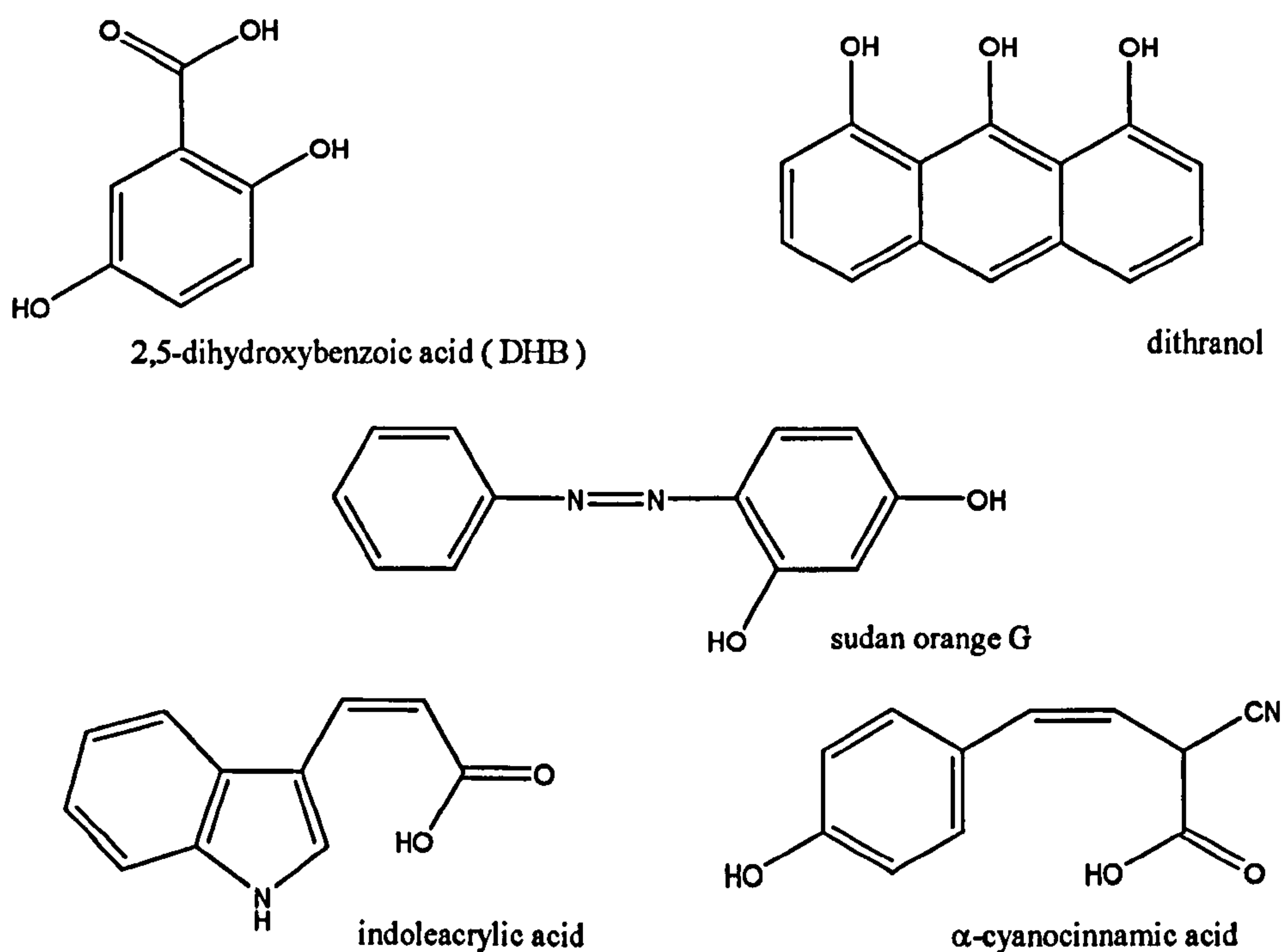


Figure 2k - Common matrix systems used in this study

CHAPTER THREE

Matrix-Assisted Laser Desorption / Ionisation

The mass spectrometric technique that has seen the greatest application to polymers is certainly matrix-assisted laser desorption / ionisation. Avoiding the solvent and multiple-charge issues of electrospray, it has been applied to routine measurement and the study of novel polymer systems.

i. Overview

This chapter outlines work using matrix-assisted laser desorption / ionisation (MALDI) as the method of ionisation for the analysis of polymeric materials. Nearly all of the results were obtained in conjunction with time-of-flight separation and detection, which is by far the most common combination of techniques in this field. Although the Fourier-transform ion cyclotron resonance instrument was equipped with a MALDI source, it was not as accessible as the other instruments and the high resolution of the instrument was not of particular benefit to this study. In most cases, where polymers were involved, the experimental aims were to monitor the mass averages and changes therein. These values were obtained from the ion intensities of the mass spectra, which were exported into Microsoft Excel as a text delimited data set. Since the actual mass values relating to the intensities were affected by the calibration and also of course were dependent on the attached cation, they were replaced by accurate mass values from the known oligomer structures. This corrected mass value was then used in the calculations to give number-average and weight-average molecular weight, which were the two statistical masses that were of interest for this work. With the information in this form, it was also possible to observe patterns in the mass distribution and derive values pertaining to the mass accuracy and reliability as will be shown in the last part of this chapter. The fragmentation of polymers ionised by MALDI will be discussed separately in chapter five.

ii. Discussion of Sample Preparation Issues

As mentioned in the introduction, the MALDI experiment can be broken down into a number of stages and each can affect the resultant mass spectrum. The first stage is the preparation of the solid sample, which incorporates the concerns of selection of matrix, solvent, absolute and relative concentrations, as well as the method of application and drying¹. This very manual task therefore has a large number of variables and many attempts have been made to simplify the procedure and also reduce the impact of the practitioner on the result². If a method can be made independent of the person preparing the slide, then it is assumed that variations from day to day will be greatly reduced.

The choices of matrix and solvent are of course sample dependent and their effects will be discussed in more detail in a subsequent section. The method of application of the sample to the slide however, is pervasive and so of prime importance to the use of MALDI. The most straight-forward technique, and for that reason perhaps the most widely used, is referred to as the “dried droplet”³. This is simply where all of the components are mixed together in a solvent and applied as a single droplet to the slide. Once dried, it is expected that a single layer of reasonable distribution and crystallinity will be formed. This expectation is of course not always borne out, with a tendency to form an uneven surface as the solvent front pushes outwards and takes much of the dissolved sample with it. This has been confirmed for a number of common matrices by observations using atomic force microscopy (AFM), which showed a flat and thin profile at the centre leading to a sharp ridge at the edge of the solvent front⁴. The thickness of this ridge varied, but was always an order of magnitude more than the vast

¹ DC Schreimer, Anal Chem, 69, 4169, (1997)

² SD Hanton, J Am Soc Mass Spectrom, 10, 104, (1999)

³ DA Allwood, IK Perera, J Perkins, PE Dyer, GA Oldershaw, Appl Surf Sci, 103, 231, (1996)

⁴ M Handschuh, S Nettesheim, R Zenobi, Appl Surf Sci, 137, 125, (1999)

majority of the sample area. The simplest approach to improve on this is to separate the different components into layers. It has been shown that applying the matrix, followed by the sample with or without added salts, can give improvements in intensity and reliability⁵.

The use of layers allows different solvent regimes to be implemented for the matrix and sample. This can be especially useful for many industrial polymers, which are often less amenable to the water-based systems typically used with most common matrices. Using a more suitable solvent, helps ensure a higher degree of uniform crystallinity, which has been observed to improve the MALDI response. There is, however, an issue here in the interaction of the different solid layers, especially given the relative miscibility of two different solvent systems. It could be rationalised that the top liquid layer partially dissolves the deposited matrix, then dries to give an intermediary layer containing both matrix and analyte. It is however unknown how important this mixing of layers is to the process. Certainly, systems where the top layer was incapable of dissolving the matrix did not show as great an improvement in performance, suggesting it is of some importance. Another slight variation reported⁶ was to use a fast-drying system, with a highly volatile solvent such as hexafluoro-2-propanol (HFIP), to minimise disruption of the lower layer or on its own to give a higher degree of uniformity across the sample spot. Although such steps gave slight improvements in work carried out here, it was often not enough to justify the extra preparatory steps needed, especially in developing methods for industry where a large number of samples have to be analysed in a shorter time than usually available for research purposes.

⁵ AM Hoberg, DM Haddleton, PJ Derrick, JH Scrivens, AT Jackson, Eur Mass Spectrom, 4, 435, (1998)

⁶ H Sato, H Ohtani, S Tsuge, N Hayashi, K Katoh, E Masuda, K Ohnishi, Rapid Comm Mass Spectrom, 15, 82, (2001)

A completely different approach to sample application has involved the use of a spraying method⁷. The goal was to establish an even layer, building up the substrate across the sample with the relevant amounts of each component. As well as physical spraying techniques using an aerosol gas, approaches involving using in essence electrospray technology have been explored⁸. With both systems, a fairly volatile solvent was required so as to prevent pooling of the liquid on the surface of the slide. This work was continued with the use of a simple artist's airbrush with an external gas supply was found to give reasonable results. This technique was particularly suitable for polymeric systems, as it gave a reliable method for the application of solvent systems such as tetrahydrofuran and dichloromethane. While these solvents are volatile, they also have low viscosity and surface tension, which means that droplets tend to spread out over a large area. In normal MALDI approaches with multiple-spot slides, this can lead to low concentrations at the centre of the sample spots or even cross-contamination of adjoining samples. Spraying overcame some of these issues, but it was rather time consuming and required some trial and error to develop a successful methodology. Early experiments in this study with Shell detergent polymer systems, using a Badger airbrush with a portable compressed air generator, gave reliable results but not sufficiently improved over carefully prepared droplet samples to warrant the extra effort. Airbrushing was however a useful tool for the advance preparation of slides of matrix, which could then be kept for a certain period before being used with an applied analyte. Such prepared systems have been commercially realised by Viscotek using a 'jet nozzle' technology which is also compatible with the effluent from liquid chromatography systems. This proprietary system centres around a fairly powerful aerosol spray mechanism and is also used as an off-line interface for liquid chromatography, in particular by gel permeation chromatography (GPC), and MALDI. While having two systems that are in essence

⁷ DM Haddleton, C Waterson, PJ Derrick, Eur Mass Spectrom, 4, 203, (1998)

mass separations after each other may seem an unnecessary duplication, it has a number of beneficial outcomes. If the original sample is a mixture, the GPC separates the components out and the mass spectrometry can then be used to speciate the simplified sample⁹. It is also one way to analyse polymers with a very broad mass distribution, which have proven to be a problem for pure MALDI approaches^{10,11}. The GPC system can be used to establish a calibrated value for the mass average, while the mass spectrometry performs sample identification, a task it is far more suited for as is shown by many of the results in this section.

iii. Presentation of Sample Preparation Results

a) Sample Application Techniques

As has been mentioned in the preceding section, organic solvents were often found to prove a difficulty for MALDI use given their tendency to spread over the slide. This was not helped by the hydrophobic nature of the stainless steel substrate that gave little impediment to the movement of non-aqueous systems. It was often the case however that adding water to improve the surface characteristics of the solvent led to two-phase systems or even the analyte or matrix precipitating out of solution. Some improvement in spotting could be achieved for the organic solvents by using a smaller volume while increasing the sample concentration. This reduced the lateral expansion but by its nature led to a very thin layer which could be even more depleted at the centre, and so did not last long in the MALDI experiment.

⁸ J Axelsson, AM Hoberg, C Waterson, P Myatt, GL Shield, J Varney, DM Haddleton, PJ Derrick, *Rapid Comm Mass Spectrom*, 11, 209, (1997)

⁹ PM Lloyd, KG Suddaby, JE Varney, E Scrivener, PJ Derrick, DM Haddleton, *Eur Mass Spectrom*, 1, 293, (1995)

¹⁰ G Montaudo, E Scamporrino, D Vitalini, P Mineo, *Rapid Comm Mass Spectrom*, 10, 1551, (1996)

¹¹ K Martin, J Spickermann, HJ Rader, K Mullen, *Rapid Comm Mass Spectrom*, 10, 1471, (1996)

On the Kratos-designed slides used with the Kompact instruments, there was a raised lip at the edge of the sample spot. This feature did not however generally give enough resistance to the movement of solvents such as tetrahydrofuran and toluene. Various templating techniques were attempted, using physical masks to restrict the movement of solvent. Most of these attempts met with limited success since it was nearly impossible to form a complete and unbroken seal surrounding the required sample spot. One technique developed that did demonstrate reliable results for a minimal investment required the use of artist's masking fluid. This fluid was basically a suspension of high-mass rubber latex in ammonia and when applied to the metal surface, it dried to give a raised profile that could be used to enclose the sample area and so contain the solvent expansion.

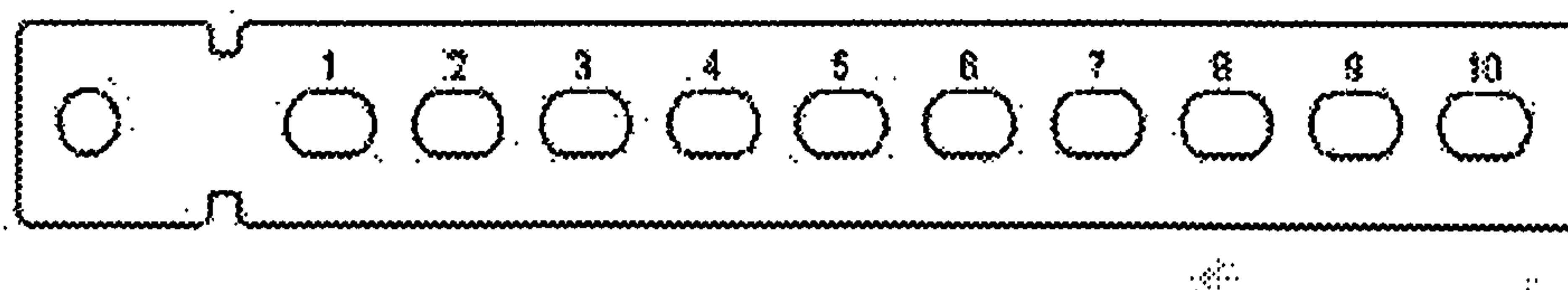


Figure 3a - Schematic of the "blank" MALDI slide for the Kratos instrument

The latex was easily applied with a small fine-tipped brush and was left to dry in a stream of air. The sample could then be applied to the open spaces left inside the mask. To test this process, a sample of buckminsterfullerene (carbon-60) in toluene and another of poly(methylmethacrylate) (PMMA) in tetrahydrofuran were used. Areas of a number of slides were prepared with and without the templating, plus the last two places on each slide were completely covered with the latex. This last step was to ensure that no contamination, resulting from any residual left by the removal of the mask interfered with the eventual spectra.

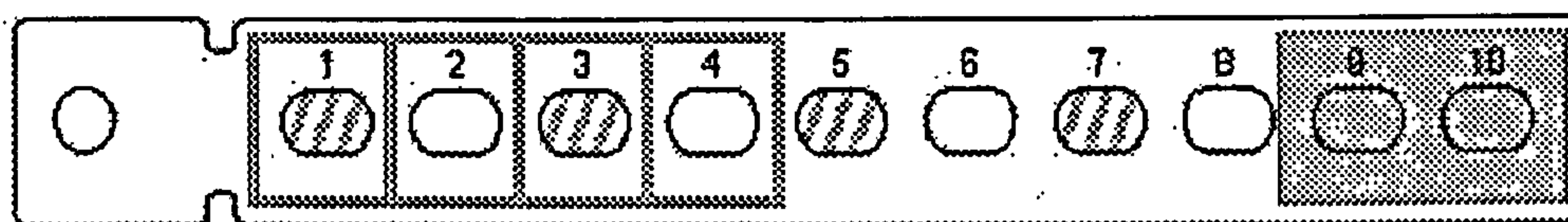


Figure 3b - Schematic of the “templated” slide showing location of the mask

After 0.5µl of the analyte had dried on each of the marked spots, the latex was carefully removed, coming away from the metal slide in a single unbroken piece in each case. Each slide was then analysed on the Kompact MALDI III instrument in linear mode, using a laser setting just above the threshold value for the sample. Fifty shots were taken across the entire sample spot at equal intervals for each spectrum. The confined spots, labelled as numbers 1 and 3, showed reasonable spectra for both the carbon-60 and PMMA samples. There was a fairly even intensity across the sample spot with only a slight increase at the edges. More importantly there was no evidence of sample on the blank spots 2 and 4, showing that the mask had successfully prevented the bleeding of the sample and allowing those spots to be used potentially for different samples. In comparison, the ‘standard’ preparation of spots 5 and 7 gave more varied intensities across the sample spots with the tendency for a large increase at the edge of the well areas, presumably due to the movement of the solvent front. This difference can be seen in the total ion intensity plots shown (figures 3c and 3d), with the *x*-axis representing equidistant points across the sample spot. Additionally with the standard preparation, the ‘blank’ spots showed evidence of low levels of contamination in over half of the cases. Finally, the two covered spots did not show any discernible level of contamination from the rubber latex, apart from possibly a small amount of low intensity noise at low *m/z* values that would not have interfered with any analyte signals.

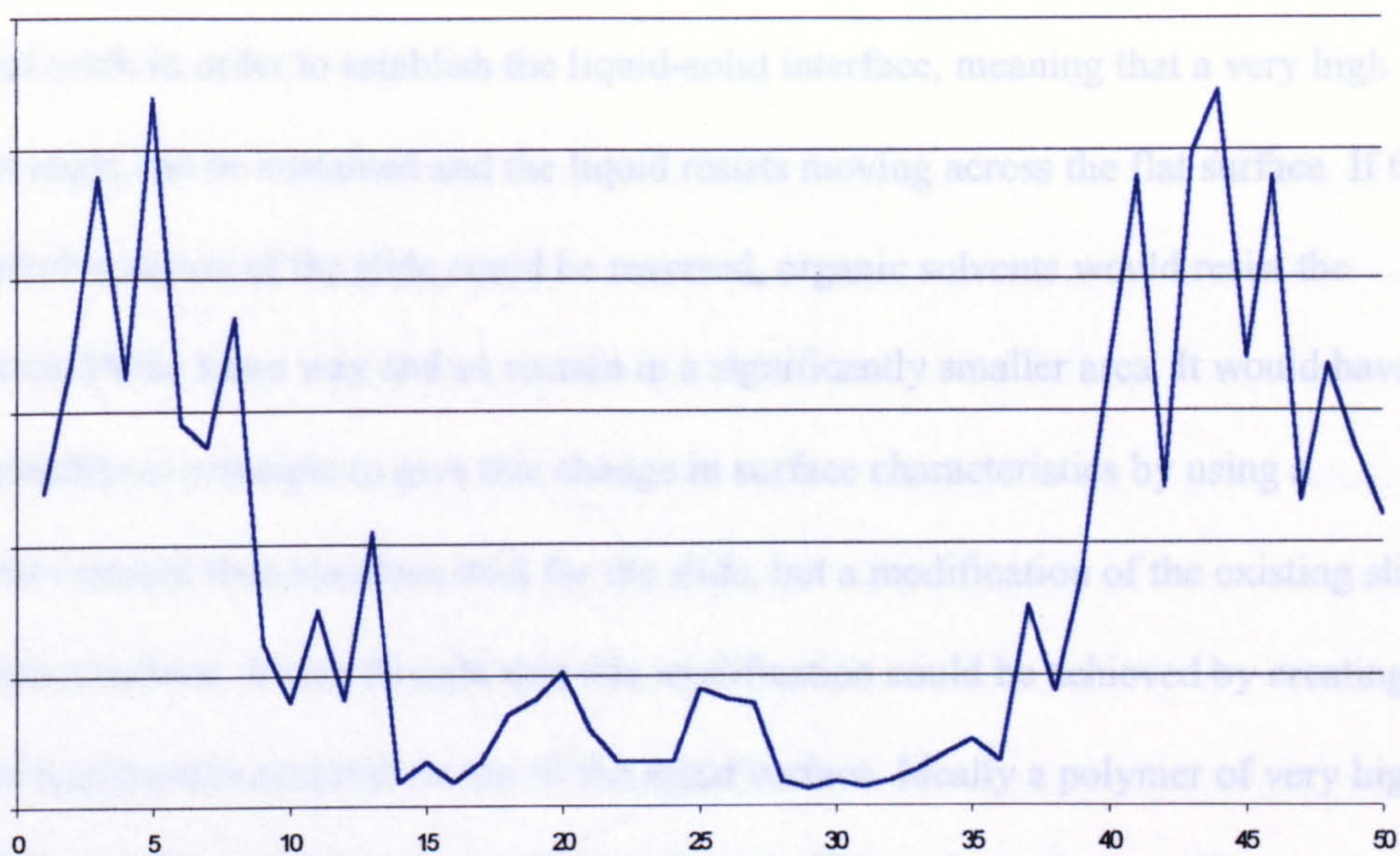


Figure 3c - Ion intensity across the sample for a non-templated slide

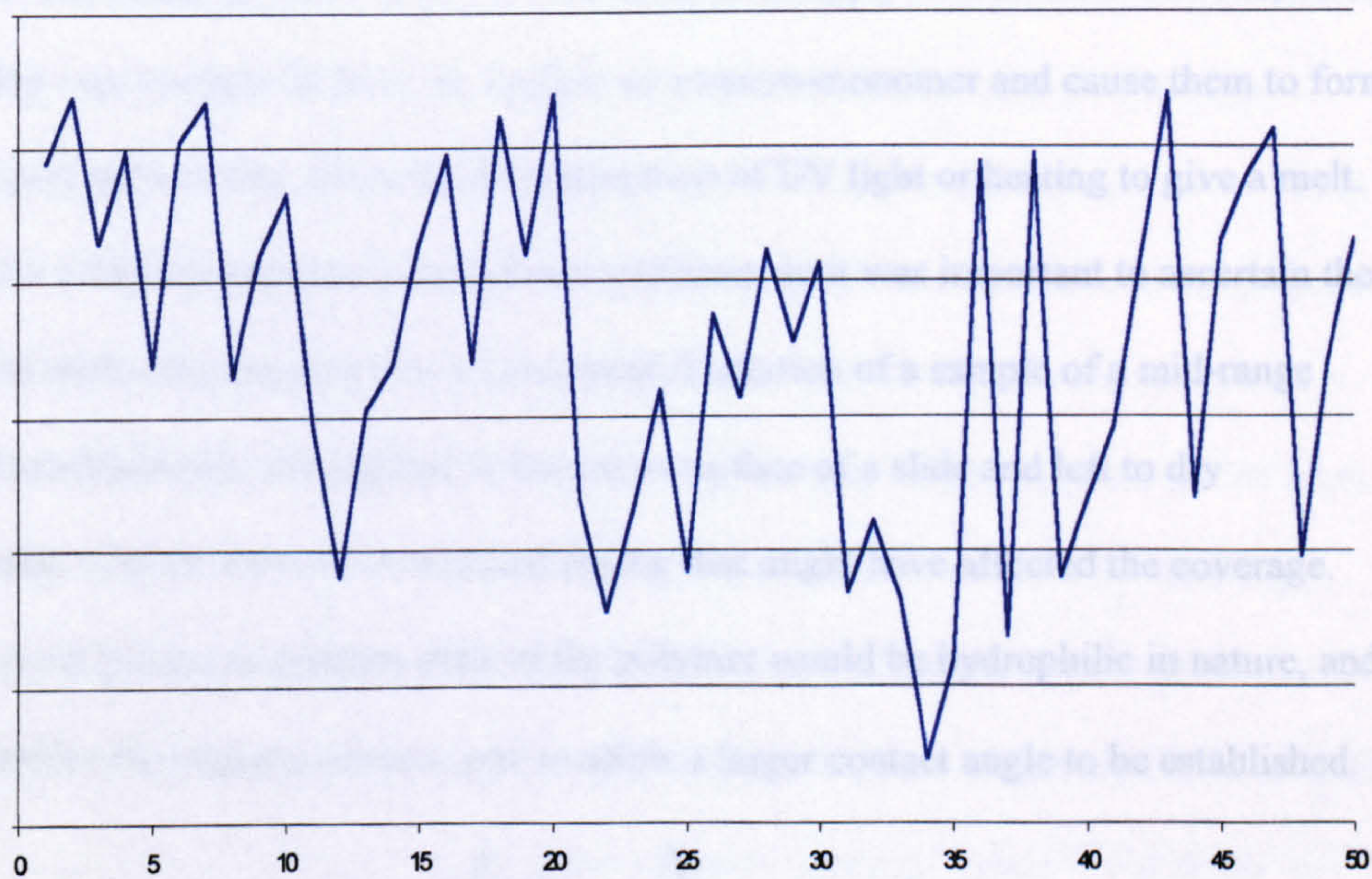


Figure 3d - Ion intensity across the sample for a templated slide

A variation on the mask principle explored was to use similar methodologies to modify the surface of the slide. The reason that polymers dissolved in organic solvents spread across the surface to such an extent was partially due to their low viscosity, but also the fact that there was very little resistance to their movement from the metal substrate. As

mentioned earlier, the stainless steel was hydrophobic in nature and so aqueous systems required work in order to establish the liquid-solid interface, meaning that a very high contact angle can be sustained and the liquid resists moving across the flat surface. If the hydrophobic nature of the slide could be reversed, organic solvents would resist the movement in the same way and so remain in a significantly smaller area. It would have been possible in principle to give this change in surface characteristics by using a different material than stainless steel for the slide, but a modification of the existing slide was more practical. It was thought that this modification could be achieved by creating a layer of a polymeric material on top of the metal surface. Ideally a polymer of very high molecular weight would have been used, as this would have been the least likely to become involved in the MALDI process or be dissolved by the action of additional solvents. Such large polymer systems were difficult to apply in their finished state, so one possibility was to apply them to the surface as a macro-monomer and cause them to form into the polymers in situ, either by the application of UV light or heating to give a melt. These two solutions required a specialised synthesis, so it was important to ascertain the benefit of such a system first. So, a concentrated solution of a sample of a mid-range glycerol-methacrylate was applied to the entire surface of a slide and left to dry completely, with no form of accelerated drying that might have affected the coverage. The glycerol groups as pendant arms of the polymer would be hydrophilic in nature, and would dislike the organic solvents and so allow a larger contact angle to be established.

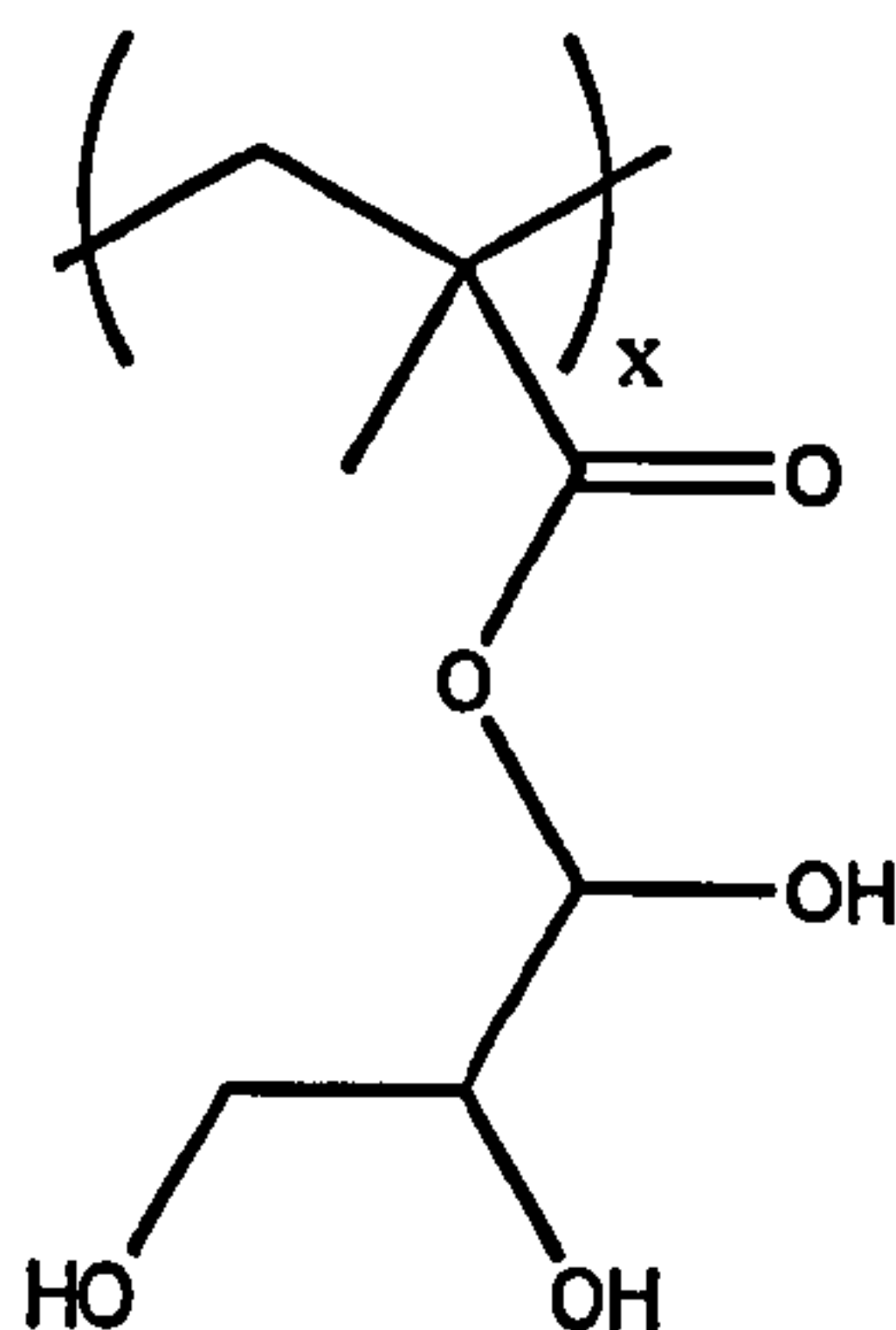


Figure 3e - Structure of poly(glycerolmethacrylate)

These modified slides were used to see if an improved method of sample preparation could be developed. Standard polymer samples and matrices were made up in tetrahydrofuran and dichloromethane, two solvents that had proved problematic in their use. Different volumes of the liquids were applied to the slide and the movement across the slide was observed. The surface did appear to give some retardation of the solvent front, but not often sufficient to prevent movement out of the well area and, with the larger volumes, even into neighbouring samples. This suggested that some degree of modification might have taken place but was not sufficient to be fully effective. Alternatively the viscosity of the solvents was such that the hydrophobic interactions were not strong enough of an impediment. The slowing of the solvent front could also have been due to dissolution of the polymer substrate. The layer of polymer was very thin however, and so it could be argued that such an effect would be very small, but it did raise concern over interference with the mass spectrum. Running a random sample of the many spots prepared gave varied results, much the same as those with any other similar sample preparation. There was no observed evidence of a series that could correspond to the masses of the polymer substrate, but, if a higher concentration of the surface modifier was found to achieve a more reliable effect, this might not have remained the case. Either way, the results from the deposition of this polymer substrate were not as good as those with the masking technique, which also has no similar issues of sample interference. A colleague ran a similar series with a hydrophobic lauryl-methacrylate substrate, which also showed little improvement over the normal stainless steel in pure “spotting” terms¹². For these reasons, it was decided not to implement the more complex approaches to polymer film deposition that had been previously described.

¹² S Bashir, *PhD Thesis*, University of Warwick, (2001)

The masking technique that was developed could also be used in conjunction with spraying methods. One of the problems with most spraying processes was that it was often difficult to limit the material to a small area without pooling occurring. By templating the slide before spraying, the deposited material outside of the sample wells could be easily removed after drying. This assisted in the creation of prepared matrix slides, where the area of crystallised solid helped control the movement of an applied analyte, as the solvent dissolves the solid material. Slides prepared in this way were shown to reduce slide-to-slide variations, which made them useful for routine analysis.

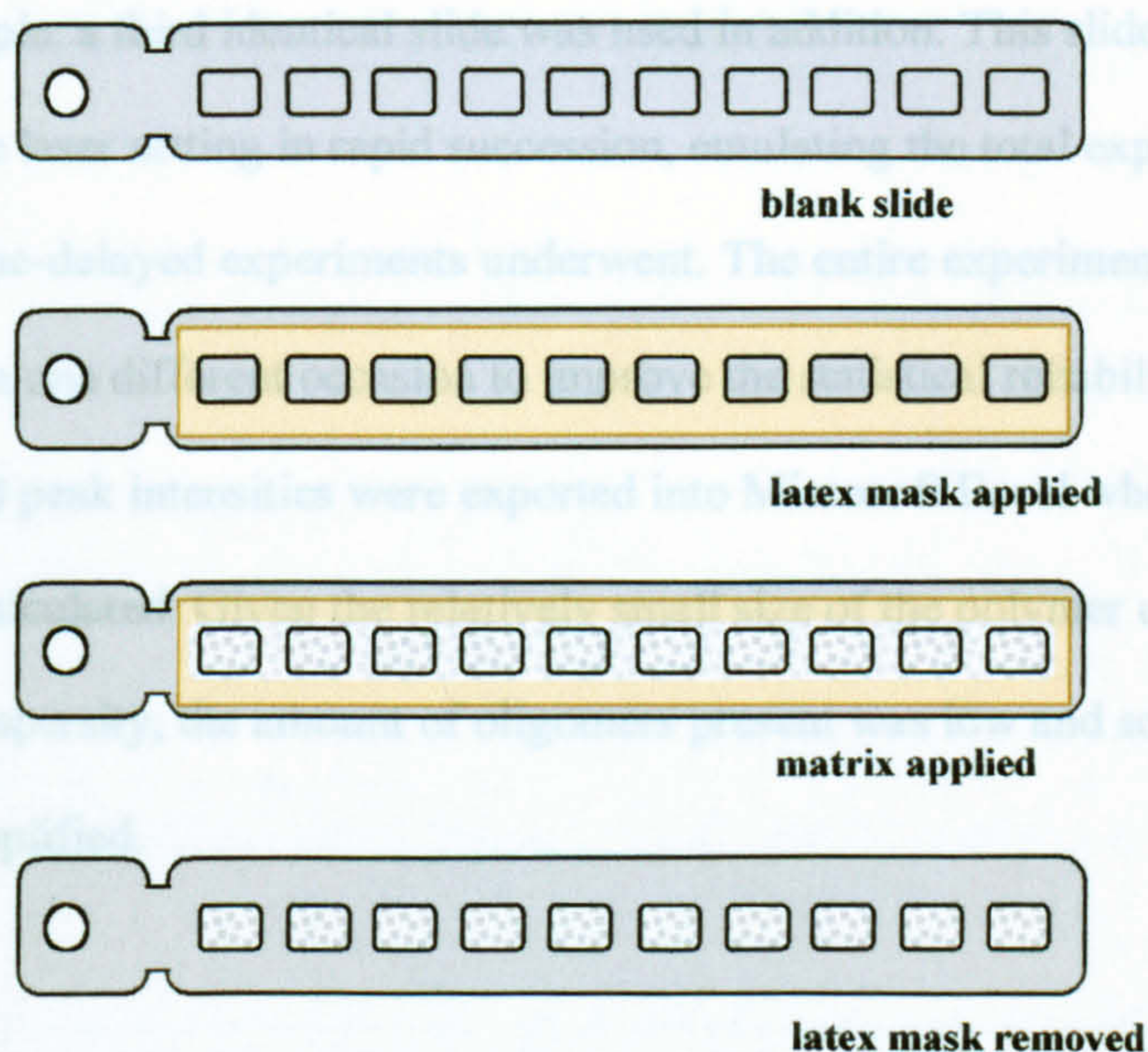


Figure 3f – Schematic of the process in preparing a templated MALDI slide

An issue with slides prepared considerably in advance and to a lesser extent with all other MALDI samples, was whether there were any variations in the quality and appearance of the spectra over an extended period of time. This effect can be broken down into three parts : changes to the sample while outside of the instrument, changes while exposed to the vacuum inside the instrument and finally changes as the laser shots deplete the sample. The former two can be thought of as being mostly related to the volatility of the sample. It may be expected that a low-mass species with a correspondingly low boiling or

sublimation temperature would be more prone to being carried into the gas-phase at the low pressures in the MALDI instrument. The possible fractional evaporation the sample was studied by preparing two slides with the simple sample system of 2,5-dihydroxybenzoic acid (DHB) as the matrix and a low-mass poly(methylmethacrylate) as the analyte. One slide was placed into and kept in the instrument while the other remained in the ambient conditions of the laboratory between acquisitions. With both slides single spectra of 50 laser shots were taken at the start and then every hour thereafter for a period of five hours. To ensure that any observed pattern was not simply due to laser depletion of the sample, a third identical slide was used in addition. This slide had six spectra taken at the same laser setting in rapid succession, emulating the total exposure to the laser that the two time-delayed experiments underwent. The entire experimental set was then repeated on one different occasion to improve the statistical reliability of the results. The masses and peak intensities were exported into Microsoft Excel where mass averages could be calculated. Given the relatively small size of the polymer used and its equally low polydispersity, the amount of oligomers present was low and so the calculations were greatly simplified.

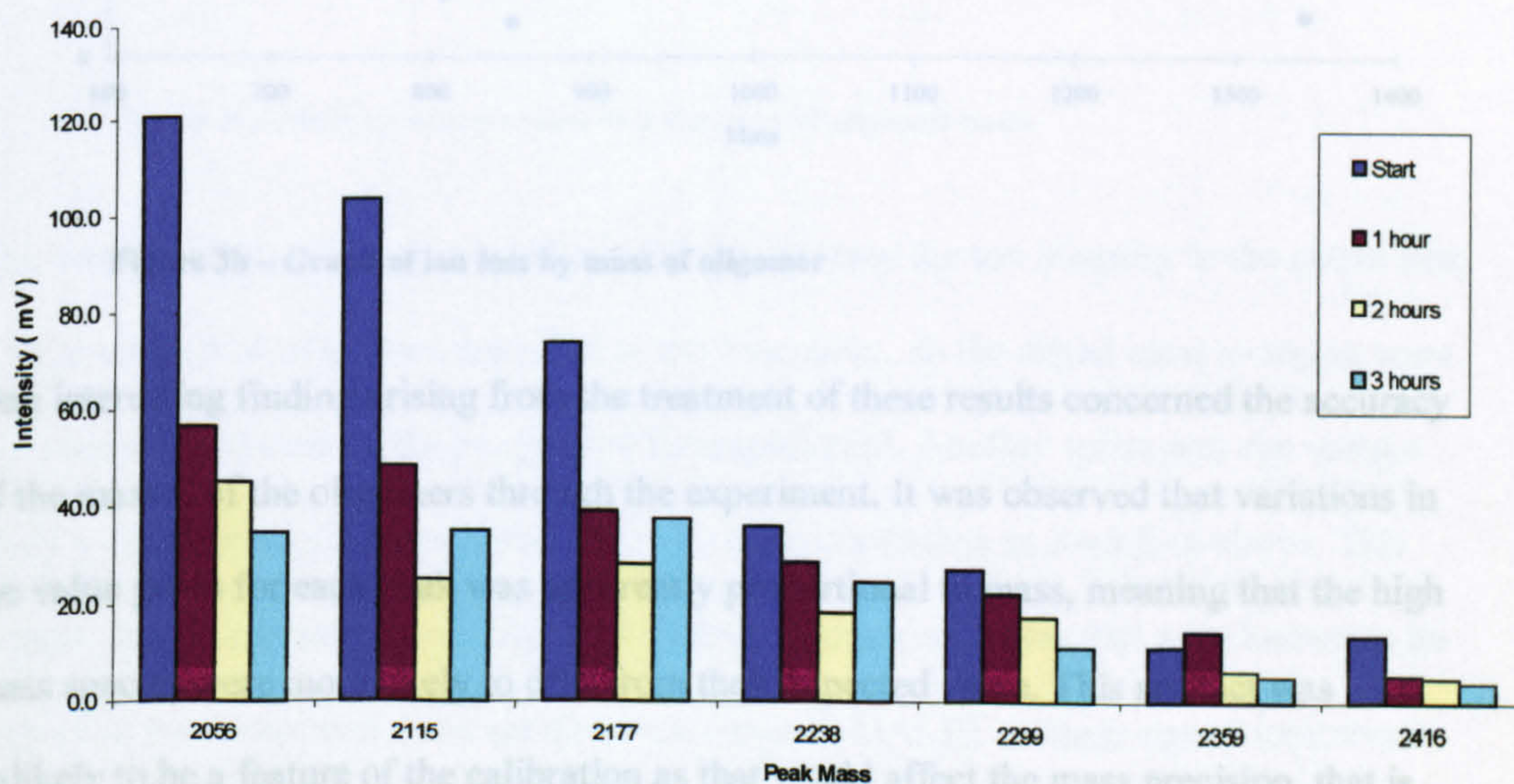


Figure 3g – Graph of ion intensity loss with time for higher mass tail

the peak. The variations were however not great enough to give doubt over assignments

Plotting the mass averages against time did not show any overriding trends for either of the environments. The results from the laser depletion also showed little mass bias, with the variations through the series of experiments demonstrating no coherent pattern.

Observing the intensities of the various oligomeric species showed a relatively steady decline, both in the time experiments and simply with the laser shots, suggesting that any trend was simply due to laser depletion and if there was any loss to atmosphere it was of less significance. This assertion is backed up by plotting the rate of ion loss against mass of the oligomer, which shows no real correlation.

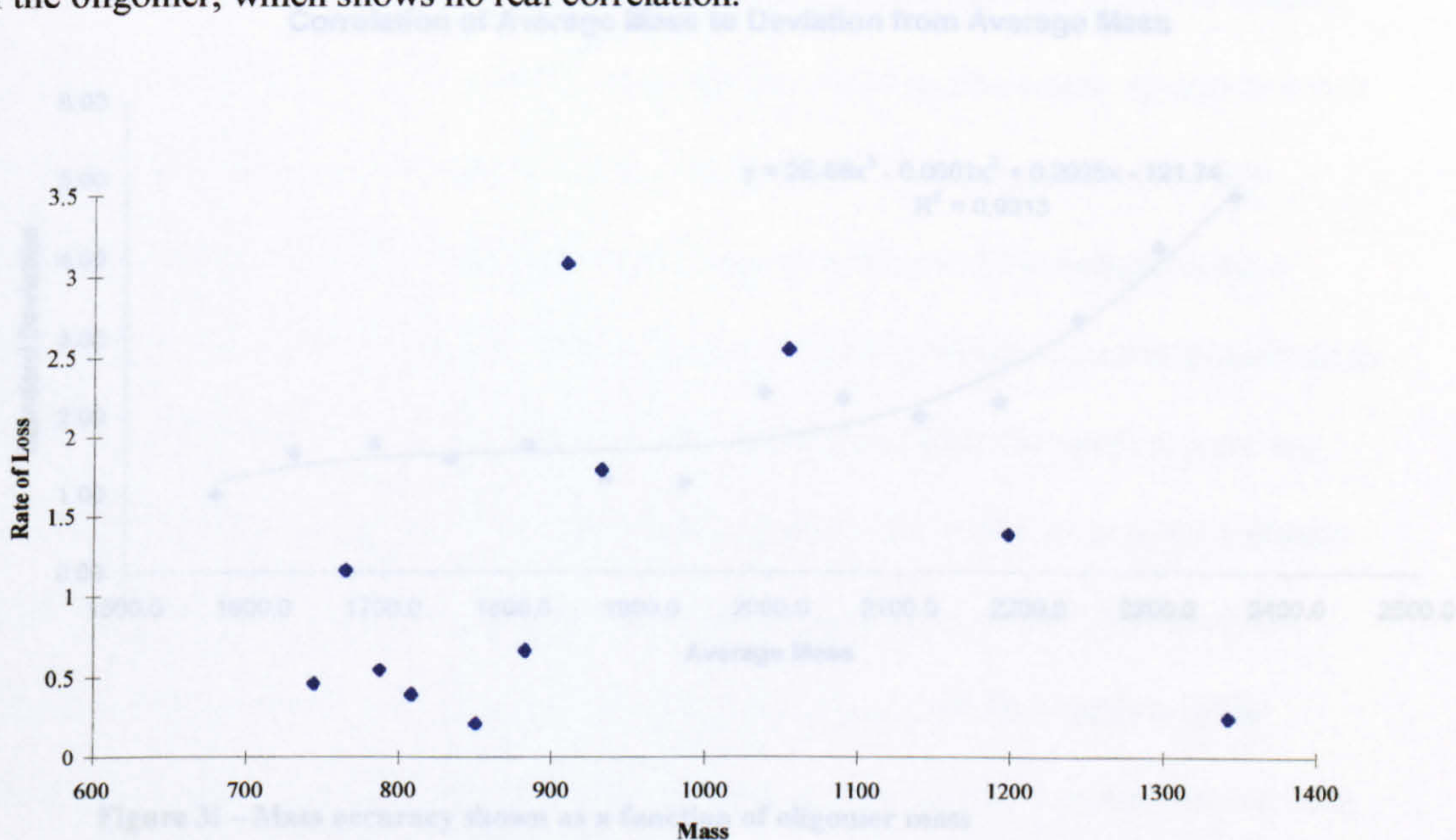


Figure 3h – Graph of ion loss by mass of oligomer

One interesting finding arising from the treatment of these results concerned the accuracy of the masses of the oligomers through the experiment. It was observed that variations in the value given for each peak was apparently proportional to mass, meaning that the high mass species were more likely to drift from their expected value. This artefact was unlikely to be a feature of the calibration as that would affect the mass precision, that is how the value corresponds to the actual theoretical mass and not effectively movement of chain being formed from the oxygen end of the molecule.

the peak. The variations were however not great enough to give doubt over assignments in this instance, since they were significantly lower than the oligomer repeat mass. The cause of the variation must arise from the time-of-flight, since the heavier mass ions will spend more time in the drift region. A similar effect was observed in the Budapest experiments discussed later, with standard deviations an order of magnitude higher for the larger masses in a polymer range of the order of 1000 m/z . The variations at high masses were also seen to be more erratic, with the presence of “rogue” signals with a large difference in mass more likely at the higher masses.

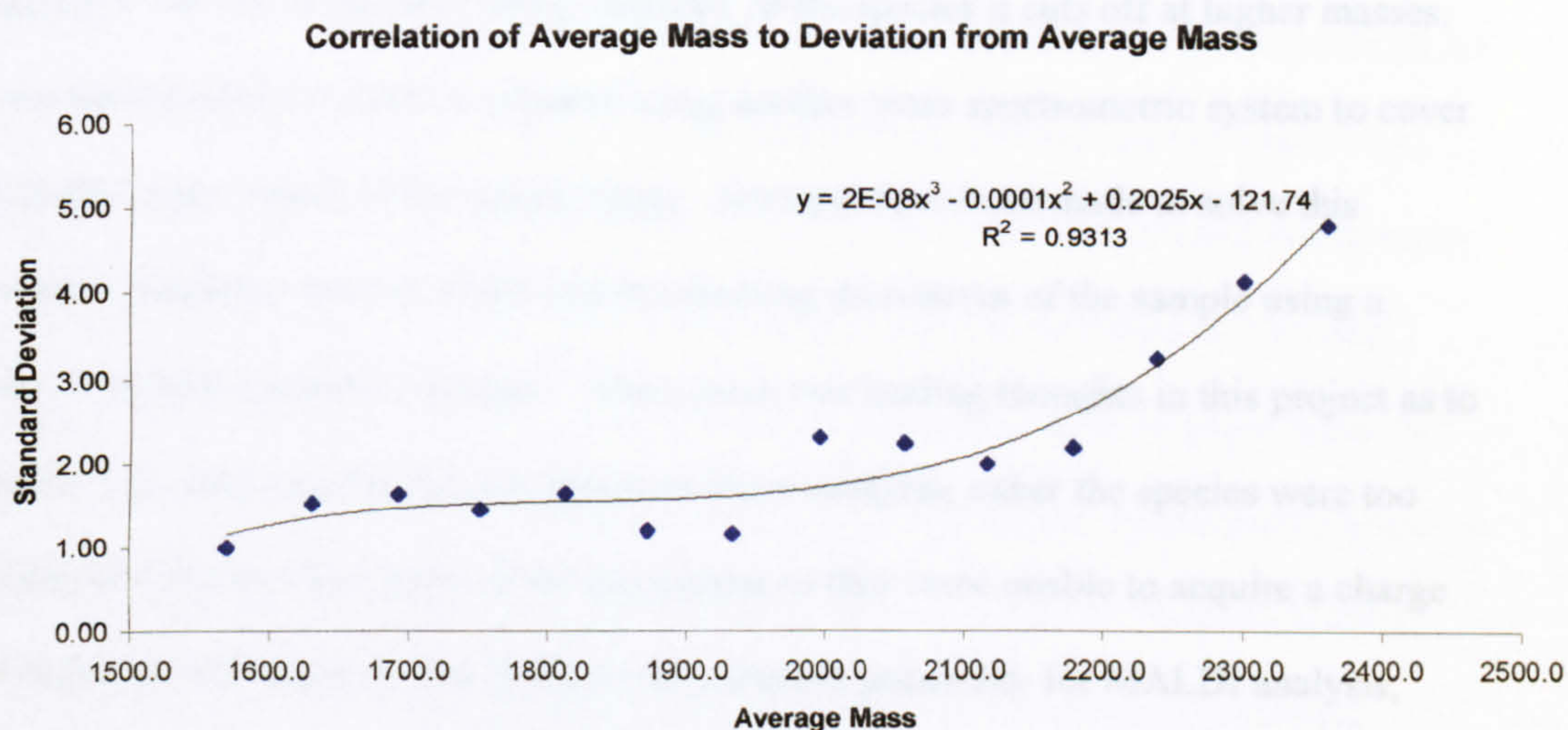


Figure 3i – Mass accuracy shown as a function of oligomer mass

The number of experiments carried out did not decrease the ion intensity to the extent that a large number of oligomers were lost to the base noise, so the actual mass averages were not seriously affected by the progress of the experiment. Another series was run using a Shell α -olefin ethoxylate detergent under the same conditions as described above. This sample was of interest as typically the first few oligomeric species that were known to be present in the compound were not observed either in MALDI or electrospray ionisation mass spectrometry. The first oligomer is the parent alcohol shown here, with the ethoxy chain being formed from the oxygen end of the molecule.

Figure 3j – Structure of parent alcohol of the C₁₂ species

b) Low-mass Polymer Samples

The currently preferred method for analysis of α -olefin ethoxylates is gas chromatography coupled to a quadrupole mass spectrometer. The total ion chromatography produced by this method contains the parent alcohol and the lowest few oligomers, but due to the decreasing volatility of the species it cuts off at higher masses. A second analytical method is required using another mass spectrometric system to cover the higher mass region of the sample range. Attempts have been made to solve this particular problem, most of which involve forming derivatives of the sample using a range of usually aromatic moieties¹³. There were two leading thoughts in this project as to why the low-mass species did not appear in direct analysis; either the species were too volatile and lost at some stage of the experiment or they were unable to acquire a charge and therefore not detected. The former was a distinct possibility for MALDI analysis, where the sample could be lost during the preparation stage or to the vacuum of the instrument. The boiling points of the material however are generally not that low so as to make it likely to argue that they could all be lost so easily during the analysis. Certainly the results documented above suggested that evaporation in the vacuum was not a major consideration for species of a similar molecular weight. Carrying out the vacuum experiments with a typical ethoxylate sample showed a similar trend to the methacrylate, or rather a distinct lack of any observable pattern. Since the parent alcohol and first two ethoxylates are not in fact observed at all in these spectra, it was dangerous however to draw too many conclusions from this result. It could be reasoned that the lowest few oligomers that were observed should have had an incrementally lower volatility and so

¹³ JC Dunphy, DG Pessler, SW Morall, Env Sci Tech, 35, 1223, (2001)

would not be lost as easily. The fact that they did not appear to decrease over time could mean that their volatility was just past a threshold where the vacuum had very little effect.

It was perhaps more likely that the first few species were unable to gain a charge in the form of a metal cation during the expected ionisation processes. From looking at their chemical structures, they would have clearly been expected to exhibit a far greater degree of aliphatic character than the higher ethoxylates and it is known that aliphatic polymers, such as polypropylene, have proven a great challenge for MALDI practitioners. This is the reasoning used by research groups that have experimented with derivative methods, as these seek to attach a group that will aid in the acquisition of charge or even exist in a charged state from the beginning¹⁴. With both the techniques of MALDI and electrospray ionisation, if the species did not acquire charge they would not be detected. The first oligomer that was typically observed was often also quite variable in its given intensity. This could be rationalised if the ion in question was not particularly stable and so prone to losing its charge, depending on the experimental conditions involved. With MALDI it might be possible to determine a combination of matrix and counter-ion that would promote the charge attachment to the low mass species. Experiments using various combinations, on the Kompact instrument at Warwick and also the Bruker system in Budapest, did give marked improvement in the quality of the existing spectra but proved incapable of resolving the missing species. Application of the sample preparation techniques described in the previous section were shown to give better intensity spectra, and seemed to resolve some of the intensity variations in the second and third ethoxylate species. While sodium was mainly used as a counter-ion, lithium and silver also gave reasonable results at the lower masses but showed a slight difference in the distribution of the higher species from that expected.

¹⁴ JP Barry, WJ Carton, KM Pesci, RT Anselmo, DR Radtke, JV Evans, *Rapid Comm Mass Spectrom*, 11, 437, (1997)

In order to investigate this low-mass issue further, two samples were obtained from the polymer research group at Warwick. These were extremely low mass methyl- and benzyl-methacrylate, synthesised by a catalytic chain transfer process¹⁵. This method uses a cobalt-centred macrocycle, which acts within the radical mechanism, transferring the active radical species between chains and so reducing the growth of the oligomers.

Through the altering of the concentration of the cobalt species and the conditions of the polymerisation, the eventual mass distribution of the polymer can be to an extent controlled. The polymers were synthesised to give in each case a mass range from the monomer up to approximately the hexamer, a range that was confirmed by measurement using the tetrahydrofuran-based gel permeation chromatography (GPC) system. These experimental series were carried out in Buapest, Hungary, at the Central Research Institute for Chemistry using the Bruker Reflex III MALDI system.

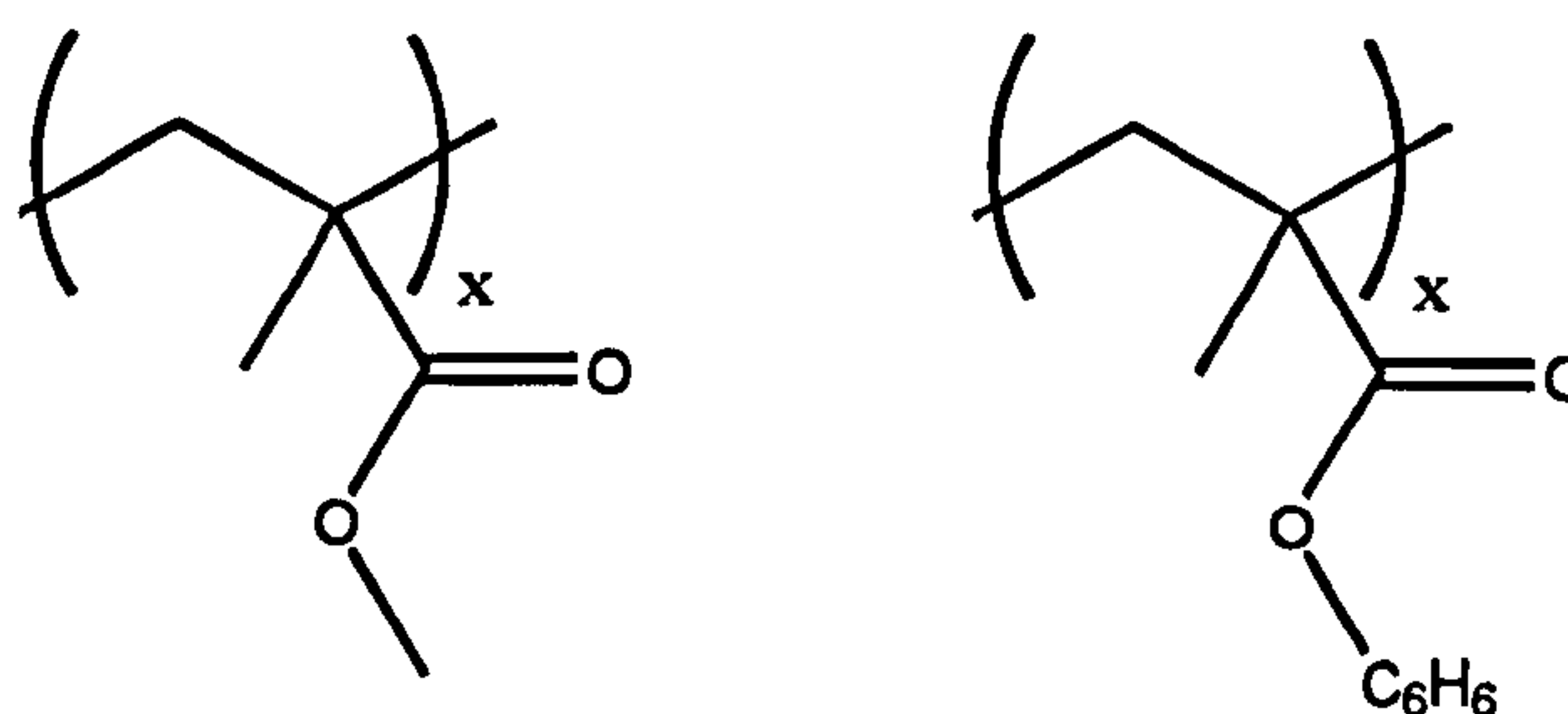


Figure 3k – Structure of methyl and benzyl polymer systems

The samples did not give consistent results on the instrument, partially as the low masses were masked by background signals. The very lowest masses were observed, although at a much lower intensities than should have been the case for the given distribution. This indicated that the lowest species were either not present at the expected levels or did not acquire charge during the MALDI process. It is also possible that these low-intensity signals were not in fact the early oligomers, such incorrect identification must be viewed as a possibility with the high number of peaks present within that region of the MALDI spectrum. It was likely that a number of these signals arose from the catalyst and other

¹⁵ TP Davis, D Kulkulj, DM Haddleton, Trends Polym Sci, 3, 365, (1995)

agents used in the synthesis and not removed by the subsequent filtration of the product. Suspicions over the sample history prompted a repeat of the GPC runs which showed a clear decrease in the low mass end over those obtained before shipment. The conclusions from the mass spectrometry could therefore not be substantiated as there were signs that material may have been lost before the sample preparation stage. It was possible that these low-mass species were volatile enough to be lost to atmosphere, either during storage or due to the conditions during shipping. The fact that the lower material could be lost in this manner was of concern, but since the timescale was unknown in this instance the significance to sample preparation could not be drawn. The experimental series described in the previous section and other samples studied in Budapest showed considerably less effect on the lowest masses over time.

iii. Mass bias effects

Typically in MALDI, sample preparation is honed in order to achieve the greatest ion intensity and repeatability. With polymeric systems however it is very important that the intensities of the different masses are all affected equally by refinements of the sample preparation. If this is not the case and some part of the mass range is favourably enhanced over others, the calculated mass averages will be changed. As mentioned previously, there are a number of parameters that can be altered in MALDI, so it is important to assess which if any of these can adversely affect the values. Then it may be possible that these parameters can be better controlled to give more consistent values.

The effect of relative variations in oligomeric species intensities was expected to be more pronounced at lower chain lengths, as here the percentage differences in mass between oligomers were greater and so the variations would have had a higher weighting on the

eventual result. Therefore, experiments were carried out on very low-mass polymers synthesised by the catalytic chain transfer process to low degrees of polymerisation. Species ranging from the monomer unit itself up to around the hexadecamer were considered. The polydispersity, or mass range width, of these samples was therefore very small and so did not give the added complication that arises from the MALDI analysis of highly polydisperse systems. In addition, at the low masses involved, it had been observed that GPC analysis often led to resolution of a number of the lowest-length species. This effect usually extended only for the first few oligomers before the species merged into the continuous curve more typical of GPC analysis. Comparisons made between GPC and MALDI results by Axelsson *et al*¹⁶ highlighted a high level of disparity in the results for these species. While the large difference at the lowest mass was reduced when the area under the resolved species was averaged continuously across the mass band instead of being discrete, it did still appear that mass spectrometry underestimated the amount of low mass species present in these polymers.

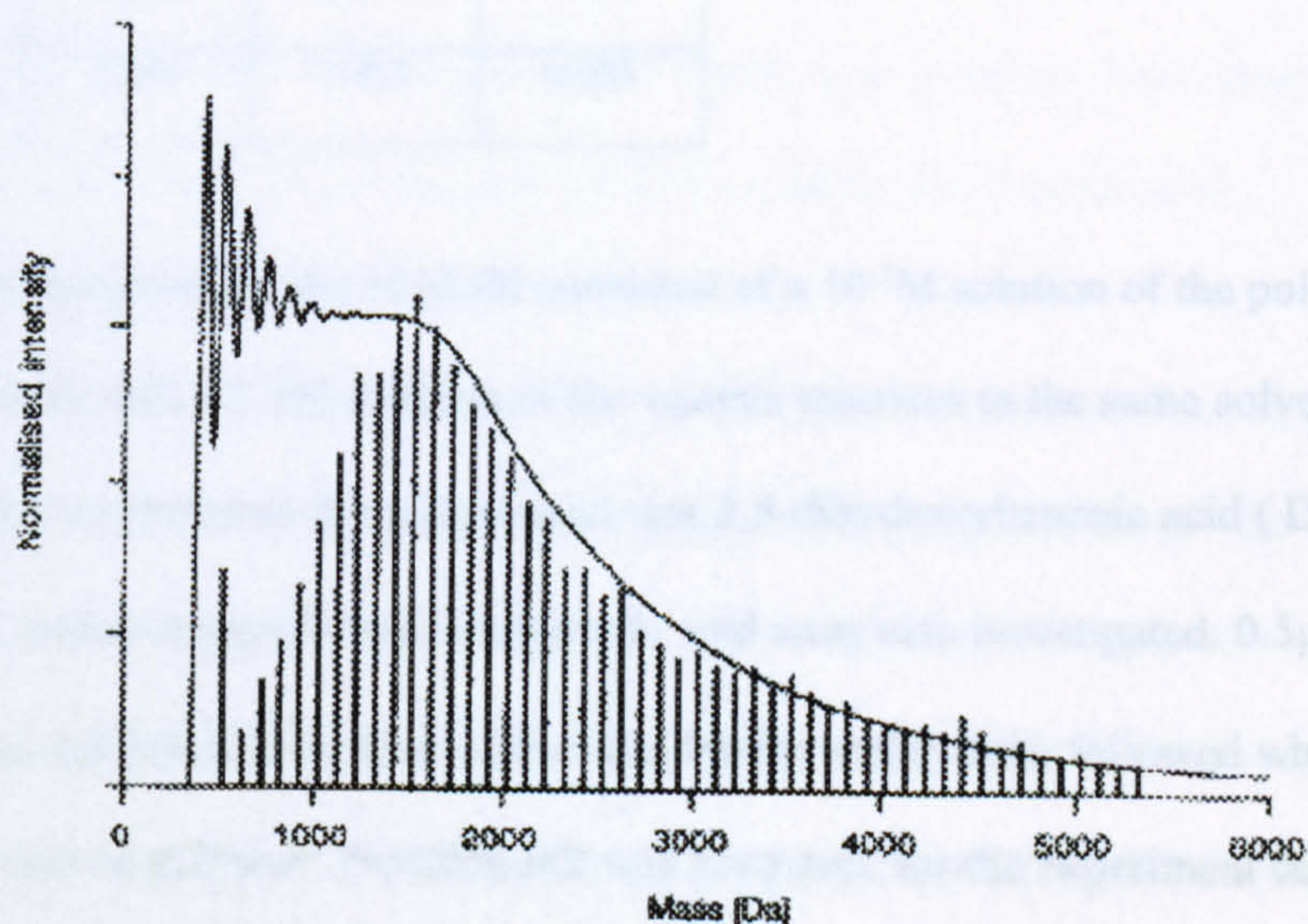


Figure 31 - Comparison of MALDI and gel permeation results at low-mass

¹⁶ J Axelsson, AM Hoberg, C Waterson, P Myatt, GL Shield, J Varney, DM Haddleton, PJ Derrick, *Rapid Comm Mass Spectrom*, 11, 209, (1997)

a) Effect of Instrumental Variables

In work carried out in Budapest, these effects were systematically studied. The main experimental sample of poly(hydroxyethylmethacrylate) (HEMA) was synthesised at Warwick by catalytic chain transfer polymerisation. Gel permeation analysis of the polymer was carried out using the Polymer Laboratories system at Warwick and the values were calibrated against a series of narrow distribution poly(methylmethacrylate) standards. Although the hydrodynamic volume of this polymer is not exactly the same as the one under study, it is a close comparison and the nearest analytical standard that was available. The values obtained by this method are given below.

	Mn	Mp	Pdi
Run 1	1736.8	2235.7	1.29
Run 2	1731.5	2219.6	1.28
Run 3	1734.7	2236.1	1.29
Average	1734.3	2230.5	1.29
St Dev	2.668	9.412	0.005

Sample preparation for the MALDI consisted of a 10^{-3} M solution of the polymer in 5:1 acetone/water and a 0.1M solution of the various matrices in the same solvent system. For most of the experiments the matrix used was 2,5-dihydroxybenzoic acid (DHB), but dithranol, sudan orange G and indolacrylic acid were also investigated. 0.5 μ l of the matrix was deposited onto each well of the 10-slot metal slide, followed when dry by the same amount of polymer. No extra salt was necessary for the experiment due to the high sodium background from the metal substrate. Spots were prepared so that each experimental series was carried out in triplicate, with 50 shots taken at each spot with the laser rastered over the surface at equal intervals. This process was found to give a more statistically viable end-result, with imperfections or the so-called “sweet spots” averaged

out across the sample¹⁷. These are areas that give a high intensity signal, but they can be shown to often not be representative of the entire distribution of the sample.

In this series of experiments, three different factors were explored for their effect on the resultant mass distribution, and hence the average mass value calculated from this series. These variables were the choice of matrix, the laser power and the acceleration potential. The matrix will be covered in more detail in later experiments, but here it was assessed in order to gauge the significance of its effect on the spectra. The choice of matrix to use in an experiment is an important decision in sample preparation for MALDI, however it is usually limited to choosing a substance that will give a spectrum of reasonable intensity and with reliable consistency. A number of the more common matrix compounds were investigated to determine whether they would give significantly different results from the same sample under similar experimental conditions. The comparison was somewhat clouded by the fact that different matrices had a slightly different threshold value, i.e. the minimum laser power needed to achieve a spectrum. The four compounds under investigation here had a similar threshold and so a common laser attenuation slightly above the threshold value of the four could be used for the experiments.

The Reflex III instrument used gave the laser power in terms of an arbitrary scale of attenuation¹⁸. The higher the attenuation, the lower was the flux of the laser. In these experiments four consecutive values were chosen starting from just above the threshold value. At higher laser powers there was the issue of fragmentation of the polymer, which will be discussed in more detail later. Finally, the last experimental condition was the acceleration voltages. These were the two electrical fields which accelerated the ions produced by the MALDI process from the source region into the field-free region of the

¹⁷ Y Kim, GB Hurst, MJ Doktycz, MV Buchanan, *Anal Chem*, 73, 2617, (2001)

¹⁸ Z Szilagyi, JE Varney, PJ Derrick, K Vekey, *Rapid Comm Mass Spectrom*, 12, 489, (1998)

TOF, and then reflected the ions back onto the detector. The reflectron voltage was usually set at 105% of the extracting voltage to ensure that all ions accelerated through the system were reflected back and did not enter the high field area at the back of the mirror. Three different values were taken for the initial voltage spanning the working range of the instrument, although at very low voltages it was often the case that insufficient ions were available for experimental use.

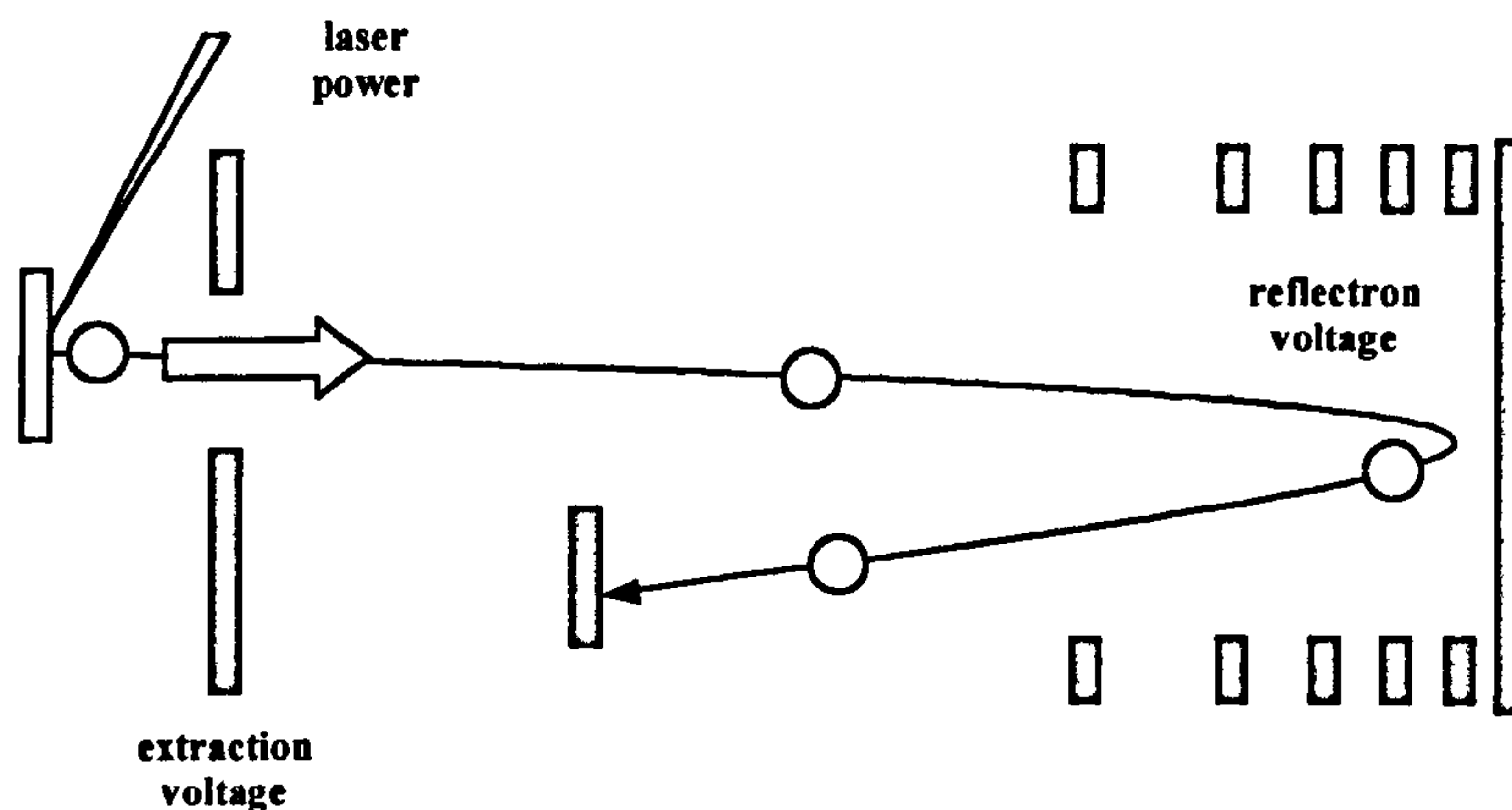


Figure 3m – Schematic of the instrument showing the variable settings

Carrying out the measurements with a single-slide preparation minimised slide-to-slide discrepancies but limited the number of settings that could be investigated for each variable. To ensure that observed trends were statistically relevant, each experimental series was carried out on more than one occasion both in the same day and on different days. Differences in values from day-to-day were found to be well below the variations attributed to changes in the experimental conditions. The results were output from the computer as intensity lists for the masses within the expected range. The sodiated adducts were identified in all cases and the intensity values tabulated, separated for each series within the experiment. Standard polymer calculations were carried out to determine the number-average and mass-average values and polydispersity.

Matrix	Mn	Mw	Pdi	St Dev (Mn)
DHB Ave	1725.2	2186.3	1.27	39.6
Dith Ave	1171.4	1484.5	1.27	41.3
IAA Ave	1505.9	1806.9	1.20	55.1
Sudan Ave	1076.6	1357.0	1.26	44.7

The four different matrices gave very different values at comparable settings. All except indolacrylic gave a polydispersity of around 1.27, however there was a spread of nearly 650 mass units in number-average molecular weight and 830 in mass-average between the two extremes of DHB and sudan orange. The DHB result was comparable to that obtained by gel permeation and gave the most consistent and also most intense spectra of the four, so DHB was chosen as the matrix for the remainder of the experimental work.

Laser Attenuation	Mn	Mw	Pdi	St Dev (Mn)
20	1793.2	2169.8	1.21	40.4
21	1833.4	2245.8	1.23	41.2
22	1866.6	2300.0	1.23	40.9
23	1789.8	2045.5	1.14	44.4

With the laser attenuation experiments it was found that decreasing the attenuation, and so increasing the laser power, at first lead to a gradual increase in mass value and then a slight drop. There was also a general increase in polydispersity at first as the laser power increased, followed by a more gradual decrease. Inspection of the mass envelopes produced by these settings shows that this arose from increased intensity of higher-mass peaks, where the highest observable mer unit potentially increased as the laser power was raised. The effect on the values for this range of settings was smaller than that for a change in matrix, with only an average maximum difference of 110 for Mn and 230 for Mw values. Standard deviation of the averages did not show any overall trend even with the slightly higher value for the 23 attenuation showing in the results above.

Acceleration Voltage	Mn	Mw	Pdi	St Dev
11.4 V	1392.5	1566.6	1.12	49.2
15.2 V	1717.5	2052.2	1.19	44.1
19.05 V	1761.5	2138.7	1.21	43.2

In the third series, the acceleration and reflectron voltages gave an increase in mass value with increasing potential. The total ion intensity at the lowest value was however significantly less in most results, leading to a large difference in the mass values calculated from those spectra. This disparity was presumably due to the fact the high-mass species which were initially low intensity were lost to the background noise and so did not contribute to the mass-average calculation. When the experiment was repeated for a smaller polymer system, better results were obtained for the lowest setting allowing the true pattern be ascertained. The increase in values in this instance were seen to have a linear correlation within the limits of the experiment, although the exact nature of the relationship cannot be fully attributed with only three discrete values. The range however of the value was significantly less than those arising from changes in laser power. In the second experiment, the average maximum difference was 75 for M_n and 154 for M_w .

Acceleration Voltage	Mn	Mw	Pdi	St Dev
11.4 V	943.8	1134.9	1.20	22.1
15.2 V	979.1	1220.0	1.25	20.9
19.05 V	1017.8	1289.3	1.27	18.6

b) Effect of Attached Cations

In a number of spectra there were high intensities of signals arising from cation attachment other than sodium. Analysis of the mass values based on the attachment of lithium, silver and potassium in these cases showed differences in the average values. Since there was an apparent mass bias in the attachment of these metal ions, spectra

where the intensities of peaks not attributed to sodium attachment were greater than 10% of the height of the equivalent sodium-bound oligomer were discounted. This was done as it was reasoned that competition between the salts could bias the sodium peak distribution and so add another effect on top of that being investigated in that series of experiments.

The second most common ion acquired from non-doped samples was usually potassium, however a number of slides in this experiment showed high degree of silver attachment. Since these results could not be used for the main body of work, the opportunity was taken to assess any bias arising from the choice of metal ion. A selection of spectra was made where a significant amount of sodium, potassium and silver were seen to be present. The ion intensities for each of the three series were separated and analysed. Since as mentioned before, the mass values used in the calculation were those without the metal ion, there was no pure mathematical bias from the difference in the masses of the three salts. The intensities of the free metal ion peak and that of the matrix-metal ion complex were also identified to give an indication of the relative amount of each present in the experiment. In the case of silver, with its two major isotopes, this represented two peaks for each oligomer which were summed to give the total silver population. This element of subtracting the salt mass from the polymer peak was important in achieving the correct mass average, and for this to occur, the counter-ion must have been positively identified. In most cases this identification was a straight-forward process since the masses of the polymer units were known, and polymer calculation algorithms within the software tended to account for the mass. Where there was more than one salt, many programs could only work with the major species. A problem would only arise if each metal ion did not produce effectively the same distribution at a scalar value of the intensity. If the affinity did show a mass relation however, the averages for each series would differ.

Observing the individual mass distributions averaged over all the experiments, there was clear indications of a difference in the silver pattern which showed far less of a Gaussian

distribution. Direct observations between the metals was difficult however due to the large difference in intensities, so the information had to be normalised on each oligomer to show the trend. This gave ion intensity in relation to the intensity of the highest signal for that particular mass. By doing this, the relatively small intensity of the lowest masses was not a problem and the relative importance of each species could be determined. All three salts gave easily distinguished signals up to the hexamer, although the actual ion intensities has dropped considerably by that point. The higher species were present and did show different metals, but the intensities were more variable than those presented.

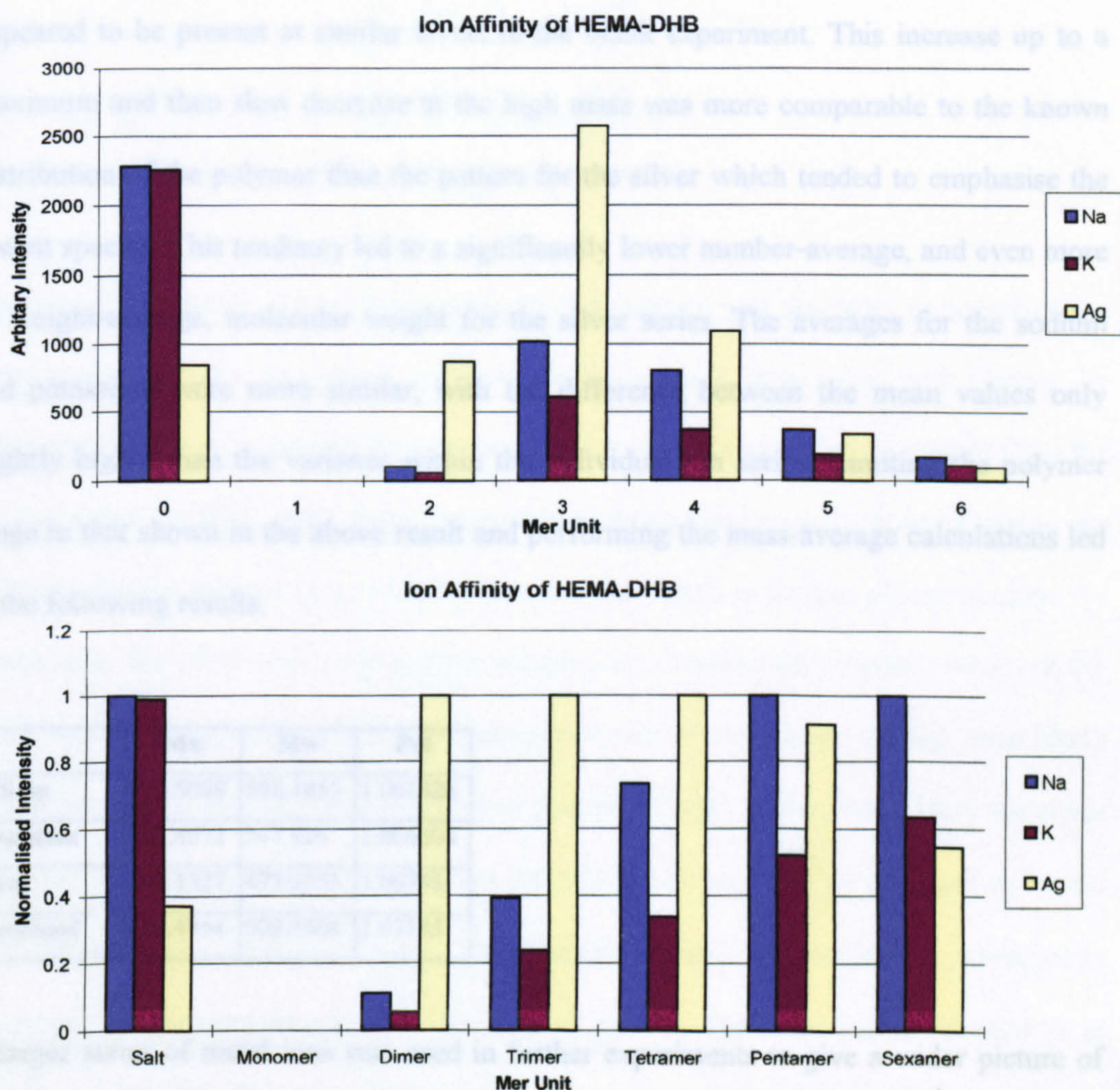


Figure 3n – Intensity and normalised bar charts of ion affinity for metal-polymer complexes

As could be seen from the bar graphs, while the silver ion appeared to represent less than half the natural abundance of the others it was the major species for the first three oligomers. In the extreme case of the dimer, over 80% of the observed polymer had a silver cation attached while it only amounted to 20% of the free salt population. The silver dominance quickly disappeared as the chain length was increased, the ratio of sodium and potassium increasing with oligomer size and by the decamer there was often no signal for the silver species. The pattern for the two alkali metals was very similar, with the sodium being the majority species of the two in all instances even though they appeared to be present at similar levels in the blank experiment. This increase up to a maximum and then slow decrease at the high mass was more comparable to the known distribution of the polymer than the pattern for the silver which tended to emphasise the lowest species. This tendency led to a significantly lower number-average, and even more so weight-average, molecular weight for the silver series. The averages for the sodium and potassium were more similar, with the difference between the mean values only slightly higher than the variance within the individual ion series. Limiting the polymer range to that shown in the above result and performing the mass-average calculations led to the following results.

	Mn	Mw	Pdi
Sodium	516.5098	548.1853	1.061326
Potassium	513.8072	547.926	1.066404
Silver	443.1327	473.0353	1.06748
Combined	474.4954	508.3508	1.07135

A larger series of metal ions was used in further experiments to give a wider picture of the effect it has on the mass value. In this case the polymer was a poly(ethyleneglycol) with a quoted most probable peak (M_p) of 764. The series were run on the Kratos instrument using a simple “dried-droplet” sample preparation. Each spot was doped with

0.5µl of a 0.1M solution of the metal chloride. The difference in this experiment is⁷ that the bias arises only from the attachment of the cation and not from a competitive process as above where more than one metal is available at a significant level. Schreimer and Li have shown that higher amount of silver, with a similar polymer system, gave less of a low-mass effect presumably due to reduced competition between the polymer chains for ion attachment¹⁹.

	Mn	Mw	Pdi	No Expt	Var
Li	745.6	775.2	1.04	25	24.47
Na	757.3	785.1	1.04	25	26.01
Cs	815.0	836.5	1.03	15	29.96
Cu	769.8	797.5	1.04	15	16.53
Ag	700.2	720.2	1.03	10	34.23

To explain this trend, it must be considered that sodium was the most preferred of the counter-ions for the oxygenate polymer over a certain mass, followed closely by potassium. When it is said that they are preferred, this indicates that these metals form the strongest and therefore most stable interaction with the electron-rich moieties within the polymer. So, by this reasoning and the view that the metals in the gas plume compete for attachment, the silver will only form a complex at a statistically smaller value. At the lower masses, the polymer-alkali metal interaction was in some way lessened, most likely due to the low number of oxygen centres or the short length of the chain. Here the silver must form a better interaction, or be less affected by the decrease in size, and so be the thermodynamically favoured product. The most obvious trait that would have a relation to the length of the polymer would be the size of the ion. The ionic radius of silver is at 126pm greater than that of sodium (102pm) however, and only slightly less than the 138pm potassium. However, these values describe inter-ion spacing in a solid crystal

¹⁹ DC Shriemer, L Li, Anal Chem, 69, 4169, (1997)

structure which could be thought of as little relevance to the gas phase complexes. A more useful value may be that of the valence shell radii, since it would be these orbitals that interact with the electrons of the oxygen centres. The *s* and *d* orbitals of the silver, at 153.2pm and 54.7pm respectively, are both significantly less than the available *s* orbital of sodium at a distance of 179.4pm²⁰. This could also explain why the potassium gave slightly greater ion intensities, since its radius is larger than sodium and so would be best stabilised with a slightly higher chain length. Ab initio calculation by Cheng and co-workers²¹ suggested that there was a minimum chain length in ethoxy systems where sodium ions could be successfully chelated by the oxygens of the polymer with ion-dipole interactions. In that case, the *4d* and *5s* orbitals of silver ions were thought to interact with *π*-orbitals of carbon triple bonds present in their sample system.

This argument assumes that the polymer chain wraps around the metal centre, presenting a certain number of oxygens for interaction with the ion. This is certainly thought to be the case with electrospray ionisation, on the basis of experiments involving ion chromatography to measure the collisional cross-section²². The difference in charge states however between electrospray and MALDI prevented a direct comparison with any confidence. The coiling model does not give a ready explanation of why MALDI analytes only attach a single ion no matter what the length of the polymer chain²³. It may be that singly charged ions are simply the most thermodynamically favoured outcome of the gas-phase reactions, with greater charge states perhaps existing in the early stages of the process. Another possibility is that the polymer remains essentially linear and a single metal cation attaches at some point along the chain.

²⁰ PW Atkins, *Physical Chemistry – Fourth Edition*, Oxford University Press, (1990)

²¹ HS Cheng, PAC Clark, SD Hanton, P Kung, *J Phys Chem A*, 104, 2641, (2000)

²² G von Helden, T Wyttenbach, MT Bowers, *Science*, 267, 1483, (1995)

²³ M Karas, M Gluckmann, J Schafer, *J Mass Spectrom*, 35, 1, (2000)

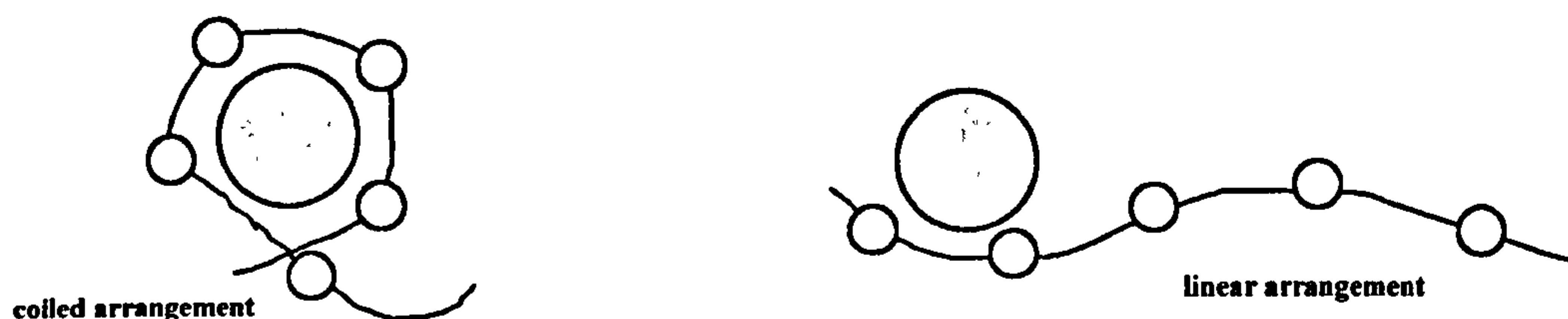


Figure 3o – Schematic showing the difference between a coiled and linear salt attachment

With a linear attachment it would be the strength of the individual interactions that would be the largest contribution to the stability of the system. With less centres for attachment and a smaller surface area, the metal-ion interaction becomes the important variable and here the values appear to match the observed trends. The AgO covalent bond enthalpy is 256 kJmol^{-1} , nearly 40 kJmol^{-1} higher than that of sodium to oxygen¹⁹. The interactions in the case of ion attachment are unlikely to be fully covalent but the values may give some clue to the strength of the affinity. As the chain length increases, the amount of available oxygens also increases so more can then interact with the metal. It is at this point that the larger radius of the sodium might come into effect. This larger sphere would now allow more oxygens to be in close contact and so the lower individual interaction strength is countered by the number of such interactions.

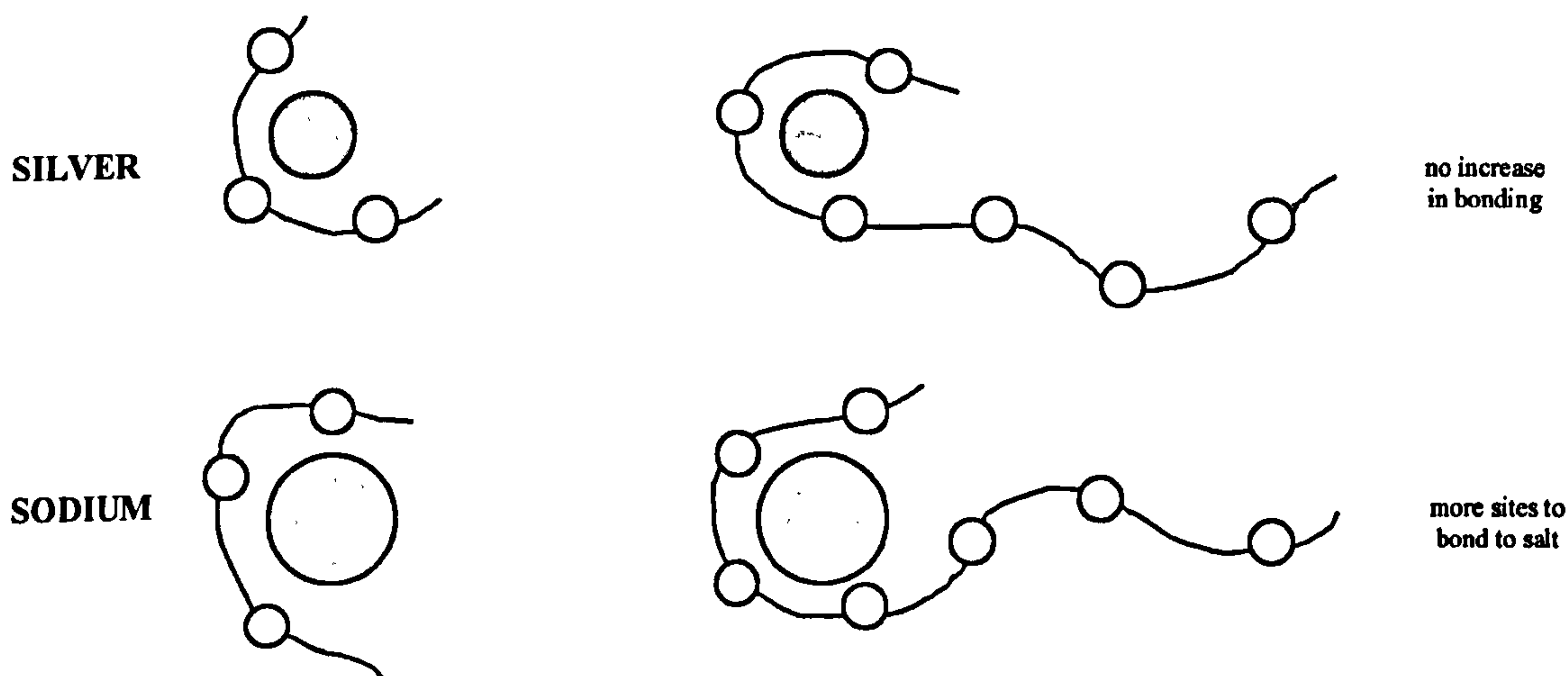


Figure 3p – Model to explain the effect of chain length on salt attachment

c) Rationalisation of Bias Effects

Returning to the subject of the laser settings, the initial increase in mass averages with an increase in laser power was rationalised as an increase in intensity of the higher mass oligomers. The larger the molecule, the more energy was required for it to desorb successfully and subsequently ionise. So, the threshold value should be considered as mass specific and as the laser power was increased, the maximum size of polymer that could be desorbed was steadily incremented. As the laser power is increased from the initial threshold value, the maximum oligomer size that was observed increased up to a limit. Above this limit, the polydispersity levelled out at a value that was usually slightly higher than those acquired from chromatographic sources.

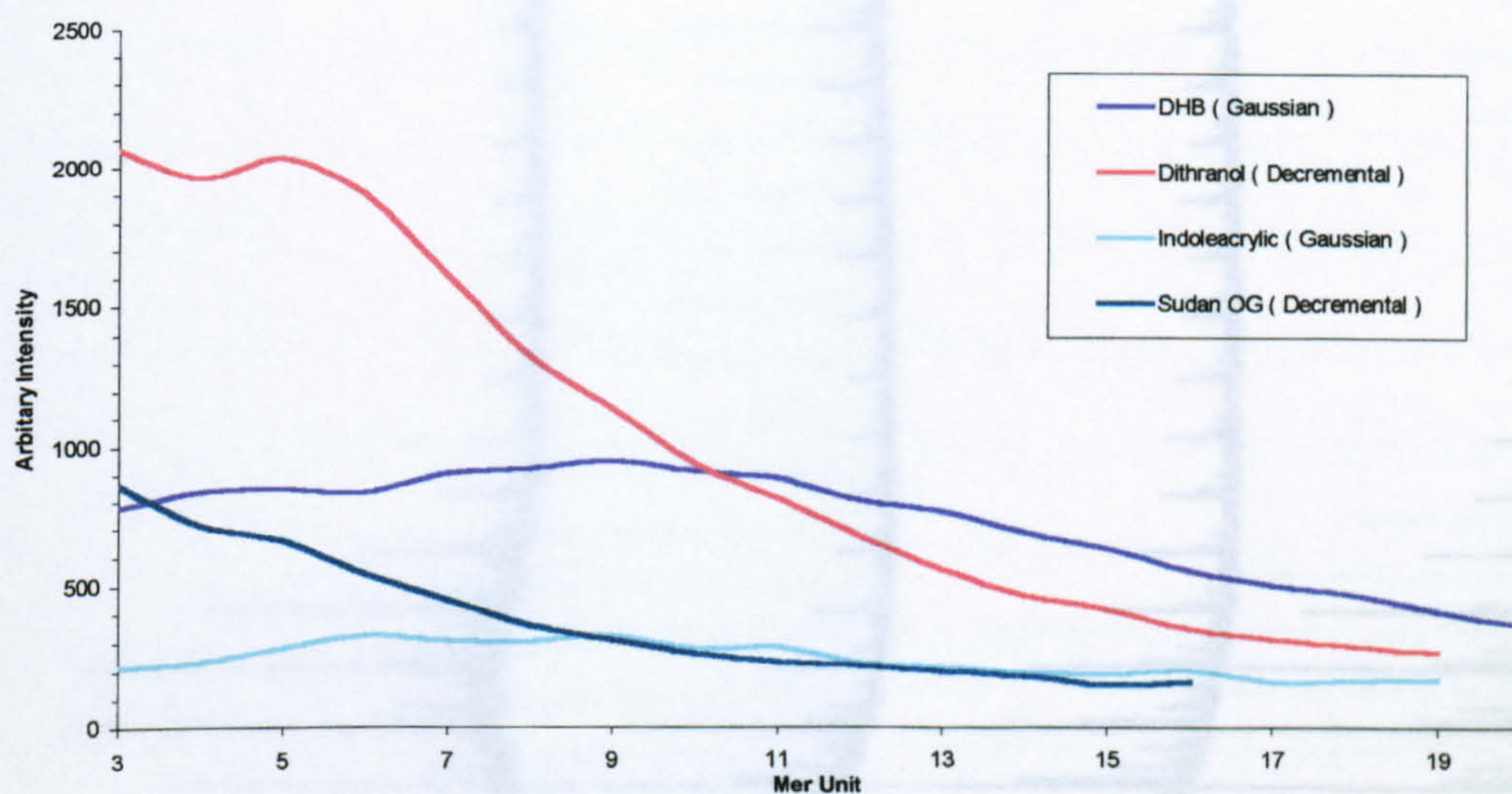


Figure 3q – Intensity plots showing both Gaussian and 'decremental' patterns for different matrices

Figure 3r – Overlaid spectra of a bimodal HEMA sample at two extreme acceleration voltages

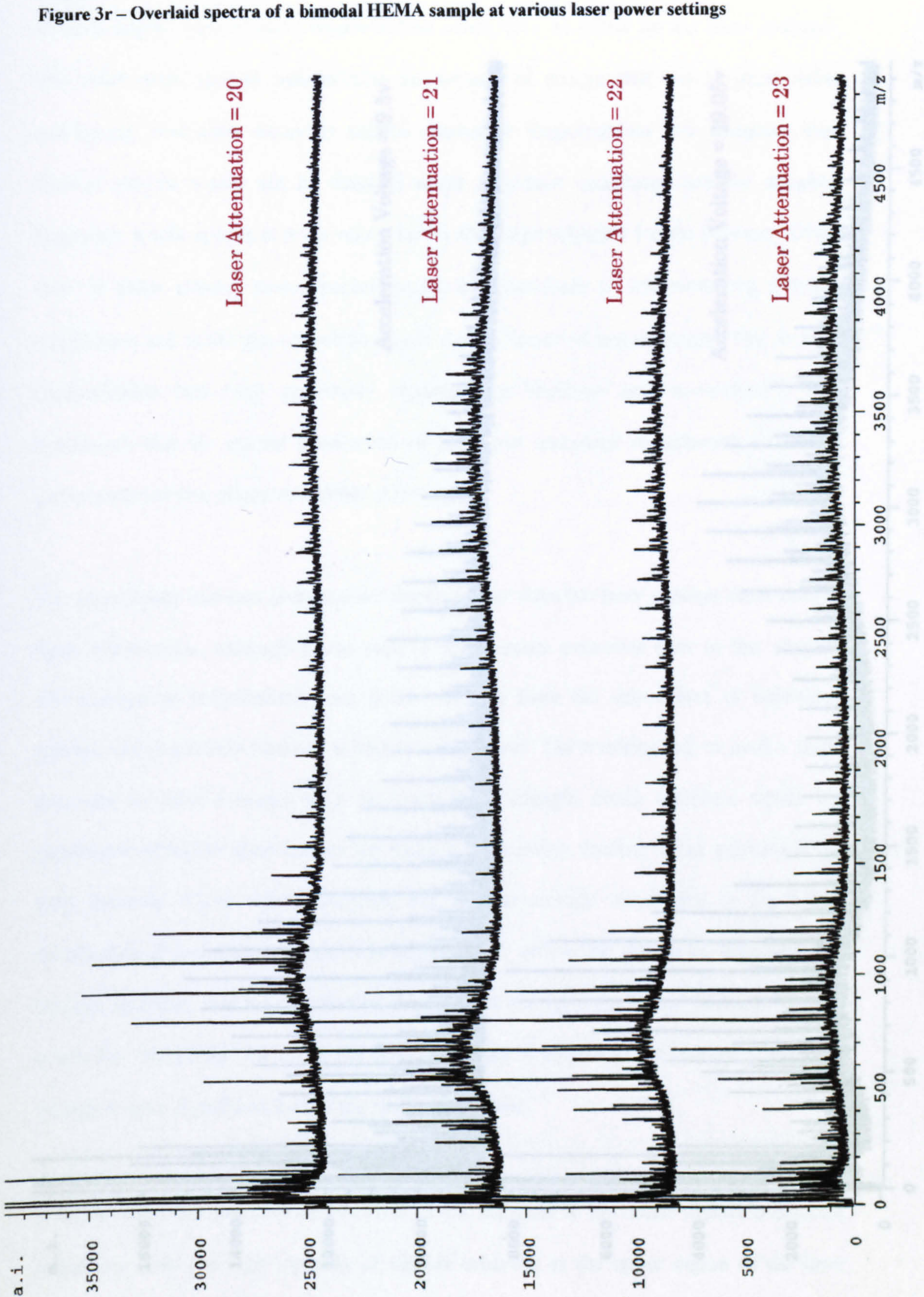
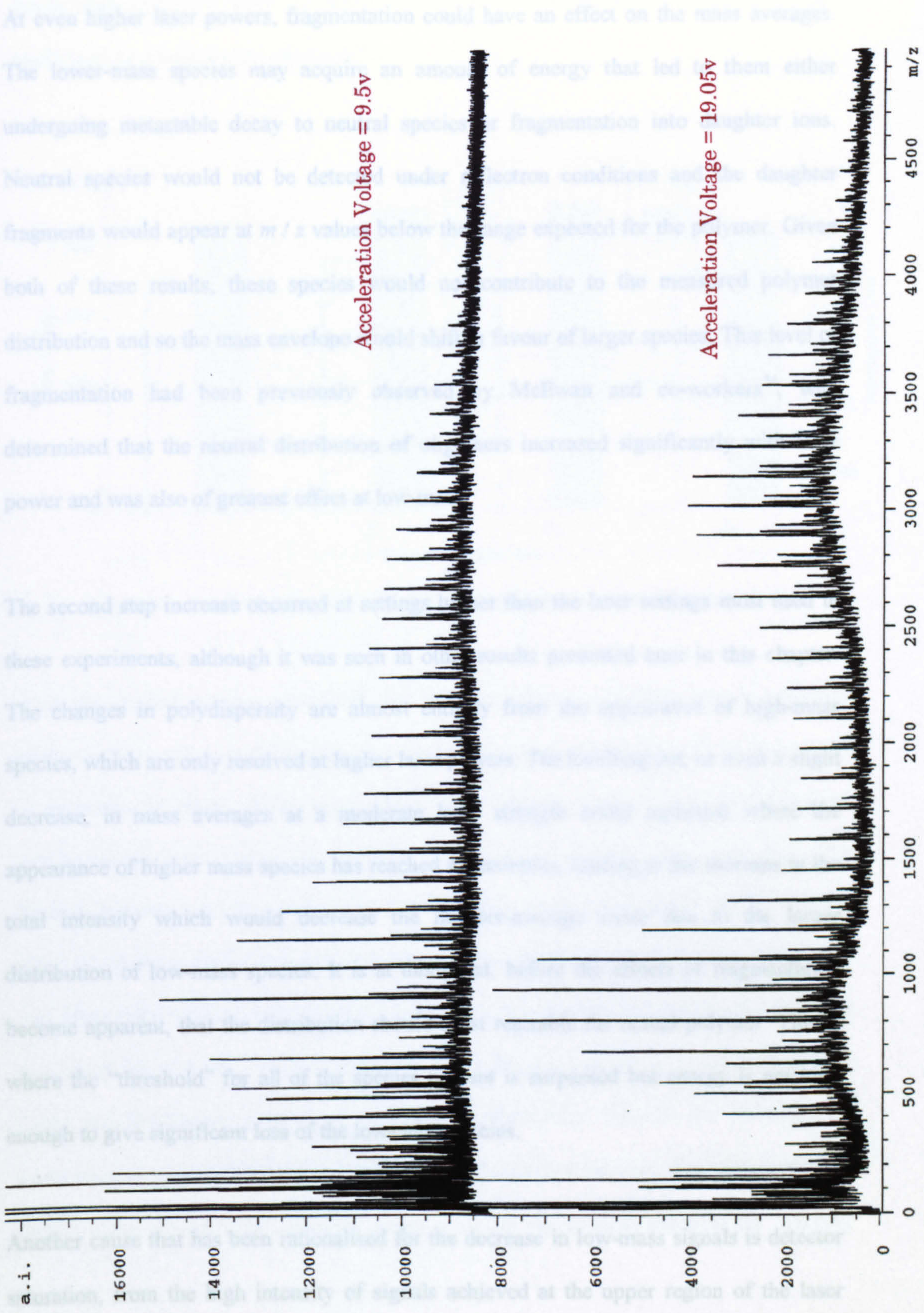


Figure 3rr – Overlaid spectra of a bimodal HEMA sample at two extreme acceleration voltages



¹⁹ CN McCreagh, C Jackson, BS Larsen, Int J Mass Spectrom Ion Proc, 160, 387, (1997)

At even higher laser powers, fragmentation could have an effect on the mass averages. The lower-mass species may acquire an amount of energy that led to them either undergoing metastable decay to neutral species or fragmentation into daughter ions. Neutral species would not be detected under reflectron conditions and the daughter fragments would appear at m/z values below the range expected for the polymer. Given both of these results, these species would not contribute to the measured polymer distribution and so the mass envelope would shift in favour of larger species. This level of fragmentation had been previously observed by McEwan and co-workers²⁴, who determined that the neutral distribution of oligomers increased significantly with laser power and was also of greatest effect at low-mass.

The second step increase occurred at settings higher than the laser settings most used in these experiments, although it was seen in other results presented later in this chapter. The changes in polydispersity are almost entirely from the appearance of high-mass species, which are only resolved at higher laser powers. The levelling out, or even a slight decrease, in mass averages at a moderate laser strength could represent where the appearance of higher mass species has reached a maximum, leading to the increase in the total intensity which would decrease the number-average value due to the larger distribution of low-mass species. It is at this point, before the effects of fragmentation become apparent, that the distribution should most resemble the actual polymer. This is where the “threshold” for all of the species present is surpassed but energy is not high enough to give significant loss of the low-mass species.

Another cause that has been rationalised for the decrease in low-mass signals is detector saturation, from the high intensity of signals achieved at the upper region of the laser

²⁴ CN McEwan, C Jackson, BS Larsen, *Int J Mass Spectrom Ion Proc*, 160, 387, (1997)

power scale. This can cause an apparent mass bias in the detection of ions by electron multipliers or channel-plate detectors²⁵.

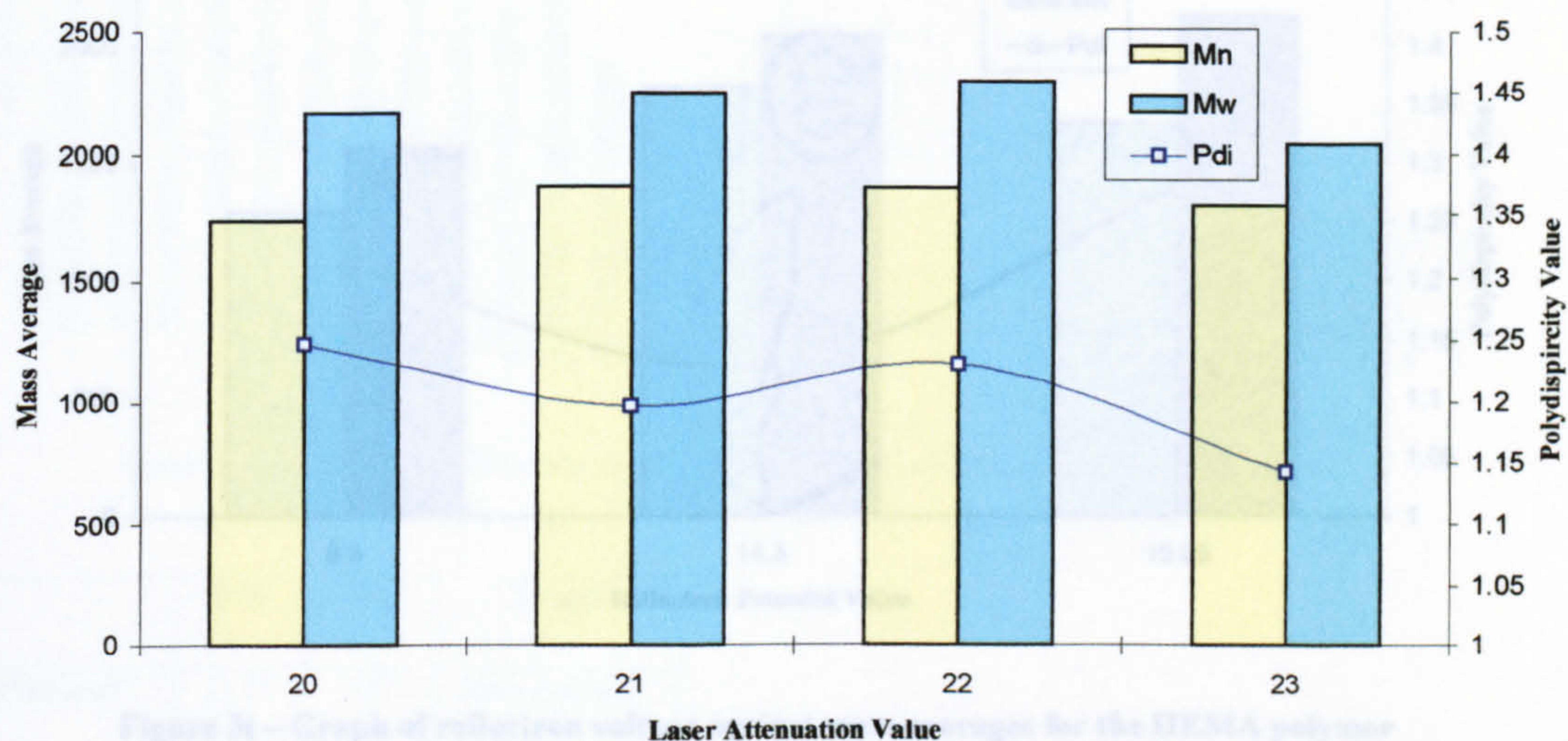


Figure 3s – Graph of laser power against mass averages for the HEMA polymer system

With the applied voltages, the field will have an effect on the ions that is inversely proportional to mass. Increasing the accelerating potential, which can also be considered as extracting in nature, brings more ions from the source region into the field-free area and so increases the overall ion intensity. The increased voltages have been shown by Tang to increase resolution and signal-to-noise ratio. These two changes might have the effect of giving a higher apparent intensity for the species in the high-mass tail, which was previously masked by background noise. Lower acceleration voltages also give rise to a lower ion velocity, which is important in the detection of the ions. Observations by Geno and MacFarlane suggest an exponential relationship between the efficiency of multi-channel plate detectors and velocity²⁶. The differences between distribution above a certain value are not great, however under a certain acceleration potential the intensity

²⁵ J Axelsson, E Scrivener, DM Haddleton, PJ Derrick, *Macromol*, 29, 8875, (1996)

²⁶ PW Geno, RD MacFarlane, *Int J Mass Spectrom Ion Proc*, 92, 195, (1989)

loss is significant enough to cause a decrease in mass average of, in this instance, over 400 mass units.

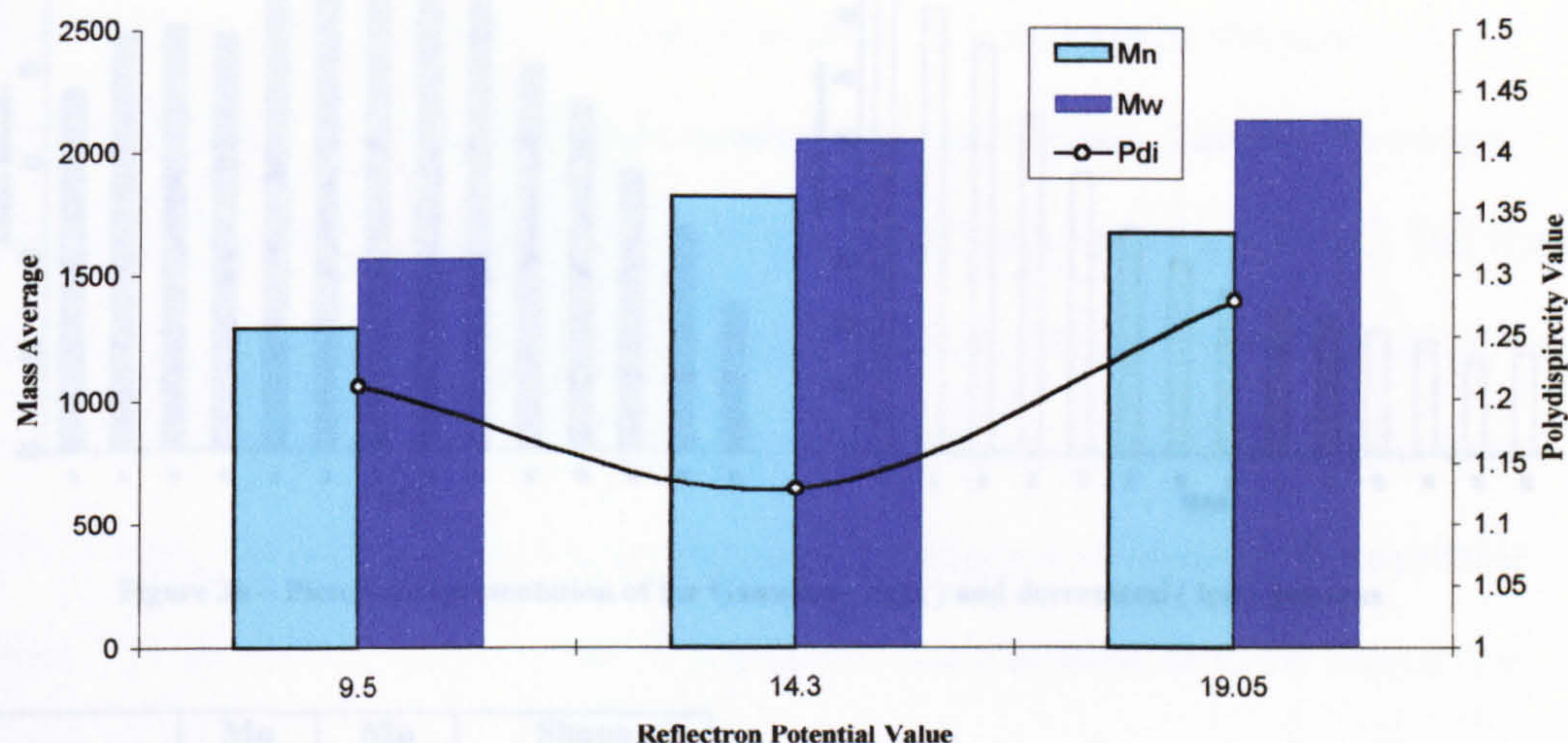


Figure 3t – Graph of reflectron voltage against mass averages for the HEMA polymer

Of the various experimental conditions, the effect of matrix was the most pronounced, with the greatest range in mass averages. With a difference of approximately 600 mass units combined with a laser power and voltage variations in the order of 100 and 75 respectively, that would mean a total possible range of nearly 800 daltons for a polymer whose average molecular weight was only around 1800. Direct observation of the mass distributions given by the four matrices showed very different profiles. The sudan orange and dithranol gave a very strong intensity for the very low mass species that quickly dropped. In fact intensities with dithranol were consistently the highest of all the matrices but only up to the decamer. Indoleacrylic acid and DHB gave distinctly more Gaussian distributions, however, the former was of such a low intensity that the high mass tail was lost to noise by the octadecamer. Of all the matrices, only DHB gave consistently discernible readings for the high-mass end of the polymer above the hexadecamer, which is why it gave the highest mass averages and polydispersity.

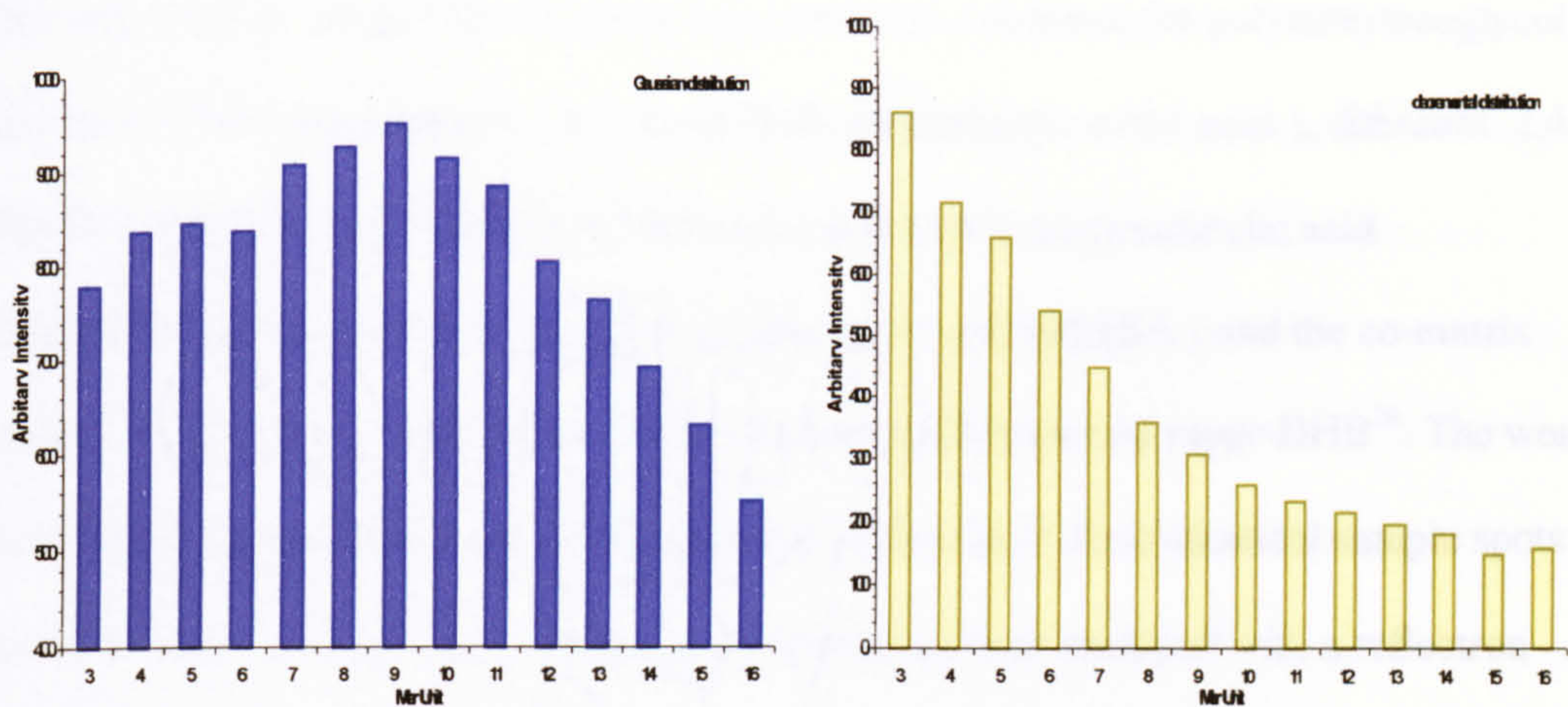


Figure 3u – Pictorial representation of the Gaussian (right) and decremental (left) patterns

	Mn	Mp	Shape
Dithranol	1171	747	Decremental
Sudan OG	1076	454	Decremental
DHB	1725	1333	Gaussian
Indole	1505	1186	Gaussian

The ultimate comparison in these two modes of distribution can be seen with the Mp values. These represent the most probable or in other words most intense ion species. The exact reasons for this large disparity are not clear from these results, but it must be due in some way to the interactions of the activated matrix with the polymer molecules. The gas-phase chemistry in the MALDI plume is still a topic of much debate²⁷, with a number of possible mechanistic routes suggested. The two different natures of distribution could suggest that there were two different processes at work here, essentially the DHB and dithranol molecules were working as matrices by slightly different routes. It was therefore of interest to extend this investigation to other common matrix systems.

²⁷ R Zenobi, R Knochenmuss, Mass Spec Rev, 17, 337, (1998)

The same sample preparation as above was used with a commercial poly(ethyleneglycol) and for the following matrices : α -cyanoxy-4-cinnamic acid (acca), dithranol, 2,4-dihydroxybenzoic acid (DHB), indoleacrylic acid (IA), aminosalicylic acid (AminoSA), SN5A, 2-(4-hydroxyphenylazo)benzoic acid (HABA) and the co-matrix system of DHB and 2-hydroxy-4-methoxybenzoic acid known as super-DHB²⁸. The work was carried out on the Kompact IV instrument, with at least three identical sample spots for each matrix on each slide. Although the instrument was equipped with a reflectron time-of-flight, linear detection was used in these experiments to maximise the available signal. The 337nm wavelength of the nitrogen laser was also suitable to the known maxima of all the matrices under study.

The two-layer sample preparation consisted of 0.5 μ l of a 0.1M solution of the matrix in a suitable solvent, followed by the same volume of a 10⁻³M polymer solution made in this instance in a 5:1 acetonitrile / water solvent system. No additional salt was added, unless a scouting run showed significant non-sodiated ions that could affect the calculated mass averages as shown in the previous work. The significance limit for non-sodiated ions was set at no greater than 5% of the related sodium-attached peak intensity. If it was higher, sodium chloride was added to the matrix solution. As also mentioned above, each combination was present at least three times of each of the 10-well slides and also on multiple separate slides. This ensured a high level of statistical reliability in the results, with spot-to-spot and slide-to-slide comparability therefore possible. Each individual spectra was composed of 50 shots scanned across the entire sample area, so as to average out any deficiencies or "sweet spots".

²⁸ M Karas, H Ehring, E Nordhoff, B Stahl, K Strupat, F Hillenkamp, M Grehl, B Krebs, *Org Mass Spectrom*, 28, 1476, (1993)

The laser power range for each matrix varied depending on the threshold value and the ability to last over a series of experiments. The minimal number of experiments was achieved with HABA which only gave three different laser powers at a separation of 10 nominal units. These spectra were all of low intensity and quickly deteriorated at high laser powers. In comparison, *acca* was able to provide twelve experimental sets from each spot with laser powers stepped by 5 from the threshold value. The matrices that tended to give the least number of sets were those that required a higher threshold laser power, which is perhaps consistent with higher powers depleting the sample spot more quickly. The nominal values given for laser powers were in themselves rather qualitative, only showing an increase in applied energy that followed a roughly logarithmic relationship. Power readings could have been taken using a suitable meter and the relationship defined. For the purpose of these experiments, the exact laser power was not of prime importance compared to the fact that it was an increase.

Plotting the mass values as a simple bar chart best showed the pattern given by each series. Each set contributed to the values for number-average and weight-average molecular weight and polydispersity. Each matrix system varied across the range, but held to the same overall pattern.

Figure 3v – Bar graph showing overall trend for the aCCa matrix system

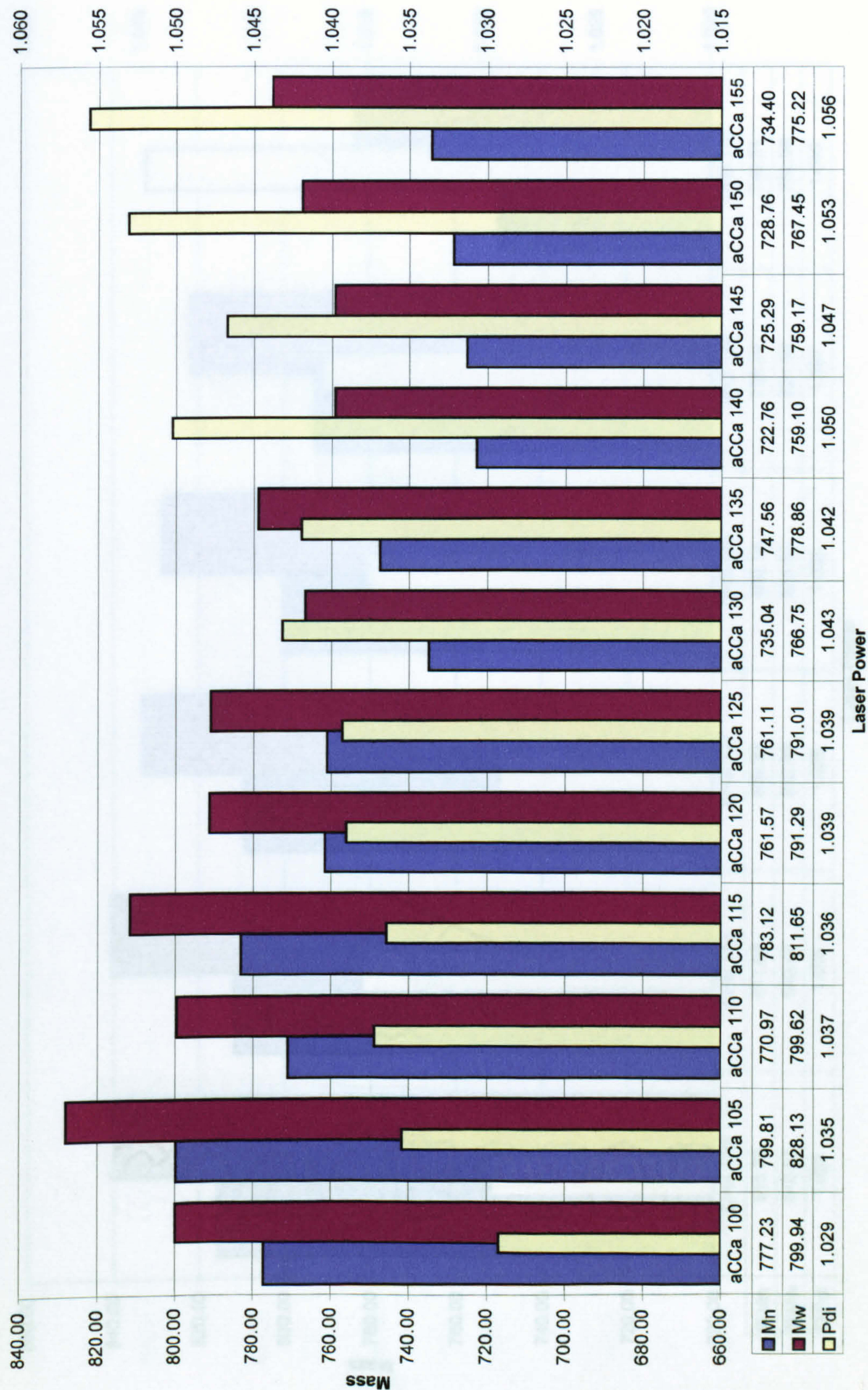


Figure 3w – Bar graph showing overall trend for the DHB matrix system

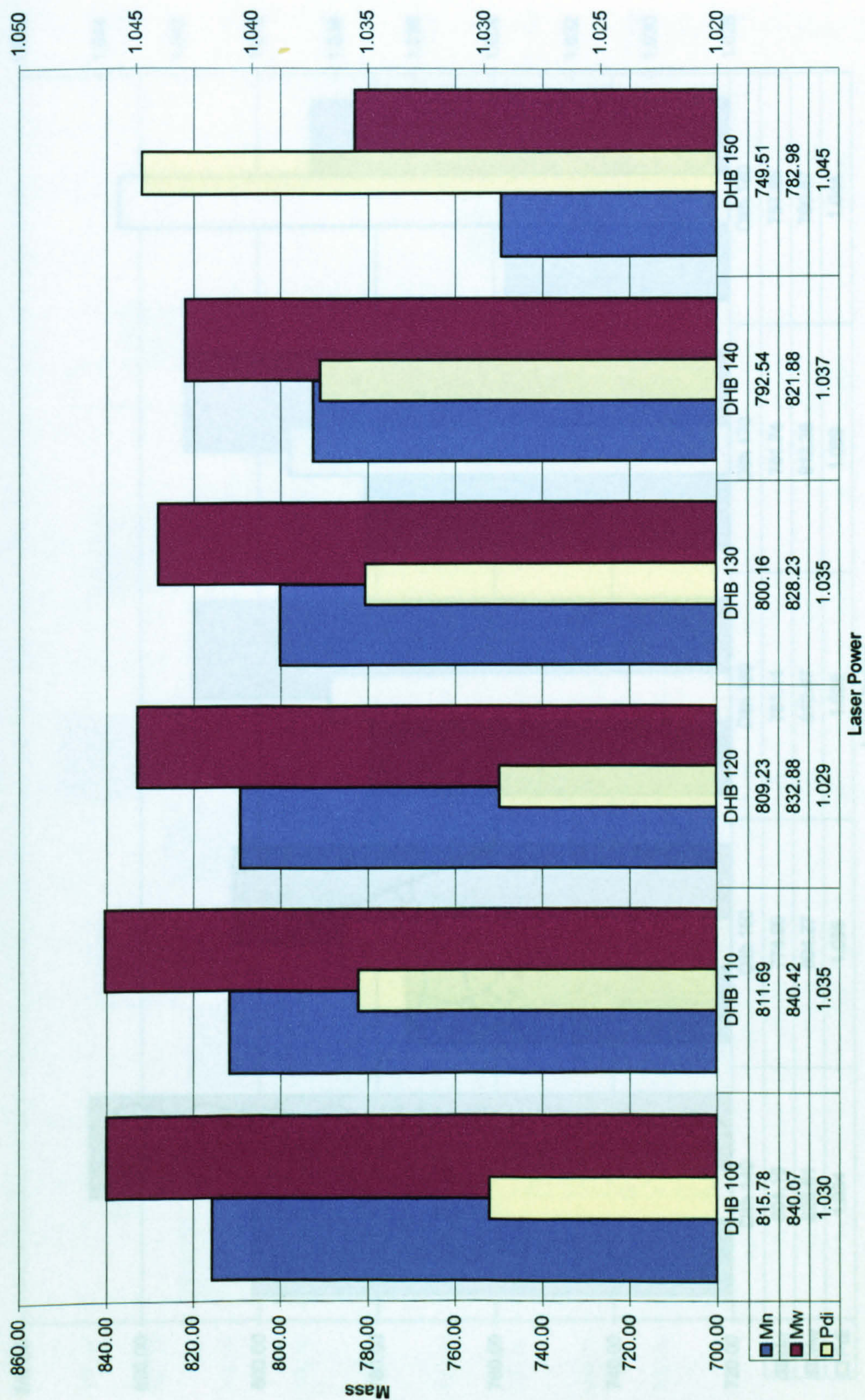


Figure 3x – Bar graph showing overall trend for the dithranol matrix system

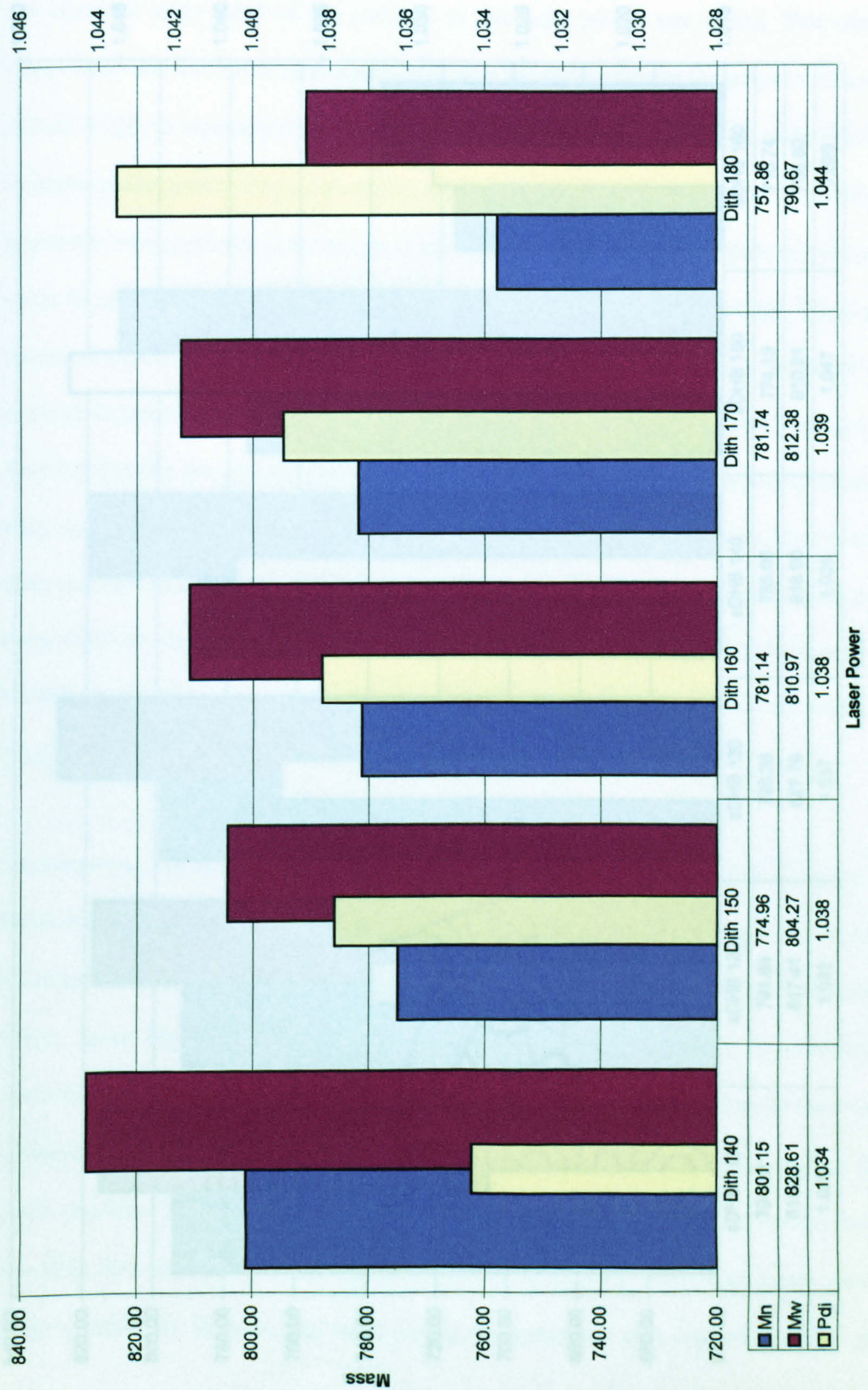
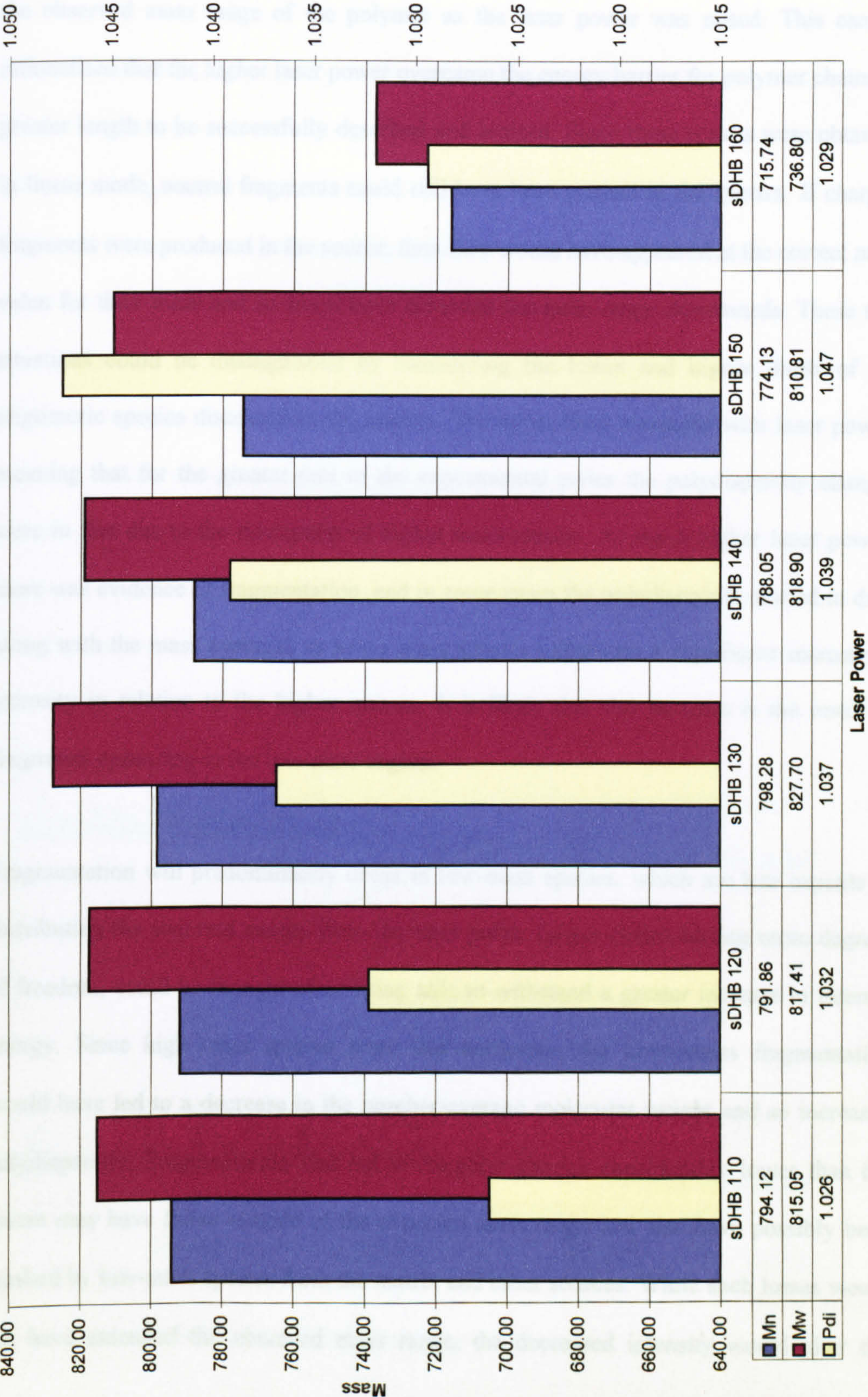


Figure 3y – Bar graph showing overall trend for the super-DHB matrix system



The most straight-forward pattern observed in all but one matrix system was a steady increase in polydispersity. As mentioned before, this represented a continual increase in the observed mass range of the polymer as the laser power was raised. This can be rationalised that the higher laser power overcame the energy barrier for polymer chains of greater length to be successfully desorbed and ionised. Since these results were obtained in linear mode, neutral fragments could still have been present in the spectra. If charged fragments were produced in the source, then they would have appeared at the correct m/z value for their mass and so could have extended the mass range downwards. These two situations could be distinguished by considering the lower and higher limits of the oligomeric species discerned in the spectra. The upper limit increased with laser power, meaning that for the greater part of the experimental series the polydispersity changes were in fact due to the desorption of higher mass species. At much higher laser powers there was evidence of fragmentation, and in some cases the polydispersity started to drop along with the mass averages as lower mass species underwent a significant increase in intensity in relation to the higher masses. It is likely that this increase is the result of fragments appearing in the low-mass region.

Fragmentation will predominantly occur in low-mass species, which are less capable of distributing the acquired energy from the laser pulse. Larger chains having more degrees of freedom, could be thought of as being able to withstand a greater increase in internal energy. Since high mass species were less numerous, the lower-mass fragmentation would have led to a decrease in the number-average molecular weight and so increased polydispersity. Fragmentation that led to daughter species considerably lower than the parent may have fallen outside of the expected mass range and also have possibly been masked by low-mass species from the matrix and other sources. While such losses would not have extended the observed mass range, the decreased intensity would alter the

number-average and so affect polydispersity, as observed in a number of experiments at the higher laser powers.

This decrease in polydispersity at higher laser powers was often very sudden and dramatic. This suggests something more than a gradual increase in fragmentation or a saturation of the higher mass species. The decrease was typically greater than any of the previous step increases and is more likely to be a result of loss of resolution of the higher mass species. As laser power increased, the peak widths also increased due to a great variance in the energies of molecules within the source region. Background noise also increased at higher laser powers and these two effects combine to affect the ability to separate out true ion peak intensities at the high mass species which tended to already be of fairly low intensity. The loss of these values from the calculation decreased the mass averages, especially the weight-average value which then has a sequential effect on the polydispersity.

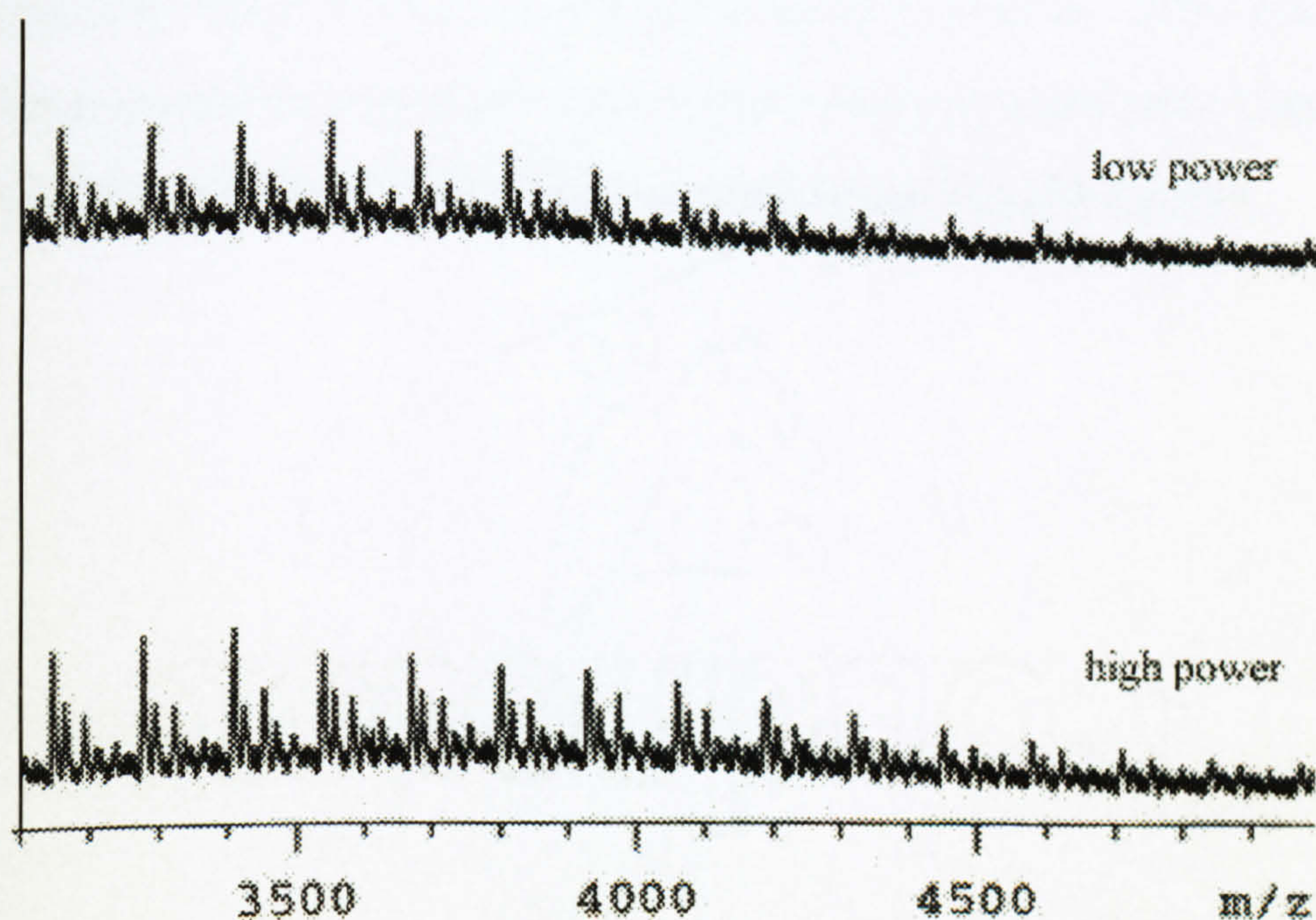


Figure 3z – Enlargement of the high mass area of the spectra

number-average and so affect polydispersity, as observed in a number of experiments at the higher laser powers.

This decrease in polydispersity at higher laser powers was often very sudden and dramatic. This suggests something more than a gradual increase in fragmentation or a saturation of the higher mass species. The decrease was typically greater than any of the previous step increases and is more likely to be a result of loss of resolution of the higher mass species. As laser power increased, the peak widths also increased due to a great variance in the energies of molecules within the source region. Background noise also increased at higher laser powers and these two effects combine to affect the ability to separate out true ion peak intensities at the high mass species which tended to already be of fairly low intensity. The loss of these values from the calculation decreased the mass averages, especially the weight-average value which then has a sequential effect on the polydispersity.

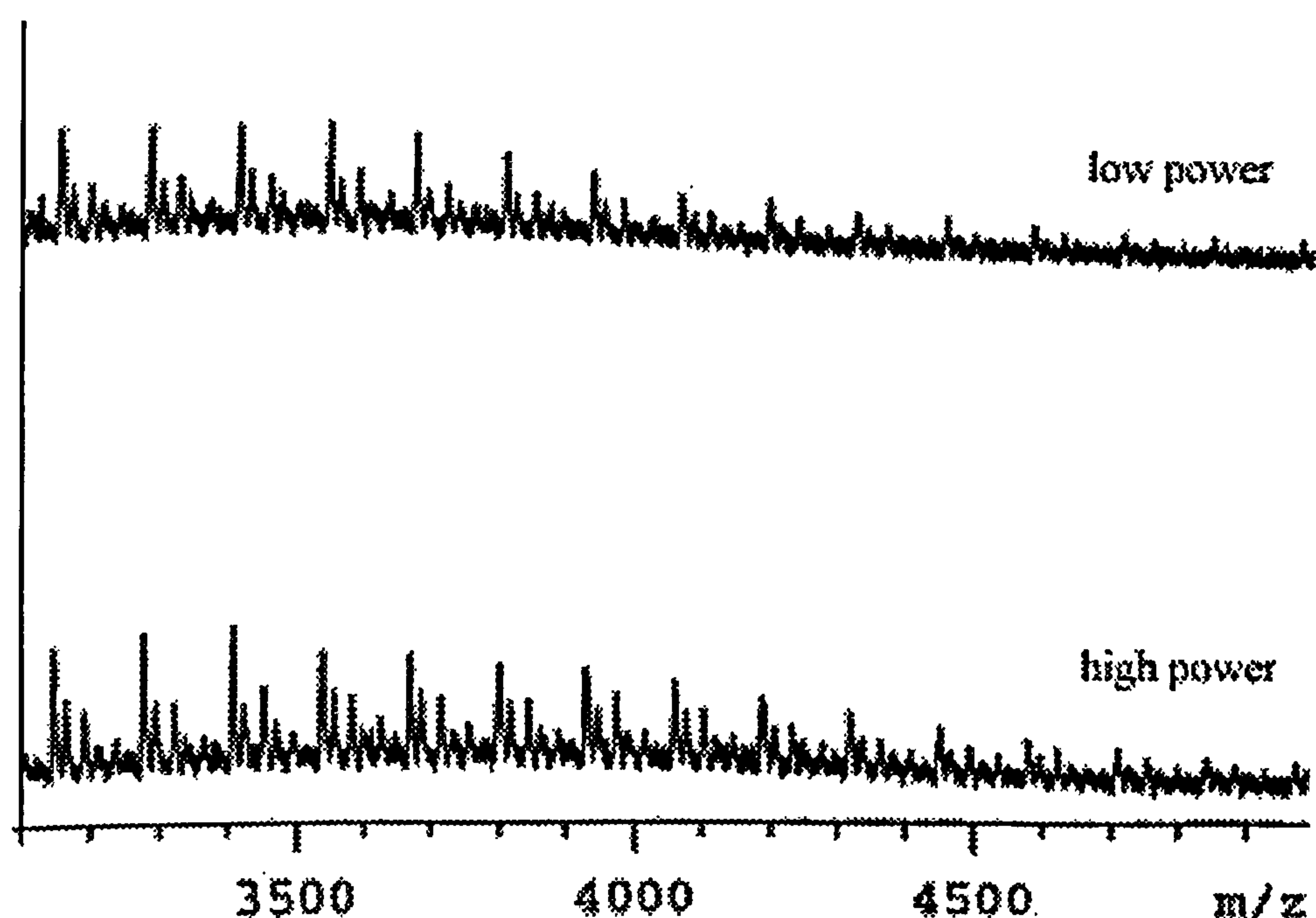


Figure 3z – Enlargement of the high mass area of the spectra

In contrast to the polydispersity, the mass averages in general decreased as the laser power went up. In many cases this was preceded by a slight increase. Previous work had shown this trend, which can be rationalised as a significant increase in the high-mass end as they acquire enough energy to successfully desorb and ionise. Once the energy crosses a threshold sufficient for all major polymer chains, then the lower mass region continues to increase at the same rate as the higher masses leading to a slower decrease in averages, especially that of number-average molecular weight. The effect of resolution loss at high-mass will have also worked towards reducing these values.

If the average mass values for all matrix systems were plotted against laser power, a more pronounced pattern was observed. All data points lay within a mass window of 50-80 Daltons and decreased as laser power increased. This was significant as it meant that matrix systems that had a higher laser threshold already started with a lower mass average than those at the low end of the scale. So while the choice of matrix had an effect on the mass value, the greater trend was with the laser power to which the sample was exposed. This accounted for the larger differences in mass values at threshold, since it was not only the matrix that differed but often the laser power used to obtain that spectrum.

Figure 3aa – Overall trend in M_n values showing variations between matrices and laser power

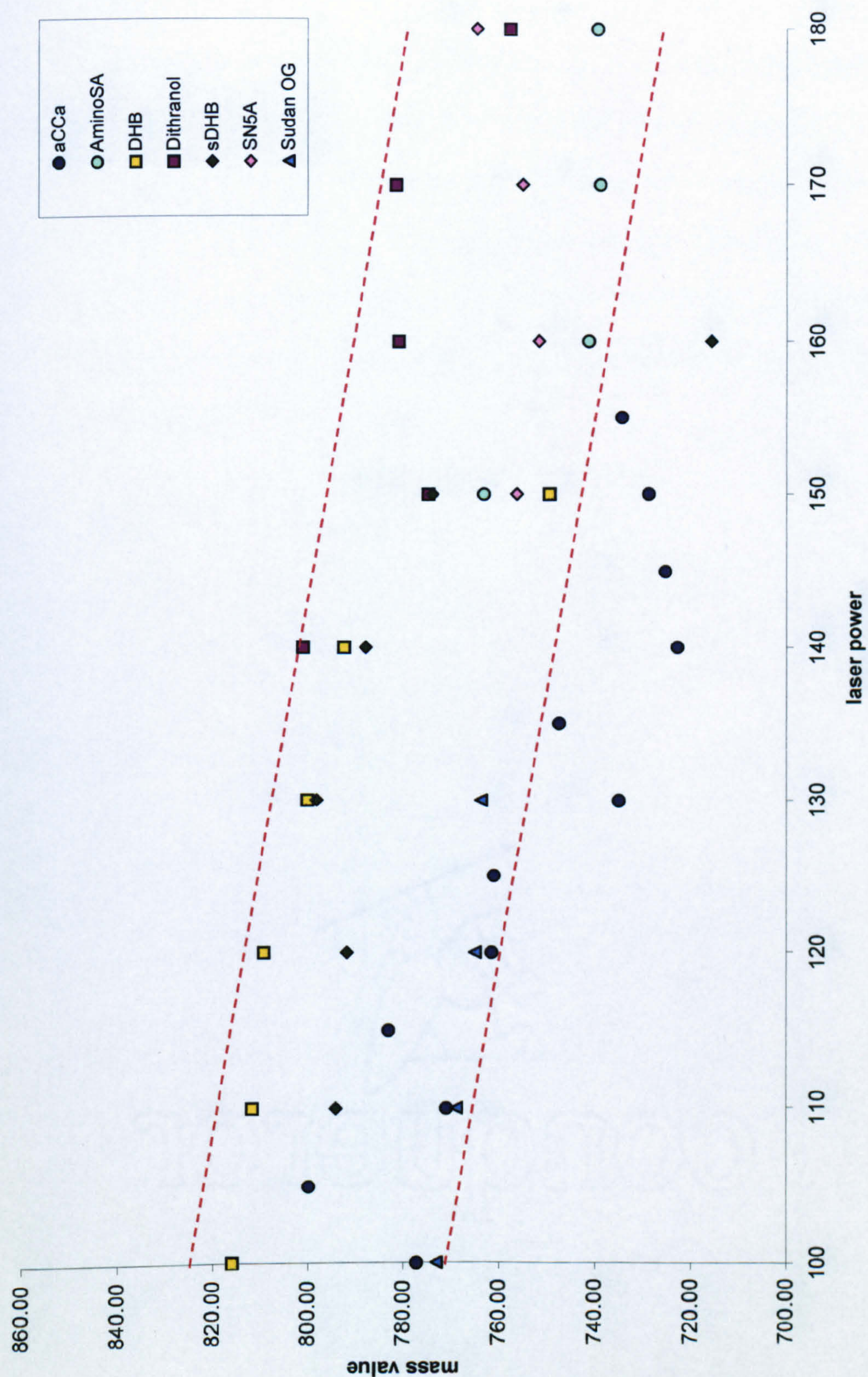
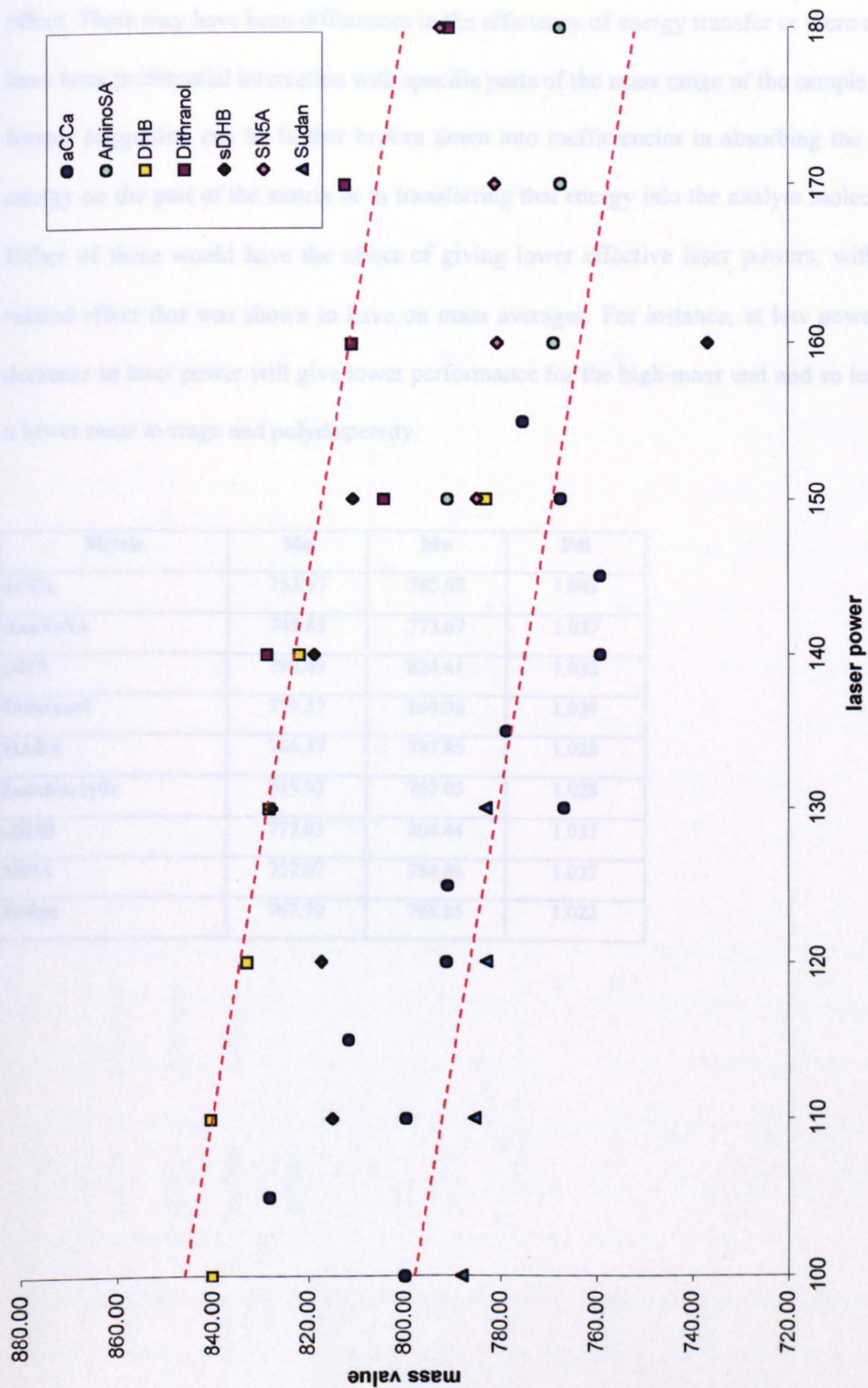


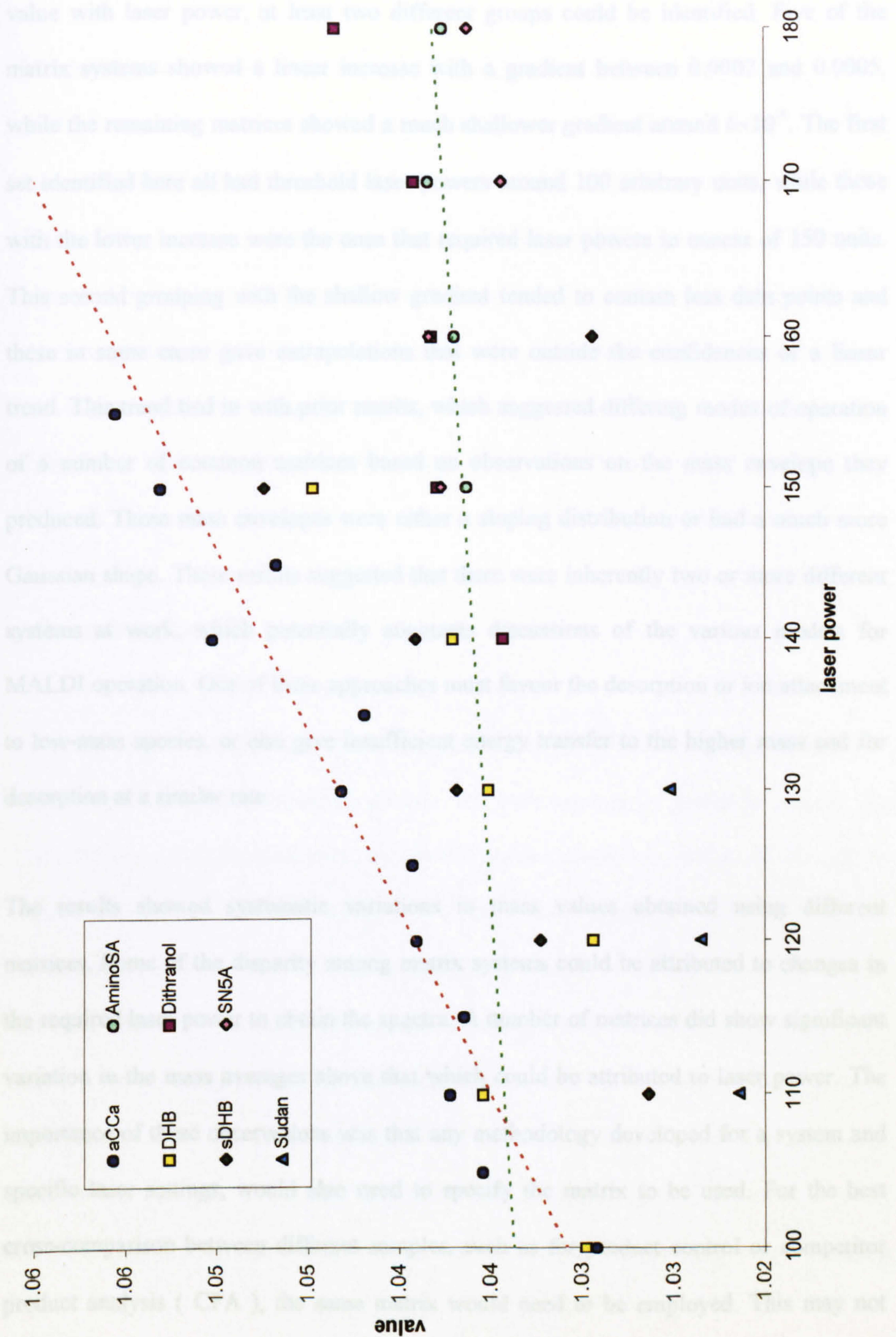
Figure 3ab – Overall trend in M_w values showing variations between matrices and laser power



This effect aside, there was still a systematic variation in mass averages between matrix systems. There are two main possibilities that could be attributed as to the cause of this effect. There may have been differences in the efficiency of energy transfer or there could have been preferential interaction with specific parts of the mass range of the sample. The former suggestion can be further broken down into inefficiencies in absorbing the laser energy on the part of the matrix or in transferring that energy into the analyte molecules. Either of these would have the effect of giving lower effective laser powers, with the related effect that was shown to have on mass averages. For instance, at low powers, a decrease in laser power will give lower performance for the high-mass end and so lead to a lower mass average and polydispersity.

Matrix	Mn	Mw	Pdi
aCCa	753.97	785.68	1.042
AminoSA	745.83	773.67	1.037
DHB	796.49	824.41	1.035
Dithranol	779.37	809.38	1.039
HABA	766.37	787.85	1.028
Indoleacrylic	745.93	767.05	1.028
sDHB	777.03	804.44	1.035
SN5A	757.07	784.86	1.037
Sudan	767.70	784.85	1.022

Figure 3ac – Overall trends in polydispersity for matrices and laser power



A more interesting pattern could be discerned within the polydispersity results viewed in the same manner. While all matrices, as discussed earlier, gave a continual increase in value with laser power, at least two different groups could be identified. Five of the matrix systems showed a linear increase with a gradient between 0.0002 and 0.0005, while the remaining matrices showed a much shallower gradient around 6×10^{-5} . The first set identified here all had threshold laser powers around 100 arbitrary units, while those with the lower increase were the ones that required laser powers in excess of 150 units. This second grouping with the shallow gradient tended to contain less data points and these in some cases gave extrapolations that were outside the confidences of a linear trend. This trend tied in with prior results, which suggested differing modes of operation of a number of common matrices based on observations on the mass envelope they produced. These mass envelopes were either a sloping distribution or had a much more Gaussian shape. These results suggested that there were inherently two or more different systems at work, which potentially augments discussions of the various models for MALDI operation. One of these approaches must favour the desorption or ion attachment to low-mass species, or else give insufficient energy transfer to the higher mass end for desorption at a similar rate.

The results showed systematic variations in mass values obtained using different matrices. Some of the disparity among matrix systems could be attributed to changes in the required laser power to obtain the spectra. A number of matrices did show significant variation in the mass averages above that which could be attributed to laser power. The importance of these observations was that any methodology developed for a system and specific laser settings, would also need to specify the matrix to be used. For the best cross-comparison between different samples, such as for product control or competitor product analysis (CPA), the same matrix would need to be employed. This may not

necessarily be the matrix that gives the best individual spectra for either system, but rather one that gives a reasonable level for both.

The observation that two different mass distributions existed was of concern as both could not represent the true distribution of the polymer. The Gaussian pattern and the more decremental system are mutually exclusive as they emphasis different parts of the mass envelope and any similarity in mass average would be down to chance. The matrices with a higher laser threshold that gave this decremental pattern resulted in a mass average that was generally lower than that given by other techniques for the sample. This suggests that these matrices were unsuitable for this application, but it must be stressed that without a clear understanding of the physical principles underlying this difference, the relative utility with other systems cannot be inferred from these results.

v. Other Samples

A number of other polymeric systems examined using MALDI did not explore issues of bias or experimental considerations directly, but were however of particular interest. As was noted in the initial introduction, one class of polymers that has resisted all attempts to acquire reasonable MALDI spectra are the truly aliphatic systems such as poly(propylene). While the standard straight-chain version is certainly common enough that GPC calibration standards are available, anything with more complicated architecture runs into the problems discussed. The linear form is used in very high-density systems, since the thin wire-like chains can pack very closely together with no side groups to interrupt the process. While such a product has a defined industrial use, it is often beneficial to create side-groups and other features to modify this packing and so decrease

the density. This can help processing or give other engineering features for the final product.

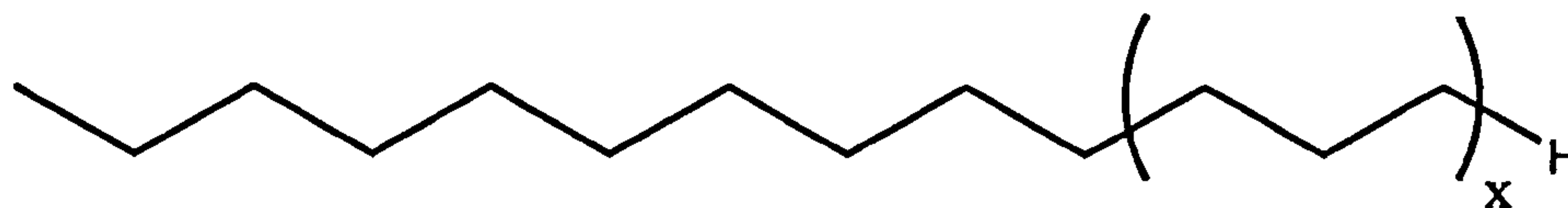


Figure 3ad – Structure of poly(propylene)

If mass spectrometry was available as a technique, it would be able to ignore the effects of the macrostructure and give a direct mass value. Even accounting for any concerns in the accuracy of the value, it would be comparable to the reliability of calibrations for such techniques as GPC. That said, the polymer does not produce any form of reliable MALDI spectra which could be due to resistance to desorption or the inability to acquire charge. A number of different sample preparations have been tried, also including the use of complex matrix systems, derivatisations and use of transition metals in an attempt to force cationisation. The techniques developed to look at bias effects were applied to a sample acquired from Shell Global Solutions main laboratory, as a minor attempt to see if such developments could improve the standing of the analysis.

Another sample class that was explored was organometallic additives used in a range of petrochemical products. These consisted of a number of transition metal centres linked by oxygen and sulphur bridges, with either alkyl or ether tails at the ends. The structure of two such compounds is shown below. The compounds have been explored previously by various mass spectrometric technique, such as atmospheric pressure chemical ionisation (APCI) and gas chromatography – quadrupole mass spectrometry (GC-MS), but those give considerable formation of clusters and other artefacts. It was hoped that MALDI may have resulted in clearer spectra that allow an easier interpretation in terms of the structure.

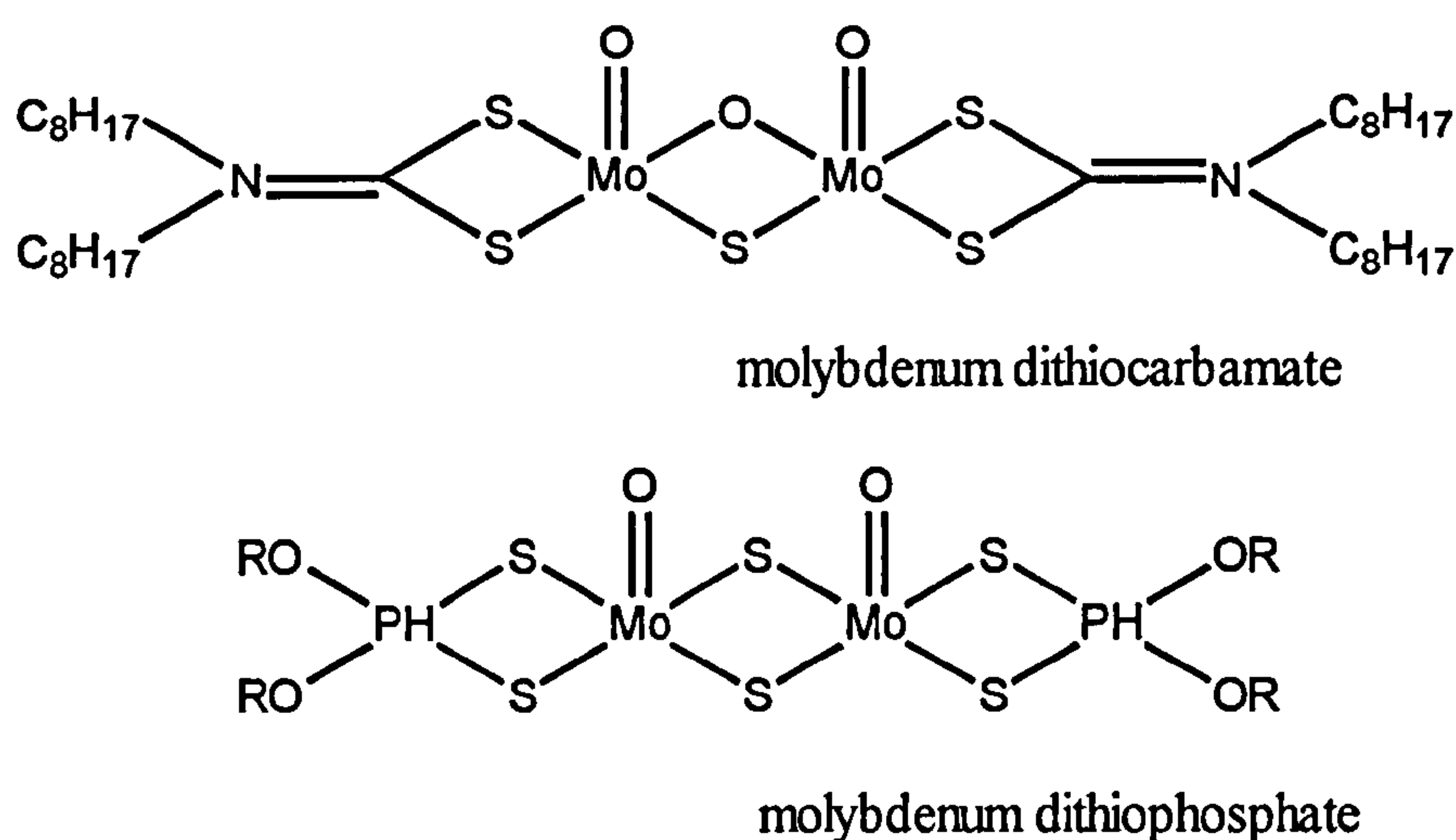


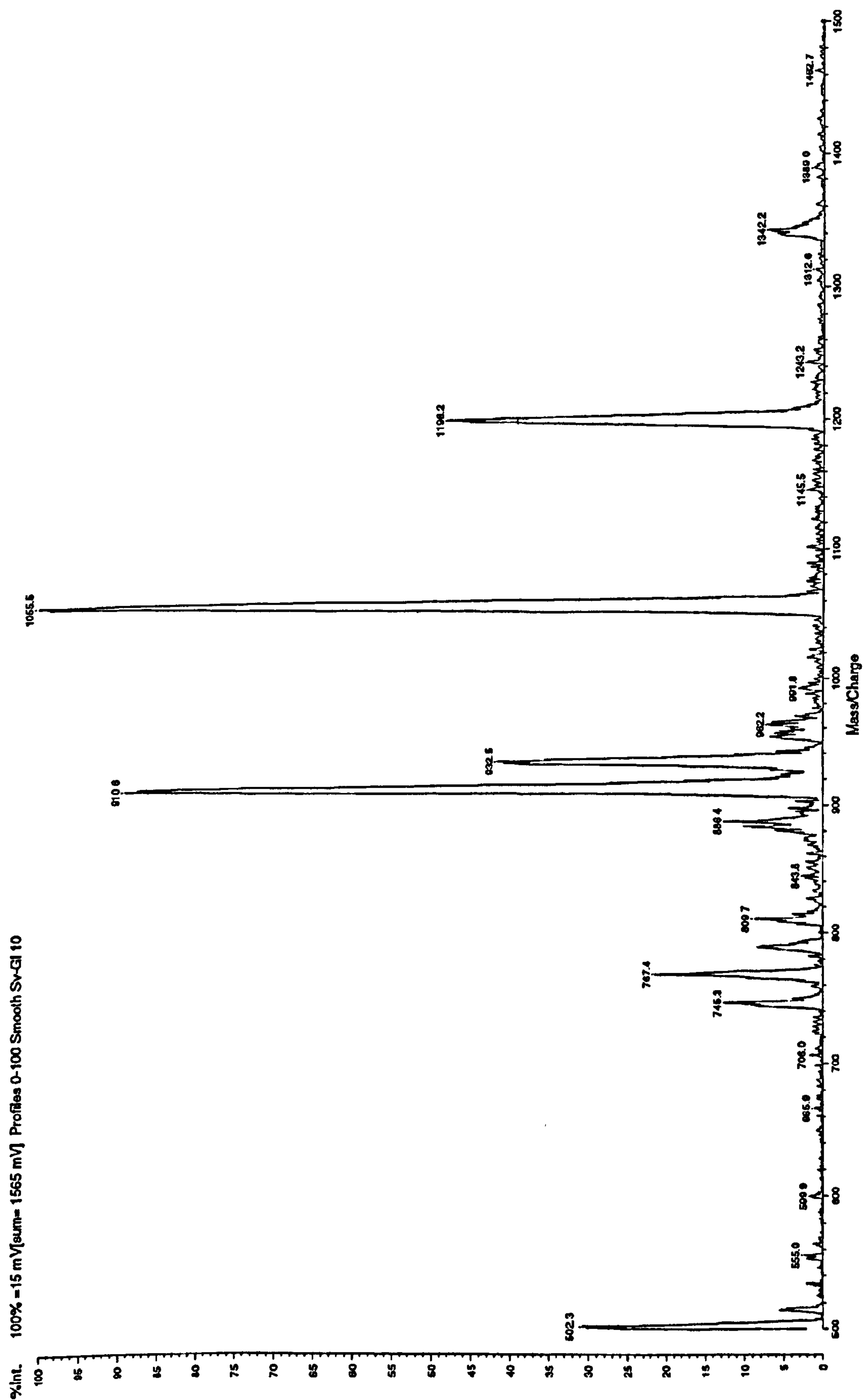
Figure 3ae – Predicted structure of two of the organometallic additives under study

The samples were prepared at a range of concentrations with a number of solvents and matrices, since no comparable information was available as to which system would be best suited to this type of molecule. While the oxygen centres and the ether groups suggested that they might act like a polyether system, the presence of the sulphurs and the charged transition metals complicated the situation. As it happened the MALDI spectra produced were not of high quality, especially when compared to the intensities of the polymer standards used to calibrate the mass scale of the instrument. While a number of true ion peaks were observed, these could not be rationalised with the supposed structure of the analyte given a single charge or the attachment of common species, such as matrix or alkali metal salts.

The three main peaks observed in the spectra appeared to arise from the sample and not from any contaminant and were visible in most sample preparations that resulted in an ion signal. The expected mass of the species was 905.12, but no peak appeared here or at a logical difference from this point. The m/z 911.2 could perhaps be rationalised as lithium attachment (expected 912.06), but since the system did not have any lithium source

added it would be very unusual to see that peak without the presence of sodium and / or potassium adduct ions at a comparable or higher intensity. The matrix used in the spectra in question was sudan orange which has a formula mass of 214.2, so this could be discounted as attached to the molecular ion as there were no peaks at all in the expected range. The fact that the three main peaks appeared to be matrix independent also suggested that they did not arise from complexes formed with any part of the matrix. The most likely source was therefore other species present in the commercial samples or parts of another organometallic molecule. That was assuming that the structures supplied were in fact entirely correct for those present in the sample. While the APCI results showed molybdenum-containing species, they again did not correspond with the molecular ion and showed clusters at above the expected m/z similar, but not identical to, those seen with the MALDI results.

Figure 3af – Spectra of the molybdenum dithiocarbamate sample



vi. Mass Reliability

With the large number of spectra acquired in this work from a wide range of different samples, it was possible to evaluate mass precision and accuracy for the systems used. The former is looking at how measured mass values for each oligomer change from one run to another, while the latter is more concerned with how close the values are to the actual known mass. Since for all of the calculations in the preceding work the mass values have been substituted, this diminished any effect of accuracy on the actual results. Accuracy is also a function of calibration, since time-of-flight is in this sense a relative technique. If the calibration is good then it would be supposed that the resultant value for any ion would be correct dependent on the precision, that is the ability to constantly produce the same flight time. So it is therefore the mass precision that is the more crucial parameter for routine analysis of polymer samples. This precision can be given between spots on a slide, between slides in an experiment or even from day to day. Mass accuracy has been seen in these experiments to be predominantly a function of the instrument, with sample preparation and matrix choice having little effect on the resultant masses.

While this considers reliability in the mass scale, the calculations shown throughout the previous sections for mass average can be thought of as describing the precision in intensity. This is where there was greater concern, as although mass deficiencies can be corrected as carried out in these experiments, it is artificial and inconsistent variations in intensity that lead to changes in the mass averages. Intensity will of course vary with sample preparation, if this was simply a linear effect there would be little concern. One exception to this is the point at which a decrease in total ion intensity due to some effect leads to the effective disappearance of mass peaks. For a typical preparation using a 780

nominal mass poly(ethyleneglycol) these were found to be of the order given in the table below. As a comparison the variation arising from the experimental effects is also given.

	Standard Deviation	% Change
Spot to Spot	6.34	1.10 %
Slide to Slide	8.29	2.31 %
Day to Day	11.47	5.01%
Laser power extremes	24.35	11.57%
Matrix selection extremes	16.83	6.79 %

From these results it can be seen that even the day to day reproducibility, given the standardisation of preparation and instrumental settings, was considerably lower than the errors arising from varying the experiment. It should further be noted that these results were for the advanced and meticulous methods of preparing the samples which would be difficult to maintain for large volumes of routine analysis.

CHAPTER FOUR

Electrospray Ionisation

Electrospray ionisation (ESI) has become one of the most widely used techniques for creating ions in mass spectrometry, especially in the application to biochemistry where the ability to work from the solution phase is most useful^{1,2}. While most separation techniques can be applied to ESI, its continual stream of ions is perhaps best suited to sectors or quadrupoles³. However, with the creative use of ion traps and other approaches it can be used with techniques more suited to pulsed sources such as ion cyclotron resonance⁴ and time-of-flight⁵. At Warwick, the Fourier-transform ion cyclotron resonance is one of the primary ESI instruments for the high-resolution analysis of a range of analyte systems and is the instrument detailed in this chapter.

i. Overview

The most obvious difference between MALDI and ESI is the phase in which the analyte is presented to the instrument. The fact that the analyte is solvated has repercussions on the experiment in that it can have an effect on the molecule and resultant ion. The largest effects have been observed with large proteins, where their conformation is determined by the solvent environment and is carried through into the gas phase⁶. While as discussed when covering the mechanism of ESI, it is not thought that ions are pre-formed in the solution phase, these macrostructures are slow to rearrange and so it is not that surprising that such situations arise. When considering a solvent system for a biological molecule, there are two possible environments that can be used. If a mostly organic solvent system is used, the protein is said to be denatured in that it is forced into a conformation that it would not necessarily take in natural conditions. For this reason, proteins are often

¹ E Gelpi, *Int J Mass Spec Ion Proc*, 118, 683, (1992)

² WJ Griffiths, AP Jonsson, SY Liu, DK Rai, YQ Wang, *Biochem Journal*, 355, 545, (2001)

³ H Murata, T Takao, Y Shimonishi, *Rapid Comm Mass Spectrom*, 8, 205, (1994)

⁴ CL Hendrickson, MR Emmett, *Ann Rev Phys Chem*, 50, 517, (1999)

⁵ PV Bondarenko, RD Macfarlane, *Int J Mass Spectrom Ion Proc*, 160, 241, (1997)

⁶ A Wattenburg, F Sobott, HD Barth, B Brutschy, *Int J Mass Spectrom*, 203, 49, (2000)

electrosprayed from buffer systems, that is a solution of a weak acid with its corresponding alkali salt. These solvent systems more resemble physiological conditions and it would be hoped lead to the protein taking a standard conformation⁷. The situation can be modified using the pH of the solution, since this will have a smaller effect on the protein through the population of protonated sites located on residues throughout the molecule⁸.

The other major issue with ESI as an ionisation technique, is that it tends to produce multiple charge states in the analyte unlike the singly-charged ions of MALDI. This does have a distinct advantage in high-mass analysis as it reduces the m/z value down into a region that is more accessible to separation techniques. It does however complicate interpretation of the spectra produced by the source, especially for polymeric systems where there are considerably more than one species present. With proteins, the charge state is often of interest as the amount of charges a molecule acquires can give some indication of its conformation as described briefly above. Many biomolecules exist in either a folded or unfolded state, depending on the environment and interactions with certain key groups in the molecule. The folded conformation is where the chains move to effectively shield residues located towards the centre of the molecule. This action of folding usually makes a number of charge-sites inaccessible so the charge state of the analyte ion produced is changed⁹.

⁷ D Lemaire, G Marie, L Serani, O Laprevote, Anal Chem, 73, 1699, (2001)

⁸ T Kashiwagi, N Yamada, K Hirayama, C Suzuki, Y Kashiwagi, F Tsuchiya, Y Arata, N Kunishima, K Morikawa, J Am Soc Mass Spectrom, 11, 54, (2000)

⁹ HP Happersberger, MO Glocker, Eur Mass Spectrom, 4, 209, (1998)

ii. Conformational Studies

The initial experiments undertaken to gain familiarity with the Fourier transform ion cyclotron resonance (FTICR) system were looking at conformational changes and the retention of water molecules in the bovine pancreatic trypsin inhibitor (BPTI) protein. This protein with a mass of approximately 6,460 Daltons is a useful analogue for a number of larger proteins with similar behaviour^{10,11}. It had been hoped that the high-resolution capabilities of the FTICR would show ions that could be attributed to water losses from the molecule. The samples were initially made up in acetonitrile : water at concentrations ranging from 20 to 40 millimolar. Buffer systems were not used at the start as it had proved difficult to achieve a stable current using commercial buffers. The spectra presented a number of signals at various masses and charges, consistent with the degradation of the analyte in the non-biological solvent environment. Changing the source conditions was also seen to have a significant effect on the charge distribution. The “harsh” conditions were when the skimmer voltages were increased and the ions retained for longer in the hexapole, leading to lower observed charge states.

The charge of each peak could be accurately determined by observing the spacing of the signals arising from the existence of carbon-13 isotopes in the molecule. Any carbon-containing species gave a small distribution of signals separated each by one mass unit. The intensity gave a purely statistical pattern based on the natural abundance of carbon-13. When the charge was greater than one, the separation was not a single unit mass but rather $1/z$, where z was the charge on the species. In this manner, it was possible to confirm the number of charges on an ion and then in turn the actual mass of the species by multiplying the m/z value by the calculated charge. Using this technique on the

¹⁰ RM Brunne, KD Berndt, P Guntert, K Wuthrich, WF Vangunsteren, *Protein Structr*, 23, 49, (1995)

¹¹ L Carlacchi, *Biopolymers*, 58, 359, (2001)

observed signals for the bovine pancreas trypsin inhibitor gave the true masses for each species and the charge state. What at first appeared to be a number of different species were, in some cases, the same species with a different number of charges and so a different m / z value.

In a number of the spectra there appeared to be a series of signals that could be interpreted as arising from water loss, however with the complexity of the spectra and uncertainty of the exact species observed such conclusions were unsafe. A model of the theoretical isotope distribution was prepared using the Bruker software to try and establish a match with observed peaks. The pattern did not give an exact match for any distribution in the spectra using the organic solvent, which was at least consistent with not observing the expected parent ion mass. Later work on the instrument gave better results with the pre-made buffer systems, which could have been used to simplify the situation but by that stage the project had moved on to focus on polymeric materials.

Figure 4a – Electrospray spectra of BPTI under 'harsh' source conditions giving 4 / 5 charges

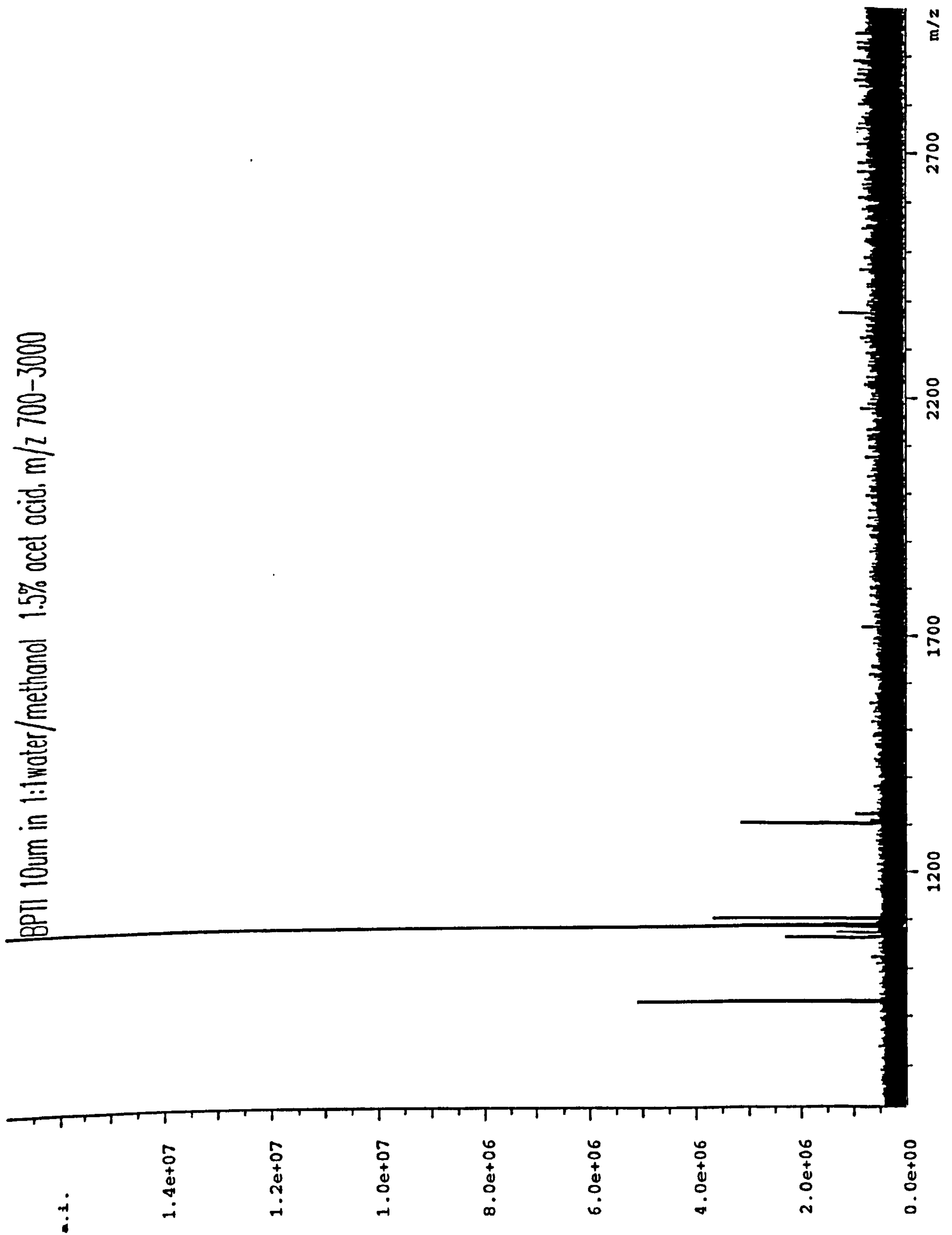


Figure 4b - Electrospray spectra of BPTI under 'mild' source conditions giving 6 / 7 charges

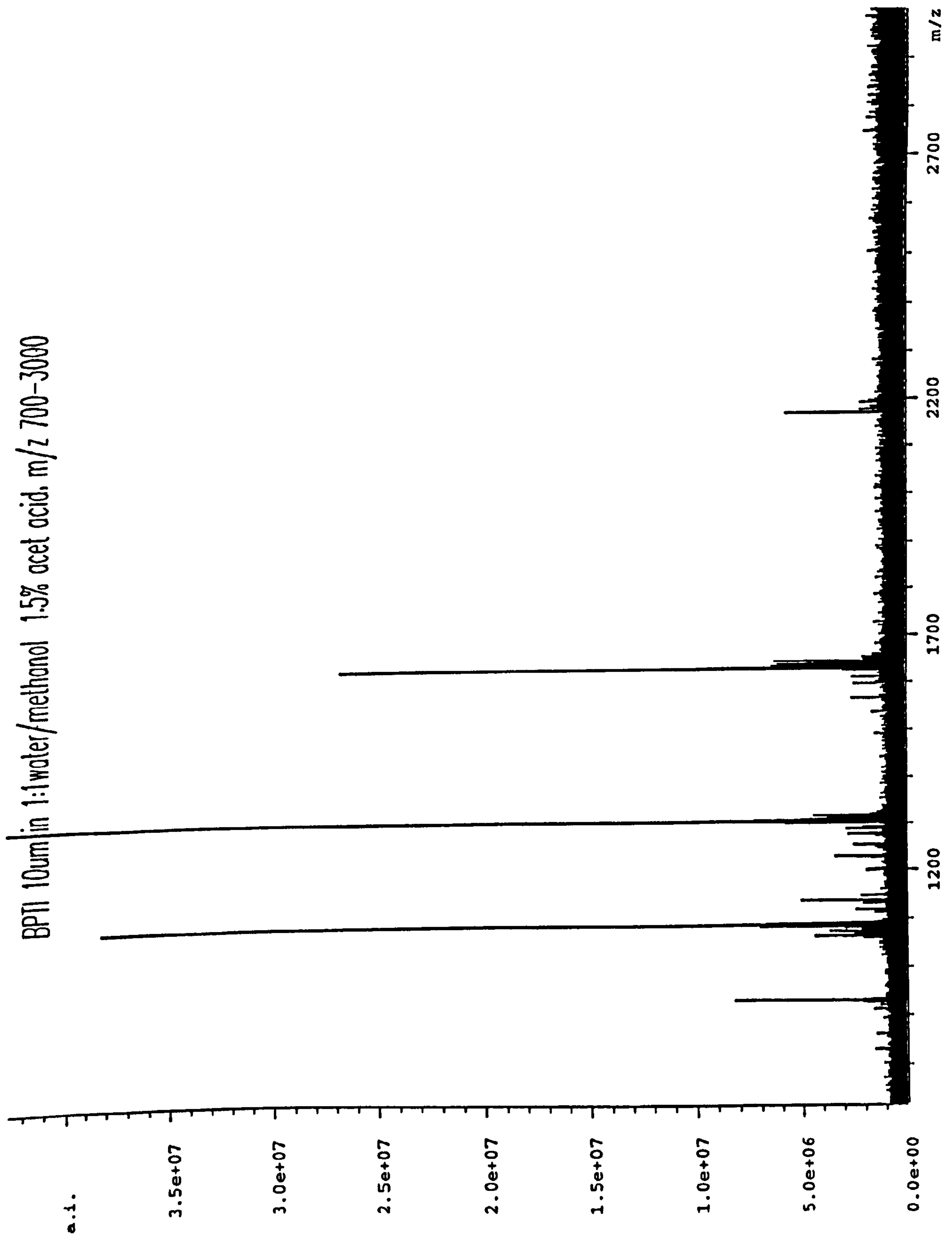


Figure 4c – Theoretical isotope distribution for the bovine pancreas trypsin inhibitor protein

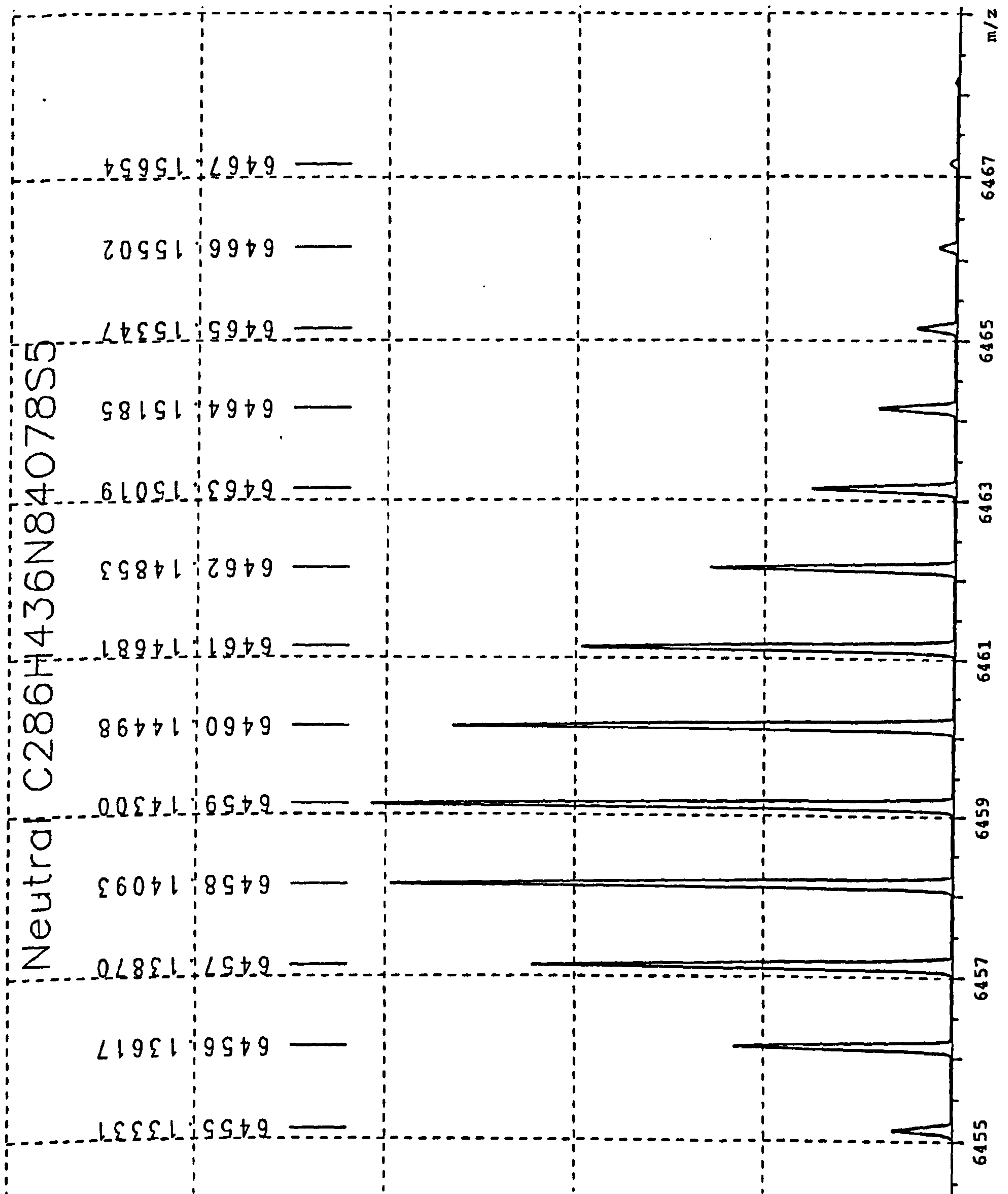


Figure 4d – Enlarged spectra showing the possible 16 mass loss for water retention

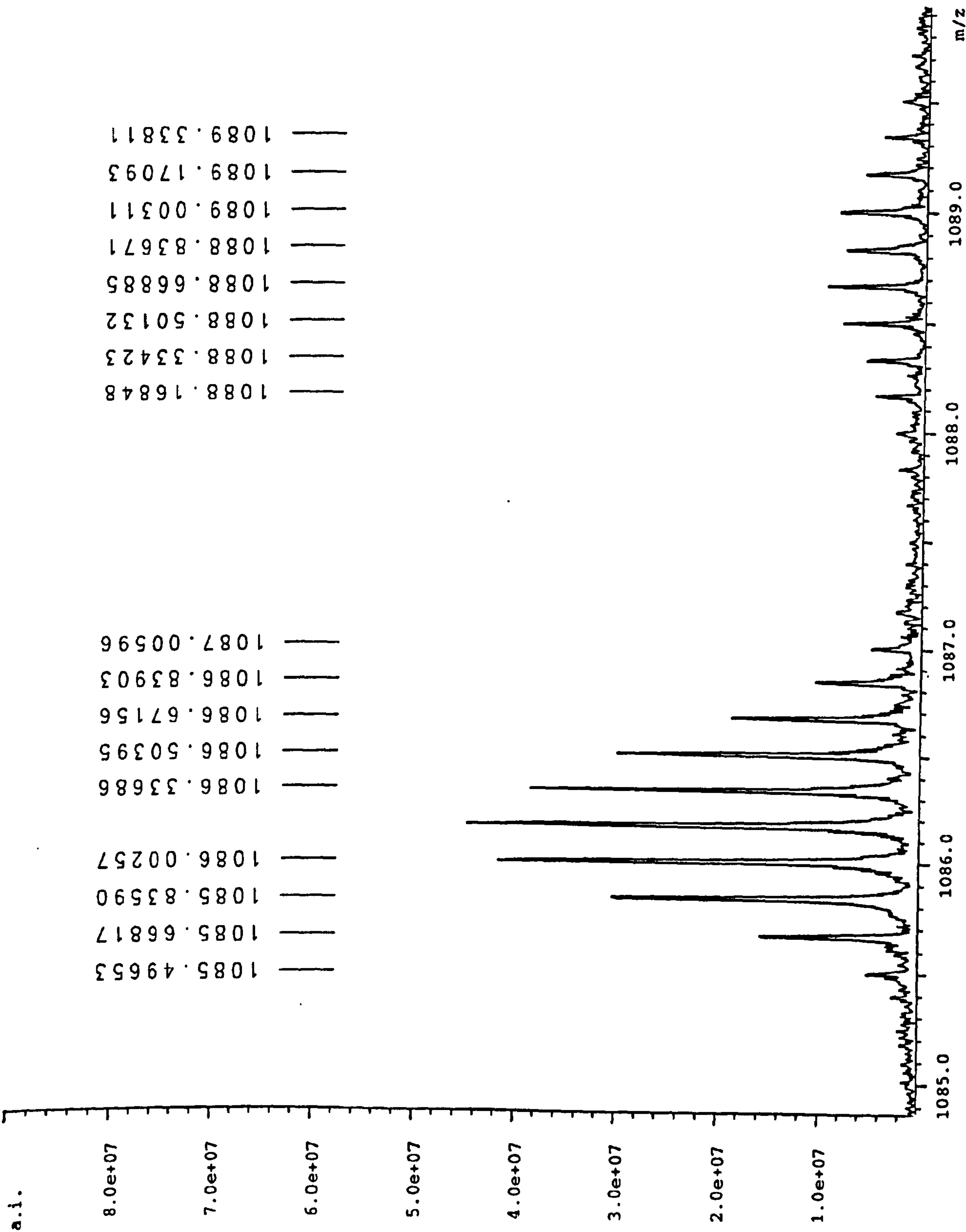
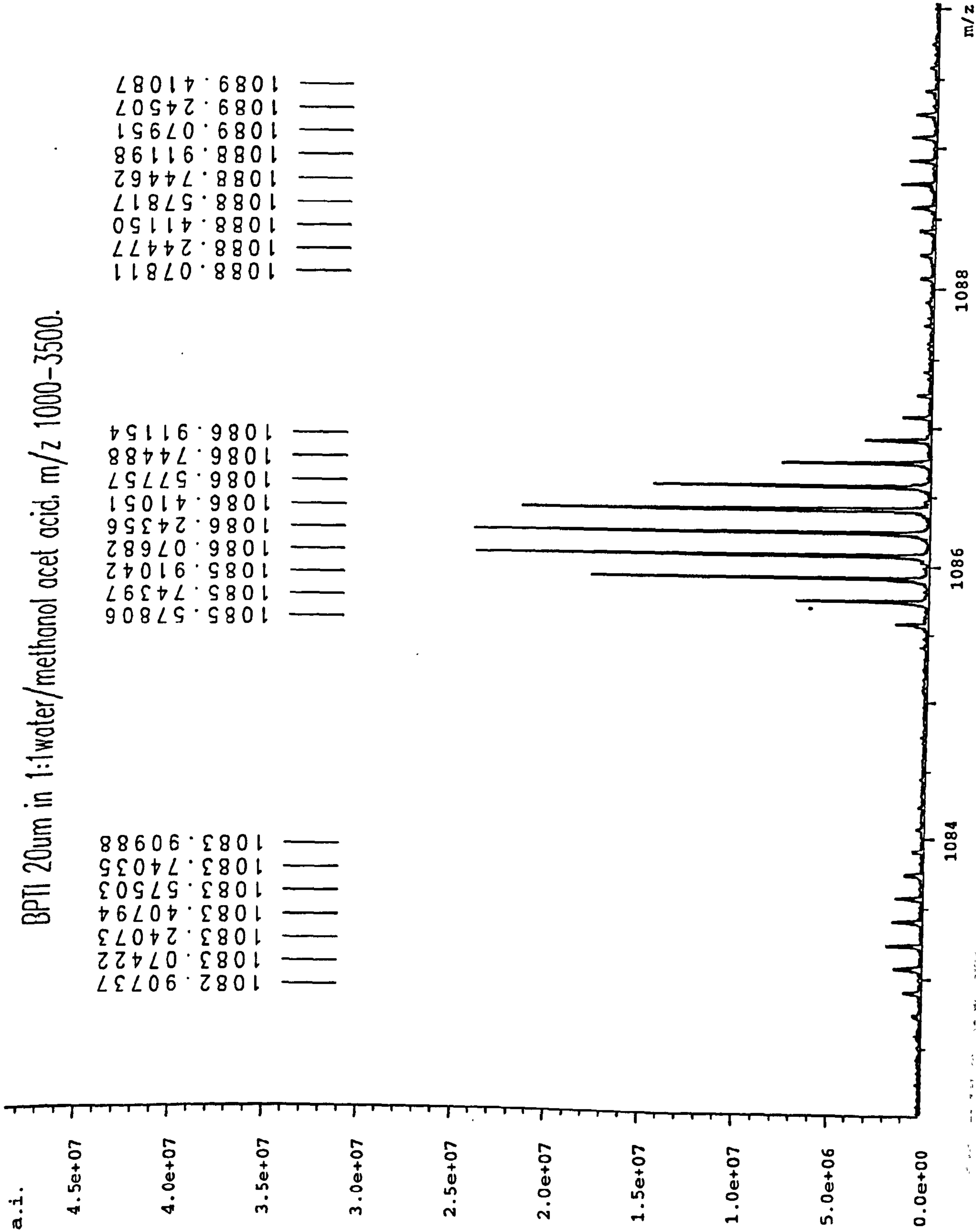


Figure 4e – Enlarged spectra showing the recurring three ion pattern



Apart from observation of changes in charge state for the conformations, there is an experimental technique that can directly observe the charge sites within systems as an indication of structure. This is H / D exchange and relies on the replacement of labile protons within an analyte ion with deuterium. Since the increase of one mass unit for every replaced proton can be observed by the high-resolution of the FTICR, it can give direct values for the number of exchangeable sites in a molecule¹². Exchange takes place in the cell on introduction of a deuterated gas at a certain concentration that makes deuterium more available than hydrogen but hopefully not high enough to cause a significant amount of collision-induced dissociation. As the labile protons disperse away from the charge sites of the molecule, it is more likely that they will be replaced by deuterium given the relative amounts present. This leads over time to the full replacement of all labile hydrogens by deuterium.

For the technique to work, the analyte must have a specific conformation and dedicated sites for the attachment of protons. In proteins this is not a problem, since the presence of hydrogen-bonding and hydrophobic / hydrophilic interactions lead to a certain shape of the molecule that is as mentioned dictated by the environment it finds itself in. Charge sites are also limited to certain amino acids that contain labile sites, usually a nitrogen or oxygen centre not involved in hydrogen-bonding or solvent interactions¹³. In a polymer this is not the case, the conformation is more variable in most chain systems with few interactions to lead to a strict tertiary structure. The charge sites also appear to be more generalised, since the charges acquired while increasing with polymer length do not relate directly to functional groups to the same extent. Certainly using the models for the ion formation in electrospray, the charge number of polymer seems to be rationalised on

¹² D Lafitte, AJR Heck, TJ Hill, K Jumel, SE Harding, PJ Derrick, *Eur J Biochem*, 261, 337, (1999)

¹³ AQ Li, C Frenslau, IA Kaltashov, *Protein Structure, Function and Genetics*, Wiley, New York, (1998)

chain length alone and the chemistry of the chain has very little significance¹⁴. Polymers also on the whole do not tend to attach protons or have labile sites that would be suited to H / D exchange. Even in certain systems where there are such locations, it is most likely that all possible sites would be exchanged over time giving effectively no structural information above the number of such sites.

A more useful structural analysis procedure that can be carried out using the FTICR is referred to as sustained off-resonance irradiation (SORI) where the trapped and isolated ion is subjected to an electromagnetic pulse that can lead to fragmentation¹⁵. This varies from collision-induced dissociation, as discussed in chapter five, where the energy for fragmentation is given by a physical collision of the molecule. Potentially this approach can be used in conjunction with H / D exchange, to correlate the location of the charge sites in a protein with a known structure. While a mass shift simply alerts to the presence of a charge site, if the shift is attributed to a fragment it may be possible to rationalise this to a particular residue in that part of the molecule. This can give some indication as to which sites are used and available in different conformations and so a general sense of the macrostructure of the protein molecule.

iii. Mass and Charge Bias Experiments

Many of the concerns discussed in the previous chapter with relation to MALDI analysis, also apply with electrospray ionisation. There are a number of settings to be considered on the experimental side, along with those for sample preparation which mainly involves a choice of solvent system. As mentioned in the introduction, electrospray ionisation is most often used for biological samples, since it is relatively gentle and the solvent

¹⁴ CN McEwan, WJ Simonsick, BS Larsen, K Ute, K Hatada, J Am Soc Mass Spectrom, 6, 906, (1995)

¹⁵ J Laskin, M Byrd, J Futrell, Int J Mass Spectrom, 196, 285, (2000)

systems can be set up to mimic physiological conditions. It is however equally as applicable to polymers although there are certain other concerns that arise from this analysis. With proteins and peptides, the issue of relative intensity and small changes in the intensity are not usually of great importance. That is except when looking at areas such as complexes or non-covalent interaction, where the differences in intensity are often used to gauge the strength of a interaction¹⁶. But as will be shown here with polymer samples, these intensities are very much dependent on the conditions of the experiment.

Experiments with polymers to investigate these conditions are complicated by the presence of multiple charges in electrospray. These charge states in themselves are also something to be observed, but they do require special consideration in determining the mass averages. Most commercial mass spectrometry software that calculates polymer values cannot account for this extra complexity, however new algorithms are now starting to appear which can deconvolute the series to allow the true envelope to be observed. These convert the mass / charge axis to a purely mass scale, so that every peak is effectively singly charged and molecular weight averages can be calculated correctly. Even without this complication of multiple charge states, when mass average calculations were carried out on a distribution with a charge greater than one, then the value achieved was actually average mass / charge. It was not always possible to simply multiple this value by the charge state, since in order to get the correct value would have required an accurate measurement of the average charge across the distribution. The manual process of working on these systems was time-consuming in the extreme, with each oligomer having to be identified and converted to a mass value. There was of course overlap between the mass envelopes of the different charge states, so these had to be summated to give the overall or total mass distribution. Although the mass accuracy of the

¹⁶ TD Veenstra, Biophys Chem, 79, 63, (1999)

electrospray-FTICR used in this work was significantly higher than for the MALDI-TOF, the mass values were still corrected to their theoretical masses for the calculation.

Each individual signal had its charge determined by the manual process from its isotope spacing. This meant that each peak could be assigned to a charge series, forming a collection of overlapping mass envelopes. It was these patterns that were changed by the experimental conditions and together gave variations in the mass averages. The experimental conditions in this regard were those within the source, which unlike the MALDI setup had both mass and charge biases that had to be addressed. Within the electrospray source were three major components, which only differ slightly from other such sources and retain their base functionality. After the spraying cone from the electrospray needle, the ions passed through a capillary and experienced the first large change in field. This was followed by an expansion from the capillary end and sampling with a cone or skimmer, which also had a variable voltage as it shaped the ion beam for transfer. Both of these sections had a single alterable voltage, but the two may also have interacted with each other to an extent. The hexapole that was by comparison a much more complex system, with voltages and timing considerations that significantly affect the ion distribution.

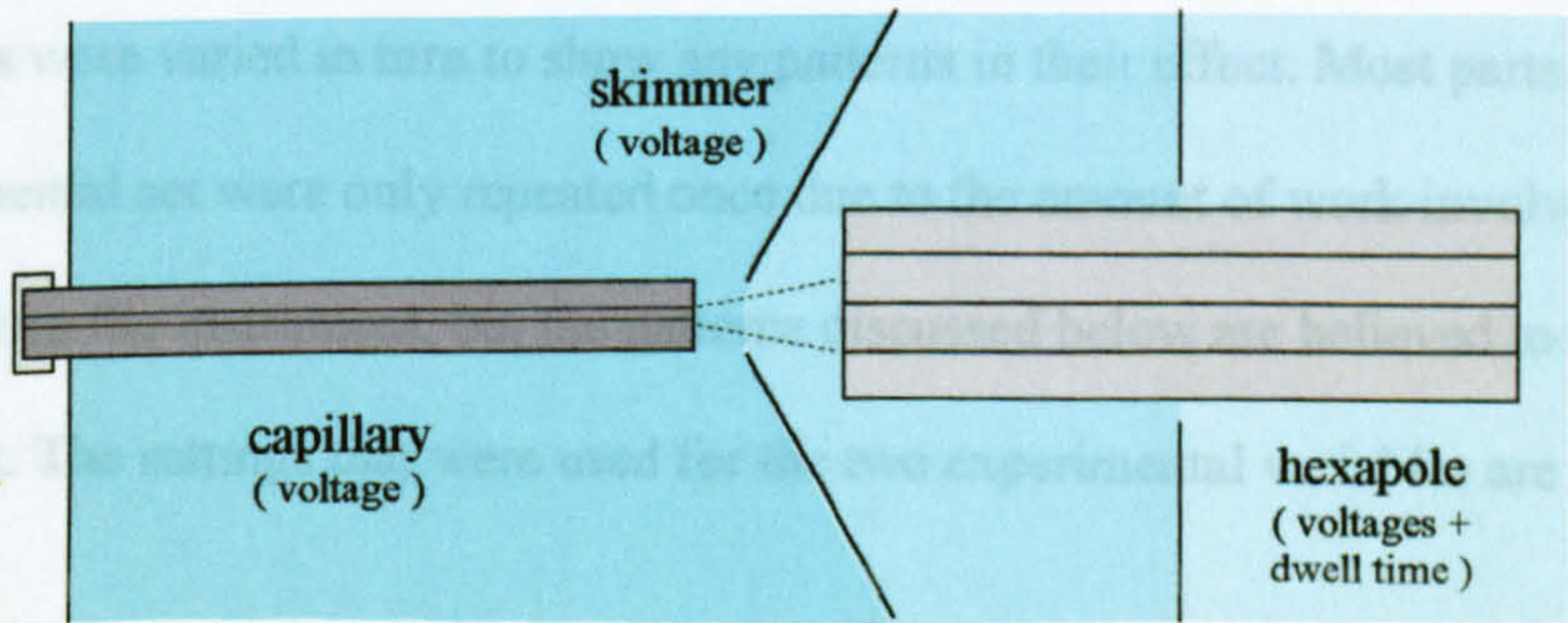


Figure 4f - Schematic of the ESI source showing the variable settings

a) Capillary and Skimmer Effects

The effect of the voltage difference between the capillary and skimmer had been partially described before^{17,18,19}. This attributed changes in charge state distribution to a charge stripping process. This stripping effect could be used to reduce the complexity of the polymer mass spectra by simplifying the number of charge envelopes. If the charge stripping conditions also affected the mass distribution however, then any resultant spectra may not be a true representation of the sample. Experiments were therefore carried out on the FTICR with its electrospray source. Two polymer systems were selected, one of quoted mass 3350 and the second of 11000, both purchased from Sigma-Aldrich as a dried solid. These were made up as a 10^{-3} M solution in acetonitrile / water with 0.1% v/v of a concentrated sodium hydroxide solution to assist cation formation. This system was shown by trial and error to give a reliable result and more importantly a stable signal that could be used for a reasonable length of time. This second feature was crucial, as for the most direct comparison, the sample and ambient conditions had to be kept as constant as possible, which was best done by a single run for each experimental series. The lower-mass polymer produced the simpler spectra of the two, with a narrower mass distribution and fewer charge states. With both systems, the capillary and skimmer voltages were varied in turn to show any patterns in their effect. Most parts of the experimental set were only repeated once due to the amount of work involved and high demand on the instrument, but the patterns discussed below are believed to be statistically relevant. The settings that were used for the two experimental variables are as follows :-

Capillary Voltage	40 - 70V (steps of 5V)
Skimmer Voltage	2 - 7V (steps of 1V)

¹⁷ GR Agnes, G Horlick, Appl Spectroscopy, 49, 324, (1995)

¹⁸ EP Maziarz, GA Baker, SA Lorenz, TD Wood, J Am Soc Mass Spectrom, 10, 1298, (1999)

¹⁹ EP Maziarz, GA Baker, JV Mure, TD Wood, Int J Mass Spectrom, 202, 241, (2000)

Each of these series was run in one go, while the occasional instance of the signal being lost during the sequence meant that the entire set of experiments was restarted from the first setting. The acquired spectra were exported as a comma-delimited file for import in Microcal Origin, as Microsoft Excel was not able to handle the high number of data points produced by the FTICR system. Every polymer peak was recorded and its charge state identified, allowing the value to be converted to an exact mass as explained previously. Once this process was completed for all of the observed oligomers, the resultant data-sheet was able to display the overall mass distribution and the pattern for each particular charge state. For each mass value it was intensity that was used for the y-axis value, although strictly this should have been the area under the peak since this corrected for peak broadening at higher masses that could lead to lower observed mass averages. With the required observations however, it was the pattern in the change of averages that was of greater importance and so it was decided that this large increase in data interpretation workload was not warranted in this particular case. The mass envelopes were then used to calculate mass averages which were plotted against the voltages to highlight the trends. The capillary voltage itself showed little evidence of an overall trend, with the variations in averages and charge states relatively small and non-coherent. This could have been due to the fact that the percentage change in voltage was small compared to the skimmer, which started at a voltage an order of magnitude lower. It was also thought that it was the difference between the two components that was of importance. In comparison, the skimmer voltage on its own did show a significant variance and a distinct pattern in the differences.

Looking first at the charge states created by the electrospray process, there was no real surprise in the comparison between the two species. The smaller 3k glycol only gave the +4 and +5 charge states, while the charge states of the much longer 11k system ranged from 10 to 14 charges. As noted in the introduction, this brought both samples down to a

m/z of around 800, with the number of charges dependent on the length of the polymer and so by that its mass. Plotting the intensities of each charge state at each voltage, normalised for comparison, showed the trend quite clearly. Increasing the skimmer voltage favoured the formation of higher charge states, this being very evident with the larger number of charge states observed with the larger of the two polymers. In figure 4g, the ion intensity of only the +4 charge state is shown for the 3350 PEG. Although it is not straightforward to observe, there was a mass shift within the charge state as the skimmer value was altered. The actual height of each line is somewhat misleading as the total ion intensity in itself has little implication for the mass average calculations.

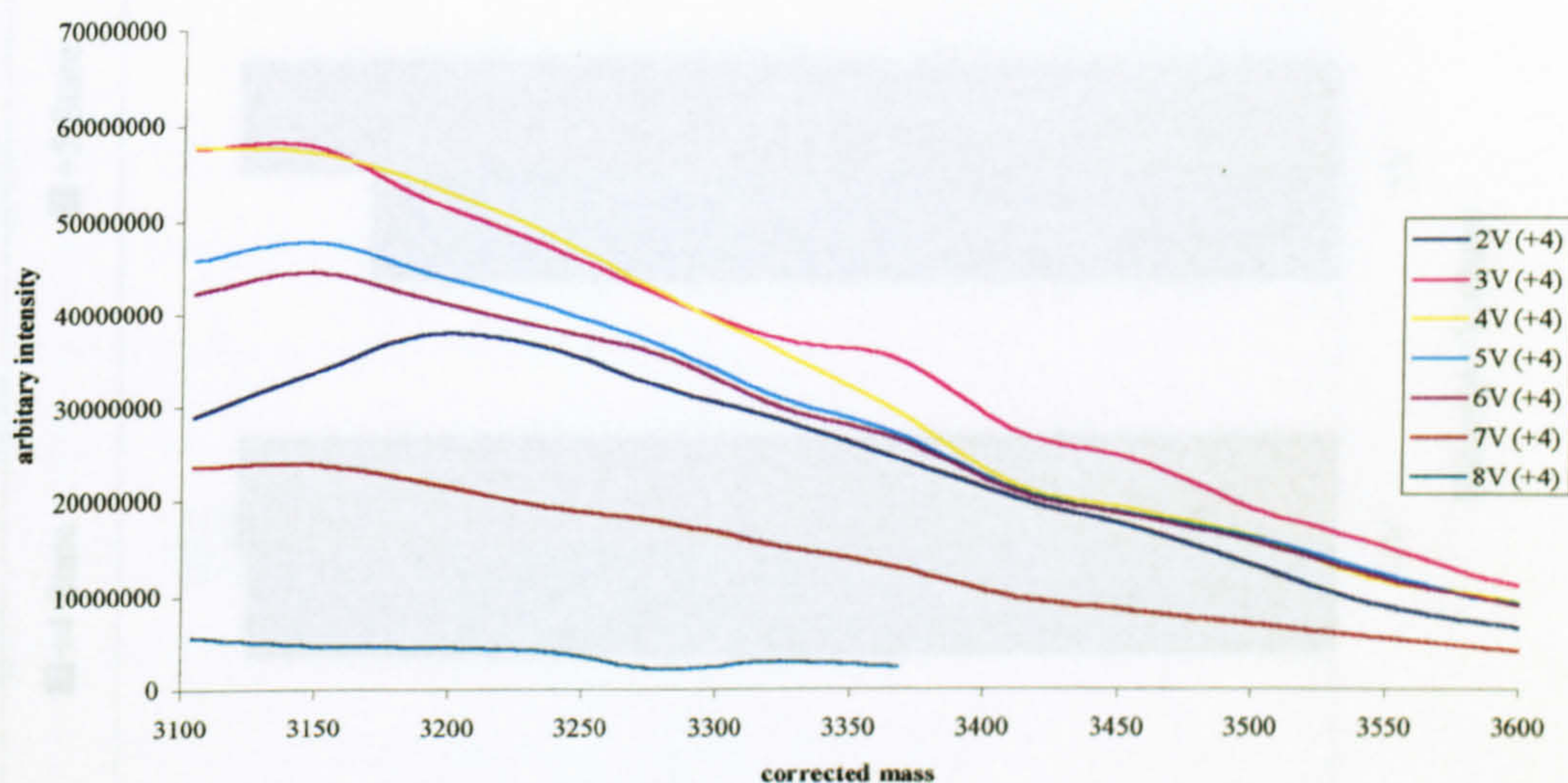


Figure 4g – Ion intensity given as a function of different skimmer voltages

Figure 4h – Charge states by each mass given by skimmer voltage of the 3k polymer

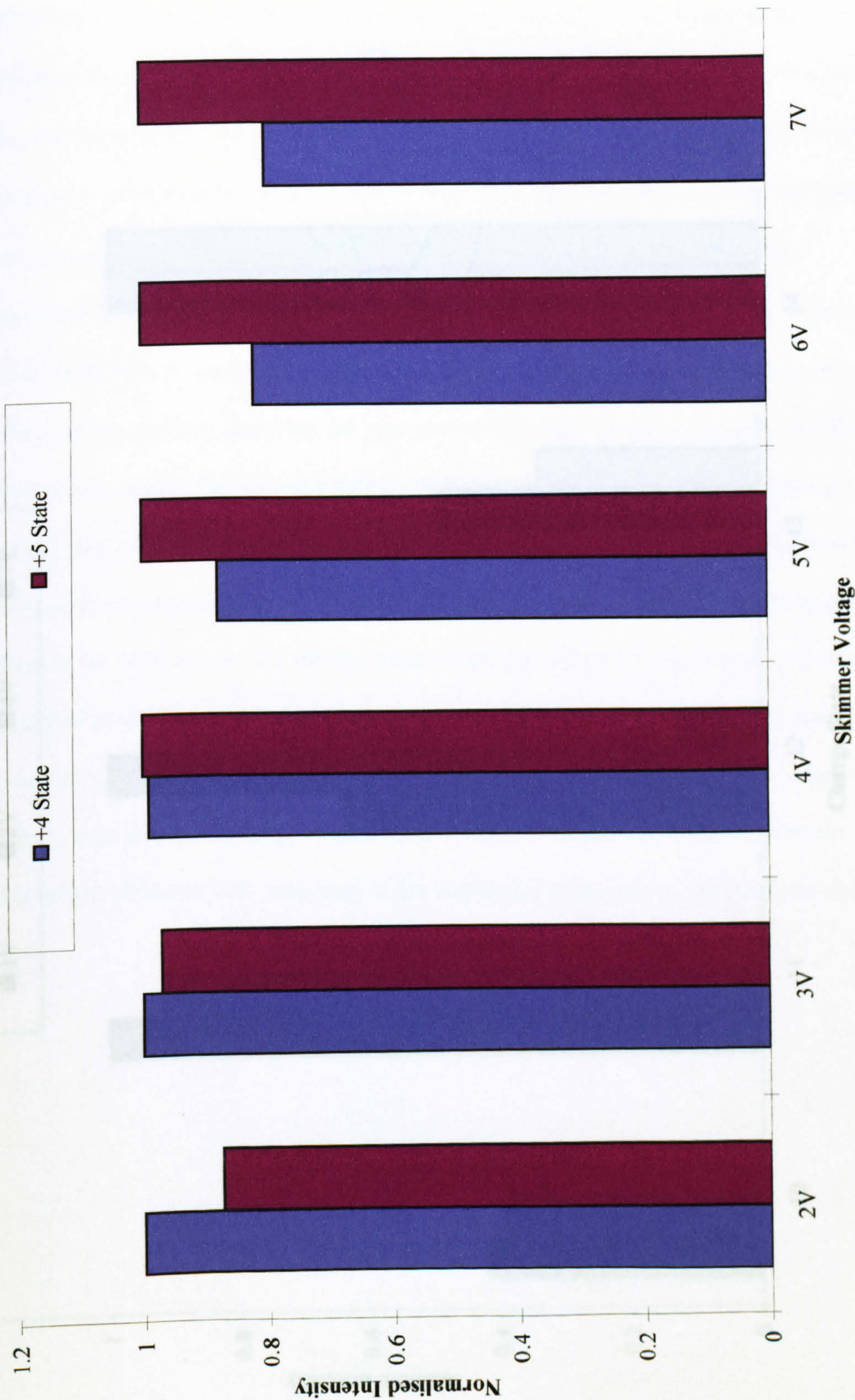
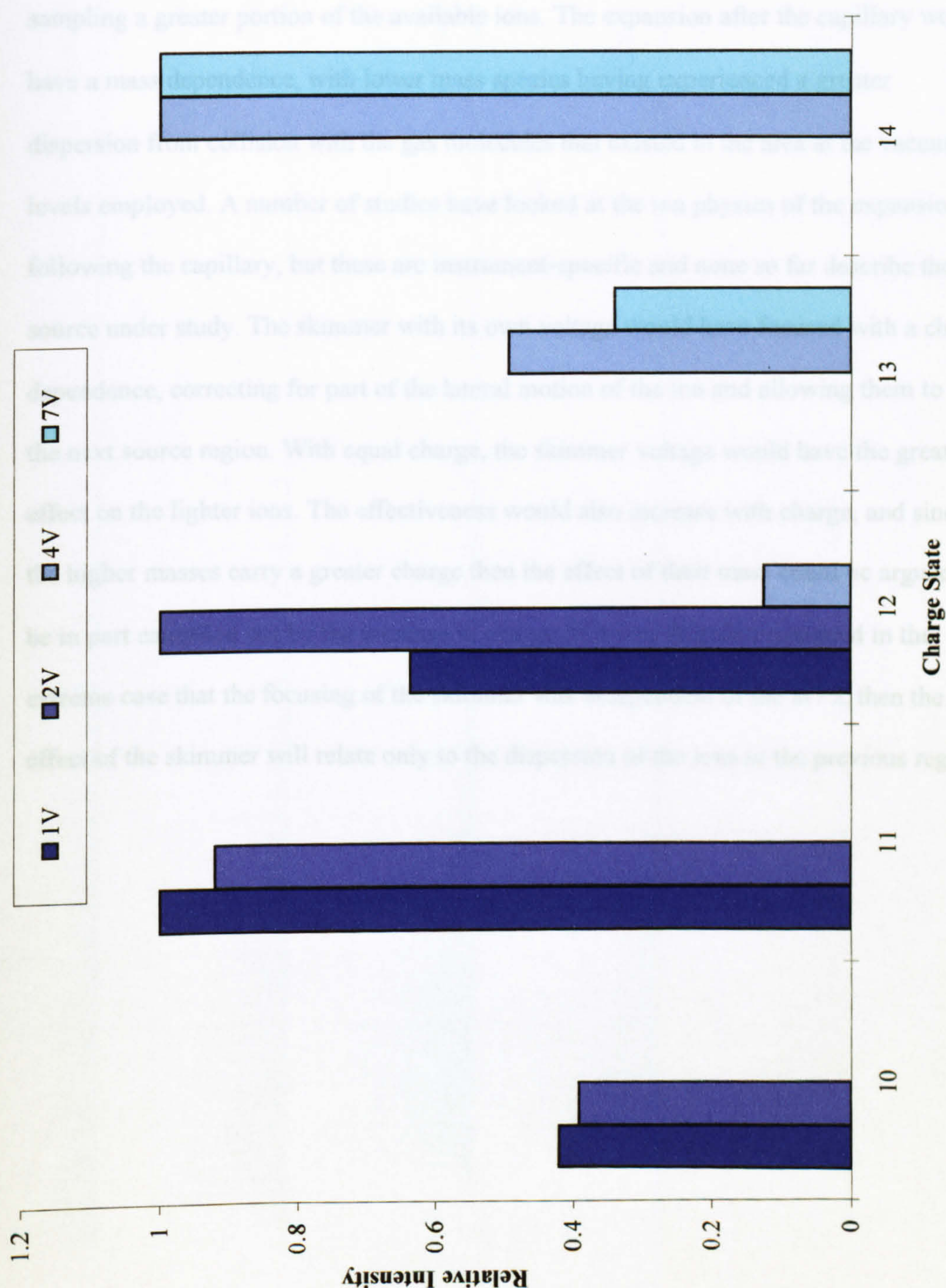


Figure 4i – Charge states by each mass given by skimmer voltage of the 11k polymer

Although this may at first appear to be the reverse of the expected effect of charge stripping, as the skimmer voltage was increased it actually decreased the drop in potential difference between the capillary and the cone of the skimmer. The change in this condition could therefore be thought to have favoured the retention of higher charges. The focusing effect of the skimmer is perhaps a more convincing argument for the effect, sampling a greater portion of the available ions. The expansion after the capillary would have a mass dependence, with lower mass species having experienced a greater dispersion from collision with the gas molecules that existed in the area at the vacuum levels employed. A number of studies have looked at the ion physics of the expansion following the capillary, but these are instrument-specific and none so far describe the source under study. The skimmer with its own voltage would have focused with a charge dependence, correcting for part of the lateral motion of the ion and allowing them to enter the next source region. With equal charge, the skimmer voltage would have the greatest effect on the lighter ions. The effectiveness would also increase with charge, and since the higher masses carry a greater charge then the effect of their mass could be argued to be in part cancelled out by the increase in charge. If it was therefore assumed in the extreme case that the focusing of the skimmer was independent of the m/z , then the effect of the skimmer will relate only to the dispersion of the ions in the previous region.

Figure 4j – Overlay of spectra showing the visible effect of skimmer voltage

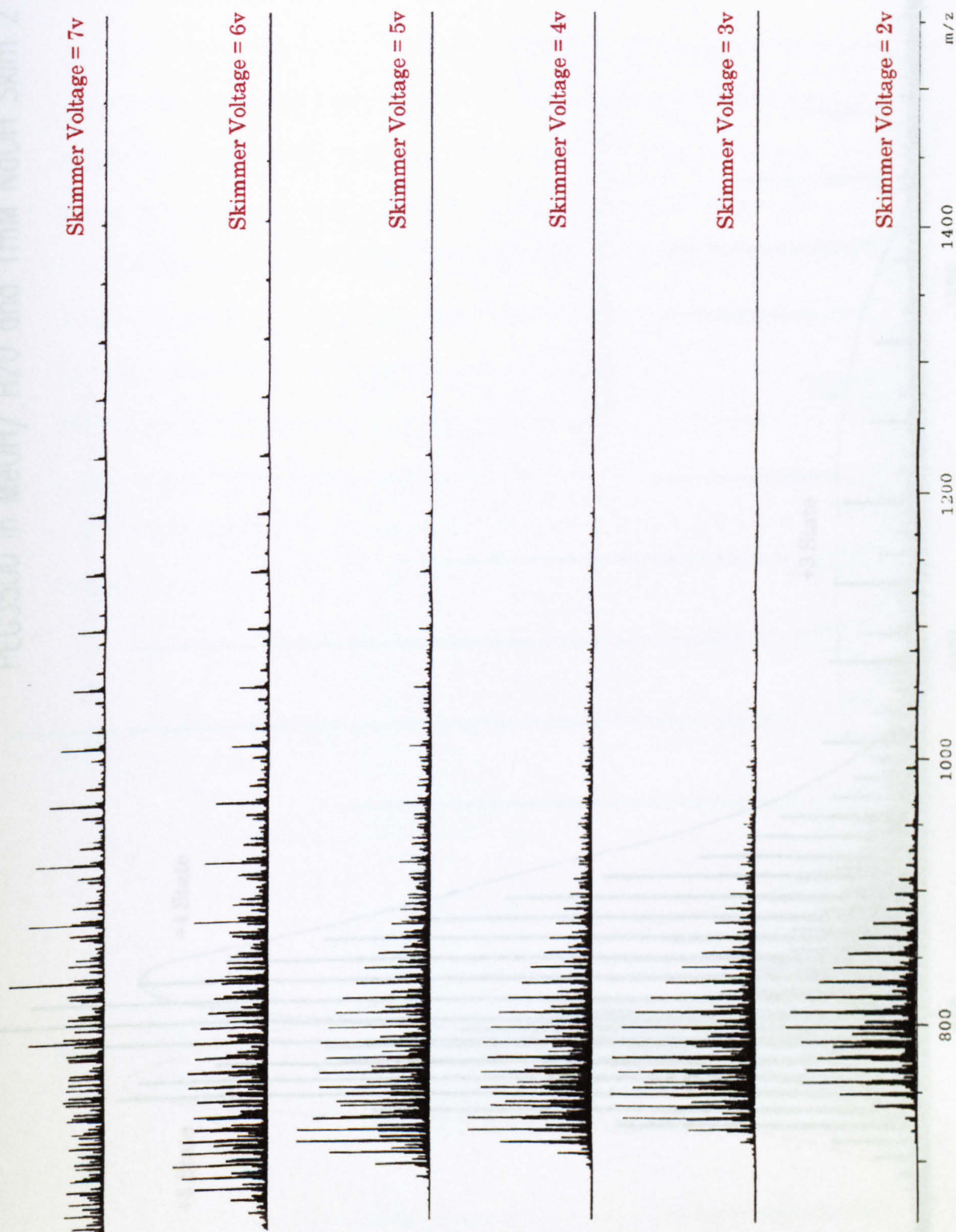


Figure 4k – ESI spectra of 3k polymer at the base settings showing overlapping charge states

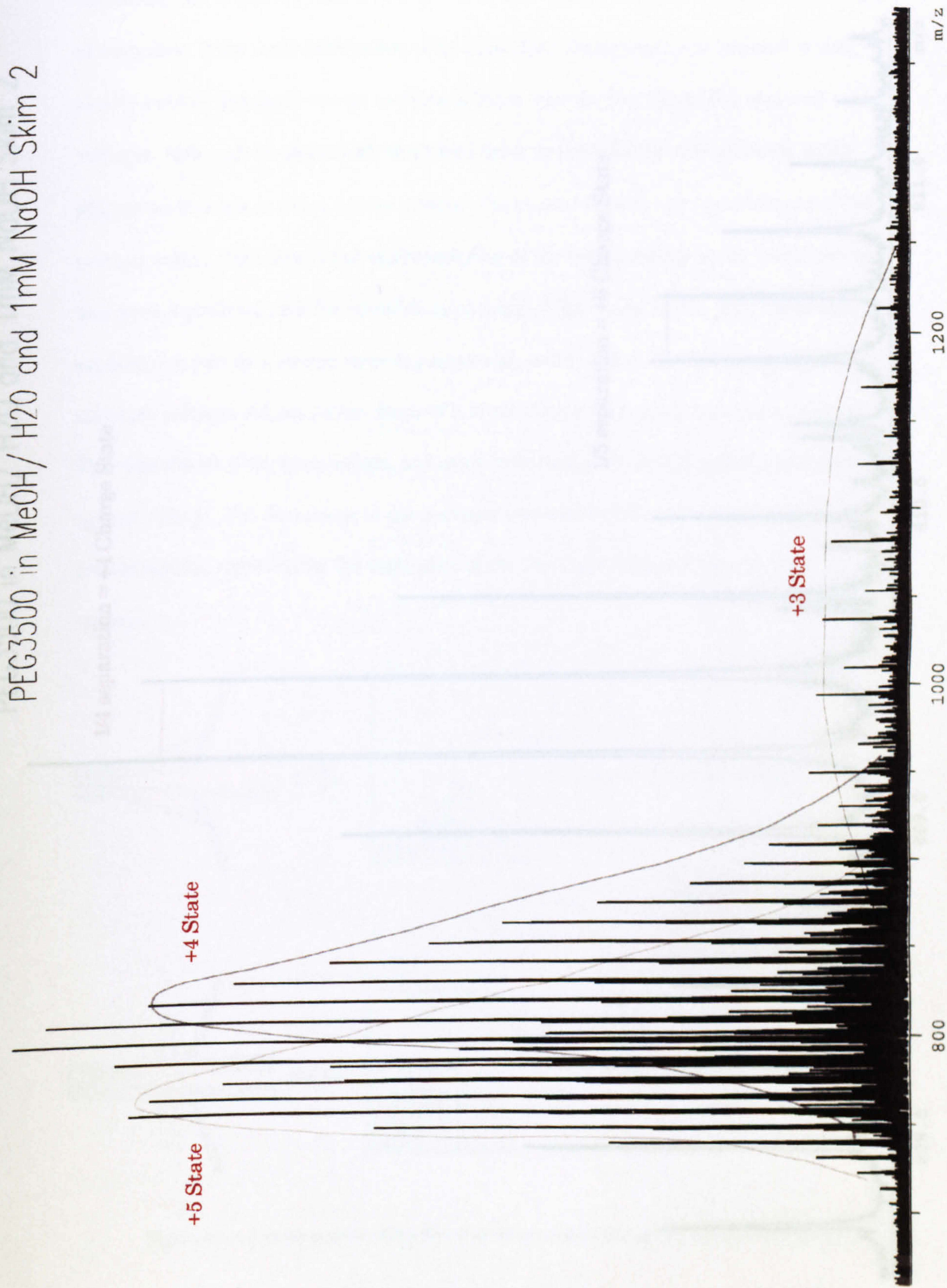
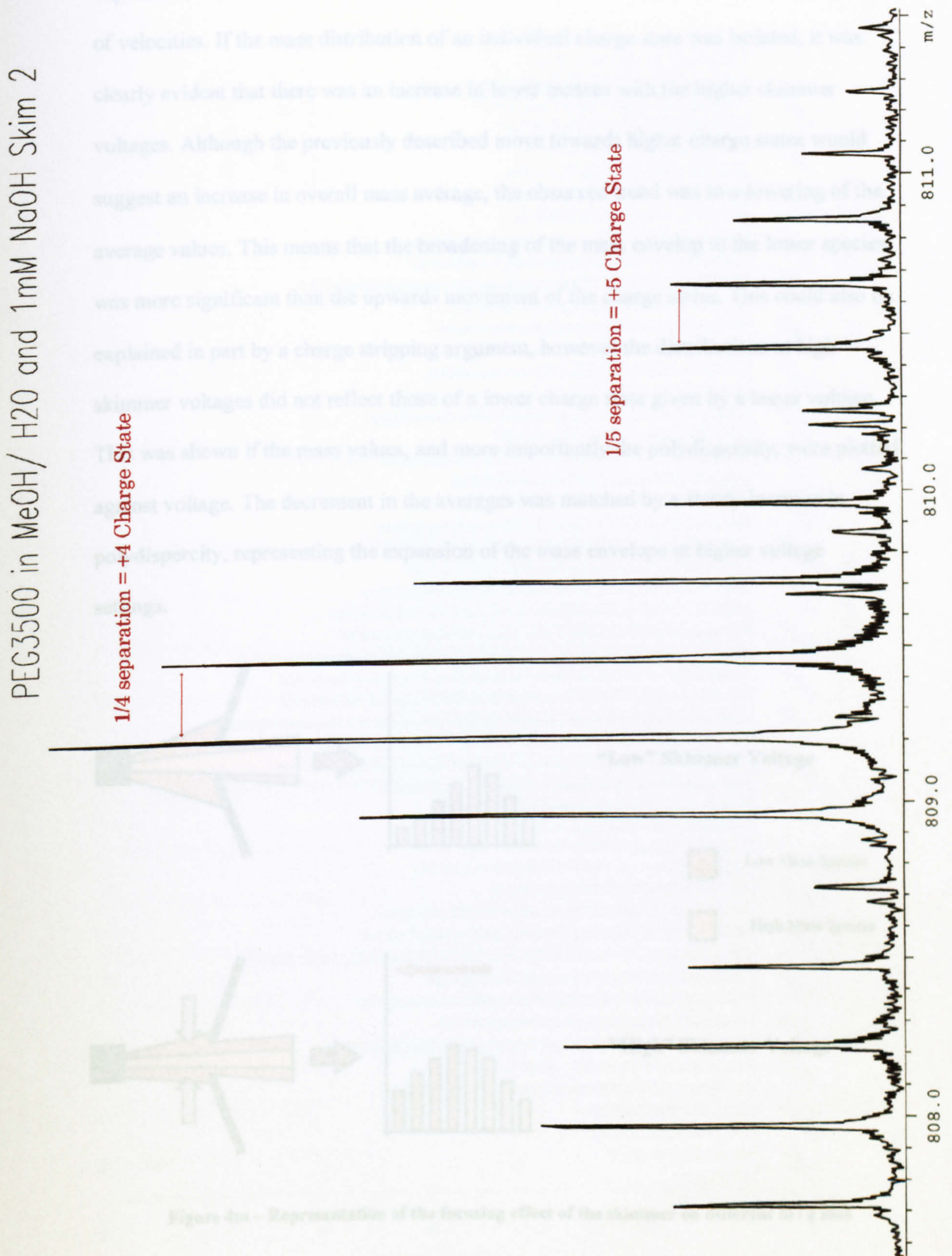


Figure 4l – Close-up of 3k polymer spectra showing the isotope pattern of a number of oligomers



The dispersion in the expansion was mass dependent or more strictly momentum dependent, but it was considered that all the ions will have acquired a similar distribution of velocities. If the mass distribution of an individual charge state was isolated, it was clearly evident that there was an increase in lower masses with the higher skimmer voltages. Although the previously described move towards higher charge states would suggest an increase in overall mass average, the observed trend was to a lowering of the average values. This means that the broadening of the mass envelope to the lower species was more significant than the upwards movement of the charge states. This could also be explained in part by a charge stripping argument, however the distributions at high skimmer voltages did not reflect those of a lower charge state given by a lesser voltage. This was shown if the mass values, and more importantly the polydispersity, were plotted against voltage. The decrement in the averages was matched by a steady increase in polydispersity, representing the expansion of the mass envelope at higher voltage settings.

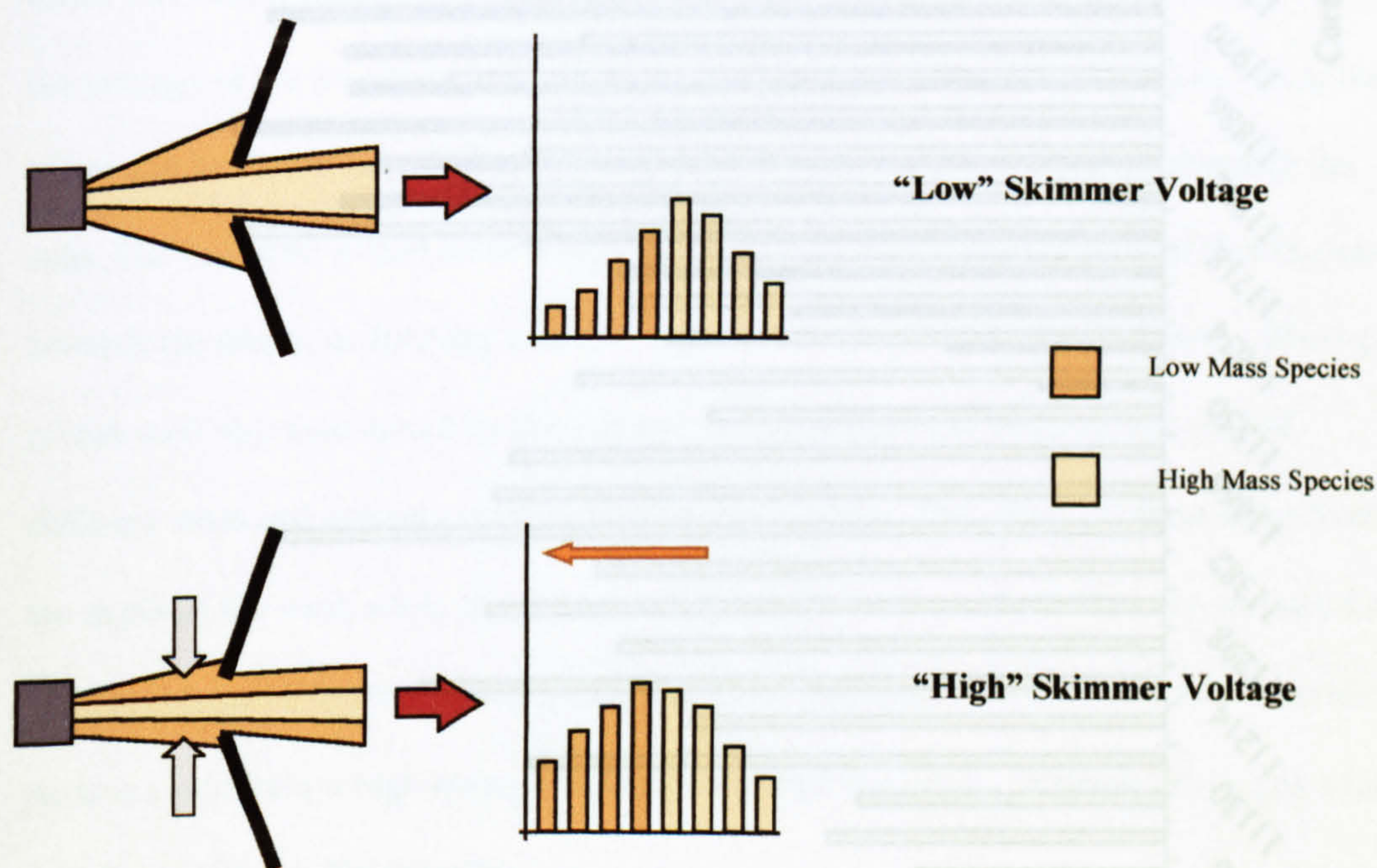
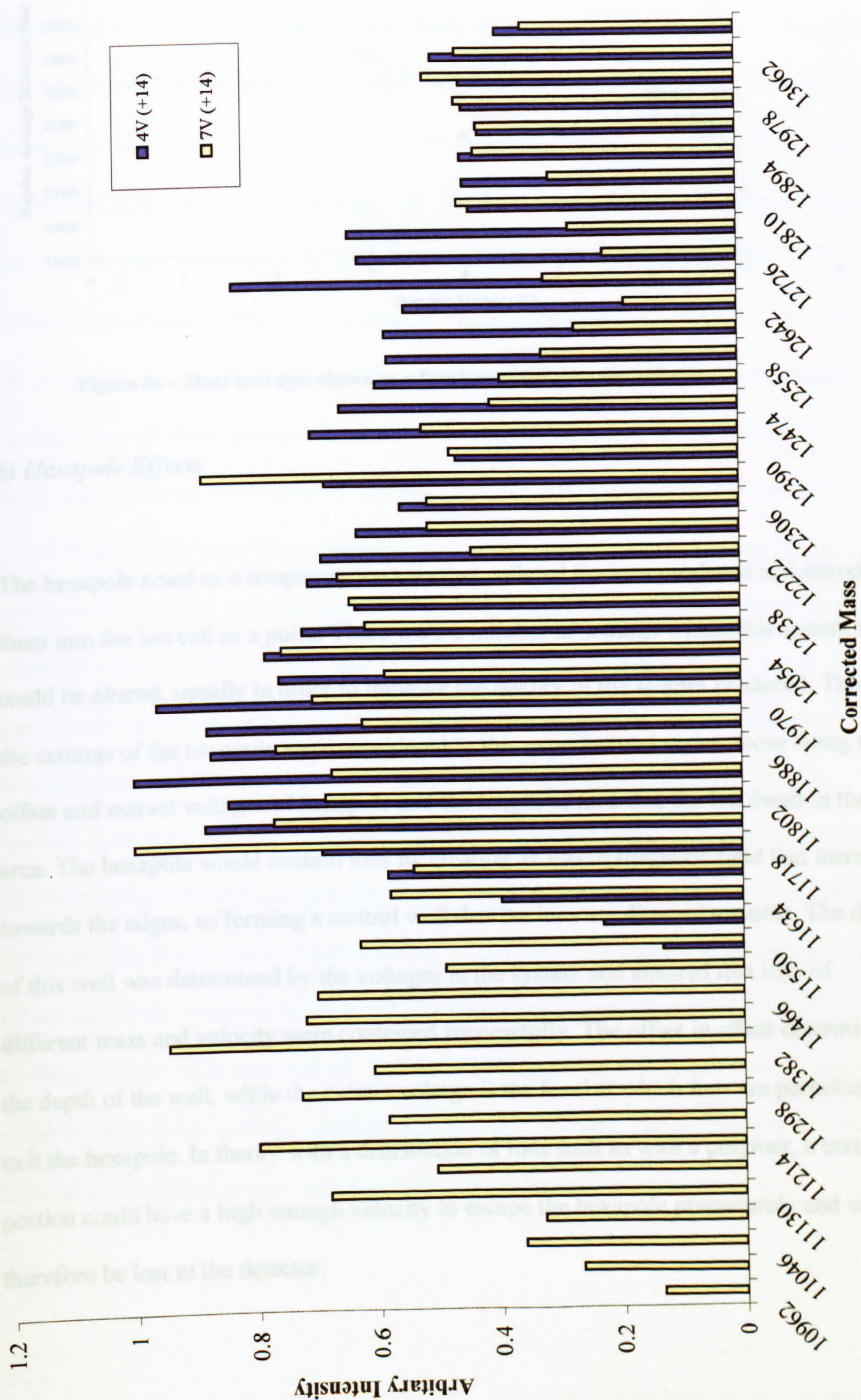


Figure 4m – Representation of the focusing effect of the skimmer on different m/z ions

Figure 4n – Comparison of the deconvoluted envelope patterns at two voltage settings



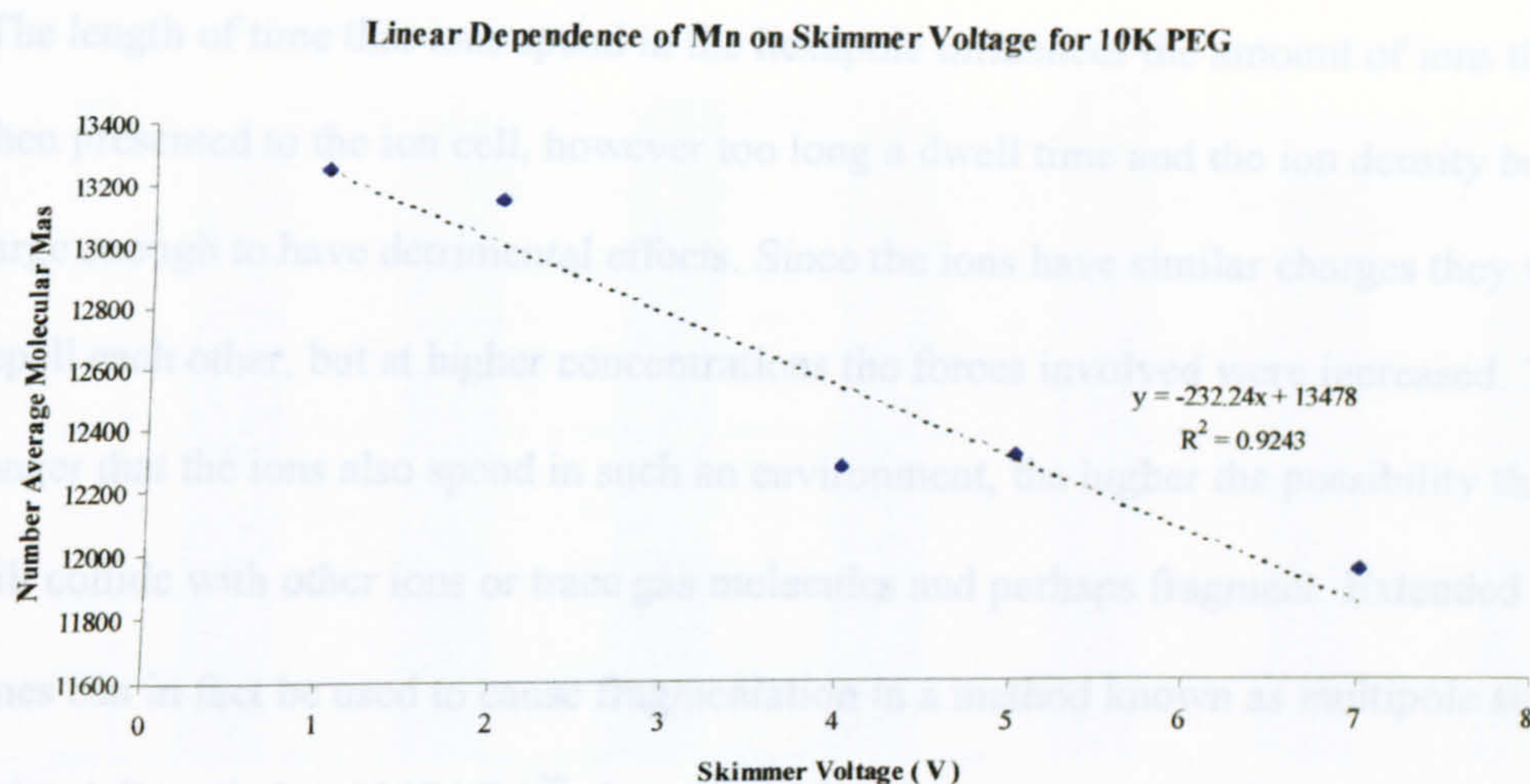


Figure 40 – Mass averages shown as a function of the skimmer voltage

b) Hexapole Effects

The hexapole acted as a temporary ion trap that collated the ions produced and introduced them into the ion cell as a pulse. There were a number of settings within this system that could be altered, usually in order to improve the quality of the spectra produced. Three of the settings of the hexapole were considered in this experimental series, those being the offset and extract voltages of hexapole and the length of time that the ion dwelt in the area. The hexapole would contain ions by creating an electromagnetic field that increased towards the edges, so forming a central well that the ions are directed towards. The depth of this well was determined by the voltages in the system and ensured that ions of different mass and velocity were contained successfully. The offset in effect determined the depth of the well, while the extract voltage is the level at which ions are permitted to exit the hexapole. In theory with a distribution of ions such as with a polymer, a certain portion could have a high enough velocity to escape the hexapole prematurely and would therefore be lost to the detector.

²⁰ K. Nakatsu-Lewis, R. H. Griffin, C. H. Krupp, J. P. Spies, R. A. Hultschiefer, *Rapid Commun. Mass Spectrom.* 13, 1997, (1997)

The length of time that ions spend in the hexapole influences the amount of ions that were then presented to the ion cell, however too long a dwell time and the ion density became large enough to have detrimental effects. Since the ions have similar charges they will repel each other, but at higher concentrations the forces involved were increased. The longer that the ions also spend in such an environment, the higher the possibility that they will collide with other ions or trace gas molecules and perhaps fragment. Extended dwell times can in fact be used to cause fragmentation in a method known as multipole storage-assisted dissociation (MSAD)²⁰. A number of different experimental runs were carried out on the system, the first looked at the dwell-time independently as it was thought to be the more crucial of the settings. With the 3k polyglycol, a series of spectra similar to those of the skimmer and capillary experiments were acquired with dwell times of 1.5, 2, 3, 4, 5, 8 and 15 seconds. The capillary and skimmer voltages were kept constant at values of 65V and 3V respectively. After processing these spectra gave a series of mass values showing the effect of the length of time the ions had spent in the hexapole. As expected the trend was very clear, at the higher values especially, and consistent with both the increase in ion population and exposure to collisional conditions. The ion intensity summated over the mass range of the polymer increased considerably at first, before levelling off and starting to decrease slightly at the highest settings. This can be rationalised by an increase in fragmentation, as the low mass fragments produced would fall outside of the measured window and so while overall ion intensity continued to increase, the area of interest did not. The mass averages showed a similar trend, with an initial increase in M_n and M_w values as well as polydispersity. Then at the higher settings, the values started to decrease once more while polydispersity stayed more level.

²⁰ K Sannes-Lowery, RH Griffey, GH Kruppa, JP Speir, SA Hoftstadler, Rapid Comm Mass Spectrom, 12, 1957, (1998)

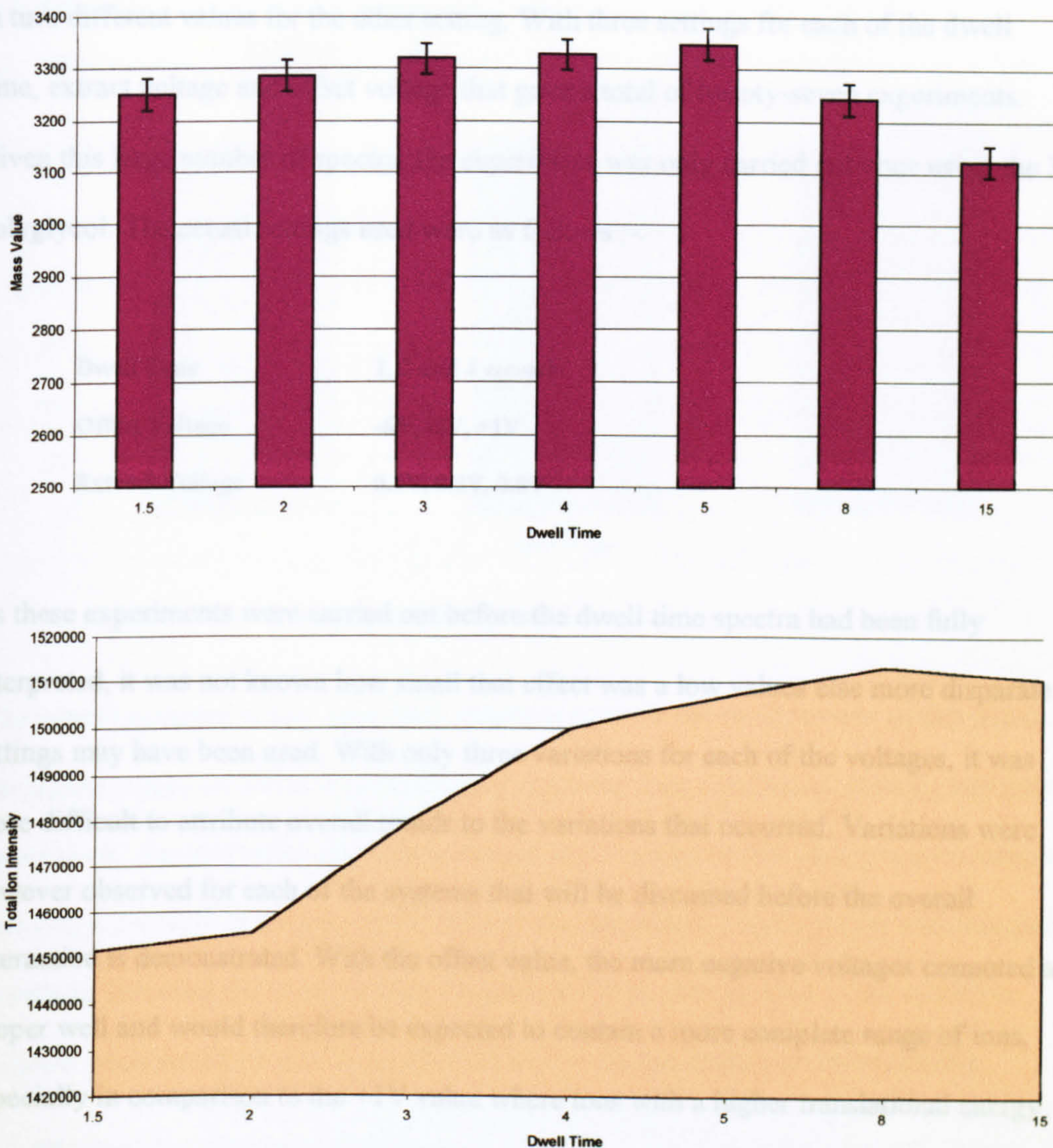


Figure 4p – Mass averages and ion intensity shown as a function of dwell time

Overall, the dwell time did not demonstrate a significant effect on the mass averages until high values were used. Certainly the levels of variation are an order less than those arising from the skimmer voltage and more comparable with those from standard experimental variance. Since it was reasonably assumed that the two voltage settings on the hexapole would have an interaction, the experiment to observe their trends was conducted slightly differently. Less settings were explored than for the other variable, however a greater number of spectra were acquired as each variation was carried out with

in turn different values for the other setting. With three settings for each of the dwell time, extract voltage and offset voltage that gave a total of twenty-seven experiments. Given this large number of spectra, the experiment was only carried out once using the 3k polyglycol. The actual settings used were as follows :-

Dwell Time	1, 2 and 4 seconds
Offset Voltage	-6V, -3V, +1V
Extract Voltage	0.3V, 0.8V, 2.8V

As these experiments were carried out before the dwell time spectra had been fully interpreted, it was not known how small that effect was a low values else more disparate settings may have been used. With only three variations for each of the voltages, it was more difficult to attribute overall trends to the variations that occurred. Variations were however observed for each of the systems that will be discussed before the overall interaction is demonstrated. With the offset value, the more negative voltages connoted a deeper well and would therefore be expected to contain a more complete range of ions, especially in comparison to the +1V value where ions with a higher translational energy would be able to escape the hexapole. This was consistent with the observed trend in mass average and polydispersity where the M_n value in particular decreased as the voltage was moved into the positive scale.

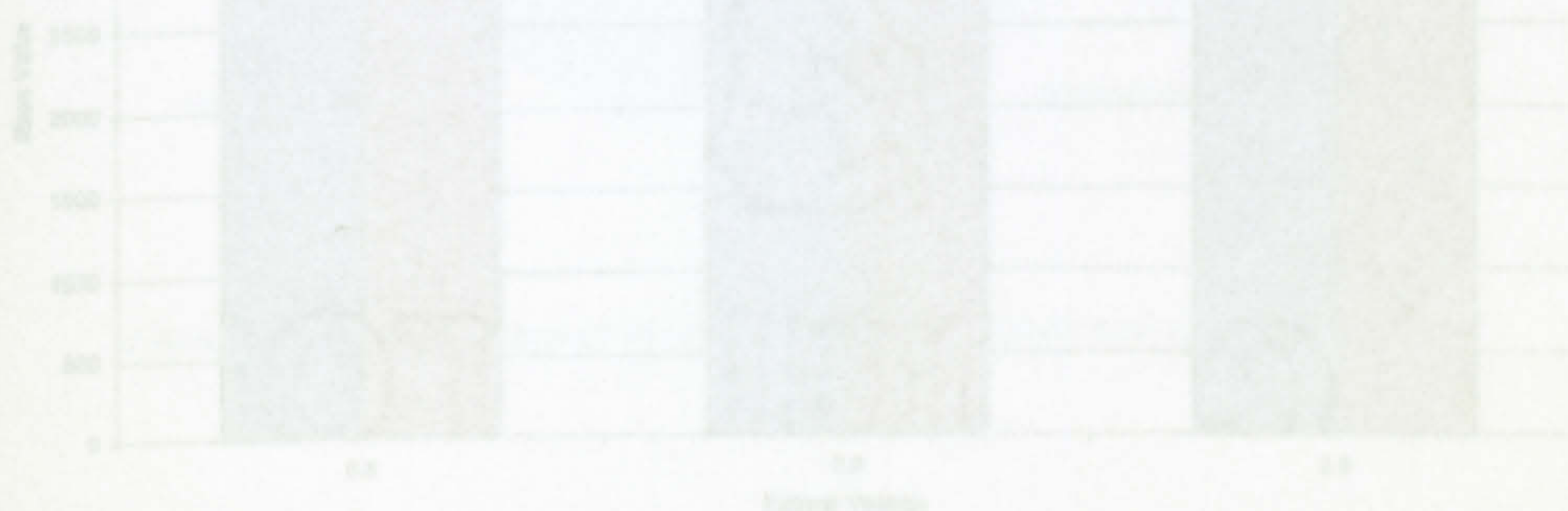


Figure 4r – Mass averages as a function of the extract voltage

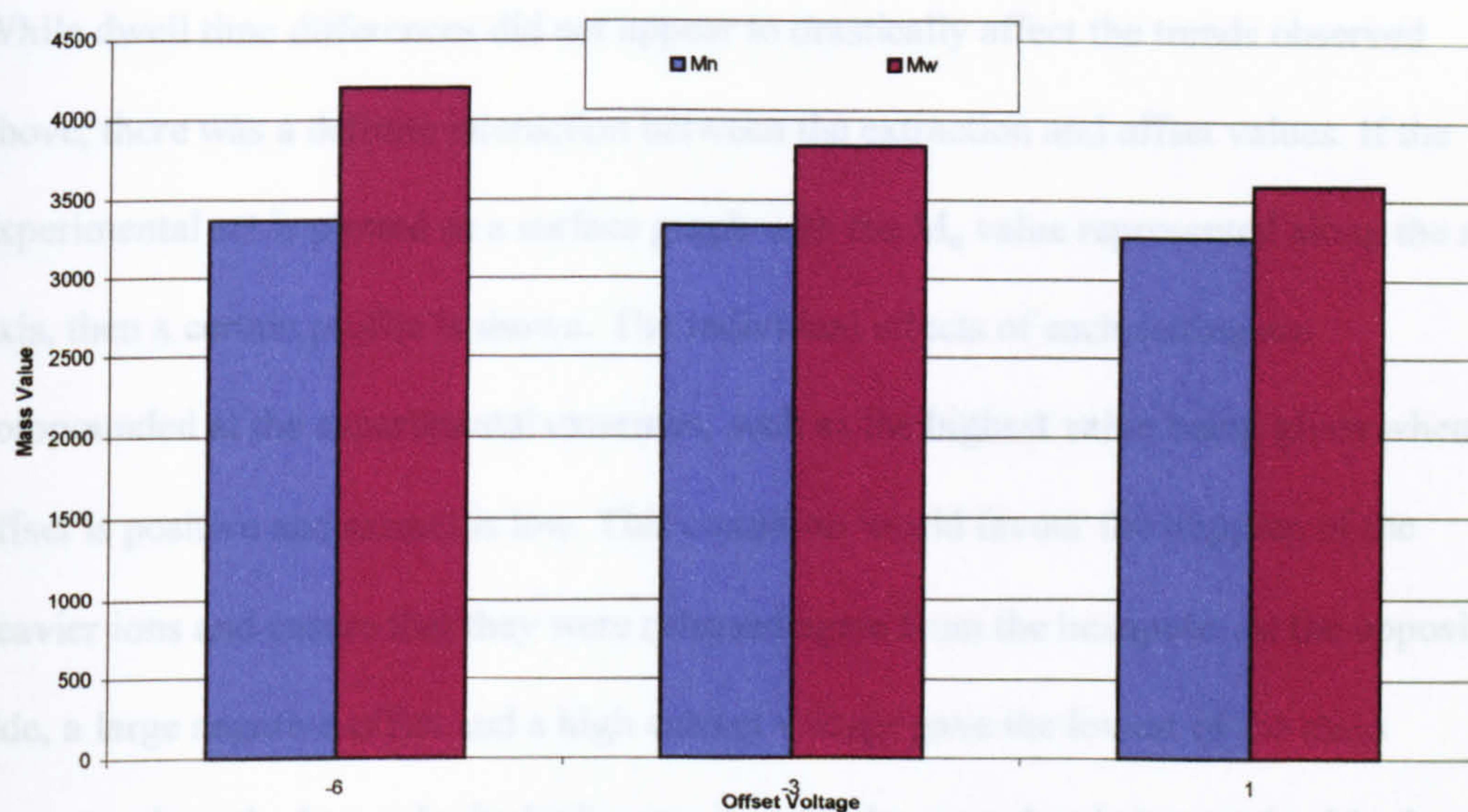


Figure 4q – Mass averages as a function of the offset voltage

The extract potential would have been expected to show the exact reverse of this trend as the higher values would have preferentially extracted ions with higher velocity and hence lower mass. Again plotting the mass averages as a function of this setting was consistent, showing a decrease in average as the voltage was increased. Polydispersity was increased in turn by lowering the extract value, suggesting that a wider portion of the available polymer mass envelope was being allowed to exit the hexapole with these settings.

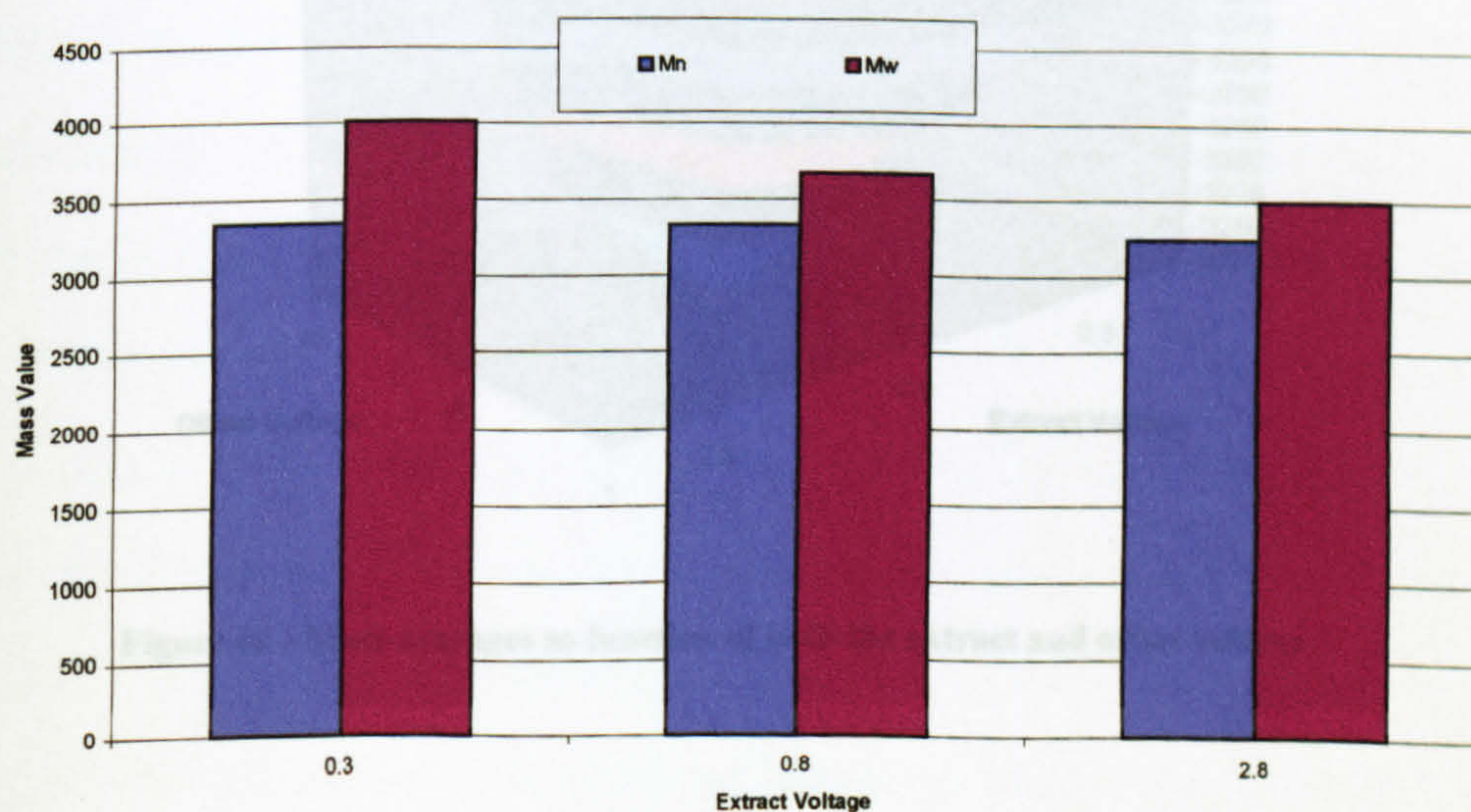


Figure 4r – Mass averages as a function of the extract voltage

While dwell time differences did not appear to drastically affect the trends observed above, there was a definite interaction between the extraction and offset values. If the experimental set is plotted as a surface graph with the M_n value represented along the z -axis, then a certain profile is shown. The individual effects of each setting are compounded at the experimental extremes, such as the highest value being given when offset is positive and extract is low. This condition would favour the trapping of the heavier ions and ensure that they were released again from the hexapole. At the opposite side, a large negative offset and a high extract voltage gave the lowest of the mass averages since the low-velocity high-mass ions can be argued as being retained in the hexapole.

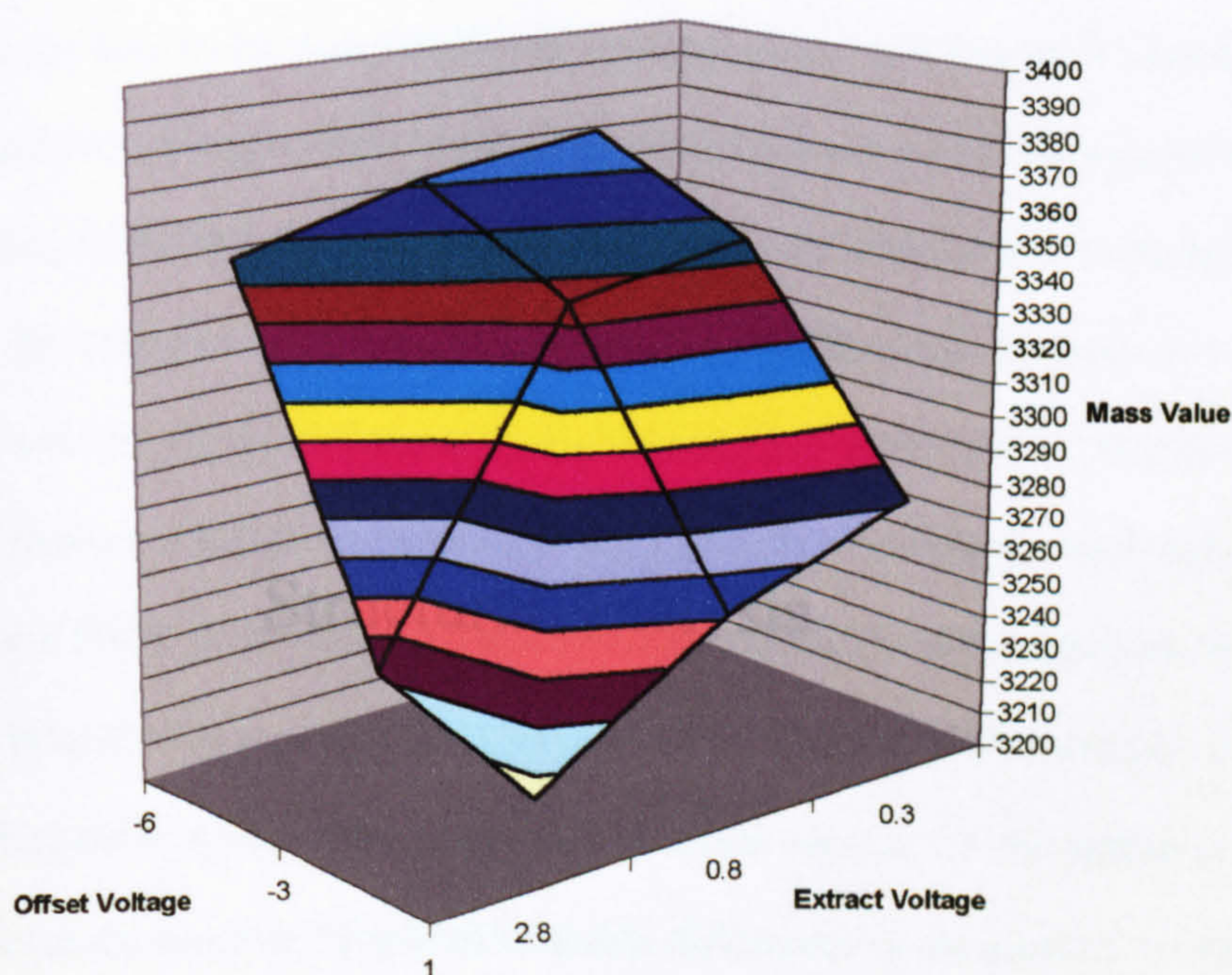


Figure 4s – Mass averages as function of both the extract and offset voltage

CHAPTER FIVE

Structural Analysis

The last two chapters have discussed issues relating to the use of mass spectrometry in the determination of mass averages for polymers. There is an area however where the nature of the technique is well suited and established. This area is the identification and structural analysis of polymers and other macromolecules.

i. Overview

In commercial analysis, there exists at the basest level two types of analyte – an unknown species and a known one that requires confirmation. In many cases an identity can be established by mass spectrometry if the mass accuracy is high enough. This process requires the use of one of the number of spectral libraries¹, where thousands of compounds are listed with their exact mass to a high degree of accuracy. Computer matching presents the most likely candidates, which may or may not be verified by the operator using sample knowledge. In order to achieve a reliable level of certainty, accuracies do need to be high. For example in order to differentiate between the compound with the empirical formula $C_{24}H_{19}N$ (m/z 321.1517) and $C_{21}H_{25}NS$ (m/z 321.1551) requires a $m/\delta m$ resolution of over 94,000. This is certainly well within the capability of FTICR. As the mass increases so does the number of possibilities. If it is not possible to identify the compound from its mass alone, further information may be able to be obtained by observation of the isotope pattern of the analyte, i.e. the pattern of masses that arises from the presence of natural abundant differences in the mass of the various elements. The most obvious element to give an isotope pattern is carbon, where the carbon-13 species exists naturally as 1.1% of all carbon atoms. Since the vast majority of samples analysed by mass spectrometry are organic and therefore carbon-containing, the pattern resulting from one or more carbon-13 atoms can give an indication of the number

¹ FW McLafferty, DB Stauffer, *The Wiley/NBC Registry of Mass Spectral Data*, Palissade Corporation, New York, (1998)

of carbons in the molecule and hopefully therefore the identification². Elements such as the halogens have very clear isotope patterns, that give good indication of their presence in the compound, but all isotope analysis relies on the intensities being true and not affected by any artefacts.

The technical difficulties of accurate mass assessment aside, these techniques only result in the determination of the empirical formula of the compound at best. In order to get an understanding of the structure of the analyte it usually requires that it be broken up and the various pieces identified. Study of the fragmentation of compounds in this way by mass spectrometry is traditionally called tandem mass spectrometry or MS / MS, which indicates its basis as two distinct mass separation stages³. The first stage isolates one particular ion, then after it is in some way fragmented, a second analysis can separate and identify all the fragment ion species that have been produced. This isolation can be either by spatial separation such as with sector instruments, quadrupoles or time-of-flight, else it can be the temporal separation that occurs in ion traps and in Fourier-transform ion cyclotron resonance (FTICR). As mentioned in the first chapter, some ionisation sources, such as electron impact⁴, have a tendency to fragment the analyte regardless due to the high energies involved. Even comparatively more gentle technique such as fast atom bombardment do lead to significant fragmentation, especially the loss of certain small groups such as water from an analyte. In the case of proteins, water molecules can also be incorporated into the macrostructure, this loss of these co-ordinated waters being observed in certain conditions and especially if the analyte is forced into another conformation⁵.

² CS Hso, Anal Chem, 56, 1356, (1984)

³ RA Yost, DD Fetterolf, Mass Spec Rev, 2, 1, (1983)

⁴ G Lawson, N Ostah, Appl Organomet Chem, 15, 749, (2001)

⁵ MF Jarrold, Ann Rev Phys Chem, 51, 179, (2000)

In general, for a molecule to fragment it must be given enough internal energy so that the covalent bonds holding it together are forced to rupture. If the fragmentation of an analyte is not intentional, it is usually because the process of ionisation has imparted too much energy for it to remain stable. There are in fact three distinct categories of ions in all mass spectrometry –

- Stable ions that reach the detector without any fragmentation
- Unstable ions that fragment within the source region of the instrument
- Metastable ions that have an intermediate lifetime stable enough for the first analyser but fragmenting before the detector

In matrix-assisted laser desorption / ionisation experiments, these last two types of ions allow particular forms of experiments. Ions that fragment in the source region are said to undergo in-source decay (ISD) and, assuming they still carry a charge, will be extracted into the field-free region at their correct m / z and can therefore be detected. This is similar to the fragmentation patterns seen in electron impact or fast-atom bombardment and can give information about the structure of the molecule⁶. Ions that are metastable and fragment in the flight-tube are more problematic, as they will have the velocity of their parent and so appear to a linear detector to be of that m / z . Neutral fragments can even be detected in this manner since they have already been accelerated by the extraction potential. However, since the fragmentation process leads to a portion of the internal energy being converted into kinetic energy, the fragments will broaden the observed peak. This type of fragmentation can be an advantage as well, in what is termed post-source decay (PSD) analysis.⁷ Using an ion gate to deflect unwanted ions off the central axis, a single parent ion can be selected. Then by use of a reflectron detector, the

⁶ Z Mincheva, P Hadjieva, V Kalcheva, R Seraglia, P Traldi, M Przyblyski, *J Mass Spectrom*, 36, 626, (2001)

⁷ Z Szilagyi, JE Varney, PJ Derrick, K Vekey, *Rapid Comm Mass Spectrom*, 12, 489, (1998)

analyte ion and any fragments can be separated out and detected. Reflectron analysis in this way also removes the presence of any neutral fragments from the spectra since they will not be deflected by the electrostatic field.

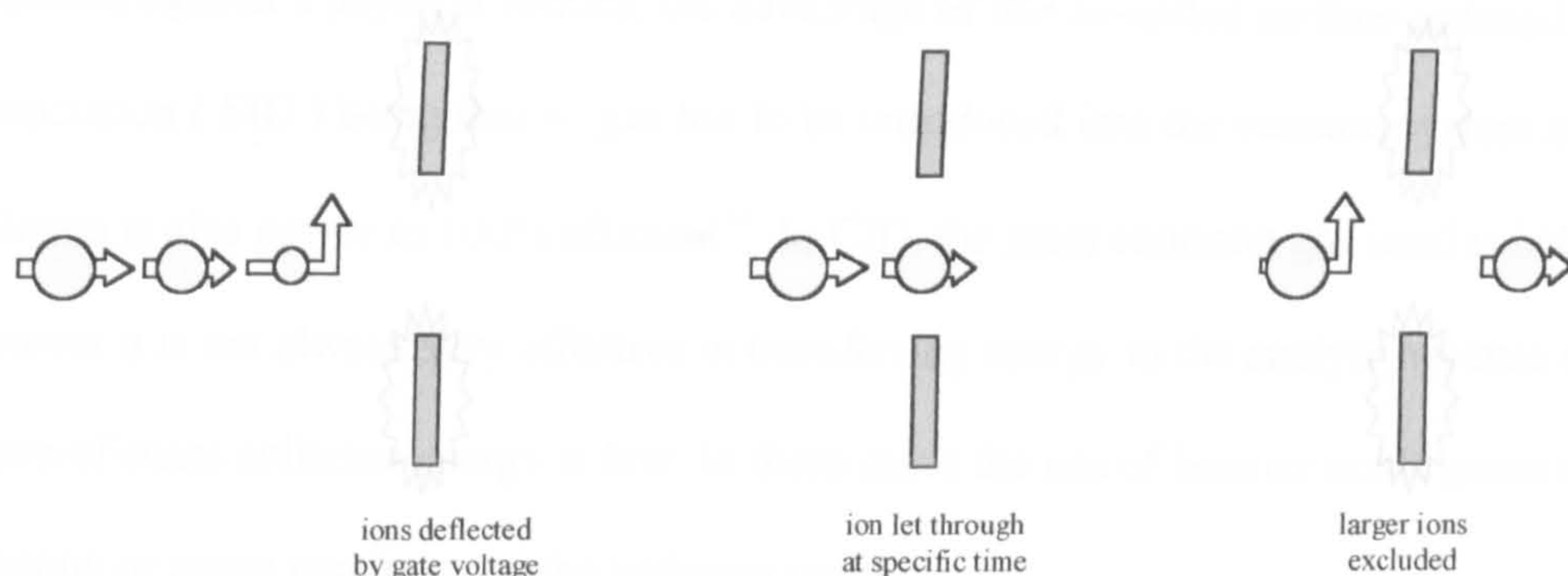


Figure 5a – Ion gating to isolate a particular mass of ion

The other option to detecting the small amount of fragmentation that occurs in the general process is to force the analyte to fragment by imparting extra energy into the system. This is generally carried out in one of two ways – either by colliding the ion with something or by irradiation. Irradiation by various sources such as a laser or other electromagnetic source directly imparts energy into the vibrational states of the molecule in a photochemical process. Such methods are well suited to ion trap and FTICR spectroscopy, where the ions are contained and so can be easily exposed to such stimuli. Techniques such as sustained off-resonance irradiation (SORI) can be used in FTICR to break apart the molecule and then detect the fragments to high degrees of accuracy, all with a relatively small amount of ions contained in the cell⁸. In comparison, colliding the molecule with another material can seem to be a more forceful approach but one that is perhaps available to a wider range of mass spectrometric techniques. The most common form of experiment is collision-induced (CID) or collision-activated (CAD) dissociation, where the analyte impacts with a non-reactive gas. The gas is non-reactive in most cases so as to prevent ion-molecule reactions occurring with the analyte that could

⁸ CL Wilkins, SJ Pastor, Int J Mass Spectrom, 175, 81, (1998)

lead to adduct formation and other species. Reactive gases can be used though, in a variant on the technique known as collisionally-activated reaction (CAR) spectroscopy that does result in fragmentation and the formation of adducts⁹. The ions can also be impacted against a physical surface, the advantage of this so-called surface-induced dissociation (SID) being that no gas has to be introduced into the vacuum system and the collision is also nearer to 100% efficient¹⁰. In CID, the most common gas used is helium, however it is not always very effective in transferring energy to the analyte because the centre-of-mass collision energy is low. In these cases the use of heavier noble gases such as xenon or argon can increase the collision yield.

Collision activation occurs as the kinetic energy of the two molecules is converted into internal energy. This is the first stage of the process and occurs in a very fast time scale (in the order of 10^{-14} to 10^{-16} seconds), followed by the comparatively much slower unimolecular dissociation of the vibrationally excited molecule¹¹. The laws of conservation of energy and momentum suggest that only a fraction of the translational energy is converted to internal energy in this way, which can be given by the following equation:

$$E_{\text{COM}} = E_{\text{LAB}} \times \frac{M_{\text{target}}}{M_{\text{analyte}} + M_{\text{target}}}$$

$$Q = \epsilon E_{\text{COM}}$$

Where E_{COM} is the centre-of-mass energy resulting from the collision, and E_{LAB} is what is known as the laboratory-frame energy. A fraction of this centre-of-mass energy is then converted into internal energy, given by Q , dependent on the efficiency of the gas

⁹ RB Cole, JC Tabet, J Mass Spectrom, 32, 413, (1997)

¹⁰ MA Mabud, MJ DeKrey, RG Cooks, Int J Mass Spectrom Ion Process, 75, 285, (1985)

molecule which is represented by a factor ε . As can be seen, the amount of energy imparted onto the analyte is proportional to the mass of the target gas, but also inversely proportional to the mass of the analyte. That means that small ions will received a higher amount of internal energy and so be much more likely to fragment than large macromolecules. It also suggests that in order to successfully fragment very large compounds for study, a heavier collision gas may be more effective as mentioned above. This can also be seen if we consider that an ion consisting of N non-linear molecules will have $3N-6$ vibrational modes, so a larger molecule will be able to distribute the increased internal energy to a greater degree than a small molecule. The advantage of using an instrument that has a high laboratory frame energy can also be seen. These high-energy collision systems, meaning energies in the kilovolt range, necessitate a electromagnetic or hybrid design such as the MAG-TOF.

The unimolecular decomposition that the molecule then undergoes is described by two very similar theories - the RRKM model of Rice, Ramsberger, Kassel and Marcus¹²; and the so-called “quasi-equilibrium” theory of Rosenstock, Wallenstein, Warharfig and Eyring¹³. These theories assume that the rotational, vibrational, translational and electronic modes are independent. It is also postulated that the proportion of ions decomposing in the time-of-flight is small. As a result of this, the spectra from many different types of mass spectrometer will be similar independent of the kinetic energy of the ions, which can range from a few dozen volts in a quadrupole to kilovolts in a magnetic sector instrument. This is especially beneficial as most of the accurate masses in the spectral libraries mentioned earlier are based on electron impact results.

¹¹ JH Beynon, RK Boyd, AG Brenton, *Adv Mass Spectrom*, 10, 437, (1986)

¹² RA Marcus, *J Chem Phys*, 20, 359, (1952)

¹³ HM Rosenstock, MB Wallenstein, A Warharfig, H Eyring, *Proc Nat Acad Science*, 38, 667, (1952)

ii. Discussion of the MAG-TOF

The hybrid-design instrument known as the MAG-TOF has been described in chapter two, but its operation was not covered in great detail. The instrument was specifically designed to give high-energy collisions at the gas chamber located just before the reflectron time-of-flight (TOF) detector. What was termed the MS1 represented the first analyser in the MS/MS experiment, its purpose was to isolate one specified ion based on its m/z value. In order to establish exactly that this mass was present and of sufficient intensity, there were two detectors before the TOF. The first was a simple linear TOF located co-axially with the MALDI source as shown in the schematic reproduced below. Unlike the other detectors in the system, this one showed all ions produced, allowing the source variables to be set to give the maximum intensity.

As with all MALDI systems, the laser power and extraction voltages could be modified to affect the result. The MAG-TOF also had the complication of varying the exact position of the sample in three-dimensions in order to fine tune the impact of the laser on the sample. While the x and y dimensions were controlled by the computer using two stepper motors in order to raster the laser across the sample, the z -axis was crucial in positioning the surface of the probe so that the laser beam struck it in the correct position to allow successful extraction. This positioning was important as the path of the ion through the machine had to be controlled so that it would eventually pass through the gas chamber and into the reflectron. If the position was out at this stage it would decrease the available ion intensity or even have led to no ions capable of reaching the destination.

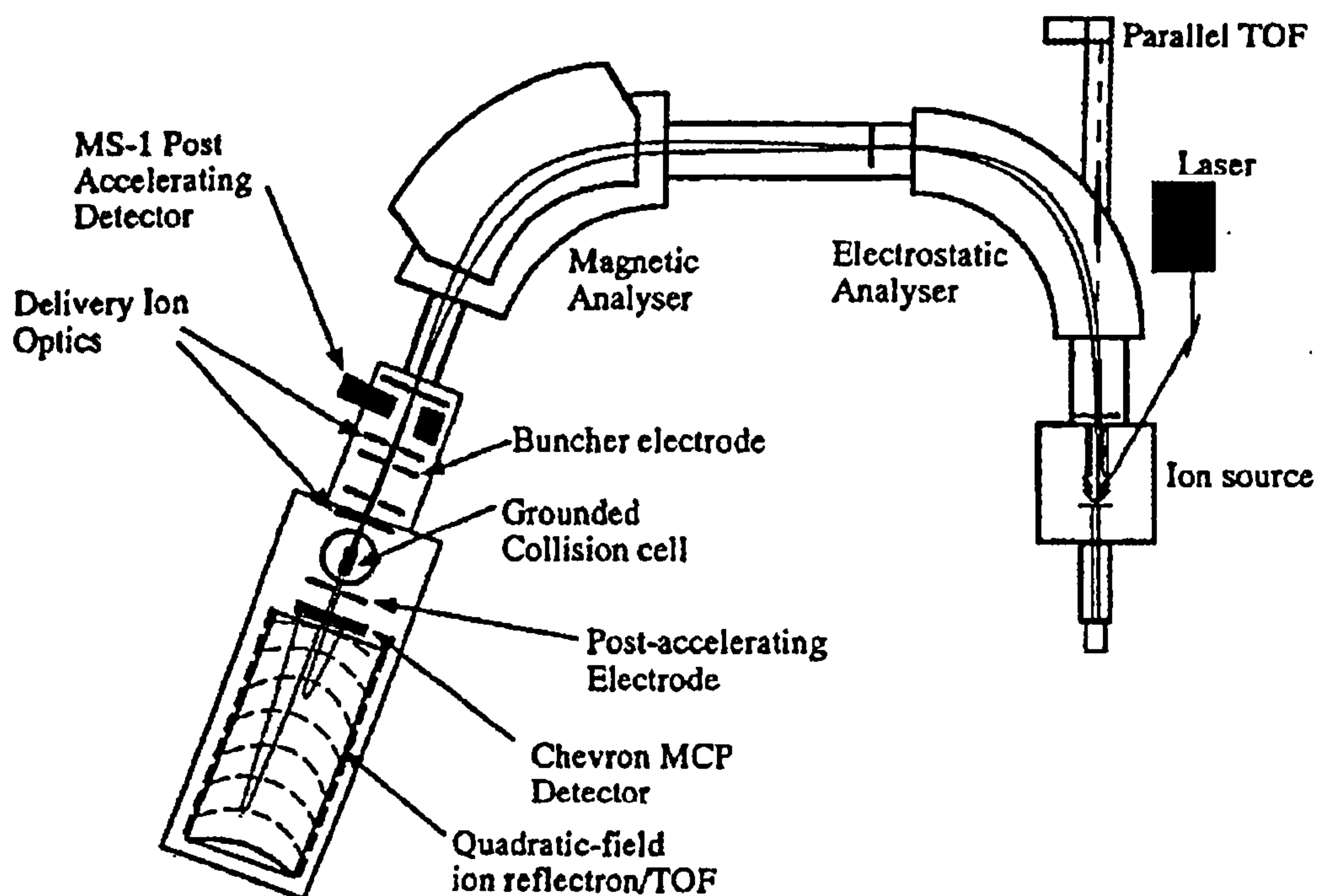


Figure 5b – MAG-TOF schematic

Due to the variable nature of the first time-of-flight region, the mass spectra that resulted from this detector had to be calibrated for each experiment if accurate mass values were to be achieved. In most instances with known samples this was not of a prime concern, but in these cases it was also the most simple procedure as the computer could be told to calibrate the m/z scale based on the masses of known peaks, including those arising from the matrix. For unknown samples, the matrix peaks were still present but a known substance had to be added to the system to give a higher mass for the calibration. Compounds such as carbon-60 and substance P were ideal for this eventuality since they gave clear signals at known masses. Once a reasonable accuracy of mass was achieved, the ion to be exposed to fragmentation could be identified and its exact mass used to set the magnetic sector and timing for the ion buncher. The magnetic sector was controlled by a UNIX computer system and only required entry of a mass value, which set the strength of the electromagnet. The value obtained from the linear TOF was a good starting point but often did not give the greatest signal strength, so another detector was

used at the exit from the MS1 in order to verify the intensity of ions present. A simple oscilloscope was used to present this result, allowing finer tuning of the electromagnet to maximise the intensity. Once the values were optimised, the ions could be allowed to pass through the ion buncher and into the collision cell. The timing of the pulse of the ion buncher was calculated based on the time-of-flight within the MS1, which was in turn dependant on the mass of the analyte ion. It was the ion buncher that effectively constrained the upper mass limit for ions accessible to the instrument, in that the calibration of its pulse time extended to a specific value above which the ions would not be coherent. The ions were focused within the collision cell, where the amount of gas could be controlled using a leak valve. As mentioned in the overview, a number of gases could be used in order to achieve a range of collision energies.

iii. Carbon-60 results

As well as being used as an internal calibrant for the linear TOF, carbon-60 was also used to verify the performance of the CID capability since its fragmentation spectrum was known and very clear. This allotrope of carbon, known as carbon-60 or buckminsterfullerene, consists of sixty carbon atoms in a roughly spherical arrangement made up of hexagons and pentagons¹⁴. The symmetry of this structure gives it rather unique properties that have led to a large body of research. The structure also gives rise to a very ordered fragmentation pattern in mass spectrometry, where it is thought that C₂ fragments are sequentially lost as the 'ball' shrinks. This gradual decline continues in series until it reaches the C₃₂ species and the strain is so great that larger fission events break up the structure entirely¹⁵. Mechanisms for such a loss have been suggested where the junction of two pentagons fuse to form a single hexagon and the C₂ pair. Essential to such a

¹⁴ H Kroto, *Angew Chem*, 104, 113, (1982)

¹⁵ T Nishimura, R Arakawa, *J Mass Spectrom*, 34, 175, (1999)

process would be a process of geometric reorganisation as in the formal carbon-60 structure there are no pentagons sharing an edge in this manner¹⁶. Dissociation energies have been calculated for the sequential fragmentation, which suggest that loss from the so-called “magic” fullerenes of C_{60} , C_{50} and C_{70} requires more energy. The quoted dissociation energies for such a fragment loss are generally thought to be in the region of 9.8eV and can also be achieved by photochemical means with a pulsed laser¹⁷.

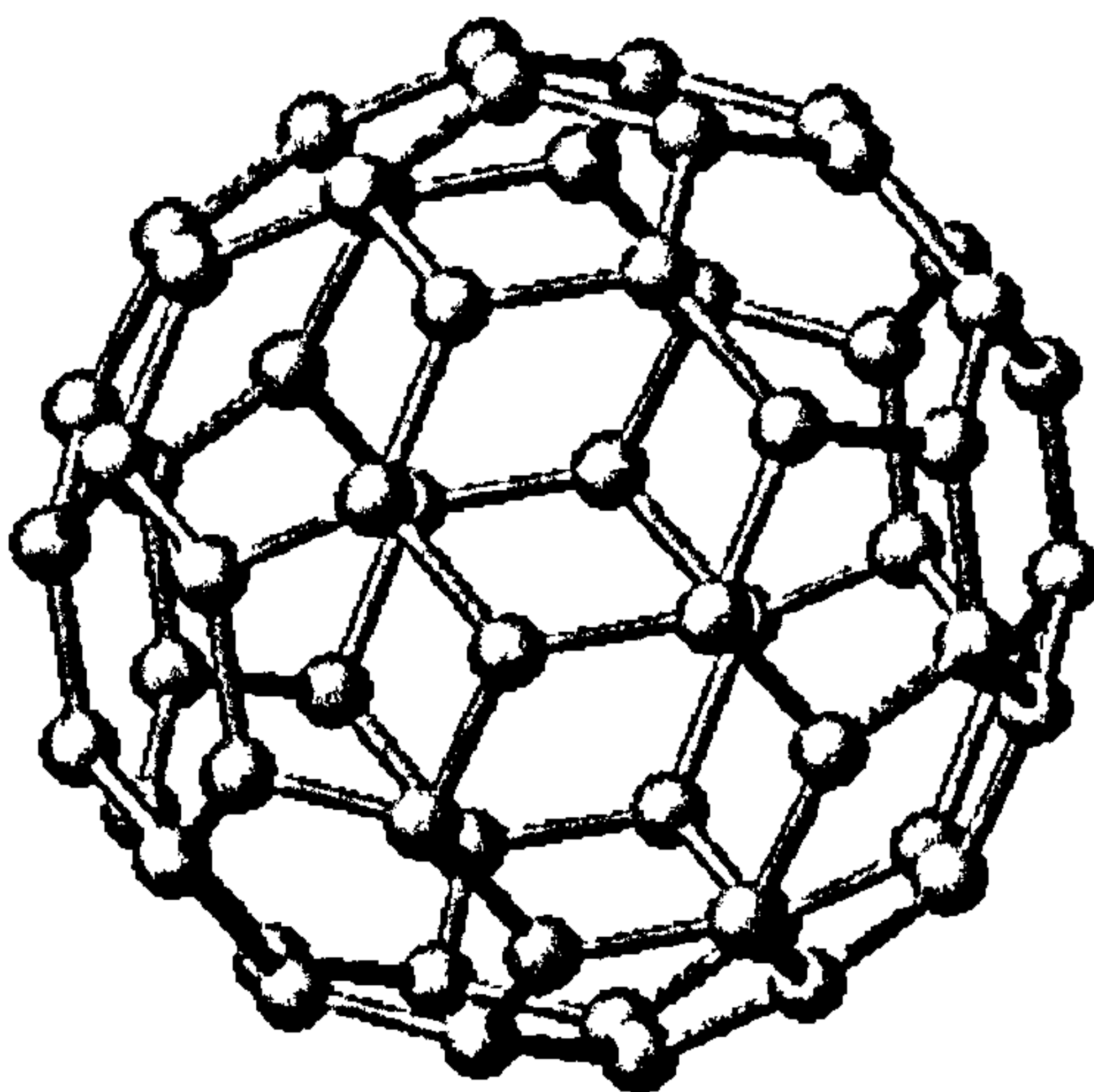


Figure 5c – Carbon-60 3-dimensional structure

When the experiment was applied to the MAG-TOF, the fragmentation gave a very clear pattern in the CID experiments, with each C_2 loss being less likely than the last and so on giving an almost exponential decay from the parent ion. The pattern was highly reproducible with similar intensities as it was considered to be given by a statistical process. It was possible to derive an experimental model for the fragmentation to explore the issue using the presence of carbon-13 isotopes. The mathematical treatment must make a number of assumptions that were consistent with what was believed to be the mechanism. Firstly that the fragmentation only proceeded by the loss of already joined C_2 units and not larger units, then also that the loss of a C^{12} atom was just as favourable as

¹⁶ SC O'Brien, JR Heath, RF Curl, RE Smalley, J Phys Chem, 88, 220, (1988)

¹⁷ S Tomita, JU Andersen, C Gottrup, P Hvelplund, UV Pedersen, Phys Rev Lett, 8707, 3401, (2001)

that of a C¹³. If a single molecule of carbon-60 is imagined as containing two C¹³s and the rest all C¹², then there are two possibilities. The C¹³ atoms can be adjacent or non-adjacent, and each of these has a certain probability given the number of permutations. When one carbon-13 atom is placed, that leaves 59 nodes where the second can be placed, of which only 3 will be adjacent.

$$P(\text{adjacent}) = 3 / 59 = 0.051$$

$$P(\text{non-adjacent}) = 56 / 59 = 0.949$$

Now, if a C₂ unit is to be lost there are probabilities that none, one or both C¹³ atoms are lost in the process. Of course, the only way that two could be lost is if they are adjacent as shown by the following Venn diagram (*Figure 5e*). The probability of each case can then be assessed based on the value already calculated for each situation.

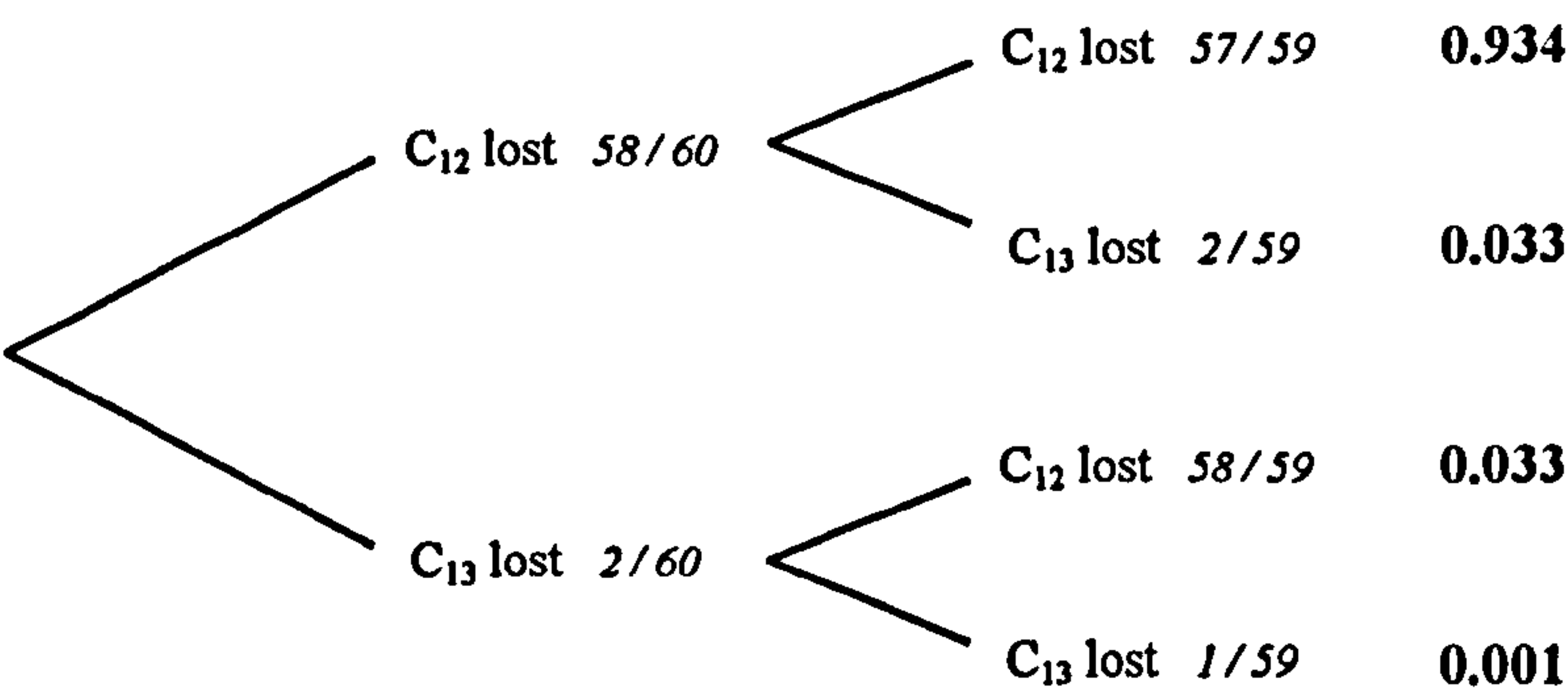


Figure 5d – Tree diagram of initial loss of a 2-carbon unit

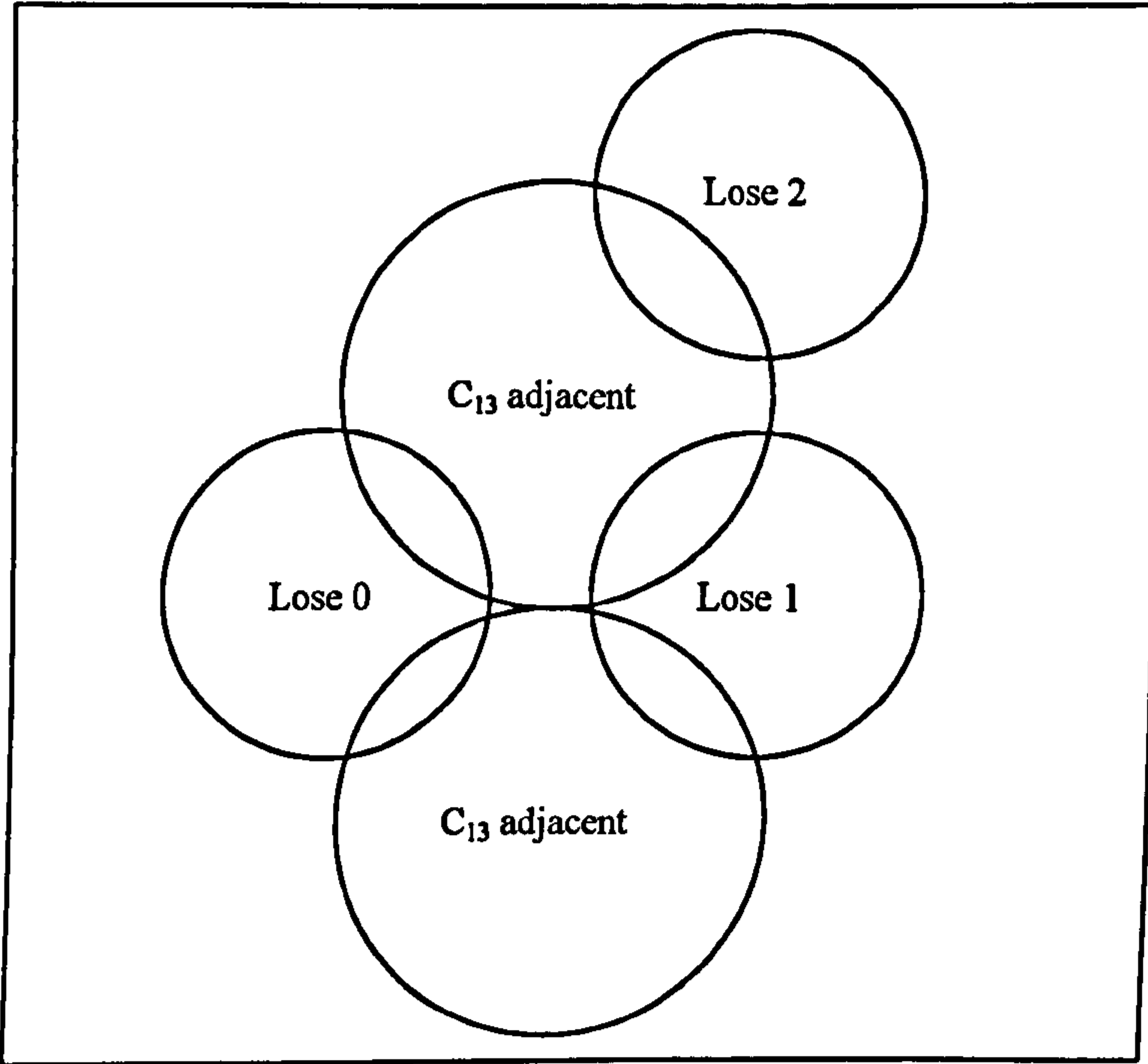


Figure 5e – Initial loss Venn diagram

$$\begin{aligned}
 P(0 \text{ remain}) &= P(2 \text{ loss}) \cap P(\text{adjacent}) = 0.001 \times 0.051 = 5.1 \times 10^{-5} \\
 P(1 \text{ remains}) &= (P(1 \text{ loss}) \cap P(\text{adjacent})) \cup (P(1 \text{ loss}) \cap P(\text{non-adjacent})) \\
 &= (0.066 \times 0.051) + (0.066 \times 0.949) = 0.066 \\
 P(2 \text{ remain}) &= (P(\text{no loss}) \cap P(\text{adjacent})) \cup (P(\text{no loss}) \cap P(\text{non-adjacent})) \\
 &= (0.934 \times 0.051) + (0.934 \times 0.949) = 0.934
 \end{aligned}$$

The statistics at this stage are relatively simple, but now become more complex as the second C₂ is considered. There are four possible starting situations, which can lead once more to the loss of none, one or both C¹³ atoms.

$$\begin{aligned}
 P(0 \text{ remain}) &= (P(2 \text{ loss}) \cap P(2 \text{ adj exists})) \cup (P(1 \text{ loss}) \cap P(1 \text{ exists})) \\
 &\quad \cup (P(\text{no loss}) \cap P(0 \text{ exist})) \\
 &= (0.001 \times 0.048) + (0.034 \times 0.066) + (1 \times 5.1 \times 10^{-5}) = 0.002 \\
 P(1 \text{ remains}) &= (P(1 \text{ loss}) \cap P(2 \text{ exist})) \cup (P(\text{no loss}) \cap P(1 \text{ exists})) \\
 &= (0.068 \times 0.934) + (0.966 \times 0.066) = 0.127
 \end{aligned}$$

$P(2 \text{ remain}) = P(\text{no loss}) \cap P(2 \text{ exist})$
 $= 0.932 \times 0.934 = 0.870$

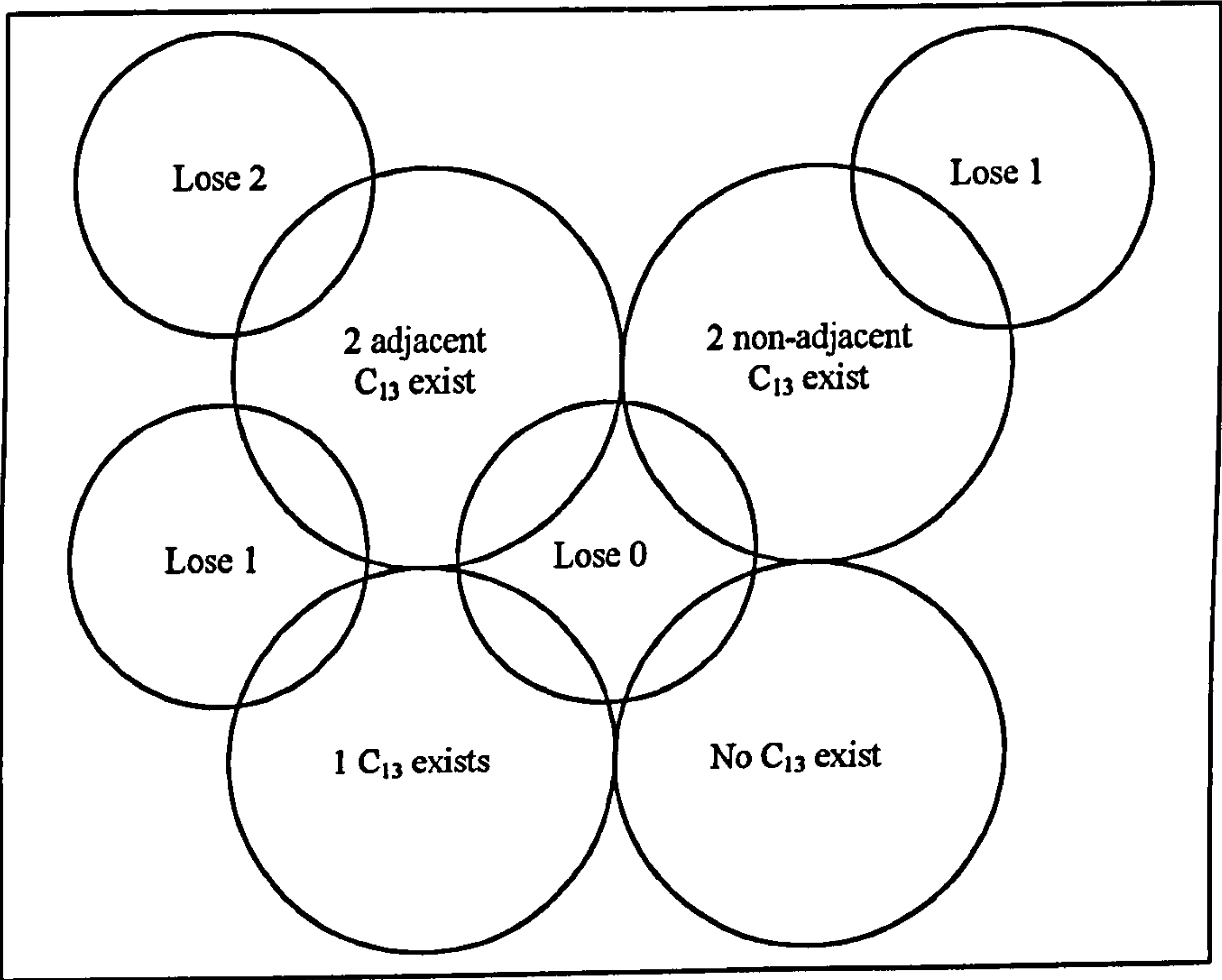


Figure 5f – Second loss Venn diagram

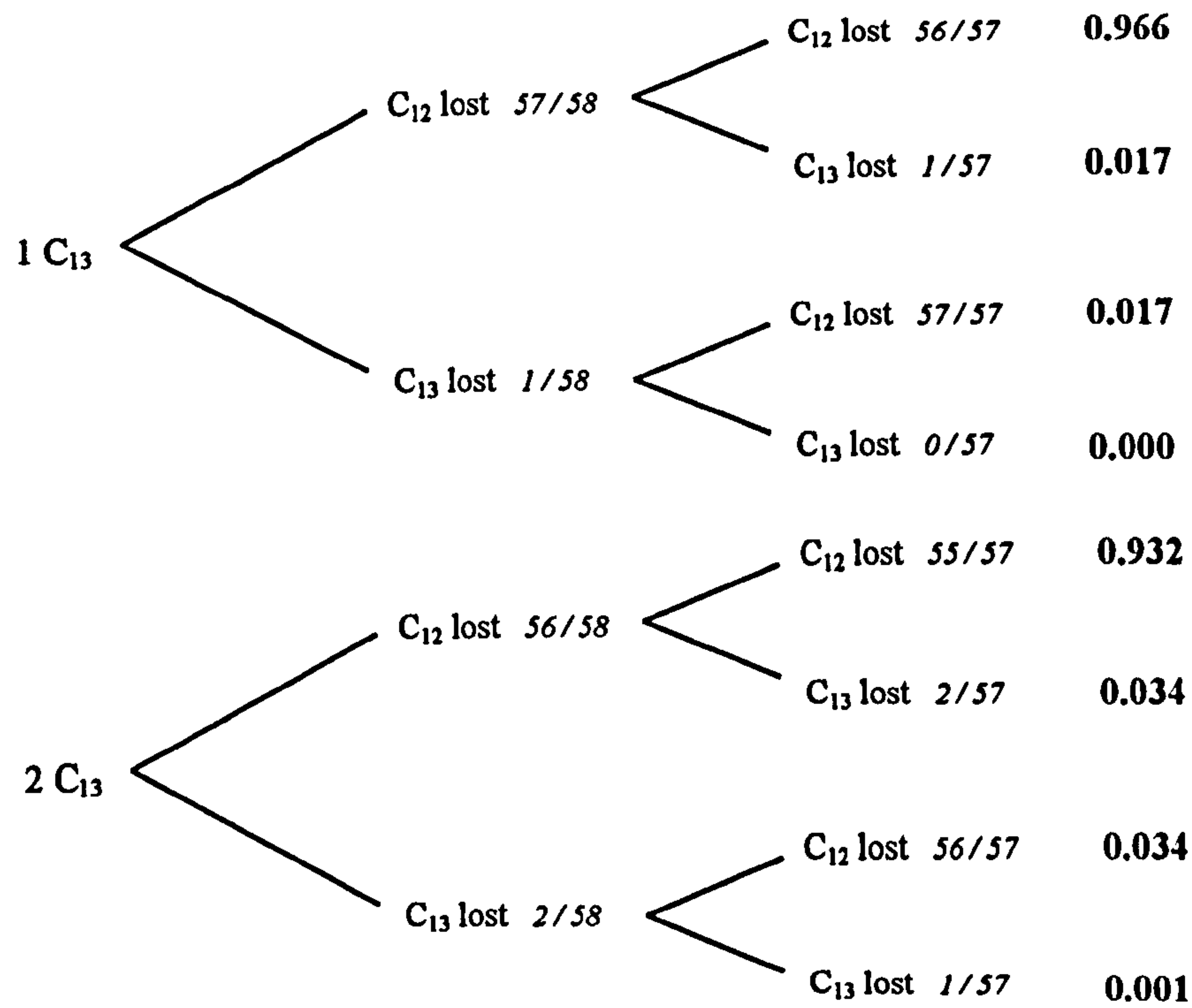


Figure 5g – Tree diagrams of second loss of a 2-carbon unit

This sequence can be repeated if required for subsequent losses, with only the probability of the existence of each of the four states changing and cascading onto the next repetition. The probabilities at each stage can relate to an ion intensity once the values for each mass are summated. This is crucial as after the first loss, there are multiple routes to certain mass values and the amount of values increases with each step in a geometric progression. For instance, the first loss from the parent ion (722 m/z) leads to three masses at 698 (representing two C^{12} losses), 697 (representing one C^{12} and one C^{13} loss) and 696 (representing two C^{13} losses). In the next stage, the same three cases can occur from each of the three daughter species, but most overlap leaving once again three peaks from m/z 674 to 672. Once the values are summated as above they could be used to compare to an observed isotope, plotted here to show a theoretical distribution. In reality there is a probability of fragmentation occurring that will decrease the size of each subsequent grouping, but it is the relative isotope pattern in each that is underpinned by the statistics described above. Only the first few groupings would need to be observed to confirm this model for the fragmentation.

As the C^{13} isotope has a natural abundance of 1.1%, the 722 mass peak with two C^{13} isotopes present represents less than 12% of naturally-occurring carbon-60. While the mass peak is visible by mass spectroscopy, the ion intensity was too low to allow CID to be carried out with current instrumentation. The solution to this problem would be to use a carbon-60 sample enriched with a higher than natural percentage of C^{13} , however such a sample was not available or economical at the time of these experiments. Experiments looking at coincident fragments, that is using two detectors for low and high mass fragments have also suggested that larger species than the C_2 fragments are present which would not be dealt with by this model¹⁸.

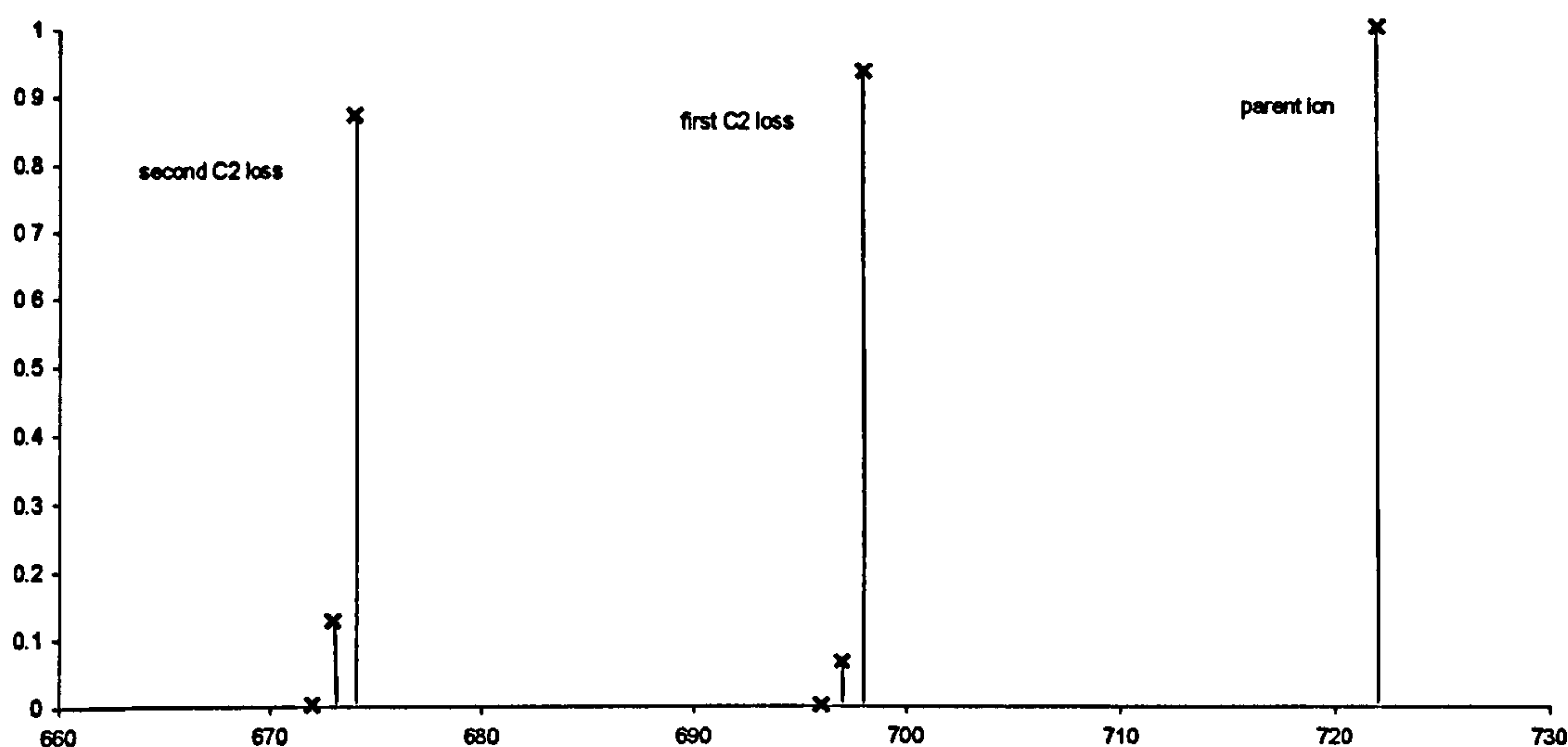


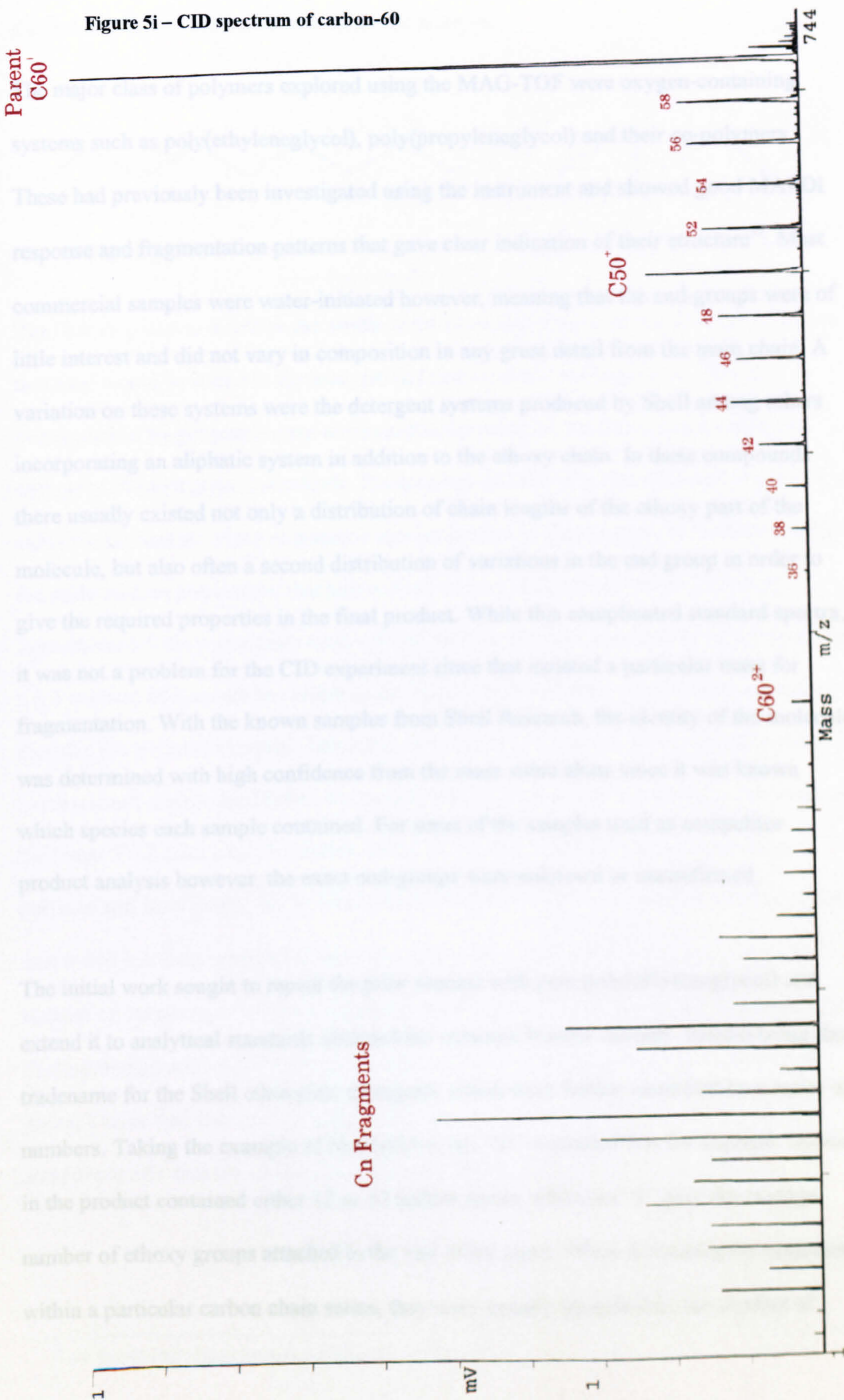
Figure 5h – Theoretical isotope distribution for the first two losses

The mathematical model aside, carbon-60 proved a useful tool in establishing the conditions for the CID experiments and tuning the ion optics of the instrument. Unlike the polymeric systems under study, the mass spectrum consisted of one strong peak and since carbon-60 could be laser desorbed without matrix there were few complications. The sample preparation only involved dissolving an amount of the solid in toluene and leaving overnight, the next day the purple solution could be pipetted directly onto the sample probe. Through a series of applications and dryings, a substantial layer of the brown substance was built up that would last for a reasonable time under the laser bombardment. Carbon-60 could also be added into sample preparations for internal calibration, but proteins such as substance P were often better since they were more suited to the solvent environments of the polymers.

¹⁸ CH Cooper, B Henry, JF Liang, R Vandenbosch, DI Will, *University of Washington electronic publication*, (1997)

iv. Fragmentation of Oxygenate Polymers

Figure 5i – CID spectrum of carbon-60



iv. Fragmentation of Oxygenate Polymers

The major class of polymers explored using the MAG-TOF were oxygen-containing systems such as poly(ethyleneglycol), poly(propyleneglycol) and their co-polymers. These had previously been investigated using the instrument and showed good MALDI response and fragmentation patterns that gave clear indication of their structure¹⁹. Most commercial samples were water-initiated however, meaning that the end-groups were of little interest and did not vary in composition in any great detail from the main chain. A variation on these systems were the detergent systems produced by Shell among others incorporating an aliphatic system in addition to the ethoxy chain. In these compounds there usually existed not only a distribution of chain lengths of the ethoxy part of the molecule, but also often a second distribution of variations in the end group in order to give the required properties in the final product. While this complicated standard spectra, it was not a problem for the CID experiment since that isolated a particular mass for fragmentation. With the known samples from Shell Research, the identity of the molecule was determined with high confidence from the mass value alone since it was known which species each sample contained. For some of the samples used as competitor product analysis however, the exact end-groups were unknown or unconfirmed.

The initial work sought to repeat the prior success with pure poly(ethyleneglycol) and extend it to analytical standards obtained for common Needol variants. Needol being the tradename for the Shell ethoxylate detergents which were further identified by a series of numbers. Taking the example of Needol23-4, the "23" indicated that the aliphatic chains in the product contained either 12 or 13 carbon atoms, while the "4" gave the average number of ethoxy groups attached to the end of the chain. When discussing the oligomers within a particular carbon chain series, they were usually identified by the number of

Figure 5k – Linear TOF spectra of the Needol sample

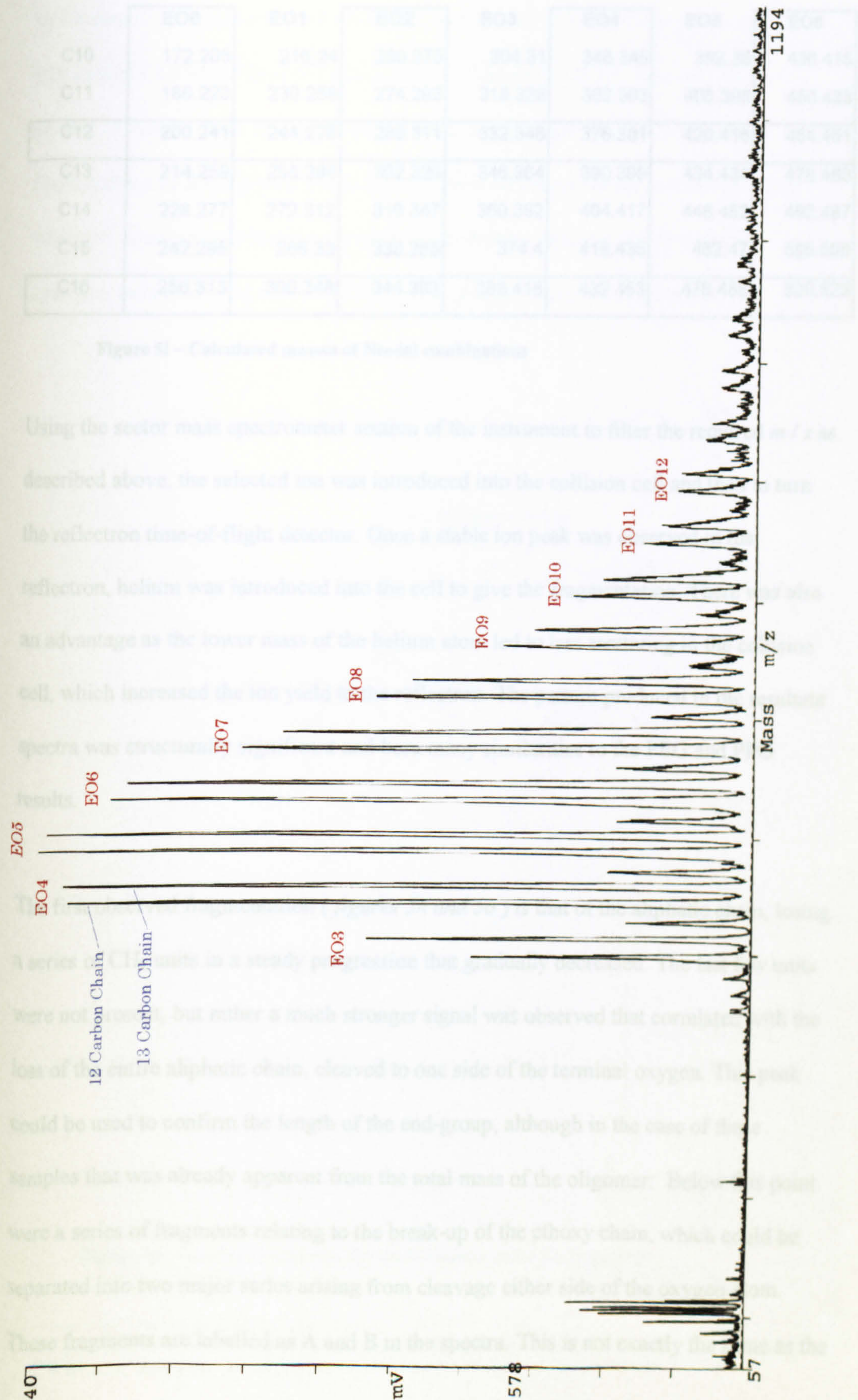
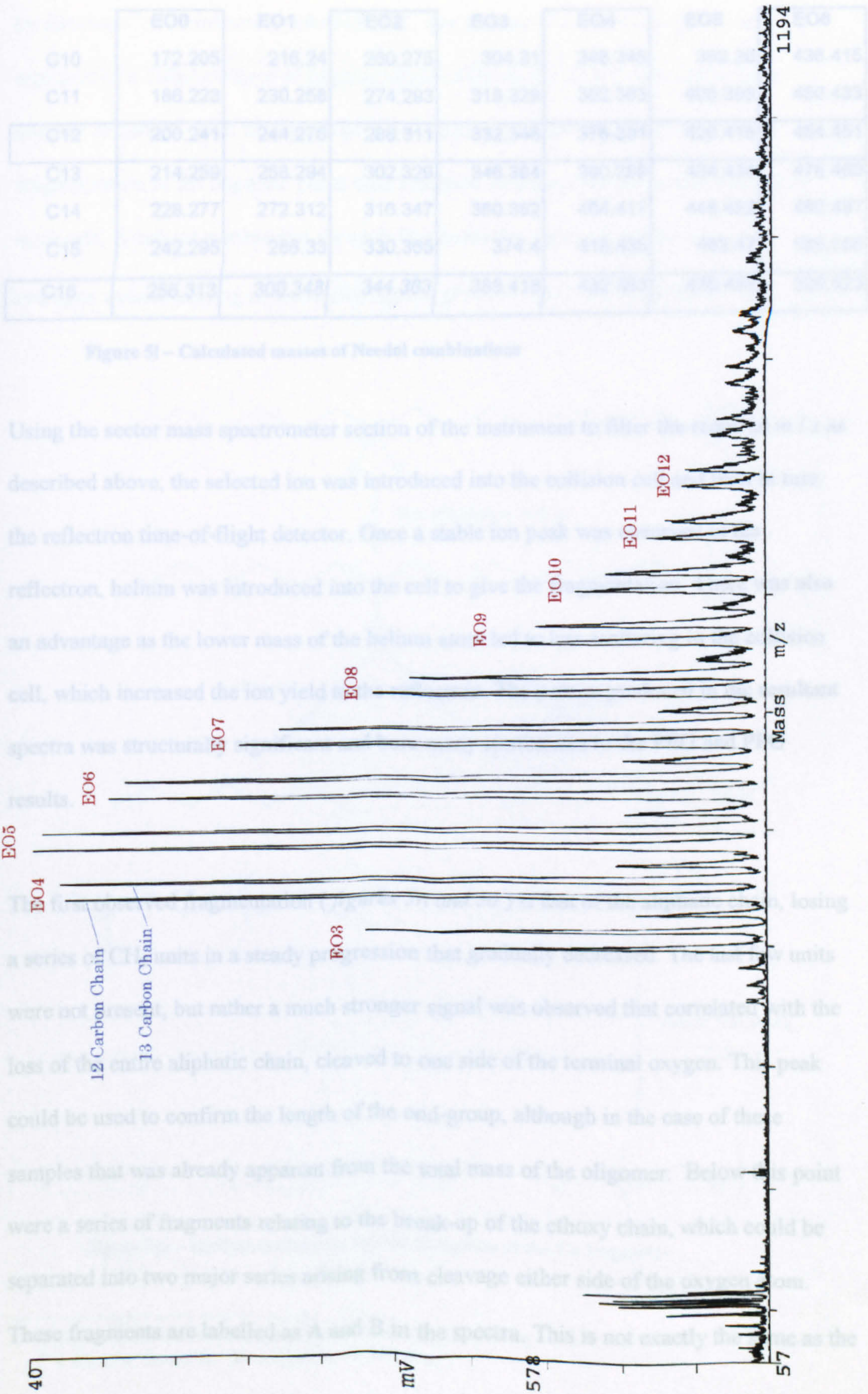


Figure 5k – Linear TOF spectra of the Needol sample



	EO0	EO1	EO2	EO3	EO4	EO5	EO6
C10	172.205	216.24	260.275	304.31	348.345	392.38	436.415
C11	186.223	230.258	274.293	318.328	362.363	406.398	450.433
C12	200.241	244.276	288.311	332.346	376.381	420.416	464.451
C13	214.259	258.294	302.329	346.364	390.399	434.434	478.469
C14	228.277	272.312	316.347	360.382	404.417	448.452	492.487
C15	242.295	286.33	330.365	374.4	418.435	462.47	506.505
C16	256.313	300.348	344.383	388.418	432.453	476.488	520.523

Figure 5l – Calculated masses of Needol combinations

Using the sector mass spectrometer section of the instrument to filter the required m/z as described above, the selected ion was introduced into the collision cell and then in turn the reflectron time-of-flight detector. Once a stable ion peak was observed in the reflectron, helium was introduced into the cell to give the fragmentation. There was also an advantage as the lower mass of the helium atom led to less scattering in the collision cell, which increased the ion yield to the reflectron. The pattern produced in the resultant spectra was structurally significant and bore many similarities to the PEG and PPG results.

The first observed fragmentation (*figures 5n and 5o*) is that of the aliphatic chain, losing a series of CH_2 units in a steady progression that gradually decreased. The last few units were not present, but rather a much stronger signal was observed that correlated with the loss of the entire aliphatic chain, cleaved to one side of the terminal oxygen. This peak could be used to confirm the length of the end-group, although in the case of these samples that was already apparent from the total mass of the oligomer. Below this point were a series of fragments relating to the break-up of the ethoxy chain, which could be separated into two major series arising from cleavage either side of the oxygen atom. These fragments are labelled as A and B in the spectra. This is not exactly the same as the

nomenclature system developed by Roepstorff et al for peptides²⁰ and developed further by Biemann²¹. A third series, labelled as C, was present at lower mass values and represented a different form of fragmentation of the chain. There were also a large number of carbon chain fragments at low masses, which are thought to arise from fragmentation of the aliphatic chain with retention of charge on the carbon side of the molecule. A radical mechanism for such fragmentation proceeds by the loss of a hydrogen radical leading to chain cleavage to give the observed C_n systems.

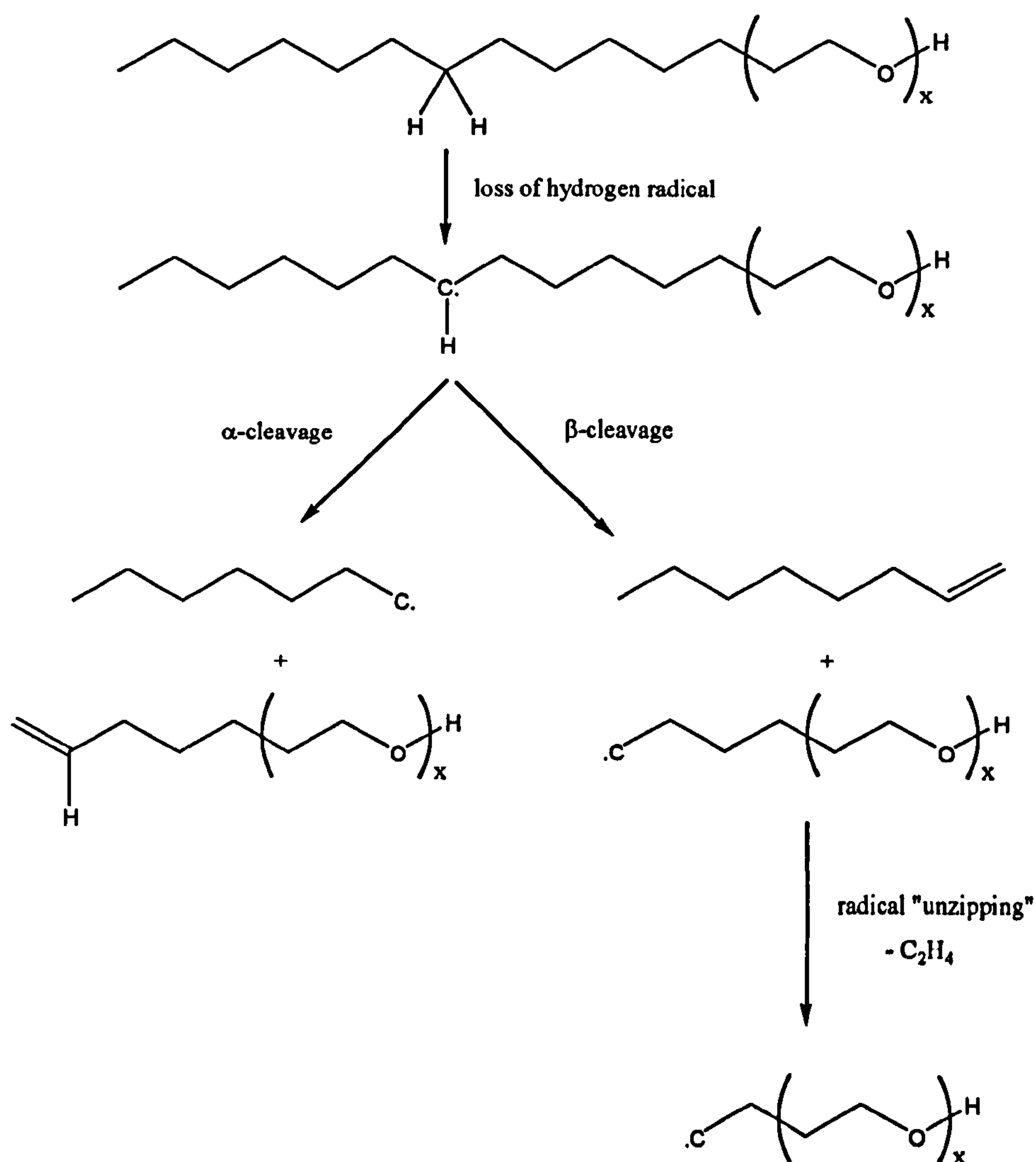
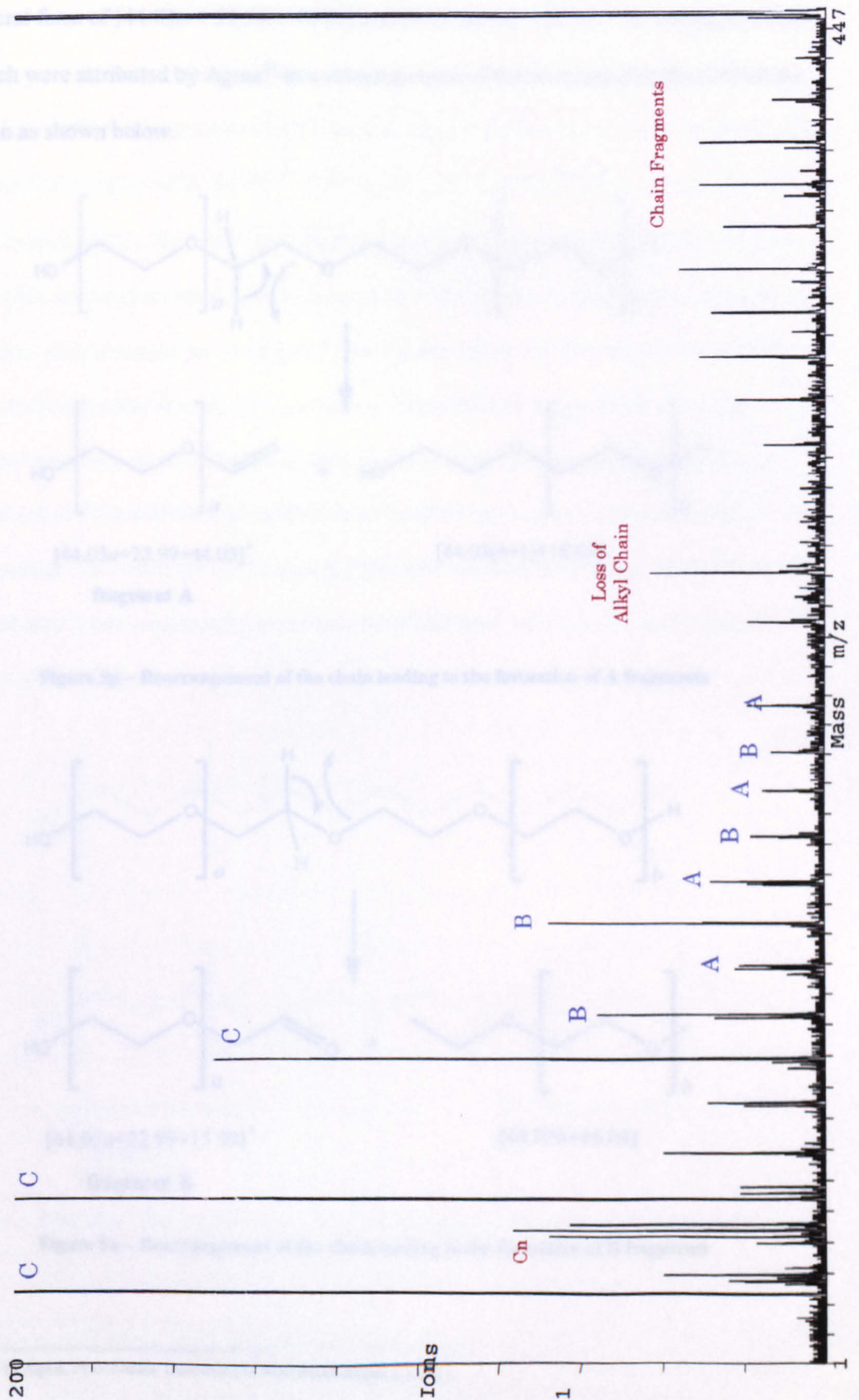


Figure 5m – Radical mechanism for the formation of the C_n fragments

²⁰ P Roepstorff, J Fohlman, J Biomed Mass Spectrom, 11, 601, (1984)

²¹ K Biemann, Biomed Env Mass Spectrom, 16, 99, (1988)

Figure 5o – CID spectra of the isolated C_{13} -EO₅ species

The masses of the peaks labelled as A and B corresponded to charged fragments with the general form of $[44.03a + 22.99 + 44.03]$ and $[44.03(a+1) + 22.99 + 15.99]$ respectively which were attributed by Agma²² to a rearrangement of bonds α and β to the C-O of the chain as shown below.

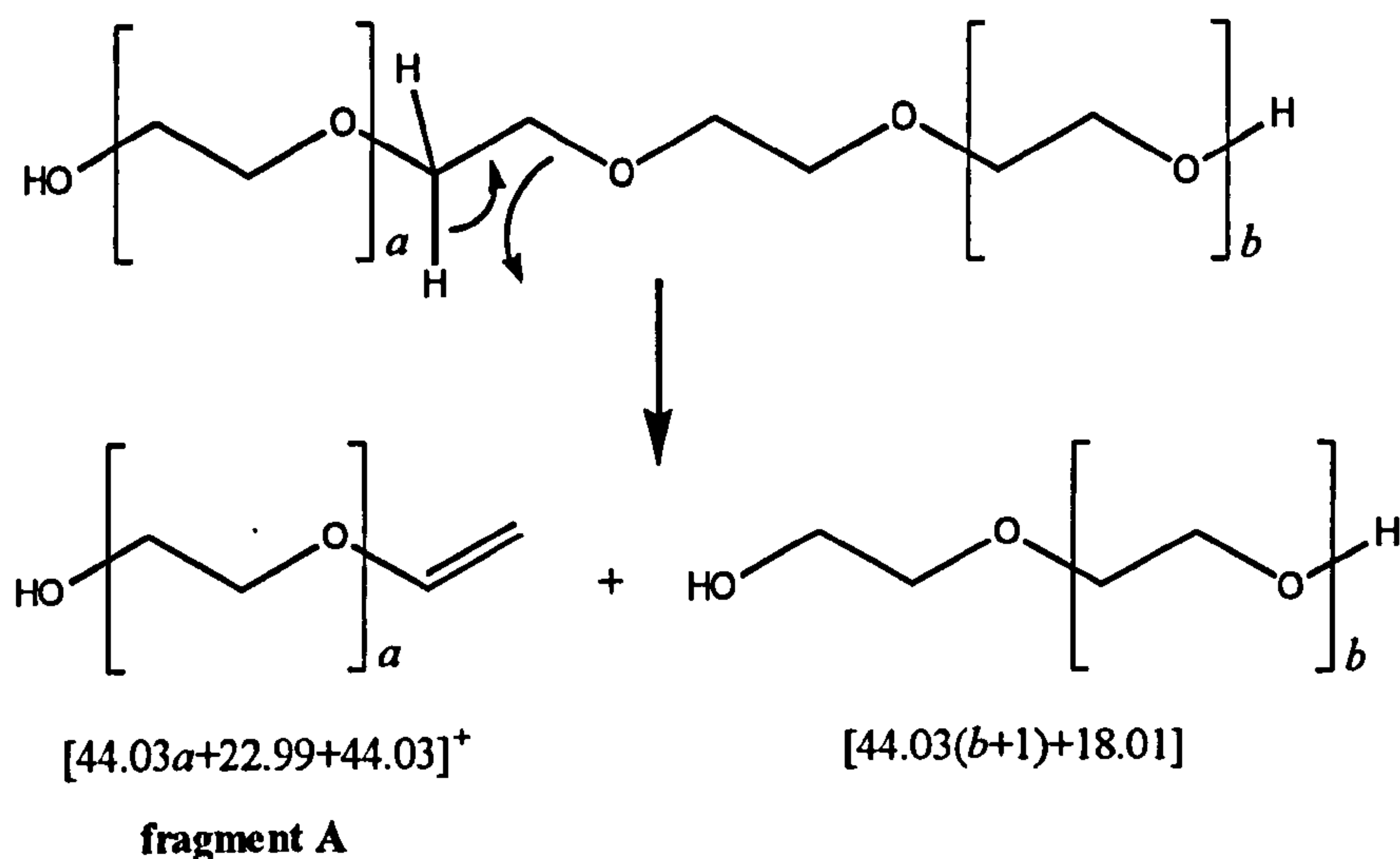


Figure 5p – Rearrangement of the chain leading to the formation of A fragments

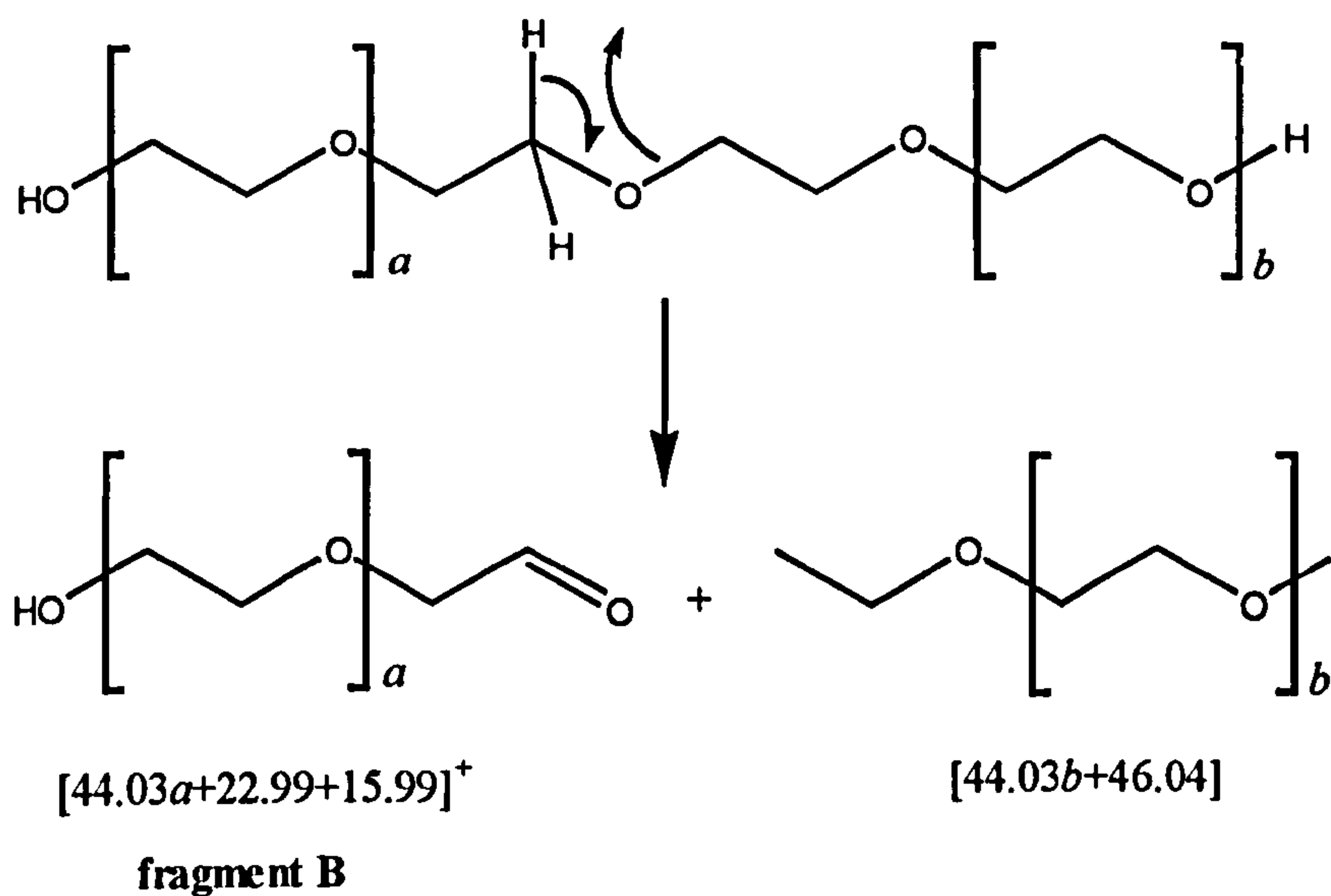


Figure 5q – Rearrangement of the chain leading to the formation of B fragments

²² M Agma, *PhD Thesis*, University of New South Wales, (1988)

The fragments labelled as C which dominated the lower mass region of the spectra can be given the general form of $[44.03a + 22.99 + 31.02]$ and unlike the other fragments seem to suggest a homolytic fission of the carbon chain adjacent to the oxygen bond. This mechanism was suggested by Craig²³ and also observed in the dissociation of alkali-metal cationised polyglycols by Bottrill²⁴. The fact that the fragments only occur at relatively low masses suggest that such bond cleavage only occurs near the centre of the chain in order for the resultant mass to be less than half of the parent. Else the radical formed leads to what is termed an “unzipping” process that moves down the chain to give the observed fragments at relatively low masses. Homolytic cleavage of the C-O bond in a similar manner was not observed in these spectra, which perhaps suggests the energy involved was not sufficient given the higher bond energies such a scission would necessitate. The value for C-C bonds at 348kJ mol^{-1} is marginally lower than C-O at 360kJ mol^{-1} , and considerably lower than the 412kJ mol^{-1} of the C-H bonds²⁵ which in principle could also be involved in the fragmentation process.

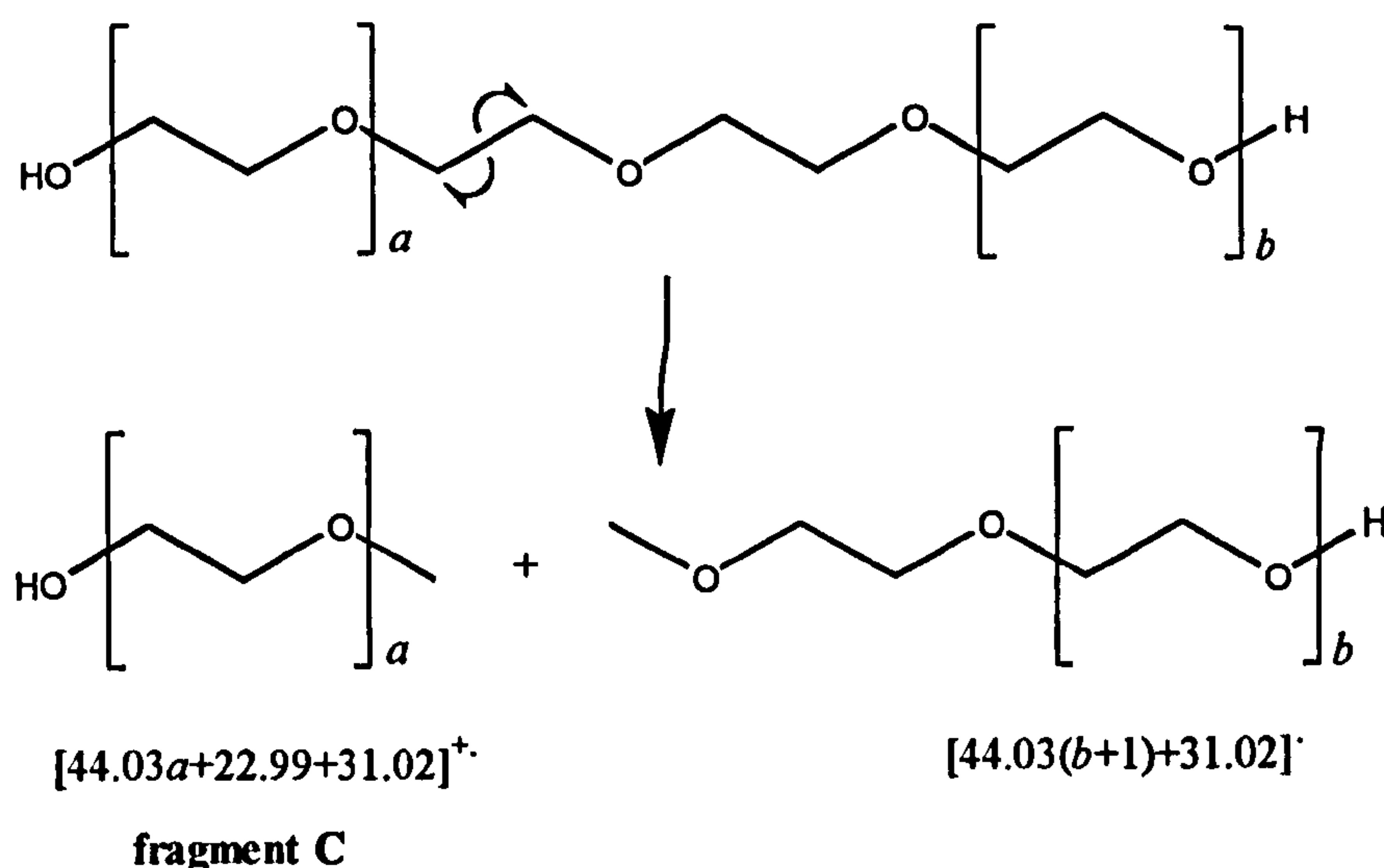


Figure 5r – Homolytic fission of the chain leading to the formation of the C fragments

²³ AG Craig, *PhD Thesis*, University of New South Wales, (1984)

²⁴ AR Bottrill, *PhD Thesis*, University of Warwick, (2001)

²⁵ NW Alcock, *Structure and Bonding*, Ellis Horwood, (1990)

An issue that arises from such observations is the retention of the charge on the polymer in the form of the attached sodium ion. The only fragments that will be observed after the reflectron are those that are charged, with the other side of the fission being lost to the detection. With the three fragmentation mechanisms shown above, the counter fragment is not observed in the spectra meaning that there exists no cases where the sodium was positioned on the other side of the cleavage point. This would seem unlikely if the charge was remote from the point of scission, suggesting that the ion was associated with a point near the fragmentation centre. If this was not the case, then statistically there should be no reason for one side of the fragmented molecule to preferentially associate with the charge. Charge migration is a possibility given the timescale of dissociation, however there is structurally little difference in the polymer either side of the breaking point other than any remaining aliphatic chain. If it is assumed that the scission occurs near the placement of the cation, then the various fragments result from situations where the sodium is associated at different points along the polymer chain. This would also account for the existence of the C_n species, as on the basis of a charge-remote argument they would be very unlikely to retain charge and so be detected.

This form of analysis was extended to look at another related chemical series, that of the Oxilube additives produced by Shell. These are similar in structure to that of the Needol class, but comprise a co-polymer system of ethoxy and propoxy groups in addition to having a wider variety of mostly aliphatic end-groups. Unlike the case with the Needols, the commercial products under study usually have only a single end-group present in each situation, which at least should have simplified the spectra in that regard. Again, each sample was subjected to analysis by GPC and in this case MALDI before the experiments on the MAG-TOF were started. The chromatography indicated that a number of the available samples had mass ranges above the experimental range of the instrument, while others had a very broad distribution with in one case a polydispersity exceeding 2.5.

Analysis by MALDI-TOF also proved difficult which suggested that CID spectra would be difficult for a number of the samples. The few that had low enough masses, a narrow mass-distribution and gave a MALDI result did demonstrate the complexity of the polymer system by the number of peaks present in the spectra.

	EO0	EO1	EO2	EO3	EO4	EO5	EO6	EO7	EO8
PO0	17.003	61.038	105.073	149.108	193.143	237.178	281.213	325.248	369.283
PO1	75.056	119.091	163.126	207.161	251.196	295.231	339.266	383.301	427.336
PO2	133.109	177.144	221.179	265.214	309.249	353.284	397.319	441.354	485.389
PO4	191.162	235.197	279.232	323.267	367.302	411.337	455.372	499.407	543.442
PO6	249.215	293.25	337.285	381.32	425.355	469.39	513.425	557.46	601.495
PO7	307.268	351.303	395.338	439.373	483.408	527.443	571.478	615.513	659.548
PO8	365.321	409.356	453.391	497.426	541.461	585.496	629.531	673.566	717.601

Figure 5s – Masses of various EO / PO combinations

Two were chosen to be run on the MAG-TOF system, with the highest intensity peaks at the centre of the distribution selected for fragmentation. However, the intensities achieved at the reflectron did not prove high or stable enough for high-quality spectra, even running for an extended length of time. The issue, as with many other polymer samples, was that the sheer number of oligomers present reduced the effective intensity of any one species that could be selected for analysis. The obvious solution to this problem was to reduce the number of species present, in the case of the Needol samples this was achieved by use of analytical standards which had a smaller number of combinations present. With the Oxilube series and other samples this was not possible, and also did not represent a general solution to the issue of low species intensity. One answer was to apply a technique used with some success for the analysis of high polydispersity samples²⁶, which was to use a chromatographic separation to create fractions containing a part of the overall distribution.

²⁶ MS Montaudo, C Puglisi, F Samperi, G Montaudo, Rapid Comm Mass Spectrom, 12, 519, (1998)

Application of preparative-scale gel permeation chromatography (prep-GPC) gave an initial mass-based separation and, using a carousel at the elution stage, fractions were collected with a smaller mass range than the initial sample. Due to the exponential relationship of the time scale in the separation, if equal volumes were taken at set times the mass ranges of each fraction would increase as time progressed and the later ones might have suffered from bias effects due to their breadth. The answer was to collect decreasing volumes, in an inverse relationship with the mass scale of the separation. The eluents were reduced down to the same volumes, both in order to give the same applied concentration and to remove the solvent added during the chromatography. In the case of the Oxilube samples, the process was carried out using an aqueous GPC system and after concentration an equal volume of acetonitrile was added to be a closer match to the solvent system of the matrix. By this approach a significant increase in oligomer intensity was achieved which allowed the collection of a small number of better quality CID spectra.

A feature observed in the initial scouting by *GPC of the samples*, was that some demonstrated a bimodal distribution. That is to say that they possessed two Gaussian-type distributions centred around distinct and separate mass values. This increased the polydispersity of the samples considerably unless each distribution was considered separately, in which case the values were more reasonable for a polymer of that type. The most likely cause of the two envelopes, which was supported by other evidence about the samples, is that more than one end-group was present and they had a significant difference in mass such as would have been the case with a combination of a C₁₂ chain and butanol as initiators. Such systems could be problematic for analysis, with techniques such as NMR unable to distinguish such features and leading to a completely incorrect mass average. Depending on the application, the two distributions could be calculated together, which would lead to a very high polydispersity, or as separate systems. For

MALDI analysis, it was fairly straightforward to separate the two mass envelopes by preparative-scale GPC with a much larger window than that used above.

An important issue with the fractioning of GPC results in this way was that, as has been shown in chapter three, the results of MALDI analysis varied significantly with each operation and sample preparation. Any slight changes in experimental conditions between the running of each fraction would have resulted in variations in intensity, that even without any bias within the defined mass envelope would contribute to a bias in the summated result. In order to try and address this issue, it was calculated to see if the matrix peak, which was omnipresent in the spectra, was capable of acting as an internal reference. In theory, if the concentration of the matrix solution was constant and the application volume was the same, then the amount of matrix desorbed should have been solely dependant on the laser power. By normalising each fractioned spectra to the height of the matrix peak, it was thought that this would have taken into account any variations in the amount of ions produced and so in turn have corrected the polymer signals so that they were summated at a comparable level. The intensity of each polymer peak was entered into Microsoft Excel and the matrix signal was used to create a normalisation constant that each intensity was multiplied by to give a new value. These values were composited to form the reconstituted spectra of the entire polymer sample. Applying mass-average calculations on these values then gave M_n and M_w results, which were compared to those from the raw results and a GPC analysis. As can be seen below, the value from this corrected calculation did bear a closer comparison to the GPC result, which could be said did not suffer from the same issue with the width of the polymer envelope. The non-normalised result also demonstrated a larger variation in the two calculated values, which is easily rationalised given the added bias in intensity arising from such a segregation of parts of the mass envelope. In effect, performing multiple spectra for a single composited system reinforces the already demonstrated intensity

variations, both as a function of mass and experimental conditions. Plotting the intensities as a series of bar charts, it can also be seen how the normalisation corrected for variations in intensity.

	Sample 1	Sample 2	Ave	St Dev
Gel Permeation Result	1551.2	1550.7	1550.9	0.35
Normal MALDI Result	1535.4	1531.6	1533.5	2.68
Fractioned MALDI Result	1528.6	1538.1	1533.3	6.71
Fractioned and Normalised MALDI	1546.4	1548.8	1547.6	1.69

Figure 5t – Number-average mass values for a wider distribution PEG sample

As with most cases of the statistical treatment of results arising from MALDI mass spectrometry, if a consideration of how artefact effects arose was taken then it was often possible to correct for these and give a perhaps more reliable result. This does however rely on the conceit that GPC is the more correct of the values, which may or may not be the case. Regardless, the variations in GPC were considerably less and as seen from these results, the simple correction was consistent with an understanding of how the spectra were acquired. Without further study of such a technique a true indication of the experimental variances could not be measured, however it would be suspected that it would be in line with those arising from the MALDI preparations already discussed. In the case of the mathematical treatment, it would be the reliability of the intensity of the matrix peak that could lead to a deviation developing in the normalised values.

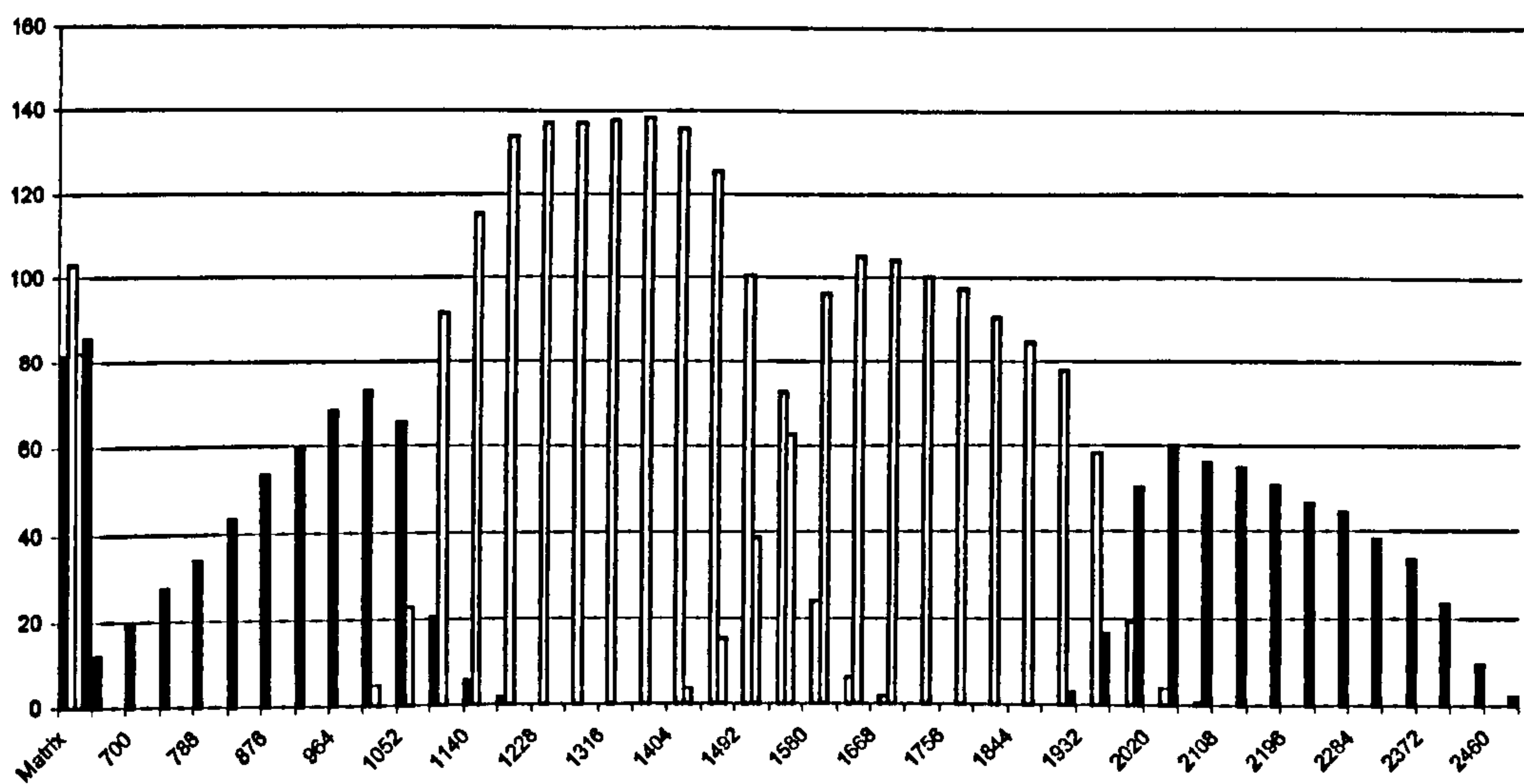


Figure 5u – Bar chart of the raw intensities of the fractions

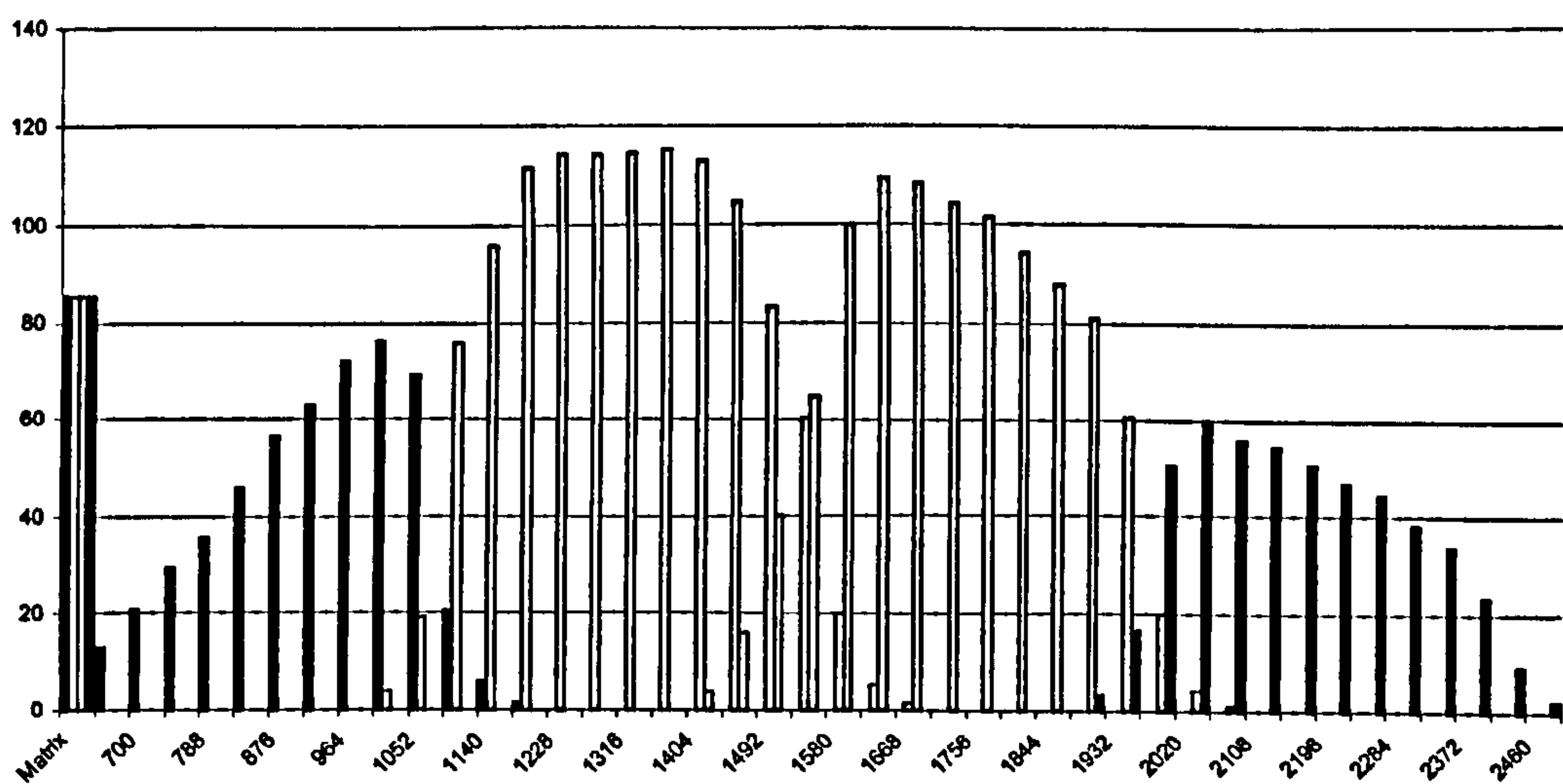


Figure 5v – Bar chart of the normalised intensities of the fractions

If the normalised intensities are summated together and presented as a single barchart, then it certainly appeared to resemble a standard polymer distribution more than that of the untreated results. There were slight variations at the very highest intensities that detracted from a pure Gaussian distribution, but it was unclear if they arose from the mathematical treatment or were truly representative of the sample itself.

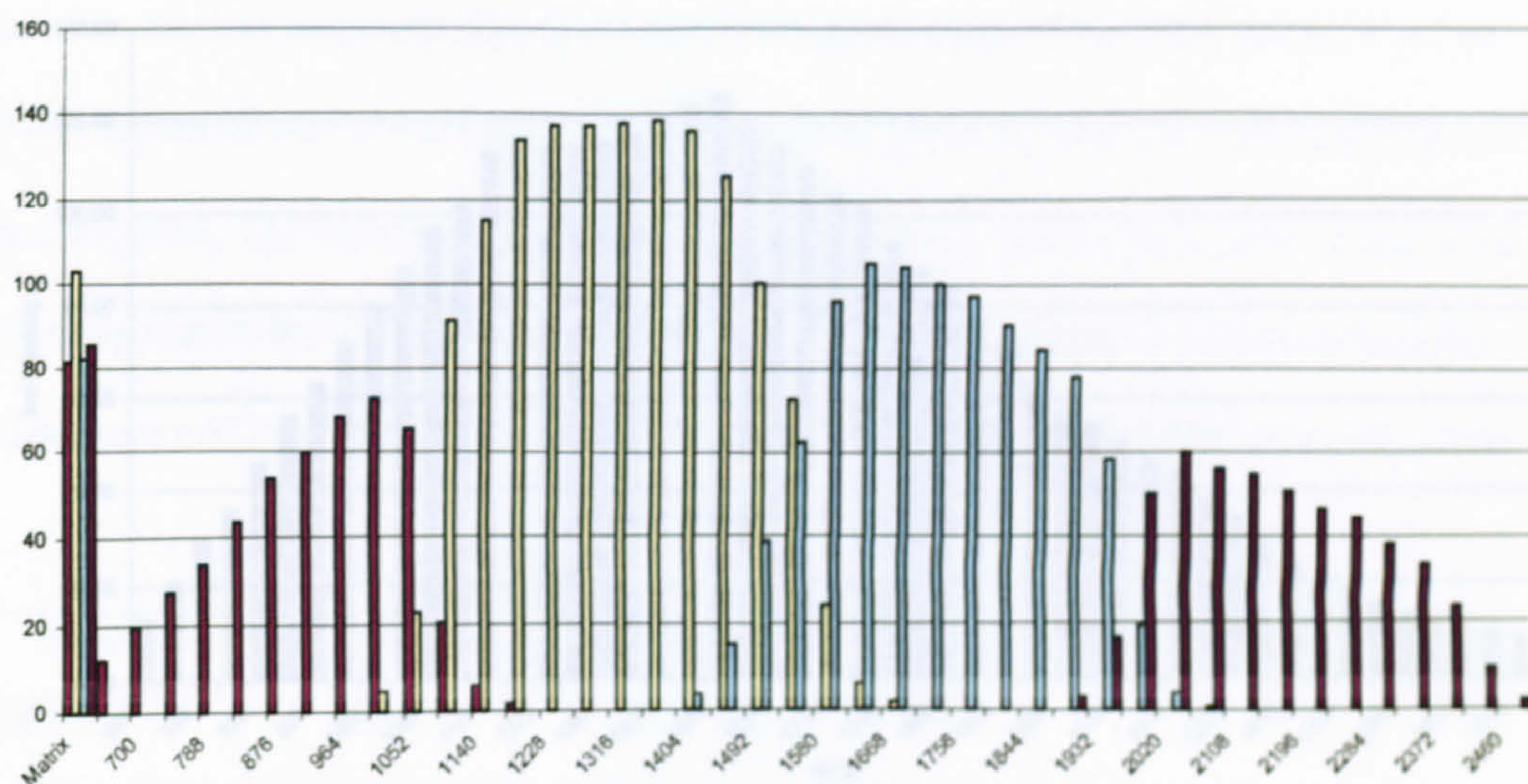


Figure 5u – Bar chart of the raw intensities of the fractions

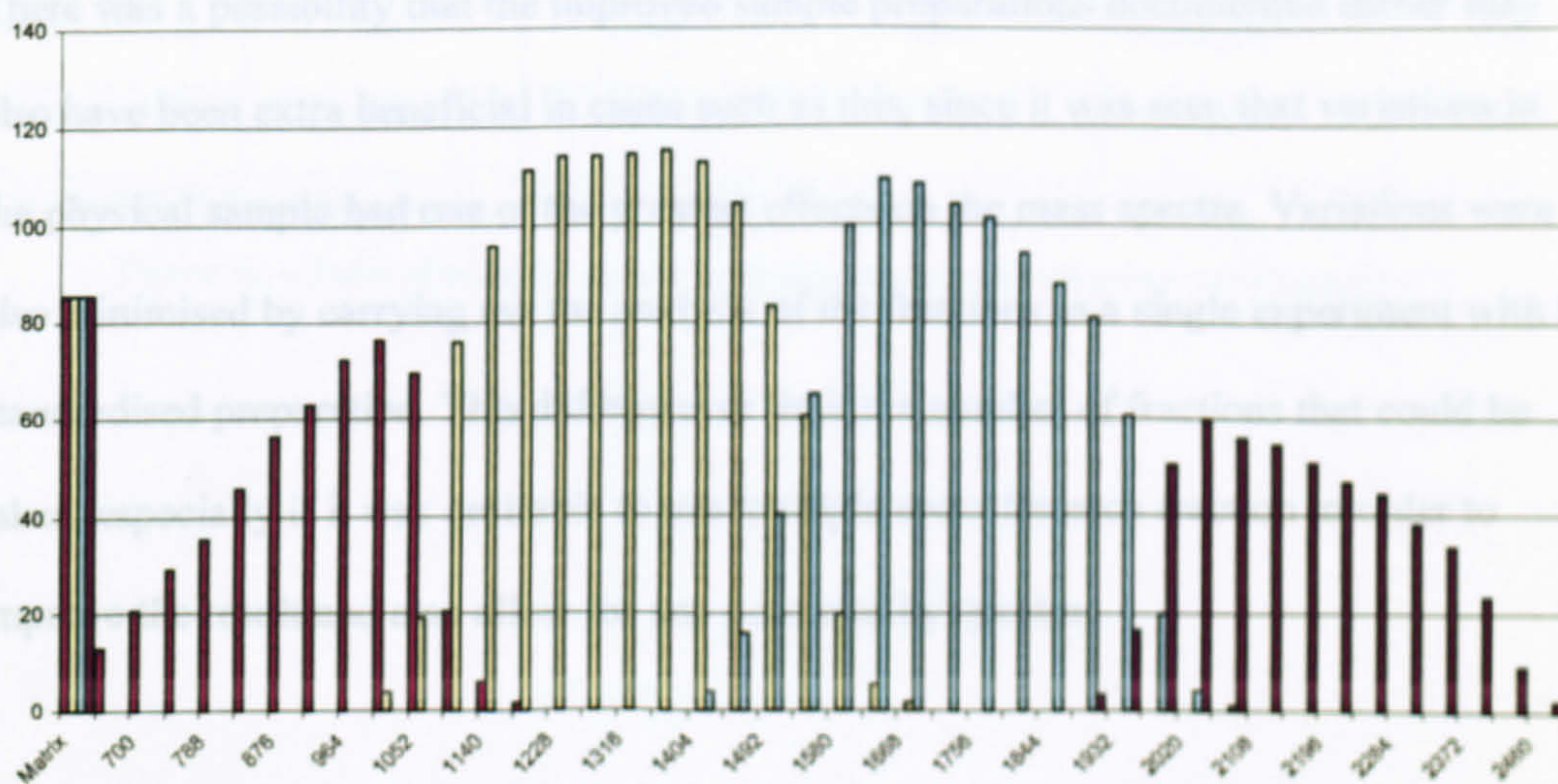


Figure 5v – Bar chart of the normalised intensities of the fractions

If the normalised intensities are summated together and presented as a single barchart, then it certainly appeared to resemble a standard polymer distribution more than that of the untreated results. There were slight variations at the very highest intensities that detracted from a pure Gaussian distribution, but it was unclear if they arose from the mathematical treatment or were truly representative of the sample itself.

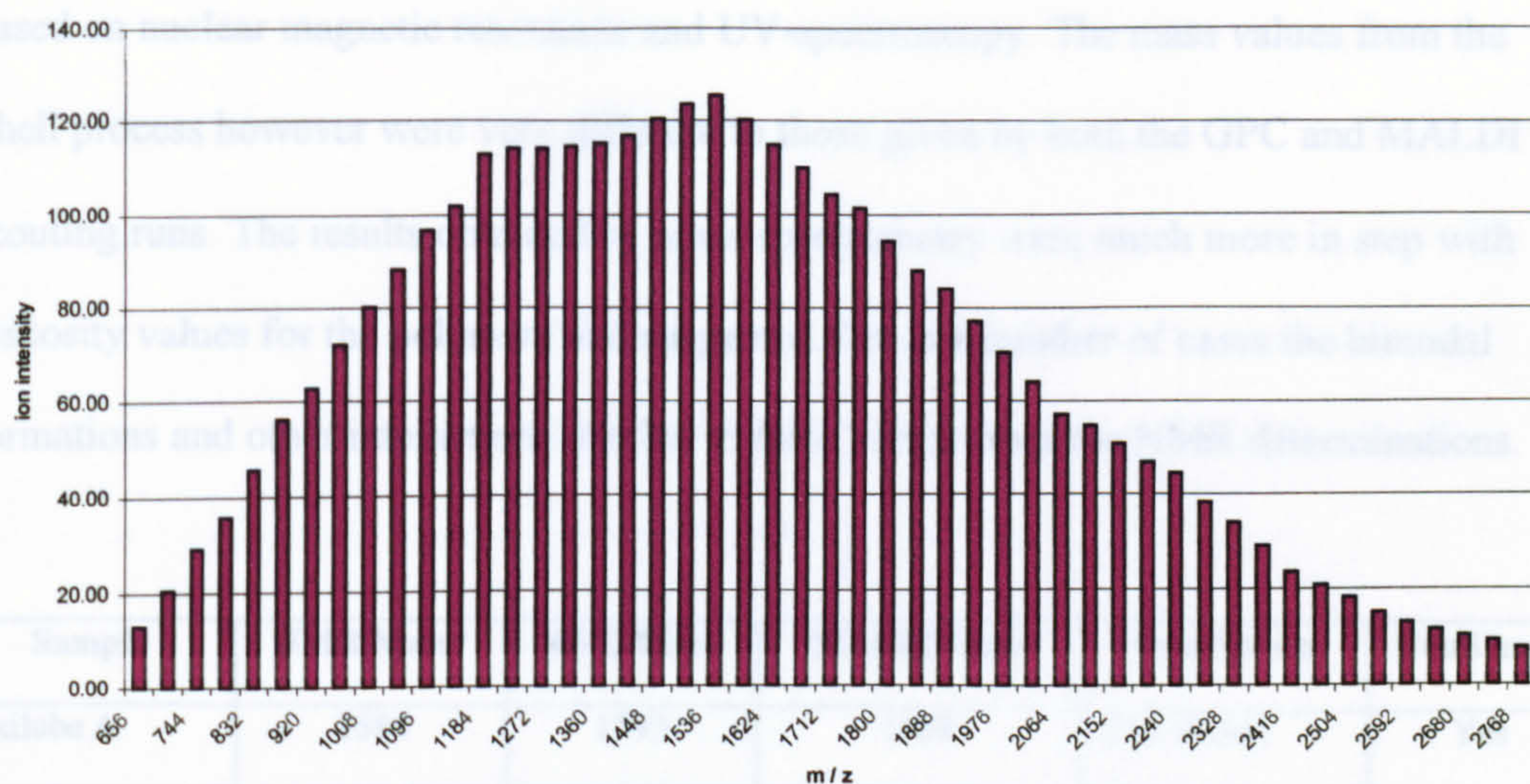


Figure 5w– Composited intensities from the normalised data series

There was a possibility that the improved sample preparations documented earlier may also have been extra beneficial in cases such as this, since it was seen that variations in the physical sample had one of the greatest effects on the mass spectra. Variations were also minimised by carrying out the analysis of the fractions in a single experiment with a standardised preparation. This did however limit the number of fractions that could be taken, especially if it was desirable to use multiple spots for each fraction in order to improve the result and also allow for any poor quality spectra.

The separated fractions were analysed by the CID method described for the MAG-TOF, with in most cases the process leading to a higher ion intensity for the peaks that were of interest. At this point however, the instrument started to develop technical problems that led to a decrease in ion production, which meant that spectra had to be acquired over a longer period and were not of the same quality as the Needol results. Of the few samples that were run, it was found that the co-polymer structure was quite random, leading to a large number of very low intensity fragments. The end-groups were easier to ascertain, which confirmed prior analysis carried out by Shell Analytical using an in-house method

based on nuclear magnetic resonance and UV-spectroscopy. The mass values from the Shell process however were very different to those given by both the GPC and MALDI scouting runs. The results obtained by mass spectrometry were much more in step with viscosity values for the polymers and suggested that in a number of cases the bimodal formations and other interactions had led to false values from the NMR determinations.

Sample	NMR Mass*	GPC Mass	MALDI Mass	End-Group	Confirmed
Oxilube A	1584	1573	1568	C12 alkane	Yes
Oxilube B	3586	3673	3652	n-butanol	Yes
Oxilube C	-	6401	6135	unknown	No
Oxilube D	2645	4437	4390	water	No
Polyglycol 15B	3347	3499	3256	n-butanol	Yes
Polyglycol 30B	4654	8809	7943	n-butanol	No

* - provided by Shell research

Figure 5x – Table of polymer results showing masses and end-group confirmations

CHAPTER SIX

Conclusions

The results presented in this thesis have demonstrated a systematic variation in the mass averages of polymeric systems analysed using both matrix-assisted desorption / ionisation and electrospray ionisation. These variations show a dependence on sample preparation and instrumental conditions that directly impact on the reliability of the results obtained. Within the range of results that can be acquired by manipulation of the experimental conditions, it is very difficult to maintain the concept of a “true” distribution for the polymer. In most cases the results of gel permeation chromatography analysis have been used as a benchmark, but these are in turn of concern regarding the exact representation of the polymer distribution, especially with it being a relative technique. That said, with the chromatographic techniques there are not the same extent of variation over that of simple sample-to-sample reproducibility.

If a known result is taken as a reference point, then it is conceivable that a specific methodology could be developed for the mass spectrometry in order to achieve the expected result. This method would require that the sample preparation and instrumental conditions are defined for each sample type. While this procedure would allow routine analysis, for example in the monitoring of batch synthesis process, it would fail for unknown samples or those lying outside a certain mass tolerance. Ironically this is similar to the main concern with gel permeation, in that accurate values are difficult to obtain for true unknowns or those outside of the range of set analytical standards used for calibrating the mass-time scale. This situation can however be addressed using “universal” calibration methods and various newer detection technology. No such simple fix as this currently exists in the case of the mass spectrometric studies.

The sample preparation steps discussed in chapter three for matrix-assisted laser desorption / ionisation were designed to minimise experimental variation. If these are carried out with a specified matrix, solvent system and alkali metal salt then the result

should have a high degree of reproducibility. This does address one of the concerns of making the procedure more operator independent and removing the biasing effect of varying sample preparation. It still remains though that the calculated mass averages will differ depending on the experimental settings. This also makes it difficult to compare values between *different instruments*, which is an important procedure for analytical science in an industrial setting. Differences in reported mass average between laboratories could arise from even small differences in laser power for instance, and not from the actual sample. It is also very true that laser powers tend to be varied in order to acquire a sufficiently resolved spectra, which would as amply demonstrated effect the distribution. Small changes may be accountable however, if the variations in averages were measured for a system over a range. This would mean that a calculation could be corrected for a change in say laser power by application of a calibrated correction factor. Such a procedure may allow such a mass spectrometric analysis to be carried out on an industrial basis with a greater degree of confidence.

The nature of the variations in mass average may be routed in the still uncertain process of matrix-assisted laser desorption and ionisation. Systematic differences between the results using a range of matrix systems strongly suggested that different situations may exist that could feed into future discussion of theory. While there are so many variables to control, it does however remain problematic to perform the empirical measurements that could potentially end the speculation over the number of proposed models.

The area that mass spectrometry is significantly more suited is in the structural analysis of polymeric systems. The fact that each oligomer is resolved with its absolute mass already provides more information than most chromatographic systems. Often by measuring the oligomer separation, the polymer can be identified and, in the case of homopolymers, the exact mass can even lead to a clue about the end-groups present. This capability is

substantially extended by application of such methods as collision-induced dissociation. Study of the fragments from a polymer can confirm identity and end-groups as demonstrated in chapter five, but it could also extend to more complex architecture. Analysis of co-polymers and cross-linked systems is problematic for other techniques, but within the scope of mass spectrometry. In this area the statistical distribution of the polymer chains is of little concern, conditions may be taken so as to give the best result in ion yield regardless of their effect on the relative intensities of other signals. As shown in the work herein, chromatography can also be used to isolate parts of a polymer distribution in order to improve results.

In summary, while the techniques explored here are useful in studying polymers, especially ones of unknown composition, it is the structural capabilities of mass spectrometry that should be of most interest to polymer science. While deficiencies in the mass analysis can be in part addressed, there is little that such methods can offer over modern chromatographic techniques. In the elucidation of macrostructure and identification of key group, mass spectrometry does present significant advantages over chromatography and other spectroscopic techniques.

FIN

**THESIS
CONTAINS CD
ROM**